OCT 16 1998
ENGINEERING SERVICES

DRAFT
Alternative Abatement Standards Application

Submitted to NMED on Behalf of SOHIO Western Mining Company for the L-Bar Uranium Mill Tailings Site

Prepared for:

Kennecott Energy

Kennecott Energy Company
505 South Gillette Avenue
Gillette, WY 82717

Prepared by:

Duke Engineering & Services
A Duke Energy Company

Duke Engineering & Services
9111 Research Blvd.
Austin, Texas 78758
512-425-2000

October 16, 1998

9903120203 990304
PDR ADOCK 04008904
B PDR

TABLE OF CONTENTS

1.0 INTRODUCTION 1
1.1 NRC License Requirements 1
1.2 State Requirements 2

2.0 SITE HYDROGEOLOGY 4
2.1 Surface Hydrology 4
2.2 Site-Specific Geology 4
2.3 Regional Groundwater Hydrogeology 5
2.4 Site-Specific Hydrogeology 7
2.5 Background Water Quality 9
2.6 Current Groundwater Quality 11

3.0 TECHNICAL INFEASIBILITY DEMONSTRATION 16
3.1 CAP Performance 16
3.1.1 Results of Corrective Action Program (CAP) 17
3.2 Groundwater Modeling Results 24
3.2.1 Source Term Characterization – Geochemical Results 25
3.2.2 Flow and Transport Studies 28
3.3 Site Security and Groundwater Protection 29
3.4 Continued CAP Cost/Benefit Analysis 30

4.0 DEMONSTRATION OF TECHNICAL ACHIEVABILITY 32
4.1 Proposed Alternative Abatement Standards 32
4.2 Natural Attenuation 33

5.0 CONCLUSIONS 37

6.0 REFERENCES 39

LIST OF FIGURES

Figure 1.1	L-Bar Site Location Map
Figure 2.1.1	Site Topography and Drainage Divide
Figure 2.2.1	Site Geology
Figure 2.2.2	L-Bar Site Stratigraphy
Figure 2.4.1	Primary Evapotranspiration Area
Figure 2.4.2	Pre-Tailings Simulated Steady-State Piezometric Contours
Figure 2.4.3	Potentiometric Surface Dec. 1996
Figure 2.6.1	pH Values (April 1998)
Figure 2.6.2	Chloride Concentrations (April 1998)
Figure 2.6.3	Sulfate Concentrations (April 1998)
Figure 2.6.4	TDS Concentrations (April 1998)
Figure 2.6.5	Nitrate Concentrations (April 1998)
Figure 3.2.1	Simulated 200-Year Tailings Fluid Concentrations
Figure 3.3.1	Final Property Boundary and Locations of Monitoring and Extraction Wells
Plate 1	Monitor Well and Piezometer Location Map – Post Tailings Cover Placement

LIST OF APPENDICES

Appendix A	"Geochemical Controls on Contaminant Migration at the L-Bar Uranium Mill Tailings Pile", Duke Engineering and Services, 1998.
Appendix B	"Projected Long-Term Flow and Quality of Groundwater at the L-Bar, New Mexico Uranium Site", Balleau Groundwater Inc., 1997.
Appendix C	Summary of Corrective Action Plan

LIST OF TABLES

Table 2.5.1	Background Water Quality in the FTH (1996-1997) at MW-29A
Table 2.6.1	Sample Results from October 1996
Table 2.6.2	Nitrate Results
Table 3.1.1.1	CAP Pumping Wells, Point of Compliance (POC) Wells, and Routinely Monitored Wells
Table 3.1.1.2	Barrier Well and Tailings Fluid Production Summary 1991 through 1997
Table 3.1.1.3	Pumpback Wells - Annual Production (1,000's liters)
Table 3.1.1.4	Pumpback Wells - Groundwater Concentrations (May, 1996)
Table 3.1.1.5	Pumpback Wells – Constituent Mass Removal Above Background
Table 3.1.1.6	Pumpback Wells – Tailings Fluid Removed Since 1990
Table 3.1.1.7	Estimated Constituent Mass Removed From Horizontal Drains
Table 3.2.1.1	Tailings Fluid Analyses from May 1996
Table 3.2.1.2	Source Concentrations
Table 3.4.1	CAP Costs
Table 4.1.1	Proposed Alternative Abatement Standards
Table 4.2.1	FTH Water Chemistry Beneath the Tailings Basin

1.0 INTRODUCTION

The L-Bar site is a Title II (UMTRCA, 1978) uranium mill tailings site located in central New Mexico and owned by SOHIO Western Mining Company. The Site Location Map is presented as Figure 1.1. The mill was in operation from 1977 through 1981, when it was shut down due to the poor economics of uranium production. A Nuclear Regulatory Commission-approved Detection and Monitoring Program (DMP) was put into place from 1981 until 1990, at which time a NRC-approved Corrective Action Program (CAP) was implemented. The mill was demolished and disposed of in 1986-1987, and interim reclamation construction took place in 1989 and 1990 to regrade the tailings, excavate diversion channels and place the radon barrier. All this work was performed in accordance with a NRC-approved reclamation plan. The purpose of this document is to provide the basis for Alternate Abatement Standards for state constituents not regulated by the NRC license.

1.1 NRC License Requirements

As part of the site's NRC license conditions, groundwater is monitored at four point-of-compliance wells; three on the west side of the site and one on the east side, and at one background well to the northeast. These wells are monitored for site-specific hazardous constituents, including nickel, selenium, radium (226 and 228), thorium and uranium. An active groundwater pumping system has been controlling seepage from the site along both the west-southwest and the northeast edges of the tailings pile.

SOHIO is currently pursuing NRC site closure, with final reclamation construction planned for Summer 1999. The final construction tasks consist of: excavating additional local sediment and weathered Mancos shale and placing it on the tailings basin cover to the original design grade; cleaning out existing sediment accumulated in the drainage channels since 1989; and, possibly place additional riprap protection along several potentially erodible slopes and at the outfalls of both the north and south channels

An Alternate Concentration Limits (ACL) application has been submitted by SOHIO to the NRC which demonstrates that groundwater contaminant conditions are as low as reasonably achievable (ALARA) and will not present a threat to human health or the environment outside of the site boundary over the next 1000 years. This application is currently under NRC review and

a copy has been transmitted to the New Mexico Environment Department (NMED), Ground Water Quality Bureau.

The state of New Mexico has unique concerns for groundwater protection in addition to constituents listed within the NRC license. The purpose of the proposed Alternate Abatement Standards is to address these additional state concerns. The Alternate Abatement Standards are needed at this site because the groundwater cannot be returned to background water quality but poses no threat to human health or the environment. In addition, the background water quality exceeds drinking water standards for several state-regulated constituents.

1.2 State Requirements

The L-Bar site operates under state discharge permit DP-150, as indicated in the discharge plan requirements of WQCC Reg. 3104. This plan was renewed in 1995 pursuant to WQCC Reg. 3109.C. As provisioned in the permit, the state requires SOHIO to monitor for several parameters in addition to those specified in the NRC license. The permit language specifically states that:

> "1. In addition to the ground water compliance monitoring report program as outlined in condition 31 of SOHIO's NRC materials license, copies of which are submitted to NMED as monitoring requirements of discharge plan, DP-150, SOHIO Western Mining Company shall augment their monitoring program as follows:
>
> a) On an annual basis SOHIO shall sample ground water from wells 16 (south side of tailings pile), 59, 62, 63, 64, (west side of tailings pile), 85, 86, and 87 (east side of tailings pile). Groundwater samples shall be analyzed for: sulfate (SO4) and chloride (Cl). pH and water elevation corrected to Mean Sea Level shall also be measured in each of these wells."

SOHIO has fully complied with these permit conditions and reports these results to the state as required. Monitor well 16 is dry and therefore SOHIO has been unable to sample this well.

Since 1996, the state has verbally expressed concern over potential nitrate contamination as a by-product of the ammonia used in the milling process. Groundwater sampling and analysis results are discussed in detail in Section 2.6 of this document.

There are a number of reasons and supporting documentation presented in this document that demonstrate why this site is eligible for alternative abatement standards as specified in WQCC Reg 4103, and stated specifically in 4103.F. The most important reason is that it is technically infeasible to return the groundwater to background water quality due to the low formation permeability and the long-term slow leakage from the tailings pile. The natural unaffected groundwater is of marginal quality, and groundwater from the affected aquifer is not used consumptively in the project vicinity. The groundwater quality is marginal even for livestock watering. Sections 3 through 5 elaborate further on these and other conditions.

Finally, related to NMED regulations, the L-Bar site is exempt from the requirement of an abatement plan as per WQCC Reg. 4105.A.4, which provides an abatement plan exemption for NRC-regulated facilities. The current site Corrective Action Program (CAP) functions as an Abatement Plan under the conditions of the discharge permit and as the state-approved abatement activities. The NRC-approved reclamation plan serves as the state reclamation program, satisfying the requirements of DP-150 condition (2). The monitoring requirements within the existing NRC license also satisfy the interim requirements of DP-150 license condition (3), which requires a post-closure monitoring plan. SOHIO anticipates that the federal Long Term Surveillance Plan, when developed, will serve as the state-approved post-closure monitoring plan.

2.0 SITE HYDROGEOLOGY

An understanding of the regional and local hydrogeology is critical to understanding why this site poses no threat to human health or the environment. The following sections describe both regional and site-specific hydrology in detail.

2.1 Surface Hydrology

The regional surface hydrology consists generally of a combination of steep-sided mesas separated by broad, gently sloping valleys. These valleys are infilled with alluvial and colluvial deposits, with primary stream channels incised through previously deposited sediments. In the site vicinity, regional drainage is to the south, first into the Rio Moquino, then the Rio Paguate, then into the Rio San Jose, then the Rio Puerco further south and east, and eventually into the Rio Grande in central New Mexico. To the north and northwest of the site, surface topography is dominated by the Mount Taylor volcanic field, which consists of broad, gently sloping basaltic flows with steep sides at flow edges. Numerous volcanic plugs occur in the project area, similar to Cerro Negro immediately to the north of the site. To the south and east, topography consists of alternating mesas and valleys.

The tailings basin is constructed at the head of a gently-sloping drainage divide, as shown on Figure 2.1.1. The divide directs surface flows to the east and west. An elevated drainage basin borders the site on the south and runoff from this basin (approximately 350 acres) flows through the south diversion channel. The north and south diversion channels accommodate all surface drainage around the site perimeter, and the embankment and cover adequately protect potentially contaminated materials within the basin. These protective features effectively prevent surface release of potentially contaminated materials.

2.2 Site-Specific Geology

Site surface geology is presented in Figure 2.2.1 and site stratigraphy is presented in Figure 2.2.2. Bedrock in the valleys around the site is predominantly masked by alluvial material. At the surface, the uppermost layer of Mancos shale is mantled by up to 35 feet of stream-deposited soils (alluvium) and talus (colluvium). These alluvial and colluvial materials are composed primarily of gypsiferous silty to sandy clays, and contain some lenticular bedded sands and

gravels. Basaltic debris, ranging in size from sands to cobble or boulder size angular blocks, can also be found strewn across the hillsides and incorporated in the alluvium/colluvium. The First Tres Hermanos (FTH) sandstone is a subunit of the Mancos Shale and is the uppermost aquifer of concern at the site. The FTH crops out on the hillsides southwest of the tailings impoundment, forming the characteristic mesa and bench topography of the area. The FTH does not come into contact with the tailings materials, but is mantled by alluvium and Mancos shale beneath the pile. Within the tailings basin, the uppermost Mancos Shale consists of a shaley sequence approximately 0 to 50 feet thick, which may be moderately to highly weathered, massive to fissile, and tends to be moderately fractured with gypsiferous fracture fillings. Beneath the tailings basin, the FTH is present from approximately 25 to 80 feet below the original land surface.

The FTH is underlain by two more alternating sequences consisting of shale/sandstone. Approximately 400 feet of shale and sandstone separate the underlying Dakota Sandstone from the FTH. The Dakota Sandstone is the closest aquifer containing potable water.

2.3 Regional Groundwater Hydrogeology

The project site is underlain by approximately 500 feet of Mancos Shale followed by a thin five- to ten-foot layer of Dakota Sandstone. The Dakota Sandstone directly overlies about 100 feet of the Jackpile Sandstone Member of the Morrison Formation. The Jackpile Sandstone overlies about 225 feet of the Brushy Basin Shale Member which, in turn, overlies about 150 feet of the Westwater Canyon Member, also a part of the Morrison Formation. Most of the water wells in the L-Bar area are completed in the Jackpile and Westwater Canyon members of the Morrison Formation (AGW Consultants, 1979). Wells have also been completed in the Brushy Basin Shale Member where sufficient thicknesses of sand have been encountered.

This description of regional trends is taken from SOHIO, 1980.

> "The oldest formations tapped for groundwater in the L-Bar region are the Permian-age Glorieta Sandstone and the overlying San Andres Limestone. The two formations join in many places to form a single aquifer. This aquifer is used as a source of water in areas northwest of the project site and near Grants, approximately 30 miles to the west. The aquifer is recharged from outcrops on

the eastern flank of the Zuni Mountains about 50 miles west of the project site. The San Andres Formation was encountered at a depth of 3400 feet, and showed low permeability.

Sandstone beds in the Chinle Formation are a source of water near Mesita, 13 miles south of the project area. Recharge of this aquifer occurs from outcrops further to the south. The Chinle Formation is not used as a source of water to the north or to the west of the site because it is overlain by more permeable formations.

The Entrada Sandstone is a minor source of relatively poor quality water northwest of Grants and in the Mesita area. The overlying Todilto Limestone and Summerville Formation are not known to be used as a source of groundwater. Water in the Todilto Limestone is slightly radioactive and contains radium concentrations above drinking water standards in the mine vicinity.

The Bluff Sandstone yields as much as 10 gpm to stock and domestic wells in the Moquino quadrangle and adjacent areas. Chemical quality of the water is generally poor. Recharge is limited by the steep cliffs the unit forms in the area of outcrop.

The sandstone units of the Morrison Formation yield 5 to 10 gpm for stock and domestic wells on the Laguna Indian Reservation, in southeastern McKinley County, and in northeastern Valencia County. Primary recharge is probably at outcrops in the area, although some infiltration from the overlying Dakota Sandstone may occur, causing poor water quality locally. Sandstones near the top of the Morrison Formation yield 20 gpm near the Woodrow Mine, four miles south of the L-Bar site. Lateral lithologic changes in the Morrison Formation result in hydrogeologic characteristics that are difficult to predict.

The Dakota Sandstone yields from 5 to 50 gpm to stock wells on the Laguna Indian Reservation. Yields from this formation in other areas, however, are generally small, and water quality is usually poor.

Within the Mancos Shale Formation, the Tres Hermanos Unit reportedly is the only sandstone that yields water to wells. Several shallow stock and domestic wells in the area adjacent to the tailings impoundment and in McKinley County to the northwest yield 5 to 20 gpm. Water quality is generally fair to poor.

Unconsolidated stream sediments (alluvium) a few inches thick to 150 feet thick form the flood plains of stream valleys throughout the region. These sediments constitute a principal aquifer along the [illegible] San Jose in the Laguna and Acoma Indian reservations and are moderately productive aquifers in the valleys of smaller flowing streams, such as the Rio Paguate and Rio Moquino. The water, however, is generally unpotable in the lower reaches of those streams.

A well drilled in the Rio Paguate (about four miles southwest of the site), which penetrated the alluvium, middle and lower sandstone units of the lower Mancos Shale, Dakota Sandstone and upper Morrison has yielded 10 gpm. This was mainly from the alluvium and Tres Hermanos Sandstone member of the Mancos Shale. Another well near the town of Paguate has yielded 15 gpm from the alluvium. It is unlikely, however, that the alluvium could be used as a reliable source of water at any considerable distance away from flowing streams."

Regional groundwater flow patterns in the vicinity of the L-Bar mine are influenced by the occurrence of recharge areas, discharge areas, and hydrogeologic characteristics of the aquifer. In general, the potentiometric surface map indicates that ground water enters the area from the north and northeast and flows south and southwest toward discharge areas. Discharge areas occur where the First Tres Hermanos crops out or is eroded by local surface drainage resulting in zones of evapotranspiration from the aquifer, but no surface flows originate from the FTH aquifer in the site vicinity.

2.4 Site-Specific Hydrogeology

The site groundwater system is characterized by upland recharge in the basaltic mesas surrounding Mt. Taylor, with subsequent arroyo discharge in the adjacent drainages. There is no evidence of base flow groundwater discharge within a mile of the site. The Dakota Sandstone is the uppermost aquifer used in the project vicinity and occurs at over 500 feet depth at the site.

The mine wellfield to the northeast is completed in the Westwater Canyon member at depths exceeding 1000 feet, and produces good quality water. According to well survey records, the FTH is sparsely used for stock watering in places, but water quality is marginal. The presence of abundant stock ponds in the area also indicate that surface runoff is the primary source of local livestock water.

Flow in the FTH aquifer in the immediate site vicinity tends to follow the general expression of surface topography, with primary flow paths toward subsurface discharge to the arroyos southwest and southeast of the site. An erosional feature in the uppermost FTH to the southwest of the site terminates groundwater flow away from the site in the alluvium. Within the arroyo, the upper FTH is eroded away and has backfilled with alluvial materials. As the groundwater flows into this bedrock depression, it is lost to the atmosphere by subsurface evaporation through the alluvium, resulting in contaminants precipitating out within the soil column. This subsurface flow mechanism is also evident by a line of tamarisk trees (salt cedar) within the arroyo, which probably delineates the FTH subcrop. Figure 2.4.1 presents the approximate location of the primary evapotranspiration area.

Monitor well MW-100 is constructed within the uppermost FTH downgradient of the southwest arroyo and produces very little water. This well typically contains 3 to 4 inches of water at the bottom of the casing when checked during the annual water quality sampling. In order to retrieve a water sample from this location, site personnel have to bail the well dry to purge for sampling, then return several weeks later and recover the sample. This condition is more evidence that groundwater flow from upgradient in the arroyo is almost non-existent.

To the northeast of the site, a small amount of subsurface seepage was detected in the form of a historic groundwater mound in the vicinity of MW-50. This groundwater mound has been treated by actively pumping MW-89 and water levels have declined significantly in this area. But the monitor wells which show elevated groundwater levels and nitrate contamination also exhibit extremely low permeabilities. Both MW-50 and MW-17B have to be purged several days before sampling to ensure that adequate recharge occurs to extract the needed sample volume from each well. Further to the east of the site, the FTH crops out in the arroyo and eventually rises to the south above the groundwater table. There is no surface discharge from any part of the tailings impoundment. Subsurface evapotranspiration is the only discharge

mechanism, although there is not enough subsurface flow to support any vegetation in the eastern-most arroyo.

The pre-mine subsurface groundwater hydraulic heads in the First Tres Hermanos have been reconstructed (BGW, 1997) as shown on Figure 2.4.2. This figure demonstrates the hydraulic gradients to the southwest and southeast. Pre-mining flow in both directions was less than 1 gallon per minute (Appendix B, BGW, 1997). These flow directions refer only to the FTH, which is eroded through or rises above the water table in both these directions.

In the past, the conceptual site model was believed to represent a continuous fully saturated column between the tailings and the groundwater. In other words, the natural strata beneath the tailings was interpreted as fully saturated from the base of the tailings to the FTH water table. Recent data from an expanded hydrogeologic investigation (INTERA, 1996) indicates a different condition. Water levels in four wells drilled through the tailings and isolated within the upper 40 feet of the FTH (MW-106 through MW-109) indicate that the tailings basin is more analogous to a perched water body. In fact, an unsaturated zone of more than 25 feet thickness exists beneath the pile. Figure 2.4.3 shows the present potentiometric surface in the FTH immediately beneath the tailings pile in 1996, including data from MW-106 through MW-109. The 1996 data is used because it represents the most extensive series of measurements for any recent year. The highest groundwater contour exists just above 6140 feet above mean sea level (amsl), and the base of the tailings occur at approximately 6170 feet amsl. Thus, the actual relationship between groundwater flow and tailings seepage is more analogous to a leaky bathtub than to a continuously saturated column. A detailed discussion of site hydrogeology is contained in INTERA, 1996, submitted previously to NMED.

2.5 Background Water Quality

During licensing, a well located northeast of the site and away from any potential mine impacts was selected as an indicator of background water quality. This well, MW-29A, is the license background well, and water quality measurements from this well have been kept continuously for more than 10 years. Table 2.5.1 summarizes the constituent concentrations of background water at the L-Bar site for 1996 and 1997. This data is representative of the historic background water quality.

Table 2.5.1 Background Water Quality in the FTH (1996-1997) at MW-29A

Constituent	Units	Feb-96	May-96	Jul-96	Oct-96	May-97	Oct-97
Temperature	(C)	-	20.16	16	17	18	16
Cl	(mg/L)	106	123	104	104	108	111
SO4	(mg/L)	3290	3420	3410	3000	3000	3000
pH (lab)	pH units	7.94	7.94	7.49	7.41	8.06	7.92
pH (field)	pH units	-	7.5	7.55	7.6	7.56	7.49
Specific Conductance (lab)	(µhmos/cm) @25*C	6960	7000	6950	7010	7020	7300
Nitrate	(mg/L)	-	<0.05	<0.1	<0.1	-	<0.05
Ammonia	(mg/L)	1.86	-	1.98	1.93	-	-
Nitrite	(mg/L)	0.07	-	<0.01	<0.01	-	-
Ni	(mg/L)	<0.04	<0.04	<0.04	<0.04	<0.04	<0.04
Se	(mg/L)	<0.002	<0.001	<0.001	0.003	<0.002	<0.002
Sb	(mg/L)	<0.1	<0.1	<0.1	<0.1	<0.1	<0.1
Bicarbonate	(mg/L)	-	561	512	512	488	561
Carbonate	(mg/L)	-	<1.0	<1.0	<1.0	<1.0	<1.0
Calcium	(mg/L)	62.8	75.9	72.9	78	78.2	75.5
Magnesium	(mg/L)	25.1	27.5	26.7	28.4	30.4	26.4
Potassium	(mg/L)	5	12	15	17	10	10
Sodium	(mg/L)	1530	1620	1600	1720	1640	1620
TDS	(mg/L)	5430	5450	5650	5660	5590	6150
TSS	(mg/L)	<4	7	<4.0	<4.0	<4.0	<4.0
U	(mg/L)	1.6	<0.6	0.001	<0.001	0.001	<0.001
Ra226	(pCi/L)	3.5	2.4	4.9	7.2	2.8	2.1
Ra228	(pCi/L)	4.2	2.3	4.4	4.3	2.5	3.5
Th230	(pCi/L)	<0.3	0.9	0.6	0.2	0.6	0.8
CN	(mg/L)	<0.02	-	<0.01	-	-	-
Si02	(mg/L)	5	5.2	5.3	5.5	5.8	5.2
Fe	(mg/L)	0.03	0.47	0.27	0.41	1.13	1.14
Fe+2	(mg/L)	-	<0.05	0.14	<0.05	<0.05	<0.05
Fe+3	(mg/L)	-	<0.05	0.13	0.41	1.13	1.14
F	(mg/L)	1.2	-	1.3	1.3	1.1	1.1

- = not analyzed

The ranges of constituents observed in the background well since 1996 include:

- chloride values ranged from 104 to 123 mg/l
- sulfate concentrations ranged between 3000 and 3420 mg/l
- pH values ranged from 7.41 to 8.06 pH units
- nitrate/nitrite ranged from 0.07 mg/l to below detection limits
- total dissolved solids (TDS) ranged from 5430 to 6150 mg/l, and
- specific conductance ranged between 6950 and 7300 µmhos/cm.

These parameters indicate that the background at the site consists of marginal to poor water quality for the upper FTH.

2.6 Current Groundwater Quality

In addition to the NRC licensed conditions the State has expressed concern primarily with nitrate in groundwater. Chloride, pH, sulfate, and TDS concentrations have been considered as secondary aesthetic concerns. Nitrate analyses have been routinely performed for several wells in accordance with the conditions of the NRC license, and these results are submitted semi-annually to the state. In 1996, the state requested that SOHIO perform some additional testing for nitrate in some wells that are not routinely tested for this compound. Sample duplicates for each of these wells were also submitted to the state for their own analyses. Table 2.6.1 presents the analytical results from each of these locations.

Table 2.6.1 Sample Results from October 1996

Constituent	Units	MW-1A	MW-2A	MW-3A	MW-14	MW-17B	MW-29A	MW-50	State Std.
Temperature	(C)	17	19	19	20	18.5	17	17	n/a
pH	(field)	7.77	6.49	7.03	6.98	6.5	7.6	7.11	n/a
pH	(lab)	7.65	6.72	7.2	7.13	6.82	7.41	7.27	6 to 9
Specific Conductance	µhmos/cm field	4626	13850	17170	10830	11560	7020	11800	n/a
Specific Conductance	µhmos/cm lab	4650	14100	17000	10800	11500	7010	11800	n/a
Cl	(mg/l)	99.8	781	668	449	373	104	516	250
SO4	(mg/l)	1600	6000	10000	6000	5000	3000	4000	600
Bicarbonate	(mg/L)	573	1350	1850	1230	1270	512	1100	n/a
Carbonate	(mg/L)	<1.0	<1.0	<1.0	<1.0	<1.0	<1.0	<1.0	n/a
TDS	(mg/L)	3370	13500	17200	9660	11100	5660	11500	1000
TSS	(mg/L)	16	4	27	30	18	<4.0	19	n/a
Fe+3	(mg/L)	0.07	<0.05	0.15	1.59	0.07	0.41	<0.05	n/a
Fe+2	(mg/L)	<0.05	<0.05	<0.05	<0.05	<0.05	<0.05	<0.05	n/a
Fe	(mg/L)	0.07	<0.03	0.15	1.59	0.07	0.41	<0.03	1
Ammonia	(mg/l)	1.03	<0.01	<0.01	2.11	<0.01	1.93	<0.01	n/a
Nitrate	(mg/L)	<0.1	280	8.4	<0.1	360	<0.1	490	10
Nitrite	(mg/l)	<0.01	0.06	0.42	0.05	0.73	<0.01	0.62	n/a
Ni	(mg/l)	<0.04				<0.04	<0.04	<0.04	n/a
Sb	(mg/l)	<0.1				<0.1	<0.1		
Calcium	(mg/L)	27.3	433	347	298	405	78	562	0.2
Magnesium	(mg/L)	11.2	631	1170	237	380	28.4	571	5
Potassium	(mg/L)	9	50	36	25	40	17	55	30 *
Sodium	(mg/L)	999	2850	3620	2230	1900	1720	1920	30 *
Si	(mg/L)	4.3	4.4	4.5	6.2	3.6	5.5	4.3	
Cn	(mg/l)					0.05			0.05
U	(mg/l)	<0.001				0.032	<0.001		
Ra226	(pCi/l)	1				10.2	7.2		
Ra228	(pCi/l)	0.3				3.5	4.3		
Th230	(pCi/l)	0.8				0.5	0.2		
Se	(mg/l)	0.005				0.003	0.003		
F	(mg/l)	1.8	0.3	0.5	0.7	0.2	1.3	0.2	

Table 2.6.1 Sample Results from October 1996 (Cont.)

Constituent	Units	MW-69	MW-72	MW-73	MW-74	MW-75	MW-89	State Std.
Temperature	(C)	15	15	16	19	15.5	16	n/a
PH	(field)	6.6	7.25	6.83	7.59	7.05	7.32	n/a
PH	(lab)	7.06	6.98	7.2	7.47	7.15	7.4	6 to 9
Specific Conductance	µhmos/cm field	11870	7350	7160	6210	6250	5760	n/a
Specific Conductance	µhmos/cm lab	12100	7670	7070	6250	6340	5790	n/a
Cl	(mg/l)	596	179	93.6	97.7	64.6	95.9	250
SO4	(mg/l)	6000	4200	3700	3000	2700	2500	600
Bicarbonate	(mg/L)	1710	488	927	451	781	537	n/a
Carbonate	(mg/L)	<1.0	<1.0	<1.0	<1.0	<1.0	<1.0	n/a
TDS	(mg/L)	11500	6880	5910	4770	4410	5000	1000
TSS	(mg/L)	<4.0	11	6	5	<4.0	<4.0	n/a
Fe+3	(mg/L)	1.88	<0.05	<0.05	0.24	0.65	0.6	n/a
Fe+2	(mg/L)	<0.05	0.05	0.05	<0.05	0.45	<0.05	n/a
Fe	(mg/L)	1.88	0.04	0.09	0.24	1.1	0.6	1
Ammonia	(mg/l)	0.72	0.05	1.51	1.89	1.92	1.43	n/a
Nitrate	(mg/L)	2.9	0.2	0.1	0.3	<0.1	0.3	10
Nitrite	(mg/l)	0.02	0.02	0.04	<0.01	<0.01	0.02	n/a
Ni	(mg/l)	<0.04					<0.04	n/a
Sb	(mg/l)	<0.1					<0.1	
Calcium	(mg/L)	389	292	206	69.1	191	110	0.2
Magnesium	(mg/L)	849	[illegible]	97	30.7	190	53.6	5
Potassium	(mg/L)	19	24	15	15	15	14	30 *
Sodium	(mg/L)	2050	1500	1490	1480	1260	1410	30 *
Si	(mg/L)	8.2	4.5	5.3	5.1	5.4	5.4	
Cn	(mg/l)							0.05
U	(mg/l)	0.91						
Ra226	(pCi/l)	7.9						
Ra228	(pCi/l)	5.3						
Th230	(pCi/l)	0.4						
Se	(mg/l)	<0.001						
F	(mg/l)	1	1.1	0.9	1.3	0.4	0.9	

Figures 2.6.1 through 2.6.5 present April 1998 results for specific constituents including pH, chloride, sulfate, TDS and nitrate, respectively.

In July, 1996, SOHIO performed additional groundwater sampling in wells which are more widely spaced across the site. This was done to gain a better understanding of the site wide geochemistry. These wells were sampled for all regulated constituents as well as the major cations and anions to determine overall groundwater chemistry, with a specific emphasis on nitrate in groundwater. The results for nitrate from all these additional analyses from May 1996 through April 1998 are presented in Table 2.6.2 below.

In summary, three general locations of nitrogen occurrence are identified at the L-Bar site. These occur in the northeast area (MW-17B and MW-50), the west central area (MW-2A) and the southwest area (MW-77, MW-92, and MW-15). However, results from predictive groundwater modeling, even without continued operation of the pumpback system, indicate that natural groundwater flow processes will prevent offsite migration of any tailings constituents over the next 200 years and probably much longer, as discussed in Section 3.2.

Table 2.6.2 Nitrate Results

Well	May, 1996	July, 1996	October, 1996	April, 1997	April, 1998
1A	0.07		<0.1		0.11
2A	357		280.06	340	360
3A		8	8.82		17.6
8	21.6				
13B	14.4				
14			0.05		0.82
15		43	68.7		
17B	420	340.4	360.73	560	480
29A	<0.05	<0.1	<0.1		<0.05
50	520	470	490.62	550	530
59		0.02	0.06		
62		0.3	1.4		
63		0.02	<0.1		
64		<0.1	0.05		
69	5.4		2.92	3.41	21.8
72		0.73	0.22		0.7
73		0.02	0.14		
74		0.7	0.3		
75			<0.1		
77		35	140		
81	39		32.04	27	57
85			<0.1		
86		0.06	<0.1		
87			<0.1		
89	<0.05	0.83	0.32		
92		181.01	200.07		
102	9.5				
108				46	
109				21.2	

Nitrate value represents combined Nitrate and Nitrite from these analyses
< or - = non detect above detection limit

3.0 TECHNICAL INFEASIBILITY DEMONSTRATION

This section provides documentation to demonstrate that continued active remediation is not required for protection of human health or the environment at the L-Bar uranium mill tailings site. The site Corrective Action Plan (CAP) has been in operation for approximately 10 years, and has been effective in controlling and treating tailings fluid seepage from the pile. However, the tailings fluid seepage continues to decline since no additional fluid is being added to the system over time. Groundwater contamination at the site is limited to the area immediately adjacent to the tailings pile, and presents no potential threat outside the property boundary, even into the foreseeable future. This conclusion is supported by the results of an extensive and thorough modeling effort performed by Balleau Groundwater, Inc. (BGW). The results of this modeling effort have been provided previously to NMED staff. Natural physical processes will continue to mitigate groundwater contamination through dispersion, dilution, and chemical reaction with aquifer materials in such a way that no potential receptors will be exposed to site groundwater. This will be assured through these natural processes as well as the long-term federal custody care agreement that will effectively control the site in perpetuity and preclude any potential future uses of the impacted groundwater. Thus, alternative abatement standards would allow the site to come into state regulatory compliance. This document provides the technical and scientific basis for NMED approval of SOHIO's proposed Alternative Abatement Standards.

3.1 CAP Performance

The detection monitoring program (DMP) was conducted from 1981 until the reclamation plan was approved, including the CAP, in 1989. As part of the CAP, an enhanced evaporation system consisting of a network of irrigation sprinklers was used to decant the free water from the surface of the tailings pond. Once the free water had been evaporated, five evaporation ponds were constructed within the Mancos shale on the eastern border of the pond to treat any additional fluids.

For groundwater protection, the final corrective action involved construction of seepage recovery wells to minimize contaminant migration from the tailings basin. These wells continue to recover the small amount of seepage water as well as the dissolved constituents and pump it to the evaporation pond network.

This type of program was technically feasible and easily modified to accommodate the mill decommissioning and other reclamation activities at the site. As a consequence of this, the CAP was relatively economical to operate and effective in treating the recovered constituents within the tailings area.

3.1.1 Results of Corrective Action Program (CAP)

The CAP had a defined goal of returning hazardous constituent levels in groundwater Point of Compliance (POC) wells to licensed concentrations. To accomplish this, seepage recovery wells, also known as pumpback wells, were installed as shown on Plate 1. Currently, other wells are monitored for either NRC or state requirements. Table 3.1.1.1 identifies all wells involved in the CAP or state discharge permit requirements.

Table 3.1.1.1 CAP Pumping Wells, Point of Compliance (POC) Wells, and Routinely Monitored Wells

Well	Well Location	Purpose	Required By
MW-1A	West	POC Well	NRC
MW-2A	Northwest	Pumping W	NRC
MW-3A	West	Monitoring Wel'	NRC
MW-12A	Northwest	Monitoring Well	NRC
MW-14	West	Monitoring Well	NRC
MW-16	Southwest	Dry	NMED
MW-17	Northeast	Monitoring Well	NRC
MW-17B	Northeast	POC Well	NRC
MW-29A	Northeast	POC Well, Background Well	NRC
MW-50	Northeast	Monitoring Well	NRC
MW-51	Northeast	Monitoring Well	NRC
MW-52	Northeast	Monitoring Well	NRC
MW-53	North	Monitoring Well	NRC
MW-55	Northwest	Monitoring Well	NRC

Table 3.1.1.1 CAP Pumping Wells, Point of Compliance (POC) Wells, and Routinely Monitored Wells (Cont.)

Well	Well Location	Purpose	Required By
MW-57	Southwest	Monitoring Well	NRC
MW-58	West	Monitoring Well	NRC
MW-59	Northwest	Monitoring Well	NMED
MW-60	Northwest	Monitoring Well	NRC
MW-61	Southwest	Monitoring Well	NRC
MW-62	West	Monitoring Well	NMED
MW-63	West	Monitoring Well	NMED
MW-64	Northwest	Monitoring Well	NMED
MW-68	Northwest	Monitoring Well	NRC
MW-69	West	Pumping Well and POC	NRC
MW-72	East	Monitoring Well	NRC
MW-73	Northeast	Monitoring Well	NRC
MW-74	Northeast	Monitoring Well	NRC
MW-75	East	Monitoring Well	NRC
MW-76	West	Monitoring Well	NRC
MW-77	Southwest	Pumping Well	NRC
MW-78	Southwest	Monitoring Well	NRC
MW-79	Southwest	Monitoring Well	NRC
MW-81	Southwest	POC Well	NRC
MW-85	Northeast	Monitoring Well	NMED
MW-86	East	Monitoring Well	NMED
MW-87	East	Monitoring Well	NMED
MW-91	Northeast	Background Well	Voluntary

Table 3.1.1.2 shows the annual production of tailings fluid in liters recovered through the groundwater mitigation elements of the CAP. Tables 3.1.1.3 through 3.1.1.6 show pumpback well recovery production, chemistry, contaminant mass removal above background, and amount of tailings fluid removed by the pumpback system. The program has demonstrated that all hazardous constituents, with the exception of uranium and selenium, are below the license established standards as measured at the POC locations. A detailed discussion of the results of the CAP is given in Appendix C.

Table 3.1.1.2 Barrier Well and Tailings Fluid Production Summary 1991 through 1997

Year	Barrier Well System Annual Production (liters)	Tailings Fluid Collected from Toe Drains (liters)
1990	15,591,812	12,490,500
1991	14,300,589	6,117,786
1992	13,195,233	4,926,064
1993	12,891,169	3,990,223
1994	10,792,663	3,337,817
1995	10,146,397	2,615,757
1996	10,083,562	1,461,010*
1997	9,560,301	*
TOTAL	96,561,724	34,939,157

* The toe drains were shut down on July 23, 1996. The 1996 total is flow up to this date.

Table 3.1.1.3 Pumpback Wells - Annual Production (1,000's liters)

Year	1990	1991	1992	1993	1994	1995	1996	1997	Total
2A	2,763	2,506	2,199	2,210	1,726	1,643	1,673	1,684	16,404
5	106	49	30	NA	NA	NA	NA	NA	185
8	988	973	901	965	852	840	863	606	6,987
10A	871	905	931	1,037	954	927	863	905	7,392
13B	185	159	151	136	98	76	72	72	950
69	753	734	715	731	674	734	738	431	5,511
77	140	132	95	95	140	110	106	106	924
82	1,048	942	416	473	556	549	454	507	4,947
83	1,310	1,885	1,911	1,306	1,450	1,488	1,469	1,427	12,244
84	1,249	1,332	1,359	1,408	1,329	1,336	1,276	1,419	10,708
89	579	492	541	568	537	507	545	413	4,182
101	344	696	761	787	674	689	594	613	5,159
102	23	64	57	57	38	45	42	26	352
Trench	5,227	3,429	3,134	3,123	1,768	1,200	1,389	1,347	20,617
Total	15,590	14,300	13,195	12,892	10,791	10,148	10,083	9,561	96,563

NA - Not Analyzed

Table 3.1.1.4 Pumpback Wells - Groundwater Concentrations (May, 1996)

MW	Cl (mg/l)	SO_4 (mg/l)	Ni (mg/l)	Se (mg/l)	Sb (mg/l)	U (mg/l)	Ra226 (pCi/l)	Ra228 (pCi/l)	Th230 (pCi/l)	NO_3 (mg/l)	TDS (mg/l)
2A [1]	750	5500	ND	NA	ND	NA	NA	NA	NA	340	12500
8	123	1930	ND	0.006	ND	0.009	1.0	1.1	0.7	21.6	3560
10A	140	2260	ND	ND	ND	ND	1.7	1.6	0.6	ND	3910
13B	678	9170	ND	ND	ND	0.72	2.2	4.9	0.2	14.4	15400
69	681	6690	ND	ND	ND	1.28	2.7	4	0.9	5.4	11500
77	290	5030	ND	NA	ND	0.027	5.4	5.9	0.4	35	8680
82	334	5140	ND	ND	ND	0.07	3.8	4.3	1.0	0.23	8660
83	319	4450	ND	ND	ND	0.004	3.3	3.3	1.0	0.25	7660
84	64	800	ND	0.001	ND	ND	0.5	ND	1.6	0.65	1860
89	58	3620	ND	ND	ND	ND	1.7	2.2	0.6	ND	5760
101	113	1650	ND	0.004	ND	ND	1.3	1.2	0.9	3.54	3060
102	91	3830	ND	ND	ND	0.8	3.0	4.5	0.9	9.5	6230
29A [2]	123	3420	ND	ND	ND	ND	2.4	2.3	0.9	ND	5450
French Drain [3]	218	4490	ND	0.006	ND	0.181	5.3	1.5	1.8	1.9	8590

[1] 1997 data, May data incomplete

[2] Background Well

[3] July 1996 data, not collected May 1996

NA - Not Analyzed

ND - Not Detected

Table 3.1.1.5 Pumpback Wells – Constituent Mass Removal Above Background

	Cl (Kg)	SO_4 (Kg)	TDS (Kg)	NO_3 (Kg)	Ni (Kg)	Se (Kg)	Sb (Kg)	U (Kg)*	Ra226+228 (pCi)*	Th230 (pCi)*
2A	10,663	37,976	112,779	5,577	0	0	0	NA	NA	0
8	161	0	0	151	0	0.042	0	0	0	0
10A	296	0	0	0	0	0	0	0	0	0
13B	549	5,686	9,287	13.7	0	0	0	0.21	0	0
69	3,202	19,316	32,377	29.8	0	0	0	4.30	0	0
77	175	1,704	2,821	32.3	0	0	0	0	267.8	0
82	1,158	9,671	15,014	1.1	0	0	0	0	0	0
83	2,682	12,841	24,918	3.1	0	0	0	0	0	0
84	0	0	0	7.0	0	0.011	0	0	0	0
89	0	1,819	565	0	0	0	0	0	0	0
101	67	0	0	18.3	0	0.021	0	0	0	0
102	0	227	213	3.3	0	0	0	0.11	0	0
French Drain	2,433	26,905	61,129	39	0	0.124	0	0	0	0
Total	21,385	116,145	259,103	5,876	0	0.198	0	4.62	267.8	0

*For Ra226+Ra228 and Th230 the mass removal is calculated as that above the background-based NRC license standards as specified in license # SUA 1472, Amendment 28. (Ra226+Ra228 = 11.01 pCi/l, Th230 = 3.12 pCi/l). For U, the mass removed is that above the 0.5 mg/l standard.

Table 3.1.1.6 Pumpback Wells - Tailings Fluid Removed Since 1990

Pump-Back Well	Total Pumped (thousands of liters)	% Tailings Fluid (based on Chloride)	Total Tailings Fluid Pumped (thousands of liters)
2A	16,404	98	16,075
8	6,987	3	208
10A	7,392	5	371
13B	950	78	742
69	5,511	66	3,637
77	924	20	186
82	4,947	32	1,582
83	12,245	30	3,675
84	10,708	0	0
89	4,182	0	0
101	5,159	0	0
102	352	0	0
French Drain	20,617	16	3,301
Total	**96,378**	-	**29,777**

These overall figures (Table 3.1.1.2) indicate that over 131.5 million liters of tailings fluid and groundwater have been treated by evaporation at the L-Bar mill tailings site. Using an estimate of 35 million liters from the tailings fluid recovery alone, the amount of contaminants removed from the horizontal drain tailings fluid is presented in Table 3.1.1.7 below.

Table 3.1.1.7 Estimated Constituent Mass Removed from Horizontal Drains

Constituent	Concentration (mg/l)	Kg Removed
Chloride	752	26,320
Sulfate	39,400	1,379,000
Ammonia	702	24,570
Nitrate + Nitrite	0.79	28
Nickel	<4	--
Selenium	0.04	1.4
Antimony	<10	--
Bicarbonate	<5	--
Carbonate	<1	--
Calcium	551	19,285
Magnesium	1,120	39,200
Potassium	400	14,000
Sodium	1,500	52,500
Uranium	137.5	4,812.5
Silicon	80	2,800
Iron (total)	4,390	153,650
Fluoride	<0.1	--
Arsenic	0.57	20
Barium	<0.01	
Cadmium	0.412	14
Chromium	3.06	107
Lead	0.65	23
Manganese	80.3	2,811

Table 3.1.1.7 Estimated Constituent Mass Removed from Horizontal Drains (Cont.)

Constituent	Concentration (mg/l)	Kg Removed
Mercury	<0.0002	--
Molybdenum	<0.05	--
Vanadium	182	6,370
Zinc	15	525
Silver	0.05	2
Beryilium	0.508	18
Cobalt	2.31	81
Copper	8.2	287
Thallium	1.9	67
Tin	<2	--
Aluminum	3,370	117,950
	Total Kilograms Removed	**1,844,468**
Constituent	**Concentration (pCi/l)**	**pCi Removed**
Gross Alpha (pCi)	318000	1.113 E 13
Gross Beta (pCi)	98900	3.462 E 12
Radium 226 (pCi)	2980	1.043 E 11
Radium 228 (pCi)	48.9	1.712 E 9
Thorium 230 (pCi)	165000	5.775 E 12

3.2 Groundwater Modeling Results

Contaminant transport studies have been performed through two separate but integrated approaches. The geochemical interactions of the tailings fluid with the native geologic materials has been studied to assess the affects of natural chemical interactions between the tailings fluid and the subsurface geologic materials (Appendix A, DE&S, 1998). This modeling provides information on contaminant source terms for the flow and transport simulations and helps support final predicted contaminant concentrations over the life of the facility. Flow and

transport was also modeled by Balleau Groundwater Inc. (Appendix B, BGW, 1997) to determine the effects of dispersion, dilution, advection, and unsaturated flow on contaminant migration downgradient from the site over the life of the facility. The predicted concentrations were expressed as a series of percent of source term isopleths in this study, without consideration of geochemical retardation effects. These isopleths were plotted in relation to the point of compliance (POC) wells, the proposed point of exposure (POE), and the proposed final property boundary. Finally, the model was re-run to include the effects of both chemical and physical processes on contaminant transport.

3.2.1 Source Term Characterization -- Geochemical Results

Characterization of the contaminant source (tailings fluid) and its extent provides the source term for contaminant transport assessments. The tailings fluid chemistry of May 1996 is provided in Table 3 2.1.1. This data has been used because this is the last time the tailings fluid was analyzed before closing the horizontal drains due to lack of production. This is also consistent with previous results.

Table 3.2.1.1 Tailings Fluid Analyses from May 1996

Constituent	Units	Results
Chloride	(mg/L)	752
Sulfate	(mg/L)	39400
PH	(pH Units)	2.03
Specific Conductance	(µhmos/cm)	32400
Ammonia	(mg/L)	702
Nitrate + Nitrite	(mg/L)	0.79
Nickel	(mg/L)	<4
Selenium	(mg/L)	0.04
Antimony	(mg/L)	<10
Bicarbonate	(mg/L)	<5
Carbonate	(mg/L)	<1
Calcium	(mg/L)	551
Magnesium	(mg/L)	1120
Potassium	(mg/L)	400
Sodium	(mg/L)	1500
TDS	(mg/L)	55100
TSS	(mg/L)	91
Uranium	(mg/L)	137.5
Radium 226	(pCi/L)	2980
Radium 228	(pCi/L)	48.9
Thorium 230	(pCi/L)	165000
Silicon	(mg/L)	80
Silicon Dioxide	(mg/L)	141
Iron (total)	(mg/L)	4390
Ferrous Iron	(mg/L)	180000
Ferric Iron	(mg/L)	<10000
Fluoride	(mg/L)	<0.1
Arsenic	(mg/L)	0.57
Barium	(mg/L)	<0.01
Cadmium	(mg/L)	0.412
Chromium	(mg/L)	3.06
Lead	(mg/L)	0.65
Manganese	(mg/L)	80.3
Mercury	(mg/L)	<0.0002
Molybdenum	(mg/L)	<0.05
Vanadium	(mg/L)	182

Table 3.2.1.1 Tailings Fluid Analyses from May 1996 (Cont.)

Constituent	Units	Results
Zinc	(mg/L)	15
Silver	(mg/L)	0.05
Beryllium	(mg/L)	0.508
Cobalt	(mg/L)	2.31
Copper	(mg/L)	8.2
Thallium	(mg/L)	1.9
Tin	(mg/L)	<2
Aluminum	(mg/L)	3370
Gross Alpha	(pCi/L)	318000
Gross Beta	(pCi/L)	98900

* Analysis by Graphite Furnace

The source concentrations for contaminant transport evaluations have been calculated from the results of the geochemical study from historical field data, and/or from tailings fluid concentration, as appropriate. Source concentrations for individual constituents are shown in Table 3.2.1.2.

Table 3.2.1.2 Source Concentrations

Constituent	Concentration	Basis
Cl	750 mg/L	tailings concentration
Ni	2.5 mg/L	tailings concentration
NO_3	285 mg/L	field data, NH_4 oxidation
pH	6.5	carbonate buffered
Ra-226	3,000 pCi/L	tailings concentration
Ra-228	50 pCi/L	tailings concentration
Sb	< 0.05 mg/L	solubility limited
Se	6 mg/L	tailings concentration
SO_4	10,000 mg/L	field data, model prediction
Th-230	165,000 pCi/L	tailings concentration
U	13 mg/L	solubility limited

3.2.2 Flow and Transport Studies

A significant effort has been focused on predictive modeling of site groundwater flow and transport to assess future potential contaminant impacts on the environment. The results of that effort are presented in Appendix B.

The model was calibrated to reproduce pre-tailings and historical water levels and the movement of non-reactive constituents. The pre-tailings condition is considered to be at steady state flow. The potentiometric surface for the pre-tailings condition was presented previously in Figure 2.4.2. As seen from this figure, a groundwater divide occurs near the northeast portion of the property, with predominant flow paths toward the southwest on the west side of the site, and toward the southeast on the east side of the site. The steady state model results indicated that the simulated water level matches the observed water levels at a distance from the tailings, as shown in Table 4 of Appendix B. The steady state flow analysis indicates that flow through the hydrologic system is about 1.4 gpm entering through the north and northwest boundaries. The southwest area discharges about 0.7 gpm and the southeast area discharges about 0.48 gpm at steady state.

The model was calibrated against historical 1977 to 1996 water level observations inside the tailings, below the tailings in the FTH, and west and east of the tailings in the alluvium and the FTH. The observed 1996 water levels from about 80 wells were compared to the simulated water levels in Appendix B, Figure 15. The results of the comparison have a correlation coefficient of 0.95. Water-level hydrographs for seven selected piezometers inside the tailings and wells in the FTH are illustrated in Appendix B, Figures 16 through 22. The results indicate that the model is capable of reproducing the hydrologic conditions inside, below, and around the tailings area. The simulation of the advective and dispersive movement of non-reactive constituents was calibrated against observed chloride concentrations. Appendix B, Figures 24 and 25 show that the simulated chloride concentration is comparable to the observed concentration spatially and over time.

A series of predictive concentration isopleths for 200 years is presented in Figure 3.2.1. The predicted concentrations are not contaminant dependent in these figures, and assume transport in the absence of any geochemical retardation effects such as would be expected for chloride. The concentration isopleths should be interpreted as fractions of the source term concentrations for

individual constituents. To determine the contaminant concentration at the 0.01 isopleth, multiply the source concentration by 0.01 to calculate the concentration for that constituent over time. This figure demonstrates that the one percent (0.01) source concentration will remain within the proposed property boundary to the east or west over the next 200 years, even excluding geochemical effects. Thus, no impacts are anticipated outside the property boundary.

Source concentrations for state constituents have been adopted from the highest observed concentrations of all the wells onsite. The calculation of actual percent concentrations is unnecessary since none of the constituents will migrate beyond site boundaries over the next 200 years.

3.3 Site Security and Groundwater Protection

At the close of SOHIO's negotiations with the Cebolleta Land Grant regarding final disposition of the L-Bar property during the mid-1980's, it was the Land Grant's desire to retain as much of the site for beneficial use as possible. The current use for peripheral land in the vicinity of the site is livestock grazing. SOHIO retained an option for additional property rights up to 200 acres beyond the present fence line. SOHIO is currently exercising that option to encompass the area of the southwest arroyo extending southwest to MW-100. This ensures that all potentially impacted areas of the site will be contained within the property boundary, even over 200 years or longer. Figure 3.3.1 presents the proposed property boundary for long-term custody. The long-term custody by the Department of Energy precludes unauthorized access to the site and prevents use of site groundwater. SOHIO considers the technical infeasibility of groundwater remediation, the natural attenuation properties of the site hydrogeology, and the property custody by the federal government to be as protective of the environment as is feasible.

Additionally, surface discharge of groundwater is not anticipated at any time at the site. Discharge to the west and east of the basin (the two groundwater flow directions) reaches the subsurface alluvial soils and is evapotranspirated in these subsurface soils. Groundwater flow velocity in the First Tres Hermanos is less than one foot/year, precluding adequate flow volume to create surface discharge. The limited drainage area also prevents any significant surface recharge, and the clay cover on the tailings cell has a net negative evapotranspiration potential of over three times the annual site precipitation. Even the nearly level cover cannot function as a recharge feature.

Drainage provisions for surface water runoff also protect the tailings and the cover. The north and south diversion channels provide adequate protection from surface flows related to the Probable Maximum Precipitation (PMP) event and resultant Probable Maximum Flood (PMF) at the site. This surface diversion system ensures that the tailings basin will maintain structural integrity over the life of the facility.

All these combined conditions can be thought of as a beneficial and effective form of natural attenuation. There is no surface discharge of groundwater and all precipitated solids and contaminants in the subsurface will be bound up at the evapotranspiration fringe within the site boundaries. Therefore the site presents no long-term threat to human health or the environment.

3.4 Continued CAP Cost/Benefit Analysis

The current CAP expenditures have resulted in restoring the environmental integrity of both surface features and groundwater at the site. For surface features, this includes mill demolition and onsite disposal, channel excavation, windblown tailings collection and disposal, and placement of the interim radon barrier or cover. For groundwater, it includes operation of the pumpback system, collection of direct tailings fluid, and treatment of both by onsite evaporation. A summary of costs to date for CAP implementation is provided in Table 3.4.1 below.

Table 3.4.1 CAP Costs

Expense Type	Year Incurred	Annual Cost	Cost-to-Date
Mill Demolition	1986-87	N/A	$1,500,000
Interim Remediation Construction	1989-90	N/A	$8,300,000
Ongoing Maintenance of Pumpback System and General Site	Annually Since 1989	$100,000-$150,000	$1,100,000
Semi-Annual Sampling, Analysis, and Reporting	Annually Since 1990	$75,000- $100,000	$750,000
		Subtotal to Date	$11,650,000

The benefits of continued operation of the active remediation system at the L-Bar site are negligible. Over 75 percent of the 1990 tailings fluid has drained from the site or been lost to evaporation. Predictive modeling demonstrates that there will be no offsite impacts for at least 200 years, even without active pumping. The natural background water quality is of marginal quality, and the subsurface geologic materials provide natural acid buffering capacity and low flow transport of contaminants. Based on a cost/benefit analysis, active remediation is not warranted at the L-Bar site.

4.0 DEMONSTRATION OF TECHNICAL ACHIEVABILITY

The contaminants that regularly exceed state groundwater quality standards are chloride, sulfate, nitrate, uranium, and selenium. However, these exceedances are expected to remain within the site boundaries and within federal control for the reasonably foreseeable future or at least 200 years. The L-Bar site corrective actions to date and favorable natural conditions demonstrate that the site has experienced minimal environmental impact and modeling of future groundwater flow and transport predicts that groundwater contamination will remain within the site boundaries. Therefore, the site presents no present or future threat to human health or the environment. The Alternative Abatement Standards for the site will bring the site into compliance with state requirements.

4.1 Proposed Alternative Abatement Standards

An Alternative Concentration Limit application for the L-Bar site has been submitted to the NRC requesting new regulatory limits for uranium and selenium. However, additional constituents must be addressed to bring the site into compliance with state standards. Site water quality parameters have historically exceeded, and will continue to exceed, state drinking water standards for chloride, sulfate, nitrate, uranium, and selenium. However, it is technically infeasible and not practicable from a cost/benefit basis to continue to actively remediate the site. Section 4.2 presents a natural attenuation explanation for why additional active remediation is not necessary at the L-Bar site.

Based on these conditions, SOHIO proposes the alternative abatement standard values for these constituents as presented in Table 4.1.1. These proposed values are taken from the highest observed concentrations for each constituent since 1990 as measured from all the wells on site, and thus represent a worst case condition. Since the tailings fluid is declining as a contaminant source term, future contaminant concentrations are expected to be less than historic levels. These conservative requested levels are technically achievable without further active remediation and will bring the site into compliance for the foreseeable future.

Table 4.1.1 Proposed Alternative Abatement Standards

Constituent	Drinking Water Standard (mg/l)	Proposed Alternative Abatement Standard (mg/l)
Chloride	250	1000
Sulfate	600	15,000
Nitrate	10	1100
TDS	1000	15,000

4.2 Natural Attenuation

The L-Bar site is an excellent candidate for the natural attenuation approach for numerous reasons. Extensive site studies and modeling efforts have indicated that only 248 million drainable liters of tailings fluid remained in the tailings cell in 1996 compared to 840 million liters drainable volume following 1990 reclamation work. As noted in the previously submitted groundwater report (INTERA, 1996), a large portion of the tailings fluid that has drained from the tailings cell is trapped in the unsaturated zone below the tailings and above the FTH aquifer. This unsaturated strata is comprised of materials that contain a large percentage of calcite, which is a very effective neutralizing agent of acidic waters such as the tailings fluid. Due to this neutralization capacity, very little low pH contaminated fluid reaches the saturated zone below the tailings pile. Geochemical studies of the site (DE&S, 1998, Appendix A) have demonstrated that the calcite content of the aquifer material and overlying strata is more than adequate to neutralize the remaining drainable tailings fluid and prevent the migration of a pH front more than a very short distance from the base of the tailings.

The First Tres Hermanos aquifer is also a very low permeability formation with flows of less than one foot per year under natural gradient conditions (BGW, 1996, Appendix B). The tailings are predicted to fully drain within the next 20 years, returning the hydrogeologic system to its pre-mine flow conditions. The tailings pile existed in a saturated state from 1976 to 1990, with ambient hydraulic head perched approximately 65 feet above the groundwater, yet the groundwater beneath the tailings pile is only slightly impacted by tailings fluid. The results of the groundwater analyses from MW-106 through MW-109 (wells drilled through the tailings into the FTH immediately beneath the pile) show that tailings-derived constituents occur primarily in MW-108 and MW-109 in the form of elevated chloride, nitrate, total dissolved solids (TDS),

sulfate, calcium, magnesium, uranium and radium 226. Table 4.2.1 presents the results of the analyses from these wells compared to the background well MW-29A and the full strength tailings fluid from the collection sump.

Table 4.2.1 FTH Water Chemistry Beneath the Tailings Basin

Analyte	MW-29A	MW-106	MW-107	MW-108	MW-109	Tailings Sump
Chloride (mg/L)	106	117	120	133	349	650
Conductivity (µmhos/cm)	6960	6620	5670	11500	8120	92100*
Fluoride (mg/L)	1.2	0.5	1.3	0.2	0.5	40
Ammonia (NH3) (mg/L)	1.86	1.62	1.71	0.1	6.56	652
Nitrogen, Nitrate (mg/L) Nitrogen, Nitrite, combined	0.07	0.15	<0.05	44.7	4.24	8.2
pH	7.94	7.25	7.62	6.96	7.04	2.0
TDS (mg/L)	5430	5690	4360	13200	7640	57800
TSS (mg/L)	<4.0	<4.0	5.0	34.0	5.0	<4.0
Sulfate (mg/L)	3290	3450	2600	8700	4320	41800
Aluminum (mg/L)	<0.05	<0.05	<0.05	<0.05	<0.05	4030
Antimony (mg/L)	<0.1	<0.1	<0.1	<0.1	<0.1	<2.0
Cyanide (mg/L)	<0.02	<0.02	<0.02	<0.02	<0.02	NM
Manganese (mg/L)	0.03	0.23	0.02	0.12	1.01	80.2
Molybdenum (mg/L)	<0.05	<0.05	<0.05	0.14	<0.05	<1.0
Nickel (mg/L)	<0.04	<0.04	<0.04	0.04	<0.04	2.3
Potassium (mg/L)	5	12	5	26	18	500
Silicon (mg/L)	5	5.4	4.7	3.7	4.3	65
Silver (mg/L)	0.01	<0.01	<0.01	<0.01	0.02	<0.2
Sodium (mg/L)	1530	1270	1090	892	1450	1740
Thallium (mg/L)	<0.1	<0.1	<0.1	0.4	<0.1	<2.0
Tin (mg/L)	<0.05	<0.05	<0.05	0.09	0.09	<1.0

Table 4.2.1 FTH Water Chemistry Beneath the Tailings Basin (Cont.)

Analyte	MW-29A	MW-106	MW-107	MW-108	MW-109	Tailings Sump
Vanadium (mg/L)	<0.05	<0.05	<0.05	<0.05	<0.05	175
Zinc (mg/L)	0.12	0.2	0.02	0.02	0.04	15.2
Arsenic (mg/L)	<0.05	<0.05	<0.05	<0.05	<0.05	<1.0
Barium (mg/L)	<0.01	0.02	<0.01	0.01	0.02	<0.2
Beryllium (mg/L)	<0.005	<0.005	<0.005	<0.005	<0.005	0.6
Cadmium (mg/L)	<0.005	<0.005	<0.005	<0.005	<0.005	0.1
Calcium (mg/L)	62.8	263	76.7	387	409	457
Chromium (mg/L)	0.02	0.02	0.03	0.02	<0.01	3.1
Cobalt(mg/L)	<0.03	<0.03	<0.03	<0.03	<0.03	2.7
Copper (mg/L)	0.01	<0.01	<0.01	0.03	<0.01	8.4
Iron (mg/L)	0.03	<0.03	<0.03	0.1	2.53	4820
Lead (mg/L)	<0.05	<0.05	<0.05	<0.05	<0.05	<1.0
Magnesium (mg/L)	25.1	178	47.2	1690	344	1090
Selenium (mg/L)	<0.002	<0.002	<0.002	<0.002	<0.002	0.073
Uranium (pCi/l)	1.6	14.3	1.0	20.3	316	142
Radium 226 (pCi/l)	3.5	35.3	2.8	14.7	90.7	207
Radium 228 (pCi/l)	4.2	3.2	1.9	5.6	1.4	3.6
Thorium 230 (pCi/l)	<0.3	<0.4	<0.3	<0.7	2.0	162000

* Field Conductivity converted to 25 deg. C

NM - Not Measured

There is also the possibility that groundwater from these wells may be impacted by vertical seepage down the wellbore or cross contamination during drilling. If this is the case, even these concentrations may not be representative of groundwater. It is also possible that the well chemistry and presence of a groundwater mound in this vicinity are a result of seepage from the tailings fluid evaporation ponds. In either case, these are short-lived impacts, since the wells will be properly abandoned during final reclamation and the evaporation ponds will no longer function as a fluid recharge source when the CAP is discontinued.

SOHIO proposes to discontinue pumping the extraction wells at the site and let natural flow and transport resume at the site. The extensive geochemical and physical flow modeling at the site demonstrates that the subsurface contaminants will remain within the site boundaries for at least the next 200 years and that the long-term custodial care arrangement with the federal government will protect human health and the environment for the foreseeable future.

As mentioned previously, the underlying formation materials beneath the pile and within the first Tres Hermanos have a very large amount of acid buffering capacity due to their high calcite content (DE&S, 1998, Appendix B). This means that pH-sensitive constituents that remain soluble in the lower pH range but precipitate out at higher pH will remain bound up in the vadose zone because the acid front is predicted to dissipate before reaching the groundwater. In fact, the tailings fluid pH immediately beneath the pile is neutral in the pH 7 range, indicating that the pH front has not reached groundwater. Since the pile acts as a declining fluid source over time, less and less tailings fluid is draining from the pile per unit time. For the more stable constituents such as chloride and sulfate, the naturally low flows within the FTH retard contaminant migration. In such a low flow scenario, dispersion plays a significant role and results in effective dilution of the contaminants throughout the aquifer matrix. This further reduces overall impacts to the aquifer. Finally, the site will be monitored in the future in accordance with the NRC Longterm Surveillance Plan to assure that the site remains in regulatory compliance.

5.0 CONCLUSIONS

The L-bar uranium mill tailings site is operated by SOHIO Western Mining Company. SOHIO has spent over $11 million dollars toward reclamation at the site and anticipates an additional $3 to $5 million in final closure construction costs to ready the site for long-term custody by the DOE.

The site groundwater Corrective Action Program (CAP) consists of a groundwater pumpback system and a direct tailings fluid collection system. Both effluents are treated on-site by evaporation. Since 1990, the groundwater pumpback system has collected and treated 96.5 million liters of groundwater. The horizontal drain system was discontinued in 1996, but collected 42 million liters of pure tailings fluid, representing approximately 1.8 million kilograms of contaminants. However, flows in the horizontal drains had diminished to a trickle by 1996, thus terminating their effectiveness.

The fluid collected and treated by evaporation is only a small amount of the tailings fluid that has seeped from the tailings pile. While approximately 35 million liters of tailings fluid has been recovered, over the period 1990-1996, approximately 594 million liters of fluid has been removed from the tailings basin through vertical seepage and evapotranspiration. Yet, groundwater from the pumpback system shows negligible tailings fluid impacts. Even the groundwater immediately beneath the pile shows relatively little impact, especially with respect to hazardous constituents.

The effectiveness of the CAP is diminishing with time. Since the horizontal drains have ceased to flow, the most effective means of tailings fluid source removal has ended. Pumping rates and flows in the pumpback system show a consistent reducing trend, an indication of declining tailings inflow to the groundwater system. Cost/benefit analyses of the effects of continued operation of the CAP show declining and minimal economic and environmental justification.

Finally, the natural properties of the conditions at the site are an ideal set of conditions for natural attenuation of groundwater contamination. Much of the tailings fluid is trapped as residual moisture in the unsaturated zone above the water table and favorable geochemical properties of the geologic strata prevent migration of the pH front. In fact, many of the chemical constituents precipitate or adsorb to the geologic strata and are, in effect, removed permanently

from the hydrogeologic system. The background water quality is marginal to poor for consumption in its unaffected state.

The low permeability of the aquifer prevents migration of the contaminants offsite. Bedding attitudes and erosional features cause First Tres Hermanos discharge to be confined to subsurface evapotranspiration within the arroyos east and west of the site, and no surface discharge occurs within one mile of the site. No future surface discharge is anticipated, especially since the tailings pond will continue to discharge less and less fluid with time.

All these conditions support granting the proposed alternative abatement standards at the SOHIO L-Bar Mill Tailings site. The uniqueness of federal custody in perpetuity also provides a strong case for valid institutional control. Granting these abatement standards will put the site in position for final closure, which is ultimately the best path to protection of human health and the environment.

6.0 REFERENCES

Balleau Groundwater Inc., 1997. Projected Long-Term Flow and Quality of Ground Water at the L-Bar, New Mexico, Uranium Site, prepared for Kennecott Energy Company.

American Groundwater Consultants, Inc., 1979. Milestone Report on Monitoring Activities at SOHIO L-Bar Property, Valencia County, New Mexico.

Duke Engineering and Services, 1990-1997. Review Reports: L-Bar Groundwater Corrective Action Program, prepared for SOHIO Western Mining Company.

Duke Engineering & Services, 1998. Geochemical Controls on Contaminant Migration at the L-Bar Uranium Mill Tailings Pile, prepared for SOHIO Western Mining Company.

INTERA Technologies Inc., 1989. L-Bar Uranium Mine Reclamation and Closure Plan, prepared for BP America.

INTERA Inc., 1996. Final Report: Hydrogeology Investigation of the L-Bar Uranium Mill Tailings Pile, Cibola County, New Mexico, prepared for Kennecott Corporation.

New Mexico Water Quality Control Commission, "New Mexico Water Quality Control Commission Regulations, November 15, 1996", Title 20 Environmental Protection, Chapter 6, Groundwater Quality, Part 2, Ground and Surface Water Protection.

SOHIO, 1980. Environmental Report: L-Bar Uranium Project Valencia County, New Mexico, in Support of Radioactive Material License Renewal Application NM-SOH-ML.

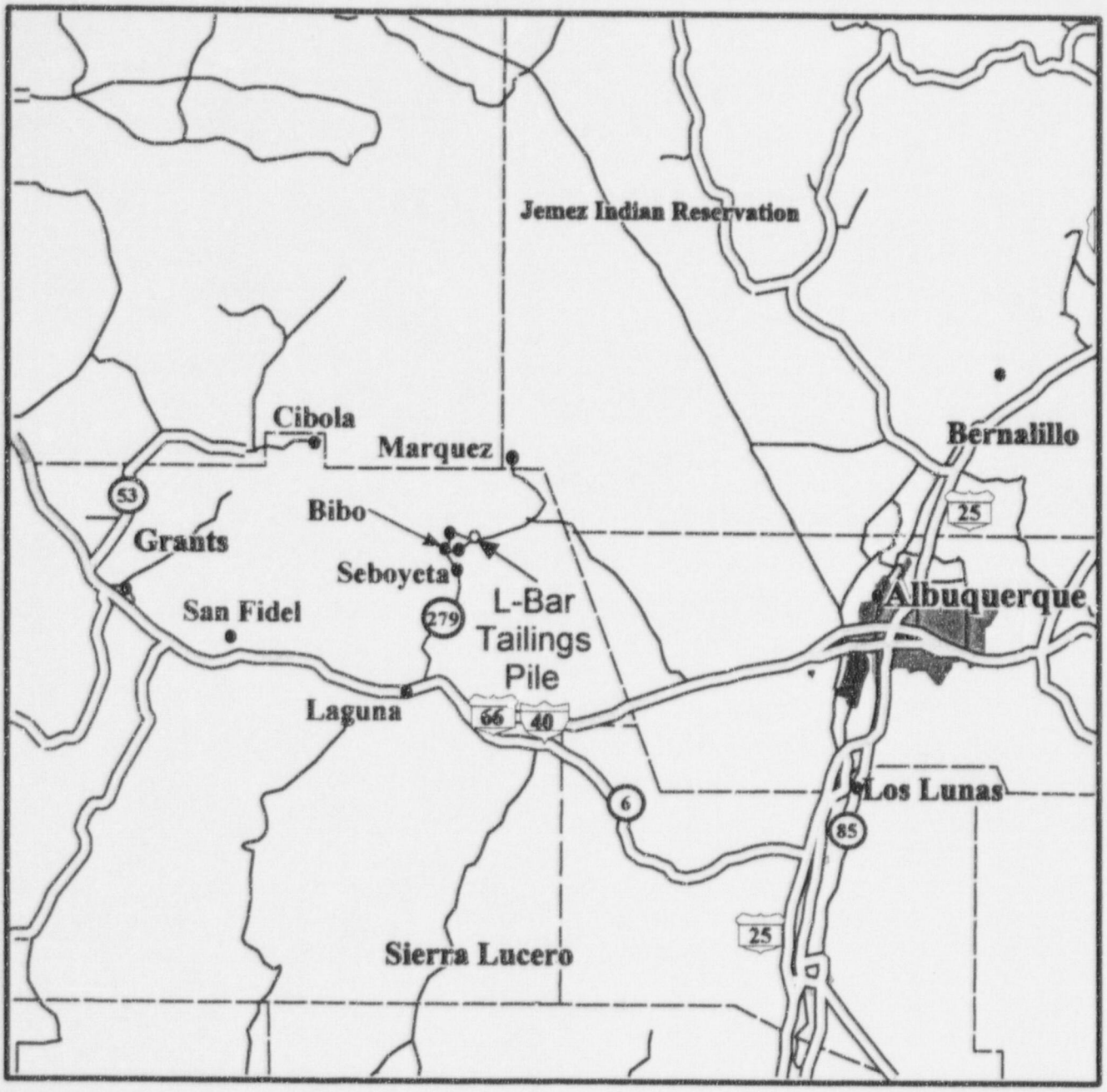

DATE: 10/14/98

REF: 00137.0C

FILE: LOCMAP2.XAR

L-BAR SITE LOCATION MAP

Duke Engineering & Services
A Duke Energy Company

NMED Alternative Abatement Standards

Figure 1.1

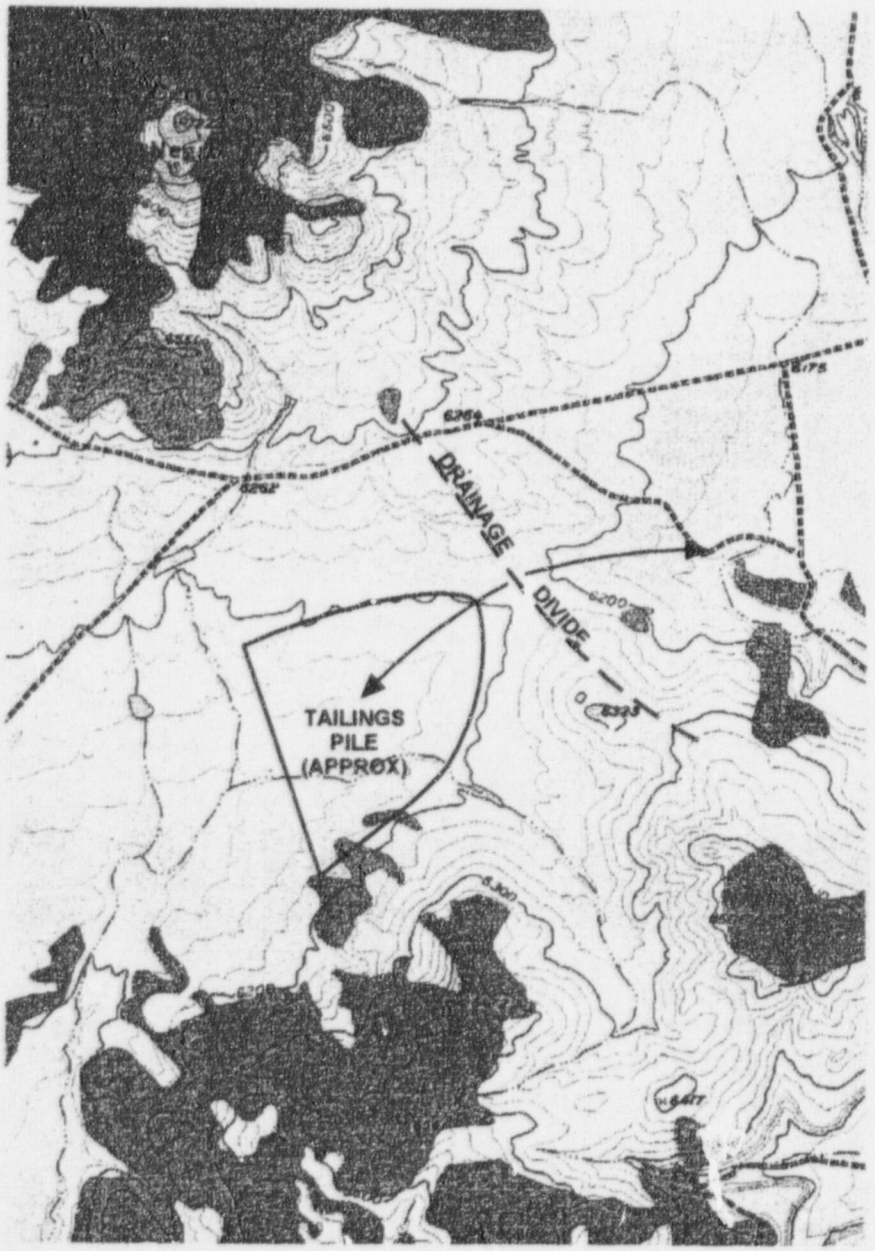

0 1000 2000

Approximate Scale
in Feet
1" = 2000'

SOURCE: USGS 1:24000 QUAD, MOQUINO, NEW MEXICO 1957.

DATE: 10/14/98	SITE TOPOGRAPHY & DRAINAGE DIVIDE	
REF: 00137.00.0001.04.00000		
FILE: TOPO.XAR		
Duke Engineering & Services, A Duke Energy Company	NMED Alternative Abatement Standards	Figure 2.1.1

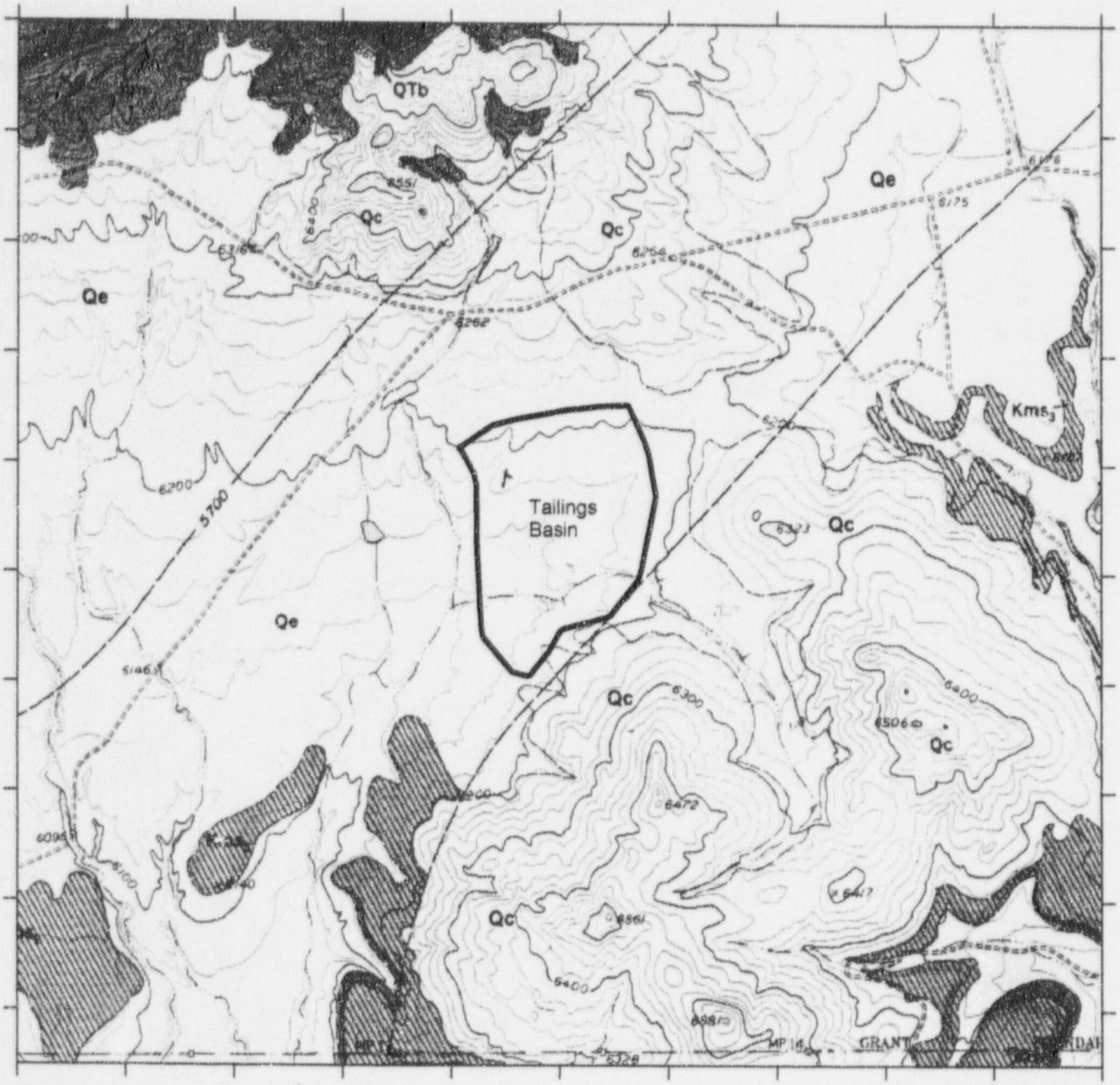

Scale: 1 inch = 2000 feet approx.

Qe	Eolian and alluvial deposits	Km	Mancos Shale; gray, friable shale with sparse beds of yellowish-gray friable sandstone. Main body about 750 feet thick.
Qc	Colluvial Deposits	Kmt3	First Tres Hermanos: grayish-orange to yellow gray, fine to medium grained, well-cemented sandstone; grades downward to siltstone and shale. About 60 feet thick.
	Gallup Sandstone		Basalt undifferentiated

Source: Geologic Map of Moquino Quadrangle, US Geological Survey, 1963

Date: 10/15/98 Produced By: KJS Checked By: KRT File Name: SITEGEOL.SRF	**Site Geology**	**FIGURE 2.2.1**
	KENNECOTT CORPORATION / L-BAR MINE **NMED Alternative Abatement Standards**	Duke Engineering & Services A Duke Energy Company

GENERALIZED STRATIGRAPHIC COLUMN OF THE L-BAR MINE AREA

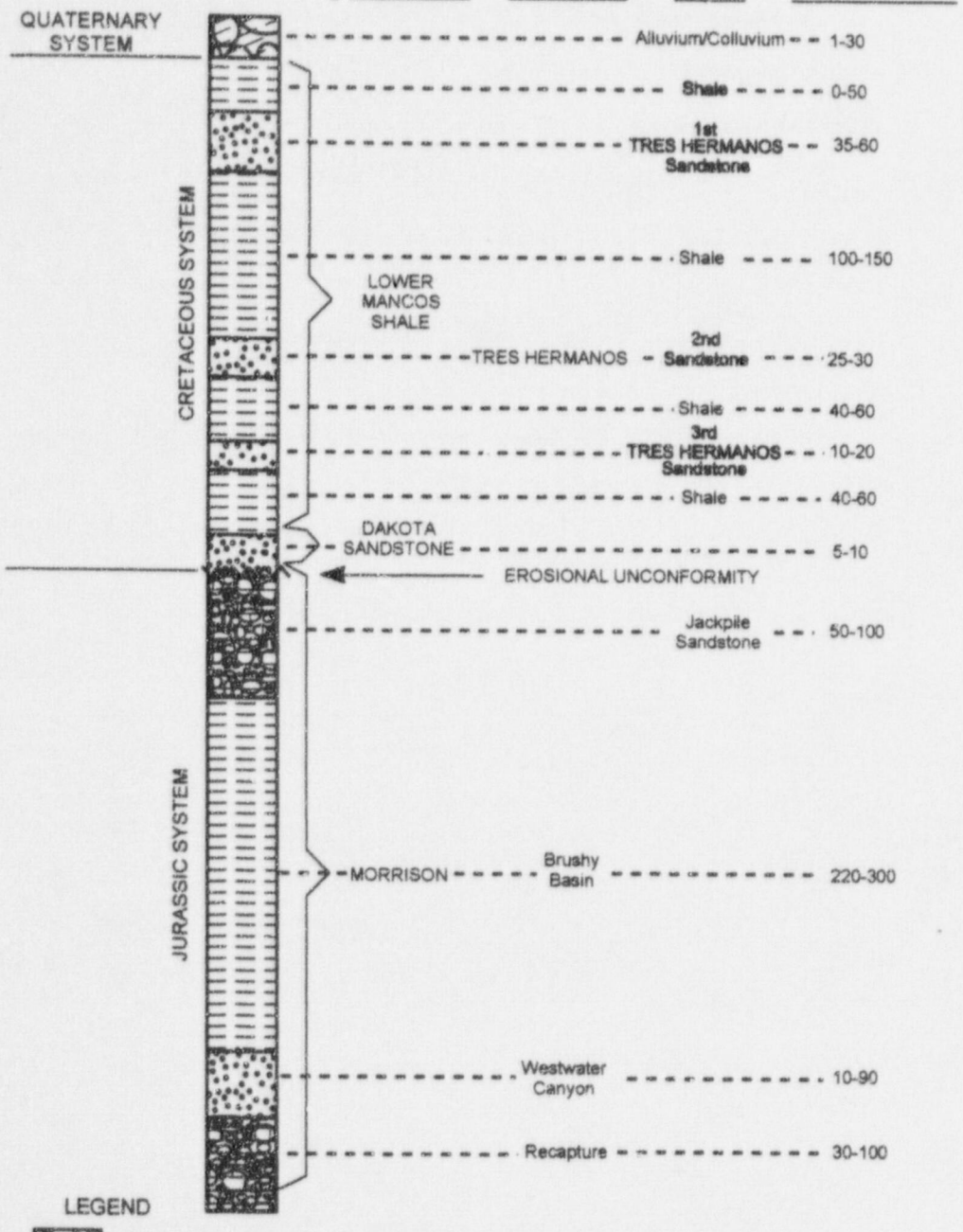

DATE: 10/14/98	L-BAR SITE STRATIGRAPHY	
REF: 00137.00.0001.04.00000		
FILE: lbarstra.XAR		
Duke Engineering & Services, A Duke Energy Company	NMED Alternative Abatement Standards	Figure 2.2.2

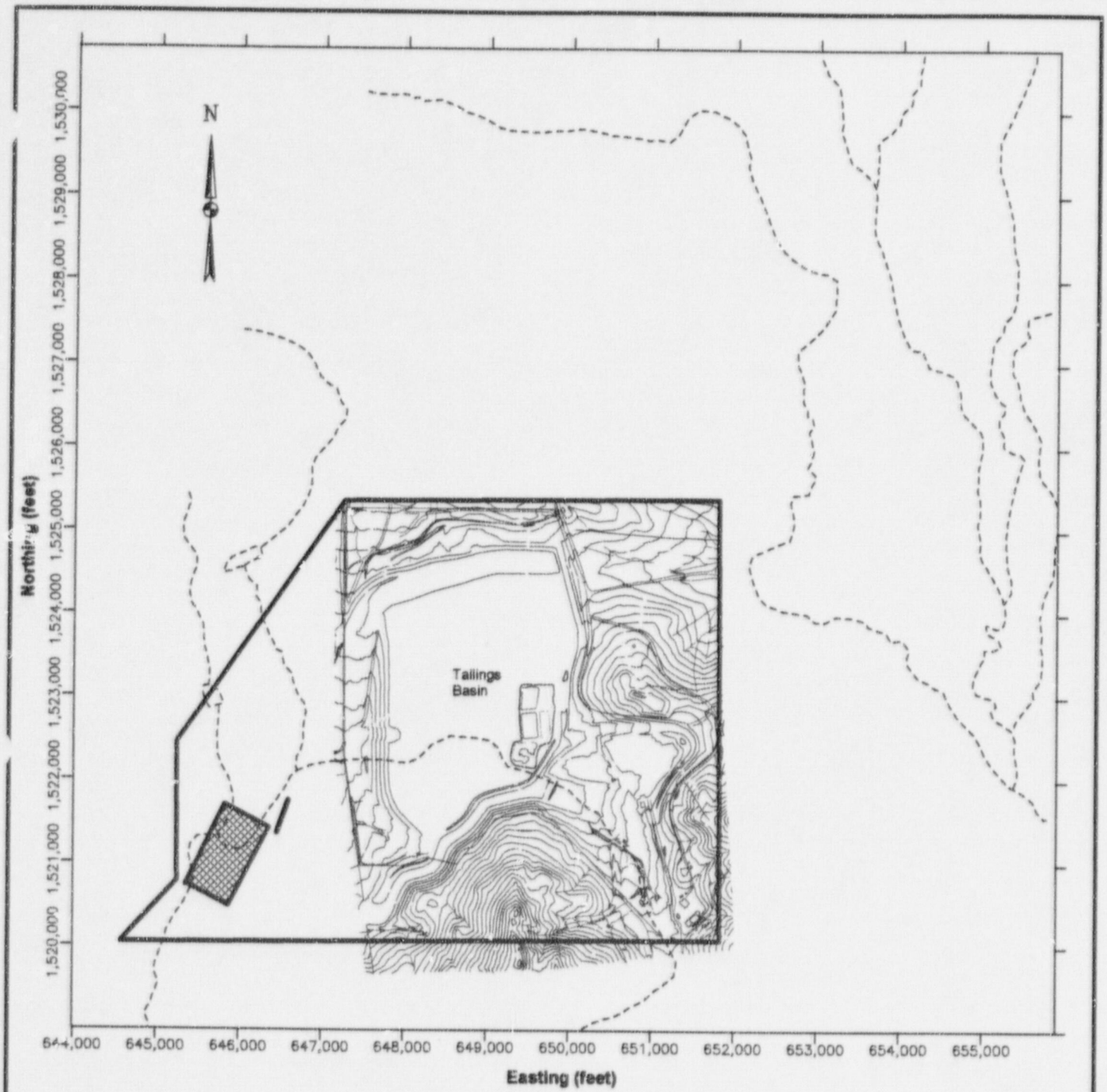

Note: Figure derived from plot by Baileau Groundwater Inc.

Date: 10/15/98 Produced By: KJS Checked By: KRT File Name: EVAPFIG.SRF	**Primary Evapotranspiration Area** **KENNECOTT CORPORATION / L-BAR MINE** **NMED Alternative Abatement Standards**	**FIGURE 2.4.1** Duke Engineering & Services A Duke Energy Company

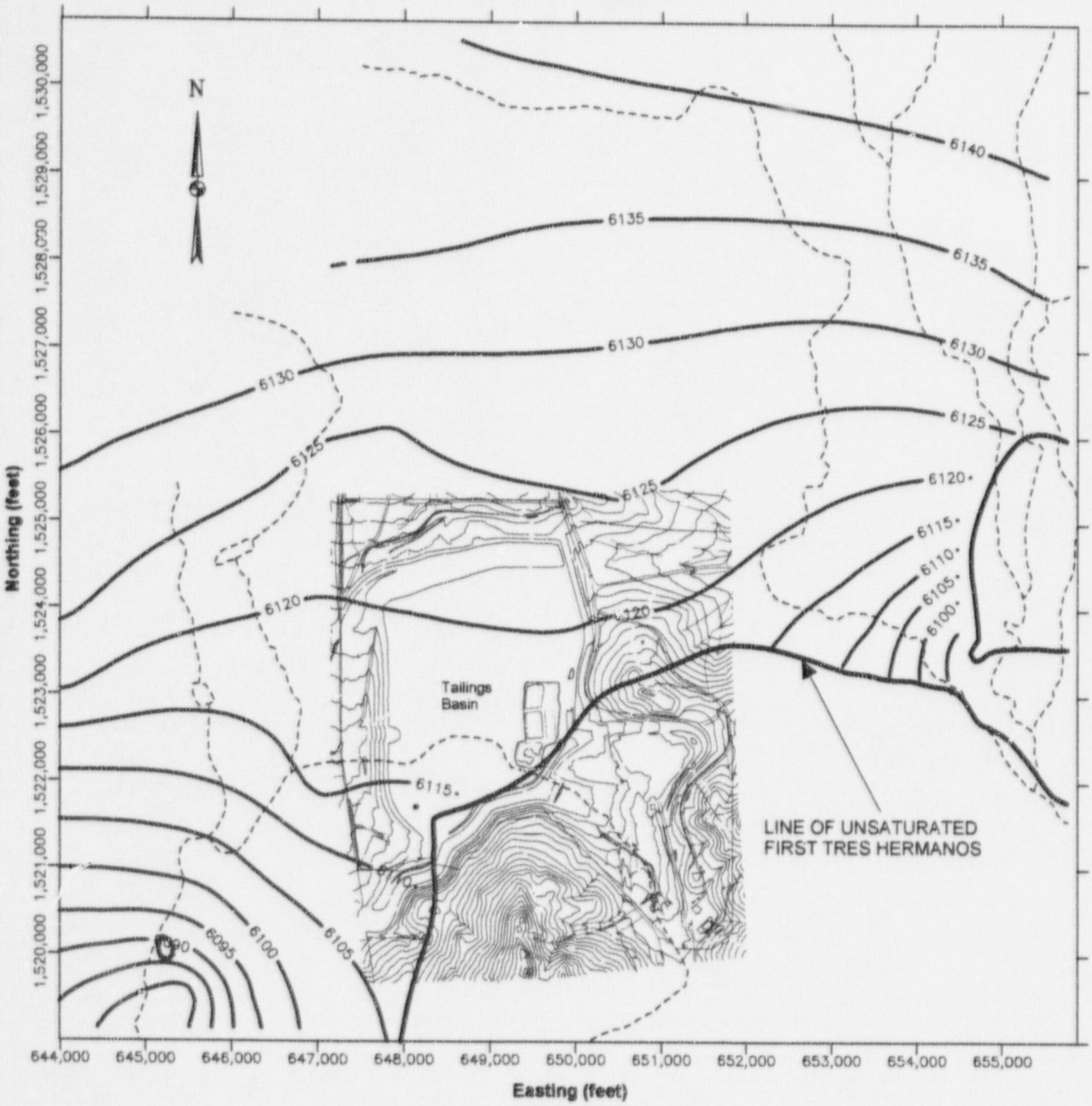

Legend

5 FT. CONTOUR INTERVAL

Note: Figure derived from plot by Balleau Groundwater Inc.

Date: 0/15/98 roduced By: KJS Checked By: KRT File Name: PRETAIL.SRF	**Pre-Tailings Simulated Steady-State Piezometric Contours**	**FIGURE 2.4.2**
	KENNECOTT CORPORATION / L-BAR MINE **NMED Alternativ. Abatement Standards**	Duke Engineering & Services A Duke Energy Company

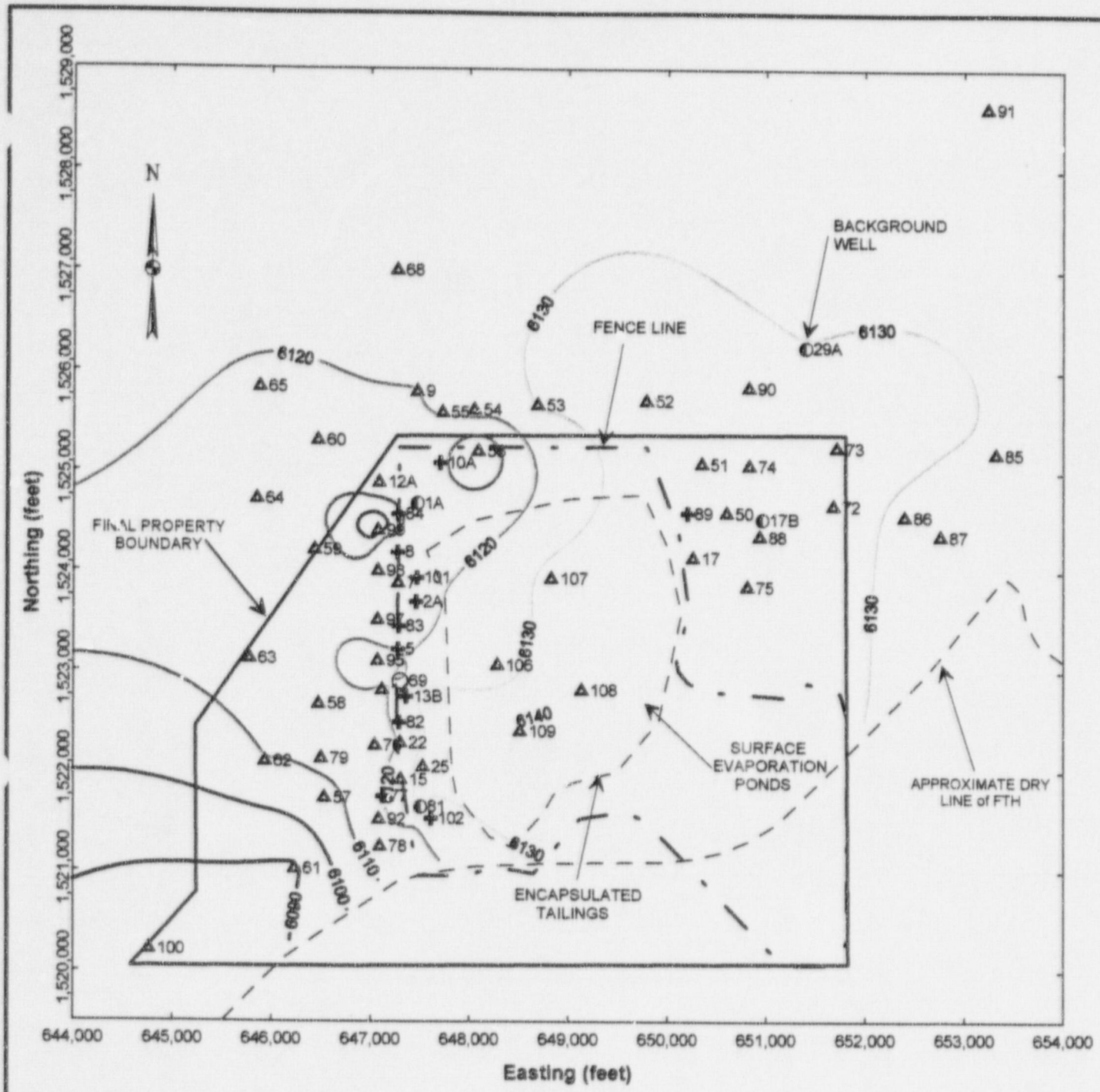

Note:
All contour lines have been extrapolated from known points at measured wells to fill the mapped area. The kriging model used provides an estimation of the potentiometric surface which is most accurate in the immediate vicinity of the tailings pile.

Legend
- Point of Compliance (POC) Wells
- CAP Monitoring Wells
- Pumpback Wells
- Pumpback and POC Well
- 10 ft. Contour Interval (Feet AMSL)

Date: 10/15/96 Produced By: KJS Checked By: KRT File Name: WLEV-96.SRF	**Potentiometric Surface Dec. 1996**	**FIGURE 2.4.3**
	KENNECOTT CORPORATION / L-BAR MINE **NMED Alternative Abatement Standards**	Duke Engineering & Services A Duke Energy Company

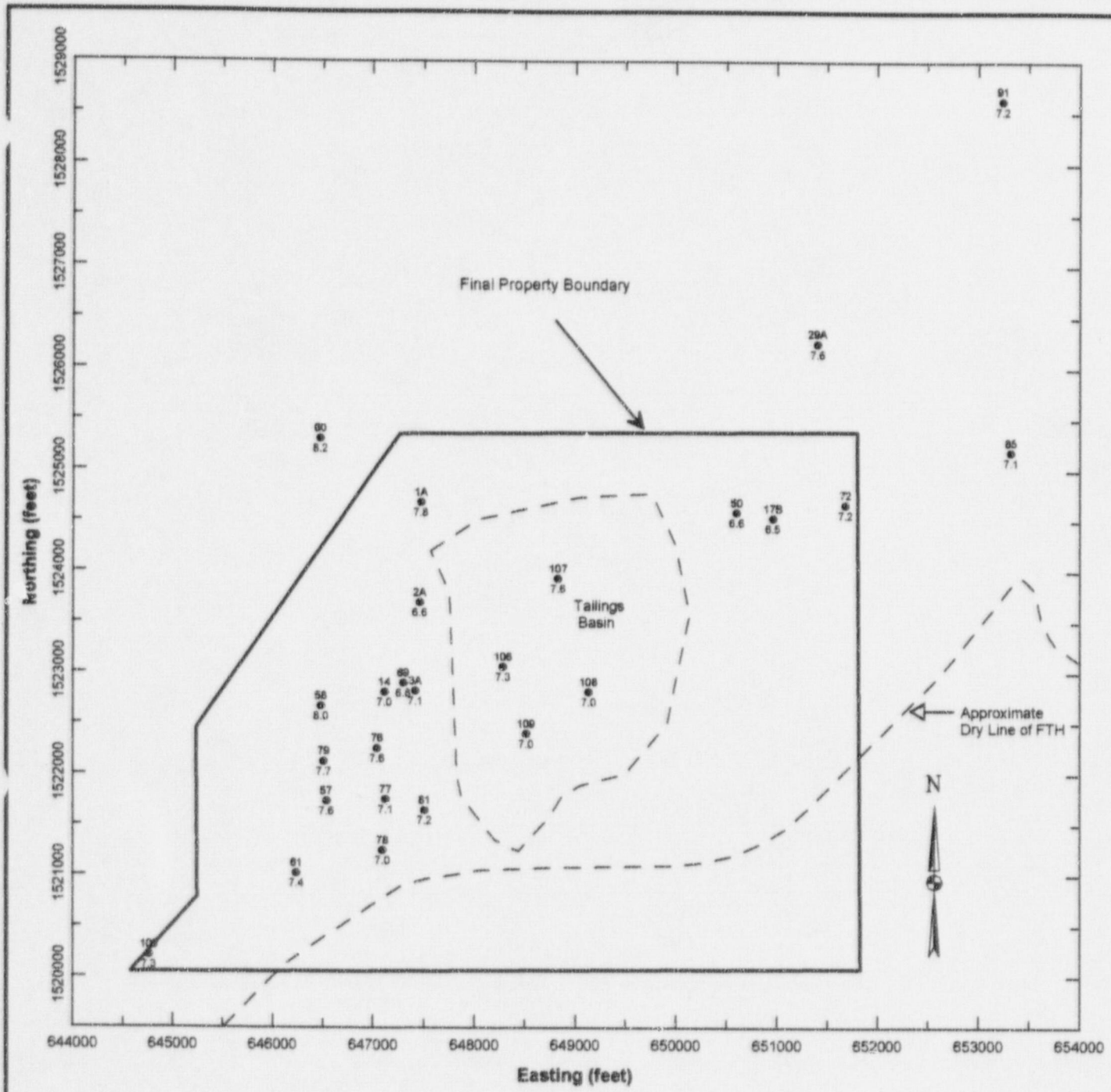

Legend

29A — Monitor Well Location and Designation

7.2 — pH Value at Location (Unitless)

Note: Analytical results for Monitoring Wells 106 - 109 were collected in February 1996

Date: 10/15/98 Produced By: KJS Checked By: KRT File Name: 98-PHP.SRF	**pH Values (April 1998)**	**FIGURE 2.6.1**
	KENNECOTT CORPORATION / L-BAR MINE **NMED Alternative Abatement Standards**	Duke Engineering & Services A Duke Energy Company

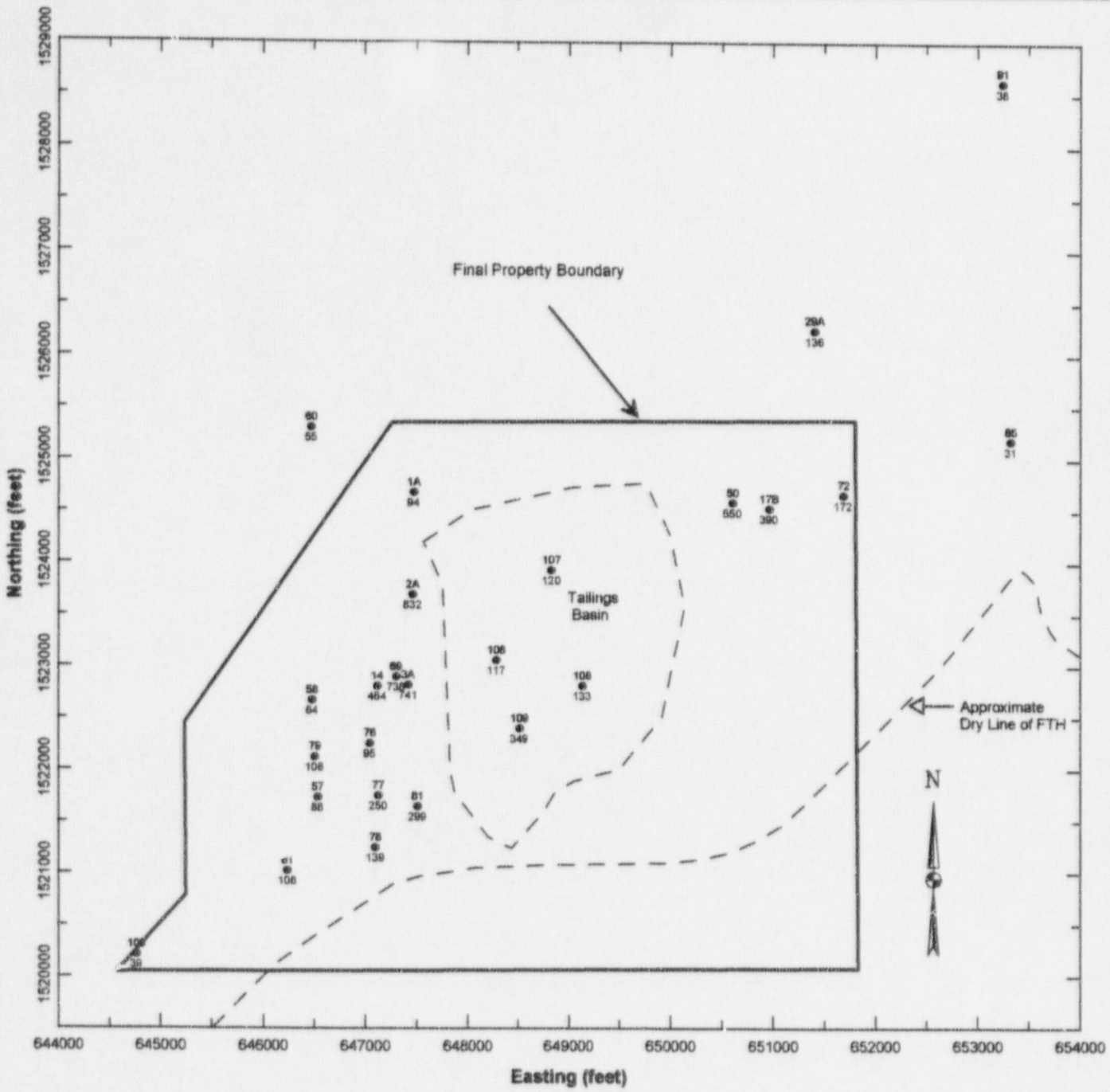

Legend

29A ● Monitor Well Location and Designation

● 139 Chloride Concentration at Location (mg/l)

Note: Analytical results for Monitoring Wells 106 - 109 were collected in February 1996

Date: 9/15/98 Produced By: KJS Checked By: KRT File Name: 98-CLP SRF	**Chloride Concentrations (April 1998)** **KENNECOTT CORPORATION / L-BAR MINE** **NMED Alternative Abatement Standards**	**FIGURE 2.6.2** Duke Engineering & Services A Duke Energy Company

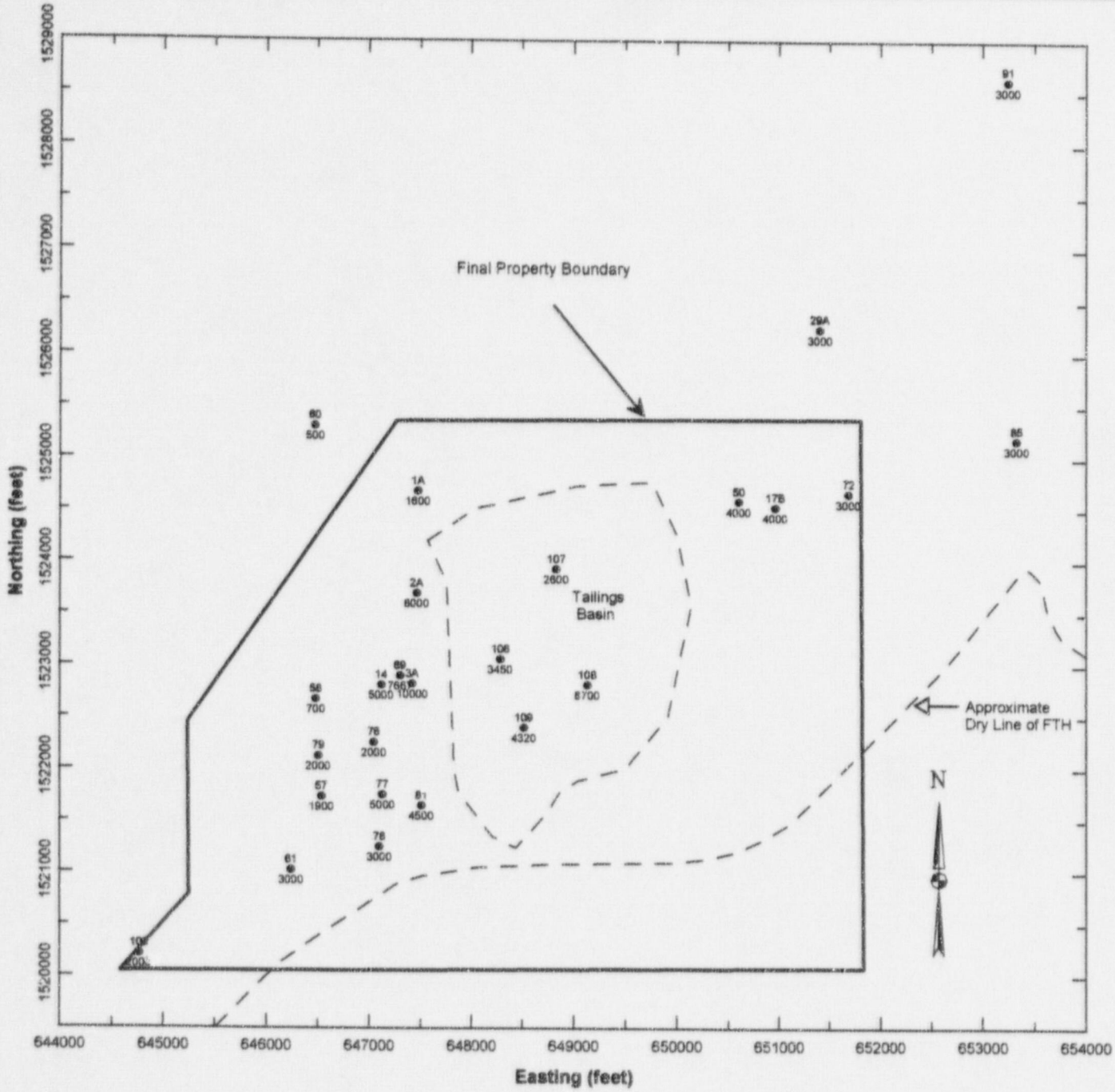

Legend

29A ● Monitor Well Location and Designation

● 2500 Sulfate Concentration at Location (mg/l)

Note: Analytical results for Monitoring Wells 106 - 109 were collected in February 1996

Date: 10/15/98 Produced By: KJS Checked By: KRT File Name: 98-SULPP SRF	**Sulfate Concentrations (April 1998)** **KENNECOTT CORPORATION / L-BAR MINE** **NMED Alternative Abatement Standards**	**FIGURE 2.6.3** Duke Engineering & Services A Duke Energy Company

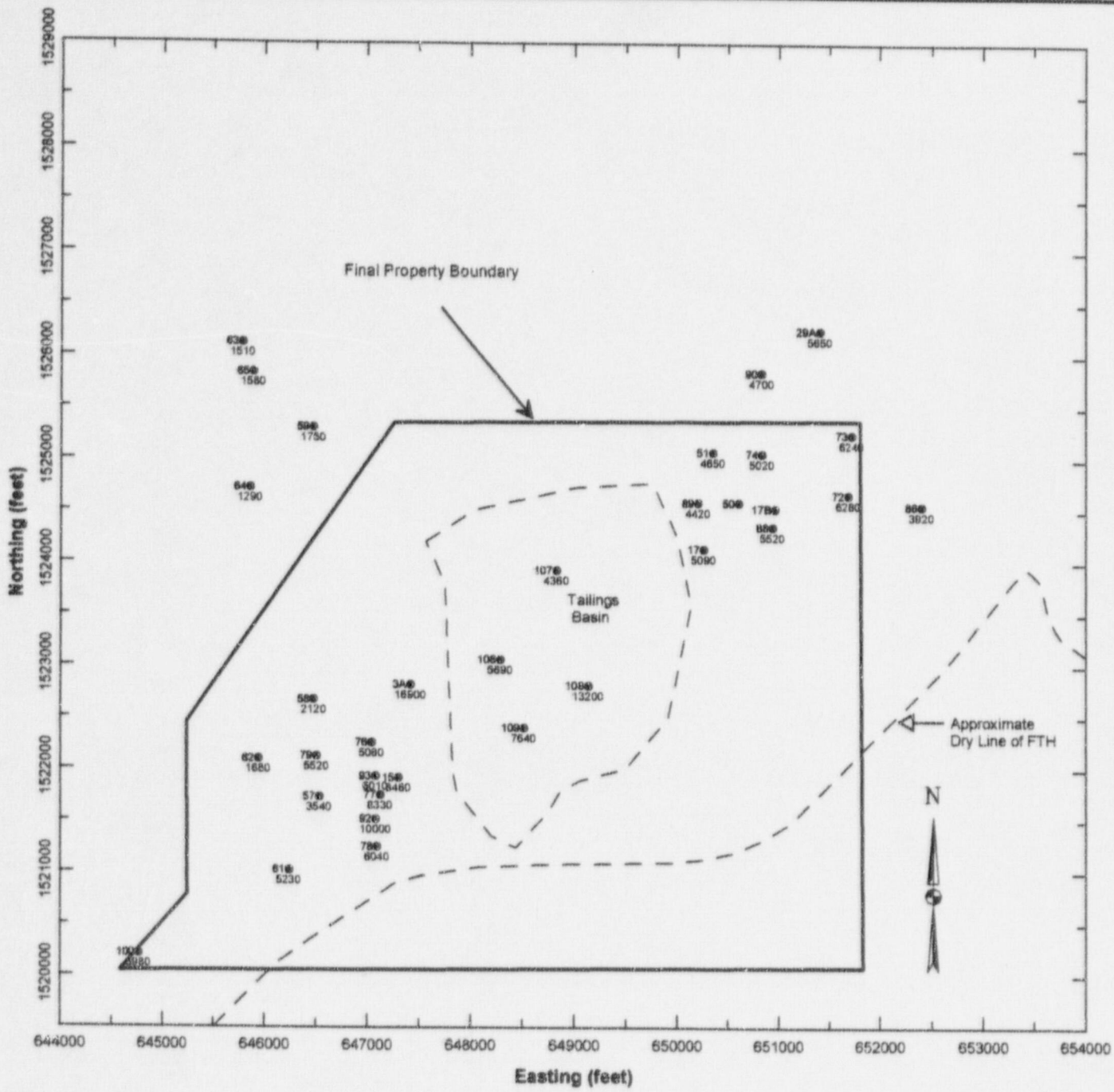

Legend

29A ● Monitor Well Location and Designation

● 139 TDS Concentration at Location (mg/l)

Note: Analytical results for Monitoring Wells 106 - 109 were collected in February 1998

Date: 10/15/98 Produced By: KJS Checked By: KRT File Name: 98-TDSP.SRF	**Total Disolved Solids (TDS) Concentrations (April 1998)**	**FIGURE 2.6.4**
	KENNECOTT CORPORATION / L-BAR MINE **NMED Alternative Abatement Standards**	Duke Engineering & Services A Duke Energy Company

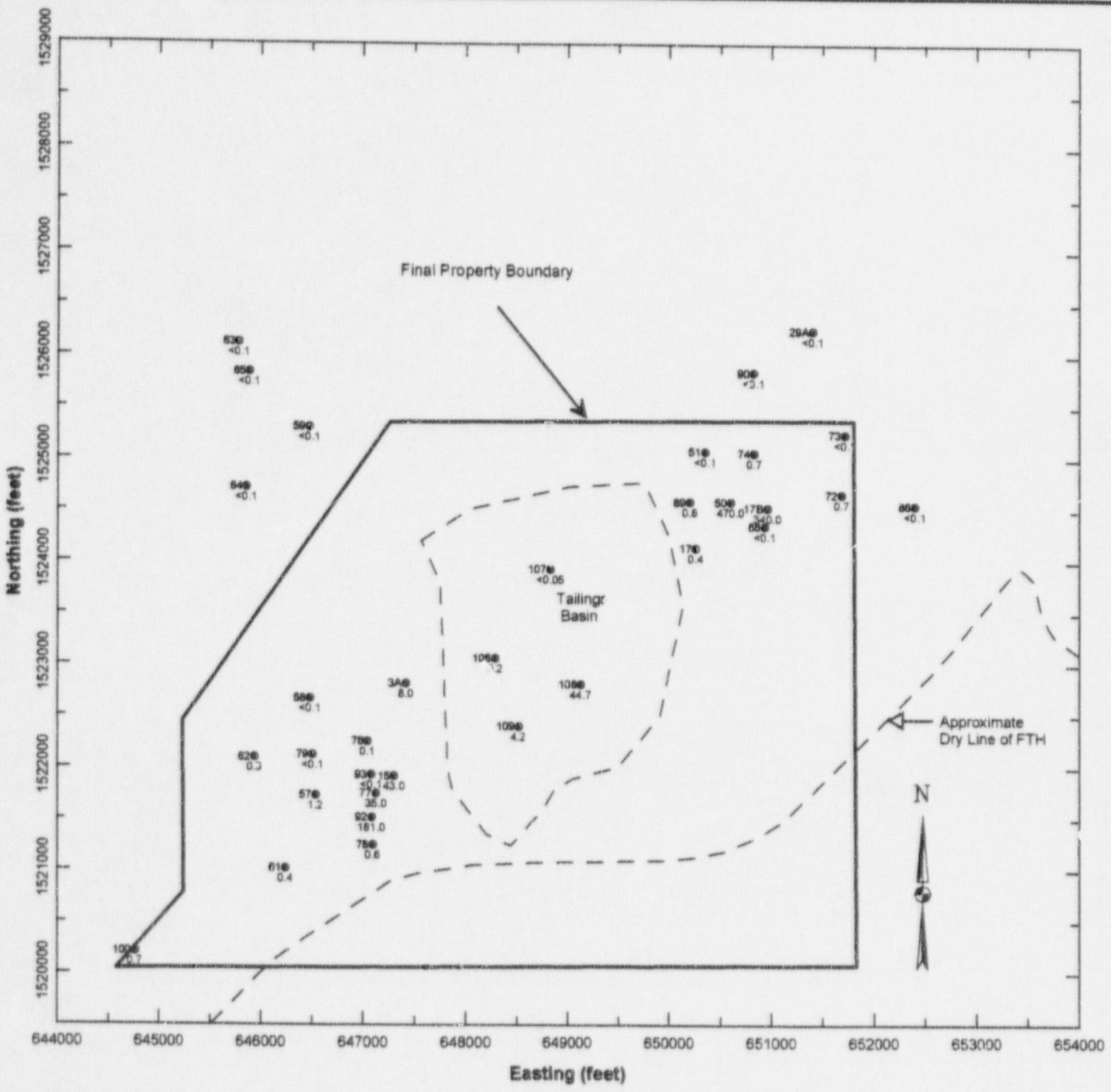

Legend

29A ● Monitor Well Location and Designation

● 35.0 Nitrate Concentration at Location (mg/l)

Note: Analytical results for Monitoring Wells 106 - 109 were collected in February 1996

Date: 10/15/98 Produced By: KJS Checked By: KRT File Name: 98-NO3P.SRF	**Nitrate Concentrations (July 1998)** **KENNECOTT CORPORATION / L-BAR MINE** **NMED Alternative Abatement Standards**	**FIGURE 2.6.5** Duke Engineering & Services A Duke Energy Company

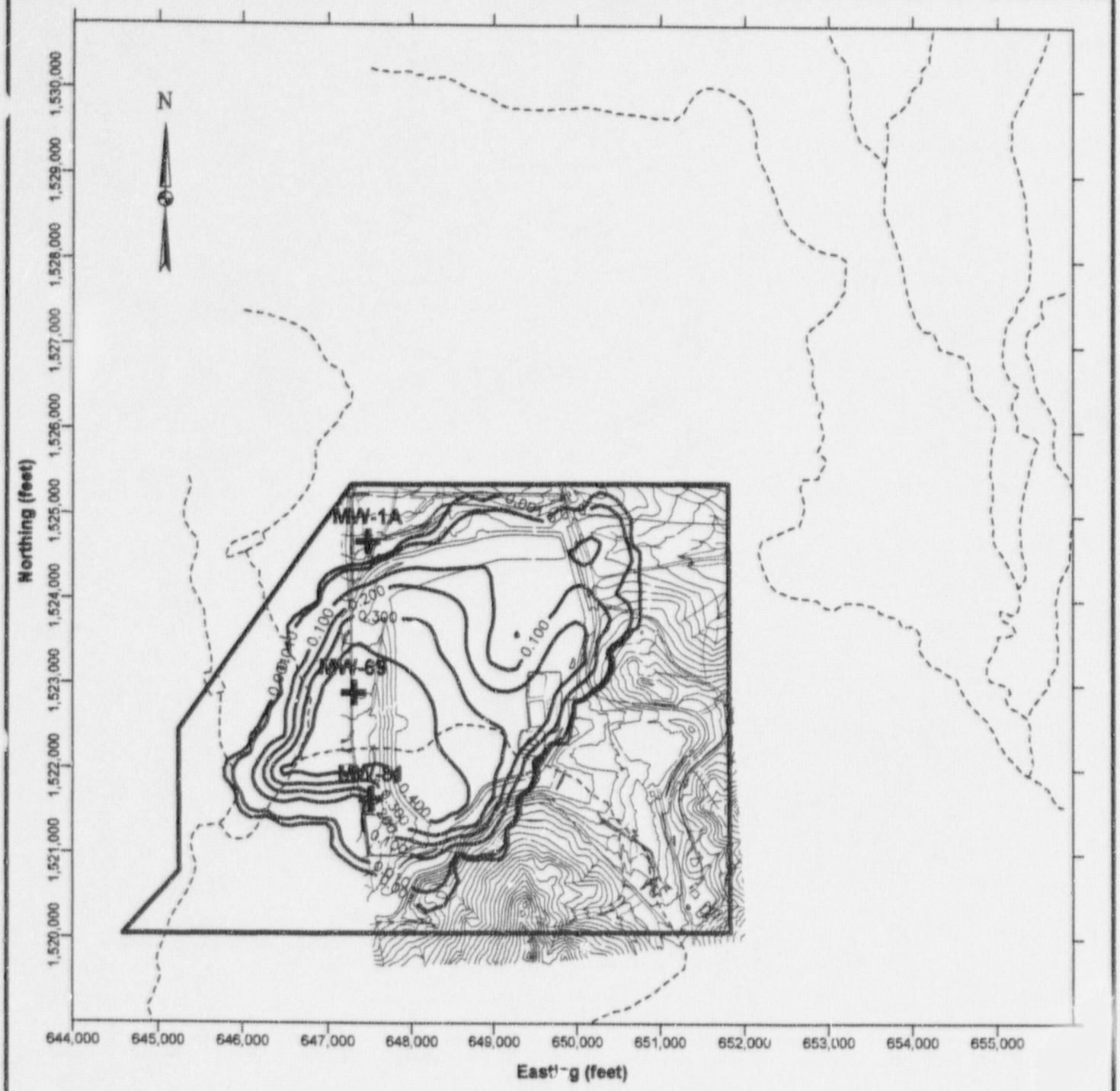

Legend

- Point of Compliance Well
- Final Property Boundary
- Contours of Relative Concentration
- 0.100 Concentration as a Fraction of Source Term

Note: Figure derived from plot by Balleau Groundwater Inc.

Date: 10/15/98 Produced By: KJS Checked By: KRT File Name: 200ALL.SRF	**Simulated 200-Year Tailings Fluid Concentrations**	**FIGURE 3.2.1**
	KENNECOTT CORPORATION / L-BAR MINE **NMED Alternative Abatement Standards**	Duke Engineering & Services A Duke Energy Company

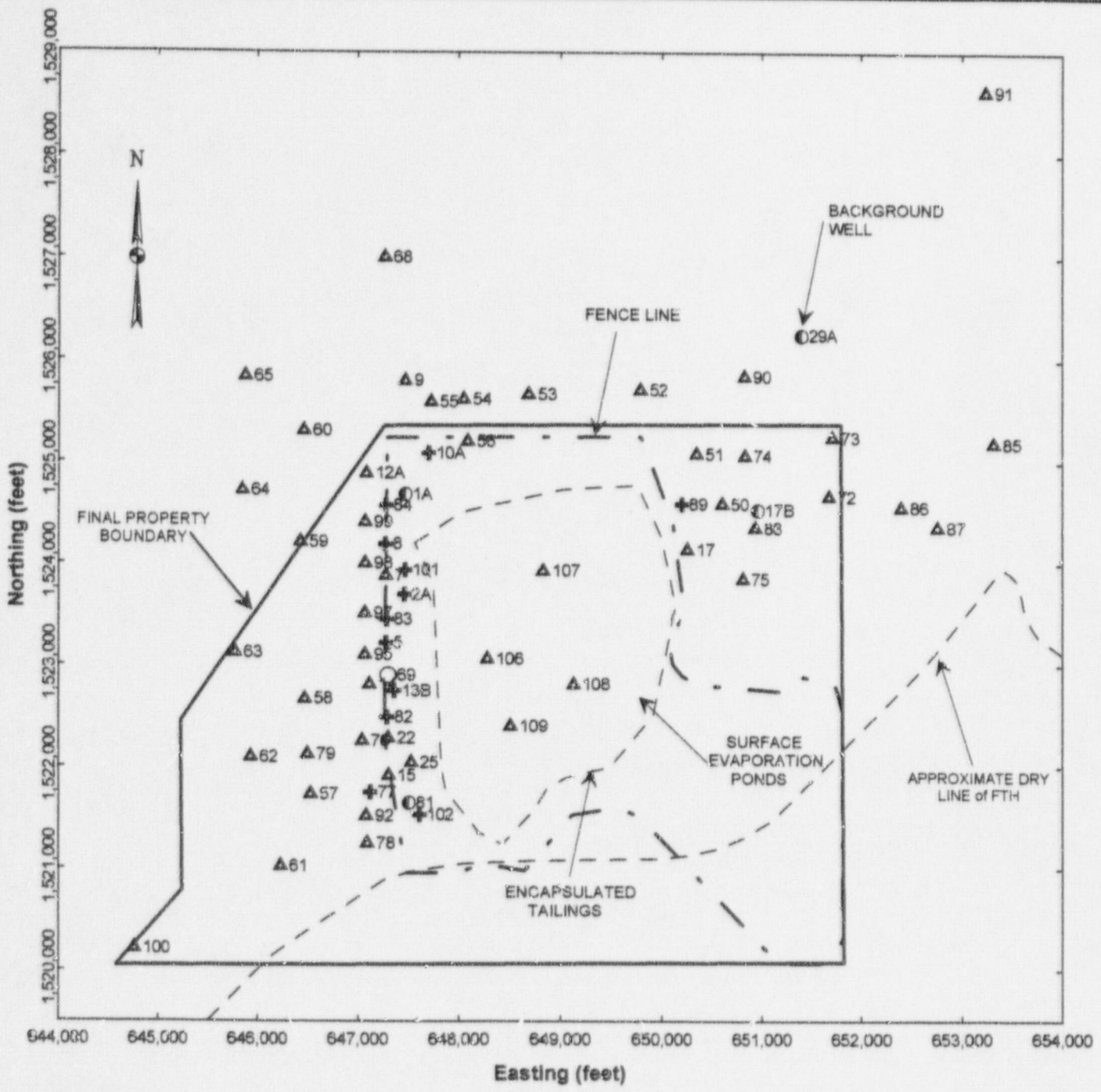

Legend

- Point of Compliance (POC) Wells
- CAP Monitoring Wells
- Pumpback Wells
- Pumpback and POC Well

Date: 10/15/98 Produced By: KJS Checked By: KRT File Name: WELLOCS.SRF	Final Property Boundary and Locations of Monitoring and Extraction Wells KENNECOTT CORPORATION / L-BAR MINE NMED Alternative Abatement Standards	FIGURE 3.3.1 Duke Engineering & Services A Duke Energy Company

Appendix A
Geochemical Controls on Contaminant Migration at the L-Bar Uranium Mill Tailings Pile

Prepared for:

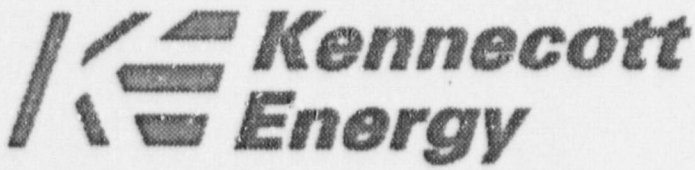

Kennecott Energy Company
505 South Gillette Avenue
Gillette, WY 82717

Prepared by:

Duke Engineering & Services
9111 Research Blvd.
Austin, Texas 78758
512-425-2000

August 10, 1998

TABLE OF CONTENTS

A-1. INTRODUCTION 1
A-1.1 Geologic Setting 1
A-1.1.1 Site Stratigraphy 1
A-1.1.2 Structural Geology 2
A-1.2 Historical Mining-Milling Operations and Tailings Cover Placement 3
A-1.2.1 Tailings Disposal 3
A-1.2.2 Tailings Cover Placement 4
A-1.3 Case Studies 4
A-1.4 Objectives 5
A-2. SITE GEOCHEMISTRY 6
A-2.1 Tailings Fluid 6
2.1.1 Composition 6
A-2.1.2 Aqueous Equilibrium Speciation 8
A-2.1.3 Mineral Solubilities 9
A-2.2 Aquifer Sediments 10
A-2.2.1 Groundwater Composition 10
A-2.2.2 Aqueous Speciation 11
A-2.2.3 Minerals 11
A-2.2.4 Mineral Solubilities 14
A-3. HYDROGEOCHEMICAL MODEL 16
A-3.1 Acid Zone 16
A-3.1.1 Acidity of Tailings Fluid 16
A-3.1.2 Acid-Neutralizing Capacity of Aquifer Minerals 18
A-3.1.3 Size of Acid Zone 19
A-3.2 Neutralization Zone 20
A-3.2.1 Calcite Dissolution 20
A-3.2.2 Kaolinite Dissolution 20
A-3.2.3 $Fe(OH)_3$ (s) Precipitation 21
A-3.2.4 Aluminum Precipitation 21
A-3.2.5 Gypsum Precipitation 21
A-3.3 Transport Zone 22
A-3.4 PHREEQM Model of Chemical Reactive Transport of L-Bar Mill Tailings 23
A-3.4.2 Model Results 23
A-4. FATE AND TRANSPORT OF TAILINGS FLUID CONTAMINANTS 25
A-4.1 Source Concentrations for the Transport Zone 25
A-4.1.1 Uranium 26
A-4.1.2 Thorium 27
A-4.1.3 Radium 28
A-4.1.4 pH 28
A-4.1.5 Sulfate 28
A-4.1.6 Chloride 28
A-4.1.7 Nickel 29

A-4.1.8 Selenium 29
A-4.1.9 Antimony 29
A-4.1.10Nitrate 29
A-4.2 Retardation in the Transport Zone 30
A-4.2.1 Chloride 30
A-4.2.2 Sulfate, Carbonate, Calcium, and Sodium 31
A-4.2.3 pH 31
A-4.2.4 Uranium 31
A-4.2.5 Thorium-230 32
A-4.2.6 Radium 32
A-4.2.7 Nickel 33
A-4.2.8 Selenium 33
A-4.2.9 Antimony 33
A-4.2.10Nitrate 33
A-5 CONCLUSIONS 34
A-6. REFERENCES 36

LIST OF TABLES

Table A-2.1.1 Detailed Chemical Composition from the Tailings Sump (1996)
Table A-2.1.2 1996 Tailings Fluid Chemistry at Multiple Locations
Table A-2.1.3 Historic Selenium Concentrations in Tailings Fluid by Graphite Furnace
Table A-2.2.1.1 Background Groundwater Composition
Table A-2.2.3.1 Summary of XRD and XRF results for 30 soil samples collected in 1996
Table A-3.5.1. Wells included in Figures A-3.5.1 through A-3.5.7
Table A-4.1.1 Source Concentrations
Table A-4.2.1 Kd Values for Constituents

LIST OF FIGURES

Figure A-1.1.1 L-Bar Site Location Map
Figure A-1.1.2 L-Bar Site Stratigraphy
Figure A-3.1 Generic Uranium Mill Tailings Model
Figure A-3.4.2.1 Initial Mineral Concentrations
Figure A-3.4.2.2 Mineral Concentrations at 2 Years
Figure A-3.4.2.3 Mineral Concentrations at 4 Years
Figure A-3.4.2.4 Mineral Concentrations at 6 Years
Figure A-3.4.2. Mineral Concentrations at 8 Years
Figure A-4.1.1.1 Uranium Aqueous Solubility

A-1. INTRODUCTION

This report addresses the geochemical controls that are important to the groundwater contaminant migration from tailings fluid and its components at the Sohio L-Bar site in New Mexico. The purpose is to identify and quantify the geochemical limits on the release and transport of aqueous contaminants resulting from the intrusion of tailings fluid into the natural sediments beneath the tailings impoundment at the site. The important geochemical controls are aqueous solubility and adsorption. These controls typically have the potential to affect groundwater migration of contaminants. The introductory sections briefly describe the site geology, history of site development, the results of similar case studies, and the objectives of this study.

A-1.1 Geologic Setting

Figure A-1.1.1 presents the site location. The L-Bar site is situated geologically in the San Juan Basin immediately south of the Mount Taylor volcanics. The geology is characterized by several thousand feet of Mesozoic and Paleozoic sedimentary rocks overlying a Precambrian age basement complex of quartzite, granite and schists. The sediments dip gently northwestward in the vicinity of the tailings pile. The sedimentary sequence consists of primarily interbedded sandstones and shales, but also includes units of conglomerate and limestone. The sedimentary sequence has been invaded locally by Tertiary-Quaternary basaltic necks and plugs, such as the Cerro Negro plug to the north of the tailings pile. The volcanic activity associated with the intrusives was geographically extensive and was related to volcanic activity responsible for the Mount Taylor volcanic field.

A-1.1.1 Site Stratigraphy

The sedimentary rocks exposed in the general area of the L-Bar tailings pile range in age from Late Triassic to Late Cretaceous. The formations of interest within the vicinity of the tailings pile, from oldest to youngest, are the Morrison Formation, Dakota Sandstone, Mancos Shale, Tertiary igneous intrusives, and Quaternary alluvium. The general stratigraphy in the vicinity of the L-Bar tailings pile is shown in Figure A-1.1.2.

The Cretaceous Mancos Shale constitutes the uppermost bedrock unit in the L-Bar area and is estimated to be 300 to 400 feet thick at the site. Only the lower portion of the Mancos Shale is present at the L-Bar Tailings pile. This lower section can be divided into seven mappable units; a lower part consisting of six alternating shale and sandstone units overlain by a thick layer of shale. The three lowermost sandstone units in the lower Mancos extend across the Laguna Mining District (Moench and Schlee, 1967). These sandstone units are locally referred to, from youngest to oldest, as the First, Second, and Third Tres Hermanos sandstones, although the middle sandstone is the only unit formally termed the Tres Hermanos. The Mancos Shale controls the

local topography, with sandstones forming high steep-walled cliffs, and the shales underlying most of the gently inclined slopes above and below the cliffs. The Mancos Shale is about 430 feet thick in the area of the L-Bar tailings pile.

The uppermost sandstone unit (the First Tres Hermanos or FTH) is the thickest of the three sandstones in the Mancos Shale and is the aquifer of concern for regulatory purposes. It is 30 to 60 feet thick, and is separated from the middle unit by 100 to 150 feet of shale and siltstone. The sandstone is orange to gray, and beds ranging from thin to thick. Quartz is the main mineral constituent. The coarsest-grained materials are found near the top of the unit and consist of well-sorted and fairly well-cemented fine- to medium-grained sands (Moench and Schlee, 1967). The unit crops out southwest of the tailings impoundment and forms the characteristic mesa and bench topography of the area. Below the tailings basin, this sandstone is present about 10 to 80 feet below the original land surface. Above the First Tres Hermanos sandstone, the Mancos Shale consists of a shale sequence 0 to 50 feet thick, which may be highly weathered and clayey to massive or fissile, and tends to be highly fractured with gypsiferous fracture fillings.

The uppermost shale layer of the Mancos Shale at the site is mantled by up to 35 feet of stream-deposited soils (alluvium) and talus (colluvium). This alluvium and colluvium are composed primarily of somewhat gypsiferous silty to sandy clays, with some lenticular bedded sands and gravels. Basaltic debris, ranging in size from sands to cobble or boulder size angular blocks, can also be found strewn across the hillsides and incorporated in the alluvium/colluvium as well.

A-1.1.2 Structural Geology

Structure maps of the top and bottom of the First Tres Hermanos Sandstone (FTH) presented in The Standard Oil Company (1980) Groundwater Discharge Plan generally show a dip to the North/Northwest and indicate no faulting or displacement of the FTH. The potential for faulting was evaluated in the context of the numerous volcanic intrusions in the area (such as the Cerro Negro volcanic plug to the north of the site). Structure contours of the base of the Dakota sandstone (Schlee and Moench, 1963) also show no faulting in the Dakota in the immediate tailings area. Several faults which exhibit displacement in the Dakota of the order of a few feet are suggested by the structure contours about 3 miles north of the site. The structure contours of the base of the Dakota sandstone indicate that the faults are not continuous to the south toward the tailings impoundment area.

Fractures and jointing, as opposed to major faulting, likely contribute to the permeability of the Tres Hermanos sandstone units within the Mancos Shale. Joint patterns measured in outcrops of the FTH (The Standard Oil Company, 1980) exhibited approximately N30E and N30W orientations.

A-1.2 Historical Mining-Milling Operations and Tailings Cover Placement

Actual mining and milling of ore at the L-Bar operations began in the fall of 1976 and continued until the spring of 1981, when the mine was closed due to the economics of the uranium industry. The L-Bar mill used a sulfuric acid-leach process, employing counter-current decantation, and solvent extraction with a design capacity of 1500 tons of ore per day. At the time of shut-down in 1981, a total of approximately 2,111,700 tons of ore had been processed through the mill; 898,500 tons of ore were from the L-Bar mine, and the remaining 1,213,200 tons of ore were processed through the mill as a result of toll milling contracts.

A-1.2.1 Tailings Disposal

Mill tailings were produced as solid waste from the milling process. The tailings were pumped as a slurry consisting of about 38 percent solids mixed with water, acid, and a variety of spent process chemicals. The mill design tailings production/disposal rate was 368 gallons per minute (gpm) (70 gpm solids and 298 gpm liquid). The tailings consisted of approximately 80 percent sand-size material and 20 percent fines (materials passing a No. 200 sieve). The finer particles are commonly referred to as slimes. It was projected that the tails would contain small amounts of calcium, potassium, sulfur, phosphorus, aluminum, and carbon in addition to appreciable amounts of radioactive materials not recovered by the milling process. A portion of the slurry fluid was returned to the mill for reuse, but the majority was disposed of in the tailings basin. As milling continued, a body of free-standing water developed in the center of the basin. It was anticipated that the majority of this water would be lost to natural evaporation.

The tailings facility was designed for a ten-year life to provide an ultimate storage capacity of 7.2×10^6 dry tons in an area of about 180 acres. An impoundment was constructed to hold the tailings by damming a natural drainage basin and pumping tailings into the basin upstream of the dam. The basin was chosen because of its relatively thick, low-permeability alluvial clay surface deposits within the impoundment and its proximity to the mill site. The starter dam on the west side was constructed of alluvial clay from within the impoundment. The impoundment bottom (the natural alluvial clay soils) was scarified and treated with NaCl (waste salt from potash mines in Carlsbad, NM) to increase the soil swelling capacity and reduce the hydraulic conductivity of the clays, thereby reducing seepage through the bottom of the tailings pile.

The tailings slurry was transferred from the mill to the pile area by a pipeline. The tails were deposited from a single pipe spigot that was periodically moved along the earthen starter dam crest to produce a wide sandy beach composed of coarse sand sized tailings. The slimes were hydraulically deposited upstream from the sands and tend to be concentrated toward the center of the tailings impoundment. The purpose of initially encouraging the deposition of the coarsest material close to the upstream side of the dam was to assist in dam stability by placing free-draining material on the upstream face, thus promoting seepage into the chimney drain and finger drain system. Over time, the discharge pipe for the tailings was eventually moved around the

entire perimeter of the tailings pond. This discharge method created a stratigraphic sequence within the tailings similar to interfingering alluvial fan deposits with grain sizes ranging from sand to clay.

A-1.2.2 Tailings Cover Placement

Three of the primary objectives of capping the tailings pile were:

- to meet NRC regulations developed to reduce the chances of the future spreading of mine- and mill-derived wastes;
- to limit infiltration of precipitation so that the pile wouldn't function as a long-term sustained source of contamination; and
- to reduce radon gas emanation from the tailings pile to NRC required levels. This was achieved by placing an NRC-approved clay cap constructed primarily of weathered Mancos Shale.

The tailings pile cap was constructed during the period of fall, 1988 through summer, 1989. Following enhanced evaporation of the majority of ponded tailings fluid, all radioactive materials were placed beneath the 6195-foot elevation contour within the tailings pond. This reduced the area to be capped to approximately 110 acres. These materials included: wind-blown tailings contaminated soil; tailings from the north, east and south sides of the tailings pond outside the contour; and mine waste-rock. A 4.1-foot minimum thickness cap composed of weathered Mancos shale and alluvium was placed over all the materials inside the 6195-foot elevation contour.

Since cap construction, the tailings fluid has continuously drained into the underlying lithologies or has been lost to evapotranspiration through the cover. The tailings fluid potentiometric levels have continuously dropped since cap placement and we anticipate that tailings moisture overall will eventually approach an unsaturated condition. At that point, the pile will no longer be capable of contributing contaminants to ground water, since the radon barrier clay cover will minimize or eliminate precipitation infiltration.

A-1.3 Case Studies

Case studies provide strong evidence of the types of groundwater plumes that may develop at uranium mill tailings sites. The surface disposal of acid-leach uranium mill tailings has affected groundwater quality at a number of sites in the western United States. PNL (1990) describes contamination at four of these sites:

1) the Riverton tailings pile in Riverton, Wyoming (also described by White, et al., 1984);
2) the Federal American Partners uranium mill in central Wyoming;
3) the Pathfinder Mill in the gas hills of Wyoming; and

4) the Sohio L-Bar site in western New Mexico (also described in Longmire and Brookins, 1982).

Other sites include the tailings piles at Falls City, Texas (Bryson, et al., 1988) and at Maybell, Colorado (Brookins, et al., 1993).

These sites, although similar in many ways, each have unique features that prevent perfect comparisons. The Maybell site has reducing conditions down-gradient from the tailings due to the abundance of pyrite. As a result, nitrate, uranium, and other redox sensitive constituents are readily attenuated by reduction. At each of the other sites, including L-Bar, oxidizing conditions prevail. Although each site differs in tailings fluid composition and the concentration of calcite and other mineral phases down-gradient from the tailings piles, there are many similarities in observed groundwater plumes.

Geochemical controls on acid neutralization, solubilities, and adsorption are discussed in detail in many of these studies. Some case studies not associated with uranium mill tailings also proved useful in this regard, such as the work by Stollenwerk (1994) on the migration of acid groundwater from a copper-mining site at Globe, Arizona.

A-1.4 Objectives

The specific objectives of this work were to:

- identify the important geochemical reactions affecting the migration of tailings fluid in the native aquifer,
- estimate the volume of aquifer needed to neutralize the remaining tailings fluid,
- explain current groundwater observations, and
- predict the natural fate and transport of contaminants within, and down-gradient from, the tailings fluid neutralization zone.

A-2. SITE GEOCHEMISTRY

Sections A-2.1 and A-2.2 present and discuss the compositions of the tailings fluid, aquifer sediments, and natural groundwater. These sections establish the geochemical inputs for the scoping and modeling calculations in later sections.

A-2.1 Tailings Fluid

The tailings fluid from the horizontal drains in recent years has been less acidic and less loaded with dissolved solids than it was in the 1980s. However, the composition has changed very little over the last five years. To varying extents, this change in composition is due to years of contact with dissolving minerals, evaporation, mineral precipitation, and dilution. Therefore, the tailings fluid relevant to this investigation is assumed to have the composition of the tailings fluid measured from the sump drainage in 1996. The following subsections focus on the model composition of the tailings fluid (A-2.1.1) the predominant aqueous equilibrium speciation of the tailings fluid (A-2.1.2) and mineral solubilities calculated for the model tailings fluid (A-2.1.3).

A-2.1.1 Composition

Tailings fluid has been regularly monitored from discharge at the tailings sump, and this chemistry has been applied as the source term in this analysis. Table A-2.1.1 presents a detailed multiple analyte suite for the tailings sump sample as measured in 1996. In the sump sample, the low pH of 2.03 is due to the high concentration of sulfuric acid in the fluid. This acid has dissolved minerals containing iron (Fe), aluminum (Al), magnesium (Mg), calcium (Ca), and other elements resulting in high concentrations of these elements in the tailings fluid. The low pH has also resulted in elevated concentrations of uranium (U), thorium-230 (Th-230), radium-226 (Ra-226), and radium-228 (Ra-228).

Table A-2.1.2 presents the tailings fluid general chemical composition from multiple locations throughout the tailings pond as measured in May 1996. This table shows that using the sump chemistry for source term modeling is conservative, because other tailings fluid samples from wells and piezometers constructed through the cover are typically less acidic and less saline. This is likely due to buffering/precipitation reactions between tailings fluid and materials placed in the pile during reclamation that had not previously come into contact with the acid (waste ore, windblown Mancos shale and alluvium). In other words, by assuming that the entire volume of remaining tailings fluid has chemistry similar to sump chemistry is a worst-case assumption.

Table A-2.1.1 Detailed Chemical Composition from the Tailings Sump (1996)

Analyte	Units	Sump	Analyte	Units	Sump
NH4	mg/L	702	Gross Beta	pCi/L	98900
NO3 + NO2	mg/L	0.79	As	mg/L	0.57
SiO2	mg/L	302	Ba	mg/L	<0.01
Fe	mg/L	4390	Cd	mg/L	0.412
Fe+2	mg/L *	2.54	Hg	mg/L	<0.0002
Fe+3	mg/L *	5080	Mo	mg/L	<0.05
Al	mg/L	3370	Ag	mg/L	0.05
Mn	mg/L	80.3	Be	mg/L	0.508
Zn	mg/L	15	Co	mg/L	2.31
V	mg/L	182	Tl	mg/L	1.9
Cu	mg/L	8.2	Sn	mg/L	<2
Cr	mg/L	3.06	TSS	mg/L	91
Pb	mg/L	0.65	Ni	mg/L	<4
F	mg/L	<0.1	Se by graphite furnace	mg/L	0.8
Ra226	pCi/L	2980	Se by Hydride	mg/L	0.04
Ra228	pCi/L	48.9	Sb	mg/L	<10
Th230	pCi/L	165000	U	mg/L	137.5
Gross Alpha	pCi/L	318000			

* These concentrations were measured for a sample collected on December 17, 1996

Table A-2.1.2 1996 Tailings Fluid Chemistry at Multiple Locations

Analyte	Units	PZ-5	PZ-8	WP-1B	MW-103	Sump
pH		8.10	2.82	6.37	2.66	2.03
Cl	mg/L	1310	1300	545	524	752
SO4	mg/L	7760	107000	6840	6950	39400
Ca	mg/L	275	786	614	655	551
Mg	mg/L	994	4040	354	924	1120
K	mg/L	130	<5.0	49	500	400
Na	mg/L	2850	4470	2850	1360	1500
HCO3	mg/L	866	<5.0	1070	<5.0	<5
CO3	mg/L	<1.0	<1.0	<1.0	<1.0	<1
Conductivity	uhmos/cm	15300	45800	10700	27300	32400
TDS	mg/L	13300	121000	10700	53800	55100

There has been a discrepancy in the values reported for the selenium over time with two different analytical methods. Historically the site has used the selenium by hydride method, primarily because contract laboratory has this equipment. Mechanical failures over the last several years have caused the laboratory to purchase new analytical equipment, including a graphite furnace for metals analysis. Split sample analysis with both techniques has yielded no distinct trends for comparison. The laboratory believes that the graphite furnace may be less affected by interference effects, and therefore more representative of sample chemistry. In the case of the tailings fluid analyses, the analysis has always been performed by graphite furnace, and these results are presented in Table A-2.1.3 below. The maximum observed concentration of 6 mg/l from these tests has been conservatively assumed as the source concentration for selenium.

Table A-2.1.3
Historic Selenium Concentrations in Tailings Fluid by Graphite Furnace

Month, Year	Se (mg/L)
May-96	0.8
Oct-95	<2.0
Apr-95	0.09
Oct-94	<2.0
Apr-94	0.01
Oct-93	<5.0
Apr-93	2
Oct-92	<2.0
Apr-92	0.72
Oct-91	0.5
May-91	6
May-91	0.074
Jul-87	<5.1
Jul-87	<10
Jul-87	<2.5
Oct-86	<0.001

A-2.1.2 Aqueous Equilibrium Speciation

At pH 2, sulfate exists in high concentrations as both SO_4^{-2} and HSO_4^-, helping to buffer the pH at 2. At these high sulfate concentrations and low pH, sodium, calcium, magnesium, manganese, iron, aluminum, and potassium form ion pairs with sulfate (e.g., $NaSO_4$, $CaSO_4^0$, $MgSO_4^0$, $MnSO_4^0$, $FeSO_4^+$, $AlSO_4^+$, and KSO_4^-). Although the free ion forms of these metals are also abundant under these conditions (e.g., Na^+, K^+, etc.), other aqueous species for these metals are not. Chlorine exists predominantly as Cl^-. For thorium, a sulfate species such as $ThSO_4^{+2}$ will likely predominate (Brookins, 1988). Similarly, a radium-sulfate ion pair, $RaSO_4^0$, may account for most of the radium in the high sulfate fluid, whereas at lower sulfate concentrations, Ra^{+2} would predominate.

According to chemical analyses conducted in December of 1996, iron in the tailings fluid predominantly exists in its oxidized form, Fe^{+3}. The ratio of Fe^{+3} to Fe^{+2} indicates an Eh value of 960 mV, indicating highly oxidizing conditions. This Eh value suggests that other redox-sensitive elements may also occur in their oxidized forms, such as uranium, UO_2^{+2}. Antimony hydrolyzes either as Sb(III) or Sb(V) to form cationic or neutrally-charged species at low pH under oxidizing conditions. Selenium in oxidizing waters at low pH occurs as $HSeO_4^-$, SeO_4^{-2}, and/or $H_2SeO_3^0$ (Brookins, 1988). The predominant form of nitrogen in the tailings fluid is ammonium, NH_4^+. Though NH_4^+ is a reduced form of nitrogen, the low pH of the tailings fluid and likely absence of nitrifying bacteria in the fluids does not favor oxidation to nitrate, NO_3^- (Brookins, 1988; Chappelle, 1993) in the tailings pile.

A-2.1.3 Mineral Solubilities

PHREEQE, a geochemical code developed by the U.S. Geological Survey (Parkhurst, et al., 1980), was used to calculate the saturation index (SI) of each potential mineral phase for the tailings fluid. The SI for a given mineral is the logarithm of the ratio of the ion activity product to the thermodynamic mineral solubility product, K_{sp} (Nordstrom and Munoz, 1986). SI for a mineral equals zero when the water is saturated with respect to the mineral. A positive value of SI indicates the water is oversaturated with respect to the mineral. A negative SI indicates undersaturation. Oversaturation implies that precipitation of the mineral is thermodynamically favored. Undersaturation implies that dissolution is favored.

The PHREEQE results indicate that the following minerals are approximately at saturation (SI ~0):

- gypsum ($CaSO_4 \bullet 2H_2O$),
- anhydrite ($CaSO_4$), and
- amorphous silica (am-SiO_2).

$AlOHSO_4$ is slightly oversaturated, but may limit aqueous Al concentrations. Highly oversaturated minerals (SI > 1) in the tailings fluid include:

- jarosite ($KFe_3(SO_4)_2(OH)_6$),
- hematite (Fe_2O_3),
- goethite (FeO(OH)), and
- quartz (SiO_2).

Most minerals are highly undersaturated (SI < -1), including:

- hydrous ferric oxide (am-$Fe(OH)_3$),
- aluminum hydroxide (am-$Al(OH)_3$),
- clays, and
- carbonates (e.g., calcite, $CaCO_3$).

A-2.2 Aquifer Sediments

The tailings pile is underlain by three geologic strata which may potentially be contacted by tailings fluid. They are, in order of increasing depth, the alluvium, the Mancos shale, and the First Tres Hermanos sandstone. The geometries, depths, and extents of these formations in the vicinity of the site are described in detail in BGW (1997). The groundwater compositions and minerals of these formations are addressed in the following subsections.

A-2.2.1 Groundwater Composition

The alluvium and Mancos shale exhibit low permeability and typically produce little or no groundwater. The First Tres Hermanos sandstone is the uppermost geologic formation that produces sufficient amounts of water for sampling at the site and is the regulated water-bearing unit. Therefore, essentially all of the groundwater samples regularly collected at the site for monitoring purposes are collected from the First Tres Hermanos.

Monitor well MW-29A is the regulatory background well at the site. However, there are many monitor wells that have not been contaminated by operations at the site that contain groundwater with slightly differing compositions. As a result, the component concentrations of natural background groundwater are chosen in this study to be approximate averages of measurements observed in several uncontaminated wells.

The resulting representative composition for natural groundwater in the First Tres Hermanos at the site is presented in Table A-2.2.1.1. This approximated background composition is compared to field data in Section A-2.2.3.1.

Table A-2.2.1.1 Background Groundwater Composition

Analyte	Concentration	Analyte	Concentration
pH	7.5	Si	5 mg/l
Cl	70 mg/l	U	0.01 mg/l
SO4	2000 mg/l	Ra (226&228)	11.01 pCi/l
HCO3	462 mg/l	Th230	1 pCi/l
Na	800 mg/l	Ni	< 0.03 mg/l
Ca	75.9 mg/l	Se	0.001 mg/l
Mg	80 mg/l	NO3	1 mg/l

A-2.2.2 Aqueous Speciation

In background First Tres Hermanos groundwater, pH is in the neutral range, SO_4^{-2} is the predominant sulfate species, and HCO_3^- is the predominant carbonate species. Sodium, chlorine, and calcium occur predominantly as free ions: Na^+, Cl^-, and Ca^{+2}.

Uranium in this neutral pH groundwater will likely be in the form of highly soluble, anionic uranyl carbonate complexes due to oxidizing conditions and the high concentrations of dissolved carbonate (Waite et al., 1994; Bryson et al., 1988; PNL, 1990). Like uranium, thorium is also expected to exist as a carbonate complex, e.g., $Th(CO_3)_5^{6-}$ (Lemire and Garisto, 1989); however, its solubility is much lower than uranium. Radium also has a low solubility in water with a pH near neutral. The predominant radium species is likely Ra^{+2} in these waters (Langmuir and Riese, 1985). Selenium and antimony react with water in oxic, neutral pH waters to form negatively charged oxyanions (Dzombak and Morel, 1990). Nitrogen occurs almost exclusively as NO_3^-. Nickel would predominantly occur as Ni^{+2}, its free ion form (Brookins, 1988).

A-2.2.3 Minerals

A total of thirty samples from core borings and surface samples of alluvium, Mancos shale, and First Tres Hermanos sandstone were collected in the fall of 1996 for analysis by x-ray fluorescence (XRF), x-ray diffraction (XRD), and petrographic thin-section analysis. XRF measures the elemental composition of the samples, while XRD and thin-section analysis measures the abundance of identifiable minerals. A summary of results pertinent to this investigation is presented in Table A-2.2.3.1. The complete laboratory results are provided in Appendix A-1.

Table A-2.2.3.1 Summary of XRD and XRF results for 30 soil samples collected in 1996

				XRD										XRF
Sample	Boring	Depth	Formation	Calcite	Dolomite	Quartz	P.feldspar	Kfeldspar	Kaolinite	Mica/illite	Smectite	Gypsum	SUM	Fe_2O_3
		(ft)		(wt. %)	(wt. %)	(wt. %)	(wt. %)	(wt. %)	(wt. %)	(wt. %)	(wt. %)	(wt. %)	(wt. %)	(wt. %)
26	surface	Alluv. N.	Alluv.	4	<3	22	5	<5	8	<5	45	4	88	4.57
28	surface	Alluv. E.	Alluv.	12	0	17	<3	<3	5	<5	52	4	90	5.48
30	surface	Alluv. S.	Alluv.	9	<5	15	5	5	16	<5	33	6	89	4.32
Representative Composition				**8**	**0**	**18**	**3**	**2**	**10**	**1**	**43**	**5**	**90**	**4.8**
7	107	23-24	Alluv.	25	0	10	<5	<5	0	<5	37	10	82	5.76
6	107	16-20	Alluv.	0	0	25	5	<5	6	0	54	3	93	6.04
15	108	21-23	Alluv.	33	0	20	<3	<3	5	<5	28	<3	86	4.94
Representative Composition				**19**	**0**	**18**	**2**	**1**	**4**	**0**	**40**	**5**	**89**	**5.6**
27	surface	w.Mancos E.	w.Mancos	34	0	12	<3	<3	<5	<5	40	<3	86	4.47
29	surface	w.Mancos S.	w.Mancos	41	0	11	<3	<3	<5	0	33	4	89	3.46
25	surface	w.Mancos N.	w.Mancos	<5	<5	11	<3	<3	<5	0	63	11	85	5.96
Representative Composition				**30**	**0**	**11**	**1**	**1**	**1**	**0**	**45**	**6**	**96**	**4.6**
1	106	50-53.5	w.Mancos	7	7	26	<5	<5	24	14	0	8	86	4.61
9	107	36-40.5	w.Mancos	40	<3	16	<5	<3	13	<5	12	<3	81	4.09
8	107	31.5-32.4	w.Mancos	35	<3	8	<5	0	0	5	37	5	90	3.94
Representative Composition				**27**	**2**	**17**	**1**	**0**	**12**	**7**	**16**	**5**	**88**	**4.2**
10	107	64-69	Mancos	<5	<5	17	<3	<5	10	12	30	0	69	3.75
17	108	49-51	Mancos	12	<5	27	<5	<3	14	20	<10	<1	73	4.35
Representative Composition				**7**	**1**	**22**	**1**	**1**	**12**	**16**	**17**	**0**	**77**	**4.05**
23	Surface	FTH-SS East 2	w.FTH.tan	0	0	83	<3	5	7	0	0	0	95	1.27
24	Surface	FTH-SS West 1	w.FTH.tan	<1	0	85	<3	<5	7	0	0	0	92	1.18
22	Surface	FTH-SS East 1	w.FTH.tan	3	<1	81	<5	<5	6	0	0	0	90	1.28
Representative Composition				**1**	**0**	**83**	**1**	**3**	**7**	**0**	**0**	**0**	**95**	**1.24**
2	106	53.5-55	w.FTH.tan	3	12	60	<5	<5	9	0	0	0	84	2.07
3	106	65-66.7	FTH.tan	0	<5	88	<5	<5	<5	0	0	0	88	1.02
18	108	52-54	FTH.tan	5	<3	80	<3	<3	<5	<3	0	0	85	1.74
20	109	46.5-48.5	FTH.tan	0	<3	86	<3	<3	5	0	0	0	91	1.47
Representative Composition				**2**	**1**	**85**	**1**	**1**	**3**	**0**	**0**	**0**	**92**	**1.4**

				XRD										XRF
Sample	Boring	Depth	Formation	Calcite	Dolomite	Quartz	P.feldspar	Kfeldspar	Kaolinite	Mica/illite	Smectite	Gypsum	SUM	Fe_2O_3
		(ft)		(wt. %)	(wt. %)	(wt. %)	(wt. %)	(wt. %)	(wt. %)	(wt. %)	(wt. %)	(wt. %)	(wt. %)	(wt. %)
4	106	67-68.5	FTH.grey	<3	<5	77	<5	<5	8	<5	0	0	85	1.27
5	106	90-95	FTH.grey	<3	<5	74	<3	<5	7	<5	0	0	81	1.98
12	107	90.5-95.5	FTH.grey	<2	<5	80	<5	<5	7	0	0	0	87	1.29
13	107	104-109	FTH.grey	7	<5	68	<3	<5	8	<5	0	0	83	2.13
14	107	115.5-120-5	FTH.grey	<1	<5	75	<3	<5	8	<5	0	0	83	1.9
11	107	77.5-80.5	FTH.grey	8	<5	55	<3	<5	12	7	0	0	82	2.27
19	108	89.3-94.3	FTH.grey	<2	<5	75	<3	<3	7	5	0	0	87	2.26
21	109	80.5-85.8	FTH.grey	12	<5	66	<3	<5	7	0	0	0	85	1.93
Representative Composition				4	1	71	1	1	8	2	0	0	88	1.9

Calcite ($CaCO_3$) was found in the alluvium, Mancos shale, and First Tres Hermanos sandstone. Surface alluvium samples contained 4% to 12% calcite while subsurface alluvium samples contained 0%, 25%, and 33% calcite. Samples of Mancos shale contained as much as 41% calcite. In the First Tres Hermanos sandstone, the calcite content is generally lower but is still found in significant quantities, ranging up to 12%. On average, the sandstone samples contained approximately 2% calcite.

Gypsum ($CaSO_4 \bullet 2H_2O$) was found in samples from the alluvium and Mancos shale but not from the First Tres Hermanos. Its concentration ranged from <3% to 10% in the alluvium samples and from 0% to 11% in the Mancos samples.

Quartz (SiO_2) accounted for between 65% to 88% of the sandstone samples but only 8% to 27% of the alluvium and Mancos shale samples. Kaolinite ($Al_2Si_2O_5(OH)_4$) content was found to range between 0% and 16% in the alluvium samples, 0% to 24% in the Mancos shale samples, and <5% to 12% in the First Tres Hermanos sandstone samples. The predominant clay in the alluvium samples and most of the Mancos shale samples, however, was smectite, which ranged from 28% to 54% in the alluvium samples and from 0% to 63% in the Mancos shale samples. No smectite was observed in the First Tres Hermanos samples.

Sixteen additional samples were analyzed under a microscope by polarized light microscopy (PLM). These analyses generally support the XRD and XRF results. Several samples from the First Tres Hermanos sandstone showed fairly high calcite contents, some containing over 10% calcite. When calcite content was very low, dolomite ($CaMg(CO_3)_2$) was found in the range of 1% to 5%. Numerous photographs show calcite precipitation where K-feldspar ($KAl(Al,Si)_3O_8$) had dissolved. Some photographs also show the presence of small amounts of gypsum. The photos are included in Appendix A-1.

Nine additional samples were collected from the fractures of Mancos shale samples and analyzed by XRF and XRD. These samples consisted predominantly of gypsum (38% to >85%). The bulk of the remaining minerals were calcite (0% to 24%), quartz (<3% to12%), and kaolinite (0% to 30%).

A-2.2.4 Mineral Solubilities

Given the pH and major ion concentrations in the background First Tres Hermanos reference groundwater (Table A-2.2.1.1), calcite is approximately at saturation (SI ~0). The bicarbonate concentration and pH imply that the equilibrium partial pressure of carbon dioxide is approximately 0.01 atm. The groundwater is undersaturated with respect to gypsum. Silica is approximately at saturation with respect to chalcedony.

Saturations for minerals involving iron and aluminum and other trace elements in groundwater not reported in Table A-2.2.1.1 were not calculated because representative aqueous concentrations of these elements are very low and not well-established. Iron and aluminum are highly insoluble at neutral pH values. In addition, colloidal aluminum and iron can pass through 0.45 micron filters. Such occurrences would result in overestimates of aqueous concentrations and, in turn, mineral saturation indices.

A-3. HYDROGEOCHEMICAL MODEL

The neutralization and fate of the tailings fluid can be described by common geochemical controls. Groundwater plumes generated from acidic tailings fluid consist of three zones: the acid zone, neutralization zone, and transport zone as depicted in Figure A-3.1 (Shepard and Brown, 1982). These zones are discussed in detail in Sections A-3.1, A-3.2, and A-3.3. In Section A-3.4, the model is simulated using the geochemical model PHREEQM (Appelo et.al., 1994).

A-3.1 Acid Zone

In the acid zone, the tailings fluid is essentially unchanged. The acid zone is denuded of calcite and other minerals that will readily dissolve at the pH of the tailings fluid, so no significant precipitation or dissolution reactions occur within this zone.

The distance that the acid zone will migrate depends on the portion of aquifer materials composed of calcite and other minerals that will be readily dissolved by the acid. It also depends on the volume and acidity of the tailings fluid and the shape of the acid plume. Each of these variables are addressed in the following subsections.

A-3.1.1 Acidity of Tailings Fluid

For the purposes of this investigation, the acidity of the tailings fluid is defined as the amount of base required to increase the pH to 6. This definition is different from mineral acidity or CO_2 acidity. The end points for mineral acidity and CO_2 acidity are around pH 4.3 and 8.3, respectively. An end point at pH 6 is used to define the tailings fluid acidity for several reasons. First, pH is buffered by carbonate at approximately this pH. Second, neutralization of acidic tailings fluid by calcite dissolution is expected to result in a pH in this range because the partial pressure of carbon dioxide will exceed atmospheric values in these regions. Finally, pH values observed in the groundwater plume at the site within 500 ft of the tailings pile are between 6.4 and 7.3. Choosing a pH endpoint of 6, as is shown later, accounts for more than 99% of the tailings fluid acidity.

In the tailings fluid, there are four primary sources of acidity: aluminum (Al), iron (Fe), ammonium (NH_4^+), and hydrogen ion (H^+). Aluminum and iron account for approximately 90% of the acidity in the tailings fluid. According to ion-specific electrode analysis, the iron is essentially all ferric (Fe(III)). At pH 2, Al and Fe are highly soluble in water, but as the pH rises to 6, they become so insoluble that greater than 99.9% of their concentrations in the tailings fluid must precipitate. The likely minerals that precipitate in the neutralization zone are amorphous hydroxides, namely $Al(OH)_3$ and $Fe(OH)_3$, and kaolinite ($Al_2(Si_2O_5)(OH)_4$) (PNL, 1986; Longmire and Brookins, 1982).

The precipitation reactions reveal the acidities associated with these metals. For aluminum, the reactions are:

$$Al^{+3} + 3H_2O \Leftrightarrow Al(OH)_3(s) + 3H^+ \qquad \text{A-3.1}$$

and

$$2Al^{+3} + 2H_4SiO_4(aq) + H_2O \Leftrightarrow Al_2(Si_2O_5)(OH)_4(s) + 6H^+ \qquad \text{A-3.2}$$

Regardless of whether $Al(OH)_3$ or kaolinite is the endpoint, each mole of aluminum that precipitates will release three moles of hydrogen ions (H^+). Therefore, each mole of aluminum in the tailings fluid is assumed to contribute three moles of acidity.

For iron precipitation, the reaction is:

$$Fe^{+3} + 3H_2O \Leftrightarrow Fe(OH)_3(s) + 3H^+ \qquad \text{A-3.3}$$

Three hydrogen ions (H^+) are generated for each ferric iron ion that precipitates. Given the total Al and Fe concentrations in the tailings fluid (3370 mg/L Al and 4390 mg/L Fe, as presented in Table A-2.1.1), the equivalent acidities are 0.37 M (moles/liter) and 0.24 M, respectively.

In an open system, ammonium may degas as ammonia according to the following reaction:

$$NH_4^+ \Leftrightarrow NH_3(g) + H^+ \qquad \text{A-3.4}$$

The formation of ammonia is highly unfavored at low pH, but as the pH rises from 2 to 6, this reaction becomes approximately 10,000 times more favorable.

Ammonium can also be oxidized to nitrate in the presence of nitrifying bacteria, according to the following reaction (Chapelle, 1993):

$$NH_4^+ + 2O_2 \Leftrightarrow NO_3^- + H_2O + 2H^+ \qquad \text{A-3.5}$$

The presence of high concentrations of nitrate in some monitor well samples suggests that at least some of the ammonium is being converted to nitrate. This reaction contributes twice the acidity as ammonia off-gassing.

The concentration of ammonium in the tailings fluid is approximately 702 mg/L. If it is assumed that one half of all ammonium is converted to nitrate and the other half is degassed, then the ammonium in the tailings fluid contributes about 0.05 M of acidity, which accounts for approximately 7% of the total tailings fluid acidity.

The hydrogen ion concentration also contributes to total tailings fluid acidity, but it only accounts for about 2% of the acidity. The pH is equivalent to the negative log activity of hydrogen ion in the fluid. Thus, the activity of H^+ at a pH of 2.03 is $10^{-2.03}$ or 0.00933. The activity coefficient calculated by PHREEQE for the ionic strength of the fluid is 0.76 L/mole. The concentration of H^+ is equal to the H^+ activity divided by the H^+ activity coefficient (0.00933/0.76 = 0.012 M). Thus the H^+ concentration is 0.012 M, which is equal to its acidity contribution.

The sum of the acidity contributions from Al, Fe, NH_4^+ and H^+ is approximately 0.68 M. Therefore, the total tailings fluid acidity is approximately 0.68 M. These calculations are presented in Appendix A-2.

A base titration was performed on a 25 mL sample of tailings fluid collected in 1996. The pH of this sample was measured to be 2.07. Approximately 20 mL of 0.5 M NaOH (0.01 moles) was needed to raise the pH of the sample to 6. Dividing 0.01 moles by 25 mL equates to an acidity of 0.4 M. Thus, the calculated tailings fluid acidity exceeds the measured acidity. The calculated acidity (0.68 M) is conservatively assumed for the tailings fluid in this report.

A-3.1.2 Acid-Neutralizing Capacity of Aquifer Minerals

The tailings fluid acidity is neutralized as it dissolves calcite. As the pH rises from 2 to 6, the predominant reaction is:

$$CaCO_3(s) + 2H^+ \Leftrightarrow Ca^{+2} + H_2CO_3^0 \qquad \text{A-3.6}$$

This reaction shows that two moles of H^+ are needed and consumed for every mole of calcite dissolved. Therefore, as the pH rises from 2 to 6, approximately 0.34 moles (0.68/2 = 0.34) of calcite is dissolved by one liter of tailings fluid.

As explained in Section A-3.2, calcium from the dissolution of calcite precipitates as gypsum and carbonate is released as carbon dioxide. Thus, as the pH returns to the neutral range, calcite does not re-precipitate, at least not abundantly. The case is different for kaolinite, which is found in considerable quantities in the First Tres Hermanos sandstone. Though the kaolinite will initially be dissolved by acidic tailings fluid, either $Al(OH)_3$ or kaolinite will be the final end point for aluminum after the pH is neutralized (PNL, 1986; White et al., 1984; Stollenwerk, 1994; Longmire and Brookins, 1982).

The dissolution of kaolinite exchanges at a ratio of 3 H^+ ions for each Al^{3+} ion, as shown by Equation A-3.2. Dissolution can only occur at low pH. As a result, dissolution raises pH slightly but does not reduce the acidity of the fluid. As calcite dissolution raises the pH above 4, aluminum has to begin re-precipitating (Brookins, 1988). If it precipitates as kaolinite, no net buffering of the tailings fluid occurs. This is also the case if it precipitates as $Al(OH)_3$, as shown by the following reaction:

$$Al_2(Si_2O_5)(OH)_4(s) + H_2O \Leftrightarrow 2Al(OH)_3(s) + 2SiO_2(s) \qquad \text{A-3.7}$$

This reaction shows that the precipitation of silica and $Al(OH)_3$ from kaolinite dissolution neither produces nor consumes acidity. Thus, if kaolinite or aluminum hydroxide are the end points of the neutralization reactions at the site, as suggested by the literature, kaolinite will not contribute to the buffering capacity of the minerals along the flow path.

A-3.1.3 Size of Acid Zone

It is difficult to estimate the current size of the acid zone without accurate estimates of the original volume and original composition of tailings fluids. No samples from monitor wells have shown pH values lower than 6, so certainly the acid zone has not migrated as far as the closest monitor well. In fact, it is quite possible the acid zone has not migrated far at all due to the large calcite content in underlying sediments.

For this investigation, the *additional* volume of underlying sediments that will become denuded of calcite due to the migration of the *remaining* tailings fluid is calculated. This is a direct calculation because the 1996 volume of tailings fluid has been rigorously estimated and its composition is well-defined.

The volume of tailings fluid remaining in the pond and underlying sediments in 1996 is estimated to be 65.5 million gallons (INTERA, 1996). Given the calculated acidity for 1996 tailings fluid (0.68 M), this volume of tailings fluid can dissolve approximately 8.4×10^7 moles of calcite, i.e., (0.68 M)*(65,500,00 gal)*(3.79 L/gal)*(0.5 moles calcite per mole acidity) = 8.4×10^7 moles of calcite. The molecular weight of calcite is 0.1 kg/mole, which implies that this volume of tailings fluid can dissolve 8.4×10^6 kg of calcite. For the alluvium and Mancos shale, the calcite content is approximately 20%. Assuming a dry bulk density of 1.8 kg/L for these formations, approximately 0.36 kg per liter of formation is calcite (1.8 kg/L*20%). Therefore, the entire remaining volume of tailings fluid can be neutralized by 2.3×10^7 liters or 820,000 ft^3 of alluvium or Mancos shale. This volume is equivalent to about 2 acres by 10 feet deep, or 0.2 feet deep over 100 acres. These calculations are presented in Appendix A-2.

From the results in Table A-2.4.3.1, the First Tres Hermanos sandstone is composed of approximately 2% calcite. Assuming a dry bulk density of 1.8 kg/L for the sandstone implies that 0.036 kg per liter of formation is calcite (1.8 kg/L*2%). Thus, if we assume that the tailings fluid percolates downward directly into the FTH, and that calcite is the only mineral that will neutralize the acid, then approximately ten times the volume of alluvium or Mancos shale (8,200,000 ft^3) would be needed. This volume is equivalent to about 100 acres by 2 feet deep. This direct contact assumption provides an additional measure of conservatism for this analysis, and in fact is not supported by field data from wells constructed in the FTH directly beneath the pile (MW-106 through -109). In fact, it is possible that the acid zone may never reach the groundwater table, but be "stalled" in the vadose zone beneath the tailings. Measured pH values in the neutral range for the FTH wells immediately beneath the pile support this scenario.

These calculations indicate that the formations beneath the tailings contain a high acid-neutralizing capacity. When compared to the total estimated volume and acidity of the tailings fluid and the scale of the site, we conclude that the acid zone will not migrate far before the total acidity of the tailings fluid is neutralized.

Field data from monitor wells installed adjacent to the pile and even through the tailings pile indicate that the acid zone has not yet migrated to the groundwater beneath the tailings pile. In

fact, the tailings pile has existed for over 20 years with a significant potentiometric head for recharge into the groundwater, and still there is no evidence that the acid zone has reached the groundwater.

A-3.2 Neutralization Zone

In the neutralization zone, dissolution of calcite and kaolinite by the acidic tailings fluid raises the pH of the water and initiates a series of precipitation reactions that lowers the aqueous concentrations of many of the tailings fluid constituents (Longmire and Brookins, 1982). These reactions are described in this section. Similar sets of reactions can be found in PNL (1990) and White, et al. (1984).

A-3.2.1 Calcite Dissolution

When acid encounters calcite, calcite dissolves. The reaction, represented by the following equation, shows that as calcite dissolves, free calcium (Ca^{+2}) and aqueous carbonate is produced. The aqueous carbonate produced is in the form of carbonic acid ($H_2CO_3^0$), a weak acid. Carbonic acid is essentially aqueous carbon dioxide which can be released to the gas phase by the reaction

$$H_2CO_3^0 \Leftrightarrow CO_2(g) + H_2O \qquad \text{A-3.8}$$

During the process of calcite dissolution, hydrogen ions (H^+) are consumed. Hydrogen ions form a complex with carbonate to produce carbonic acid, which in turn may be converted to water by the out-gassing of carbon dioxide. Regardless of the fate of the hydrogen ions, the free hydrogen ions (H^+) are consumed, thereby raising the pH.

The dissolution of calcite ceases when the pH rises to a critical level, in this case around 6 to 6.5, depending on the concentrations of dissolved carbonate and calcium. At this critical level, the water is no longer undersaturated with respect to calcite, so no calcite will dissolve. As a result, this calcite-equilibrated water may migrate into the calcite-rich transport zone where no significant calcite dissolution occurs.

Calcite often contains a considerable magnesium (Mg) content, typically by isomorphous substitution of magnesium for calcium in calcite minerals. Thus, dissolution of calcite containing magnesium often results in increasing aqueous magnesium concentrations.

A-3.2.2 Kaolinite Dissolution

Dissolution of kaolinite consumes free hydrogen ions, thereby raising pH in acidic waters. However, it does not neutralize tailings fluid acidity because re-precipitation of dissolved aluminum produces as many free hydrogen ions as kaolinite dissolution consumes (refer to Section A-3.1.2).

A-3.2.3 $Fe(OH)_3$ (s) Precipitation

The high ferric iron, Fe(III), concentrations in the tailings fluid begin to react with water and precipitate when the pH increases to about 3 (Brookings, 1988). Fe(III) precipitates predominantly in the form of amorphous hydrous ferric oxide, $Fe(OH)_3$ (s), as shown in Equation A-3.3 (PNL, 1986; Stollenwerk, 1994).

Though recrystallization and redox reactions may convert precipitated iron into minerals such as magnetite, these more highly ordered and more complex minerals are slow to form and are difficult to model. They are also believed to have a negligible impact on the evolution of the tailings fluid as it migrates through the neutralization zone and into the transport zone.

Application of Le Chatelier's principle to this precipitation reaction implies that a decrease in the concentration of H^+ (increase in pH) will result in additional reaction of Fe^{+3} and H_2O, producing $Fe(OH)_3$ (s) and more H^+. Thus, as H^+ is consumed by calcite dissolution, Fe^{+3} precipitates and additional H^+ is produced. As discussed in Section A-3.1.1, generation of H^+ contributes to the acidity of the tailings fluid. This acidity contribution from iron helps to buffer the pH around 3. Therefore, as calcite dissolution continues to consume H^+, the pH will rise well above 3 only after nearly all of the iron in the water is precipitated.

A-3.2.4 Aluminum Precipitation

The high aluminum concentrations in the tailings fluid will precipitate as kaolinite (Longmire and Brookins, 1982) or as $Al(OH)_3$ (s) (PNL, 1986). The main difference is that aluminum does not precipitate in large quantities until the pH rises above 4 (Brookins, 1988). Thus, nearly all of the ferric iron will need to precipitate before the pH can rise to the range where the aluminum precipitates, at which point the pH will be buffered around 4 until nearly all of the aluminum precipitates.

A-3.2.5 Gypsum Precipitation

The calcium concentration in the original tailings fluid appears to be controlled by gypsum, $CaSO_4 2H_2O$(s) PHREEQM calculates a SI (saturation index, see Section A-2.1.3) of approximately 0.1 for gypsum in the 1996 tailings fluid described in Table A-2.1.1. This SI indicates approximate saturation with respect to gypsum.

As calcite dissolves, the calcium concentration increases, causing the fluid to become oversaturated with respect to gypsum. As a result, gypsum precipitates. The reaction is

$$Ca^{+2} + SO_4^{-2} + 2H_2O \Leftrightarrow CaSO_4 \bullet 2H_2O(s) \qquad \text{A-3.9}$$

$$CaCO_3(s) + 2H^+ + SO_4^{-2} + 2H_2O \Leftrightarrow CaSO_4 \bullet 2H_2O(s) + H_2CO_3^0 \qquad \text{A-3.10}$$

Combining this reaction with Equation A-3.6 implies the overall reaction

Thus, the calcium released from calcite dissolution precipitates as gypsum.

Along with free hydrogen, sulfate is consumed in the process. In moles, the amount of sulfate consumed is equivalent to the number of moles of calcite dissolved. Although other sulfate minerals, such as jurbanite and alunite may become oversaturated within the neutralization zone, gypsum appears to be the dominant sulfate precipitate resulting from neutralization of tailings fluids at similar sites (PNL, 1986). As a result, the aqueous concentration of sulfate will decrease within the neutralization zone, limiting the source concentration of sulfate for the transport zone.

A-3.3 Transport Zone

A contaminant plume in the transport zone is primarily limited by its source concentration, groundwater flow rates, and adsorption. The source concentration of a contaminant in the transport zone is limited by one of three factors, whichever provides the lowest concentration:

- the contaminant's concentration in the tailings fluid;
- the contaminant's solubility in the transport zone; or
- the contaminant's minimum solubility reached within the neutralization zone.

Other potentially important factors include the dilution effects of infiltrating surface water and the concentrating effects of evaporating groundwater. Precipitation is not a major process in the transport zone except, perhaps, when evaporation is considerable.

Groundwater flow rates and adsorption are the primary controls on the rate of migration of contaminants in the transport zone. Adsorption is typically represented by the distribution coefficient, Kd. The Kd of a constituent is an equilibrium ratio defined as

$$K_d = \frac{S}{C} \qquad \text{A-3.11}$$

where S is the adsorbed solute concentration (mass of constituent adsorbed per mass of aquifer material) and C is the aqueous solute concentration (mass of constituent dissolved per volume of groundwater). By definition, a Kd for a particular constituent is constant for a given set of environmental conditions, e.g., pH, groundwater chemistry, redox condition, temperature, etc., regardless of the solute concentration in solution. The Kd value is typically expressed in units of mL/g.

For migration in the saturated zone, the Kd and retardation factor (Rf) are related by the equation:

$$R_f = 1 + \frac{\rho_b}{\theta} K_d \qquad \text{A-3.12}$$

where ρ_b is the dry bulk density of the aquifer matrix and θ is the porosity. For a porosity of 0.3 and a ρ_b of 1.8 g/cc, which are reasonable values for the First Tres Hermanos sandstone, a Kd value of 0.1 mL/g corresponds to a R_f of 1.6. Similarly, a Kd of 1 mL/g implies a R_f of 7, and a Kd of 10 mL/g implies a R_f of 61. The retardation factor represents the ratio of the average velocity of groundwater to the average velocity of the contaminant.

Source concentrations and Kd values for the transport zone are addressed in detail in Section A-4.

A-3.4 PHREEQM Model of Chemical Reactive Transport of L-Bar Mill Tailings

A numerical code called PHREEQM (Appelo et.al., 1993) was used to simulate the chemical reactive transport of acidic tailings fluid through aquifer media containing calcite. The model is not intended to account for all known complexities at the site such as compositional variations in formations, heterogeneities, etc. Rather, it is intended to provide a simple conceptual model to elucidate the major chemical controls on the ground-water transport of tailings fluid components. Section A-3.4.1 describes the PHREEQM code and Section A-3.4.2 presents the results of PHREEQM simulations.

A-3.4.1 Description of PHREEQM Code

PHREEQM is a modification of PHREEQE, a code developed by the U.S. Geological Survey. PHREEQE is a code designed to model geochemical reactions based on ion-pairing and known thermodynamic equilibrium constants (Parkhurst, et al., 1980). PHREEQE can calculate mass transfer, pH, redox potential, and equilibrium concentrations for multi-phase mixtures. PHREEQM, developed by Appelo, et al. (1993), couples a one-dimensional transport code to PHREEQE so that chemical reactive transport can be simulated. When modeling the advection of a reactive solution through aquifer materials, a code like PHREEQM is required to conserve mass and maintain thermodynamic equilibrium for all components.

A-3.4.2 Model Results

The model simulates the transport and geochemical reactions that would occur in the First Tres Hermanos sandstone given an influx of sump tailings fluid having the major ion composition presented in Table A-2.1.1. The sandstone is assumed to contain calcite at a solid weight percentage of 2% prior to reaction with tailings fluid. For the modeling results presented in this report, kaolinite was not considered because it adds no acid-neutralizing capacity to the system (refer to Section A-3.1.2). The precipitating form of aluminum is assumed to be $Al(OH)_3$, as is the case in other similar models (PNL, 1986; White et al., 1984; Stollenwerk, 1994). In addition to calcite, a $Fe(OH)_3$ (s) content of approximately 1.8% is assumed based on the XRF results in

Table A-2.2.3.1. Background aqueous concentrations in the sandstone are assumed to be equal to the concentrations presented in Table A-2.2.1.1.

A simulation can demonstrate the effect of geochemical reactions on chemistries in the groundwater flow path. Figures A-3.4.2.1 through A-3.4.2.5 show the model results for aqueous and solid concentrations in the sandstone as a function of distance from the point at which tailings fluid is simulated to enter the sandstone. In the first figure, the tailings fluid has not yet entered the sandstone, so concentrations are constant at background levels. Groundwater flow is to the right in the direction of increasing distance and has an assumed linear velocity of 0.75 ft/yr (Nabil Shafike, Balleau Ground Water, personal communication, 1997). This velocity is derived as a representative average velocity based on pre-tailings contours and model results throughout the tailings pond operation. Normal background hydraulic gradients produced a flow of approximately 0.3 feet per year, while the current induced gradient from tailings seepage produced flows of approximately 2 feet per year. This artificial gradient is predicted to equilibrate back to the natural gradient as the pile dewaters over the next 20 years, so 0.75 feet per year is a conservative value for flow over the next 1000 years. A detailed discussion of groundwater flow is presented in Appendix B (BGW, 1997).

When the tailings fluid enters the sandstone, an immediate effect on aqueous and mineral concentrations is observed. Figures A-3.4.2.2 through A-3.4.2.5 show the concentration profiles at 2, 4, 6, and 8 years. As time increases, the length of aquifer that is denuded of calcite increases. At 8 years, calcite is dissolved from approximately 1.3 feet of aquifer while gypsum is precipitated in its place. Thus, the neutralization front is approximately located at 1.3 feet. Behind this front, the groundwater is acidic. There is a two-tiered decline in pH that develops in the neutralization zone between the neutralization front and the tailings fluid source. This result is due to the sequential precipitation and re-dissolution of Al and Fe, as explained in Sections A-3.2.3 and A-3.2.4.

Though the neutralization front reaches 1.3 feet in 8 years, the ground-water plumes of Cl, Na, Ca, SO_4, and H reach approximately 6 feet, assuming no retardation in the transport zone. The ratio of these distances implies that the retardation factor of the migration of the neutralization front is approximately 4.6. In the Mancos shale and alluvium, where calcite content is ten times higher than in the sandstone, the retardation factor would be about 46. Thus the natural retardation of contaminants in the geologic system beneath the tailings pile is quite significant.

A-4. FATE AND TRANSPORT OF TAILINGS FLUID CONTAMINANTS

The ground-water constituents of concern at the site are pH, Cl, SO_4, NO_3, U, Th-230, Ra-226, Ra-228, Se, Sb, and Ni. License-mandated concentrations of these constituents must not migrate to point-of-compliance wells within the regulatory time-frame. Slow ground-water advection of constituent plumes, low dispersion, adsorptive retardation, solubility constraints, and natural dilution can prevent potential non-compliance.

In this chapter, two geochemical controls are addressed that affect the fate and transport of important tailings fluid constituents: aqueous solubility limits and adsorption. These controls are discussed in Sections A-4.1 and A-4.2, respectively.

A-4.1 Source Concentrations for the Transport Zone

The pH changes from 2 to at least 6 as tailings fluid flows from the acid zone into the neutralization zone. This change alone results in a wide range of aqueous solubilities and partition coefficients for chemically reactive constituents. This change combined with the changing concentrations of other aqueous components in the neutralization zone results in changes of aqueous solubilities and partition coefficients that can only be predicted using a chemical equilibrium code such as PHREEQE.

This section addresses the solubility constraints that will limit the concentrations of certain constituents released to the transport zone. The minimum solubilities attained within the neutralization zone will limit the mobilities of constituents whose concentrations in the tailings fluid are greater than the minimum solubilities attained in the neutralization zone. For these constituents, the minimum solubilities obtained can be used as the predicted source concentrations for the transport zone.

Table A-4.1.1 summarizes the estimated source concentrations of the important constituents for the transport zone. Among these constituents, those having estimated source concentrations that are below tailings fluid concentrations are limited by solubility constraints. Each constituent is addressed in the following subsections.

Table A-4.1.1 Source Concentrations

Constituent	Concentration	Basis
Cl	750 mg/L	tailings concentration
Ni	2.5 mg/L	tailings concentration
NO_3	285 mg/L	field data, NH_4 oxidation
pH	6.5	carbonate buffered
Ra-226	3,000 pCi/L	tailings concentration
Ra-228	50 pCi/L	tailings concentration
Sb	< 0.05 mg/L	solubility limited
Se	6 mg/L	maximum tailings concentration
SO_4	10,000 mg/L	field data, gypsum precipitation
Th-230	165,000 pCi/L	tailings concentration
U	13 mg/L	solubility limited

A-4.1.1 Uranium

In the neutral pH range under oxidizing conditions, aqueous uranium is predominantly hexavalent and forms stable complexes with carbonate and phosphate. In groundwater under oxidizing conditions, uranium has been observed to migrate without considerable retardation (PNL, 1990; Hodge et al., 1996; Duff and Amrhein, 1996). The high mobility is typically attributed to the formation of highly stable uranyl carbonate complexes. However, in the case of uranium mill tailings sites, the concentrations of uranium in these plumes are usually far below the concentrations in acidic source tailings fluids and considerably below solubility limits in the transport zone. The reason appears to be a concentration-limiting pH value encountered in the neutralization zone.

The PHREEQM calculations in this report show that the continuous supply of calcite along the flow path ultimately raises the pH of the migrating L-Bar tailings fluid above 6. The solubility of uranium under these conditions was investigated using MINTEQA2, a USEPA chemical equilibrium code developed by Allison, et al. (1991).

MINTEQA2 calculations indicate that the aqueous solubility of the uranyl ion reaches a minimum between pH 5 and pH 6, depending on the partial pressure of carbon dioxide. The results of these calculations are depicted by the curves in Figure A-4.1.1.1. The theoretical maximum solubility is limited to approximately 13 mg/L by UO_2CO_3 around pH 5.8 in the neutralization zone if the partial pressure of carbon dioxide is 0.025 atm. At a partial pressure of 0.1 atm, the calculations predict that the minimum solubility occurs at pH 5.4 and equals 12 mg/L. Such high partial pressures of carbon dioxide will result due to the production of carbonic acid from calcite dissolution. The high carbonate concentrations in the groundwater samples collected near the toe

of the dam combined with the corresponding pH values indicate partial pressures of carbon dioxide that exceed 0.1 atm. As the pH of the migrating fluid rises above the pH of minimum uranium solubility, the uranium solubility increases considerably. However, because the precipitated uranium is immobilized in the neutralization zone and does not migrate with the fluid, the uranium in the fluid that migrates into the transport zone becomes undersaturated with respect to uranyl minerals. Thus, for modeling purposes, the minimum solubility attained in the neutralization zone can be used to establish the uranium source concentration for the transport zone.

The May 1998 field data indicate that the maximum observed uranium concentration in the groundwater plume down-gradient from the tailings source zone is around 3 mg/L in MW-69. This well is both a point-of-compliance well and a pumping well. It produces anomalously high flow rates when purged prior to sampling and is likely influenced by fracture flow, possibly directly from the tailings pond. This concentration is not far from the 12 to 13 mg/L minimum solubility predicted by MINTEQA2. Thus, based on 1) the observed concentrations within the uranium plume, 2) the widely-reported conservative behavior of uranium in the transport zone, and 3) the fact that MINTEQA2 predicts a minimum solubility limit of approximately the same magnitude as observed in the field, it is considered conservative to assume a transport zone source concentration at the theoretical solubility limit of 13 mg/L for uranium.

A-4.1.2 Thorium

The predominant thorium aqueous species in the neutral pH range depends on the pH and the concentration of dissolved phosphate. It is not subject to oxidation or reduction. In the absence of phosphate, $Th(OH)_4^0$ is the predominant thorium species above pH 5. In the presence of phosphate, even at concentrations as low as of 0.1 ppm, thorium phosphate complexes, such as $Th(HPO_4)_3^{-2}$, predominate in the pH range of 4 to 7 (Langmuir and Herm 1980). Alternatively, in the presence of high concentrations of carbonate above pH 6, thoriu rbonate complexes may predominate (Lemire and Caristo, 1989).

According to MINTEQA2 calculations using the database of Lemire and Garisto (1989), the formation of $Th(CO_3)_5^{6-}$ should increase thorium aqueous solubility to a thorium concentration on the order of 10 mg/L within the carbonate plume at L-Bar. One pCi/L of Th-230 equates to approximately 5×10^{-8} mg/L, or 0.05 parts per trillion. In most natural groundwaters, the *reactivity* ratio of Th-230 to Th-232 is approximately 0.8 (Langmuir and Herman, 1980). The reactivity of a compound in this case is the number of disintegrations of the compound per time per volume of water. In uranium mill tailings, the reactivity ratio has been reported as high as 1607, but on a mass basis, Th-232 still accounts for essentially all of the dissolved thorium (Langmuir and Herman, 1980). Assuming a Th-230 to Th-232 reactivity ratio of 1607, the corresponding isotope mass ratio is 0.0091. If this ratio is assumed for the tailings solution, which has a Th-230 radioactivity around 165,000 pCi/L (equivalent to a Th-230 concentration of 0.0084 mg/L), then the total thorium concentration in the tailings fluid would be around 1 mg/L. This concentration is an order of magnitude lower than the estimated solubility of thorium within the carbonate plume at L-Bar. Thus, the mobility of thorium in the neutralization and transport

zones may not be limited by solubility. As a result, it is assumed for conservative purposes that the source concentration for the transport zone equals the concentration in the tailings fluid. However, as discussed in Section A-4.2.5, significant retardation occurs by thorium adsorption to local aquifer materials.

A-4.1.3 Radium

Below pH 8, radium aqueous solubility is limited to approximately 0.001 mg/L by $RaSO_4$ (s) because of the high aqueous sulfate concentration at the site. This solubility is estimated using MINTEQA2 and the radium thermodynamic database of Langmuir and Riese (1985). The tailings fluid reactivities of Ra-226 and Ra-228 are approximately 3,000 and 50 pCi/L, respectively. These are equivalent to concentrations of 3×10^{-6} and 2×10^{-10} mg/L, respectively. Because these concentrations are far lower than the predicted aqueous solubility of radium, solubility likely will not limit radium migration at L-Bar. Consequently, the source concentrations of Ra-226 and Ra-228 for the transport zone are assumed to equal the concentrations observed in the tailings fluid.

A-4.1.4 pH

The pH is limited in the transport zone in a manner analogous to solubility. The PHREEQM model adopted in this report assumes a completely open system. As a result, it indicates that the pH will rise to approximately 7.2 before it can migrate in the transport zone without dissolving calcite. In a closed system, the pH would not rise past 6 because the carbonate would not be allowed to off-gas as carbon dioxide. The field data near the toe of the dam shows pH values in the range of 6.5, suggesting that the system is neither completely open nor completely closed. This is likely due to slow or limited off-gassing. Based on these data, it is assumed that the pH of the neutralized tailings fluid that enters the transport zone is around 6.5.

A-4.1.5 Sulfate

As calcite dissolves in the neutralization zone, the released calcium combines with dissolved sulfate to precipitate gypsum. This reduces the sulfate concentration from nearly 40,000 mg/L to around 10,000 mg/L. This decrease is predicted by the model and is supported by field data. Thus, the source concentration of sulfate for the transport zone is assumed to be 10,000 mg/L.

A-4.1.6 Chloride

Chloride is highly soluble in water and will not be limited by solubility at the concentrations observed at L-Bar. The source concentration of chloride for the transport zone is assumed to be 750 mg/L, which is approximately equal to the tailings fluid concentration and the concentrations observed in groundwater west of the dam.

A-4.1.7 Nickel

Below pH 7.5, the aqueous solubility of nickel is greater than 10 mg/L and increases with decreasing pH (Brookins, 1988). The concentration of nickel in the 1996 tailings fluid is below the detection limit of 4 mg/L. Therefore, the concentration of nickel entering the transport zone will not be limited by solubility.

In the case of nickel, with a variable detection limit not specifically tied to the drinking water standard, we refer to the arithmetic average of the 1991 through 1996 analytical results to estimate the source concentration at 2.5 mg/L.

A-4.1.8 Selenium

The oxidized form of selenium has a valency of +6 and is highly soluble in water (Brookins, 1988). The highest concentrations of selenium measured in the tailings fluid since 1991 is 6 mg/L, so this value is assumed to be the source concentration.

A-4.1.9 Antimony

Antimony has never been detected in the tailings fluid, even at detection levels as low as 0.1 mg/L, although this element is present in natural groundwater at the site. By using one-half of the minimum detection limit, we assume that the source concentration attributed to tailings fluid is 0.05 mg/L.

A-4.1.10 Nitrate

As explained in Section A-3.1.1, some of the ammonium in the tailings fluid will be oxidized to nitrate while much of the remainder will be released to the gas phase as ammonia. The field data suggest that only a small portion of the ammonia is converted to nitrate. Nitrate is known to migrate in groundwater without retardation under oxidizing conditions when there is no vegetation to intercept it (Drever, 1988). Thus, if we assume for conservatism that half of the total ammonia (570 mg/L total) is off-gassed and half is converted to nitrate, then the source concentration is identified at 285 mg/L.

A-4.2 Retardation in the Transport Zone

Retardation coefficients (Kd values) can vary over many orders of magnitude. For example, some thorium Kd measurements exceed 10^6 mL/g while others are negligible (see Section A-4.2.5). The large variation is due to the sensitivity of the Kd value to the various environmental conditions. For those elements that exhibit a high sensitivity to environmental conditions, estimated Kd values are rounded to the nearest order of magnitude. Kd values of zero are assigned when an element is assumed to migrate approximately as fast as water. Source values for the Kd terms in this study have been derived from literature values, results of adsorption modeling, and comparison of field velocities of contaminant plumes to groundwater velocities. A summary of the Kd values recommended for the important constituents is presented in Table A-4.2.1.

Table A-4.2.1 Kd Values for Constituents

Constituent	Kd (mL/g)
Cl	0
Ni	10
NO3	0
pH	0
Ra-226	10
Ra-228	10
Sb	0
Se	5
SO4	0
Th-230	100
U	0.1

A-4.2.1 Chloride

The movement of chloride (Cl^-) in an aquifer is representative of the movement and velocity of the groundwater because chloride does not appreciably adsorb to aquifer materials or precipitate (PNL, 1990). As a result, the Kd value for chloride is assumed to be zero.

Other source constituents entering the transport zone either closely track the movement of the chloride or travel more slowly. Those that move more slowly in the transport zone participate in adsorption/desorption reactions. Although the adsorbing constituents migrate as fast as chloride while dissolved in the water, their overall velocities are slowed by the fraction adsorbed at the same time. Those constituents with higher Kd values spend a higher percentage of time adsorbed and thus migrate more slowly than those with lower Kd values.

A-4.2.2 Sulfate, Carbonate, Calcium, and Sodium

Observations at L-Bar indicate that many of the major ions, including sulfate (SO_4), bicarbonate (HCO_3), calcium (Ca), and sodium (Na), move essentially as fast as chloride. As a result, these constituents are also assumed to have Kd values of zero.

Bicarbonate (HCO_3) is a special case because it is not present in the acidic mine tailings. Instead, it is produced by the dissolution of calcite in the neutralization zone. The close match in the trends of the chloride and bicarbonate concentrations is due to unretarded transport of bicarbonate in the transport zone down gradient from the neutralization zone. Slow off-gassing of carbon dioxide likely explains the decreasing bicarbonate concentrations with distance from the toe of the dam.

Sulfate (SO_4) trends suggest essentially unretarded transport in the transport zone but at concentrations far lower than in the tailings fluid. The reduced concentrations are due to the precipitation of gypsum ($CaSO_4 \bullet 2H_2O$) in the neutralization zone.

A-4.2.3 pH

The low pH of the tailings fluid (pH 2) will move slowly due to the pH buffering capacity of the alluvium, Mancos shale, and First Tres Hermanos formations along the groundwater flow path. However, as discussed in Section A-4.1.4, a small pH effect is observed in the transport zone, as predicted by the geochemical transport model. The field data indicates that the pH of fluids passing through the neutralization zone into the transport zone is approximately 6.5. At this pH, the hydrogen ion concentration can migrate nearly as fast as the groundwater because it is not high enough to react with, and dissolve, calcite or kaolinite. This trend is observed in the monitor well data, suggesting that a Kd of zero can be applied to a pH of 6.5 in the transport zone.

A-4.2.4 Uranium

Various studies of uranium adsorption under various conditions have been performed in the laboratory. One of the most thorough studies of the effects of carbonate concentration on the adsorption of uranium is documented in Waite et al. (1994). This study focused on adsorption to ferrihydrite, $Fe(OH)_3$, a generally ubiquitous natural adsorbent that tends to dominate adsorption reactions in aquifers. Waite et al. (1994) show that high concentrations of carbonate in groundwater considerably reduces the adsorption of uranyl complexes at neutral to high pH. The cause appears to be two-fold. First, adsorption of the aqueous uranyl carbonate species is low (Waite et al., 1994), and second, carbonate itself adsorbs strongly to ferrihydrite. In fact, adsorbed carbonate can occupy a large percentage of adsorption sites on oxide surfaces, considerably limiting adsorption of other ions, such as uranyl carbonate species (van Geen et al., 1994).

Field studies have shown that uranium mobility may be only slightly retarded by adsorption in the neutral pH range. Plumes of uranium and sulfate are coincident in groundwater down-gradient from a tailings pile in Riverton, Wyoming (White et al., 1984; PNL, 1990). Uranium mobility is also observed at the Federal American Partners uranium mill site in central Wyoming (PNL, 1990). Other studies also show low adsorption of uranium in the presence of carbonate (Hodge, et al., 1996; Duff and Amrhein, 1996). We have therefore conservatively assumed a Kd value of 0.1 mL/g for uranium in the transport zone.

A-4.2.5 Thorium-230

Thorium mobility in the transport zone is likely highly retarded by adsorption. High concentrations of carbonate have been shown to sharply decrease the adsorption of thorium on iron oxides (Murray and Coughlin, 1992) and alumina colloids (Righetto et al., 1988), but Kd values cannot be inferred from these studies for the conditions at L-Bar. In the absence of carbonate, adsorption to silica is low above pH 6 (Osthols, 1995). In a different study, Rancon (1973) measured Kd values on the order of 10^5 mL/g for a quartz-illite soil at pH 6. Carbonate was likely absent from these tests. In the same study, a Kd value of 10^6 mL/g was measured for quartz-illite-calcite-organic matter soil at pH 8. In this case, the presence of organic matter may have been responsible for the high adsorption observed, as shown by Langmuir and Herman (1980).

Consistent with these studies, a pH of 4 to 6 should allow for high adsorption of thorium to aquifer materials. This is the pH range of the neutralization zone. At these lower pH values, the thorium carbonate complex is less stable. Very high thorium adsorption in the neutralization zone is expected to prevent nearly all of the migration of thorium into the transport zone. The very small amount of thorium that does manage to enter the transport zone may be adsorbed to colloids (Murray and Coughlin, 1992).

Although very low concentrations of Th-230 may be only slightly retarded due to potential colloid migration, a thorium Kd value of 100 mL/g is proposed as a conservative estimate for the majority of thorium along the flow path. This Kd value is at least four orders of magnitude lower than those measured by Rancon (1973). Nevertheless, with a conservative Kd of 100, the thorium is effectively immobilized in the formation.

A-4.2.6 Radium

The radium concentrations in the tailings are much lower than radium aqueous solubilities. Therefore, precipitation will not occur. Instead, radium mobility will be limited by adsorption.

The Kd for radium adsorption to kaolinite is approximately 800 mL/g between pH 6 and 7, and increases as pH increases (Langmuir, 1997). Copenhaver et al. (1993) measured radium Kd values of approximately 60 mL/g in Connecticut aquifer solids. Radium also adsorbs strongly to silica (Langmuir, 1997). Based on these data, a conservative Kd value estimate for radium at the site is set at 10 mL/g.

A-4.2.7 Nickel

Nickel adsorbs fairly strongly to mineral surfaces. An overview of soil/surface sediment databases used in high-level radioactive waste repository performance assessments, Kd values for nickel ranged from 10 to 1000 mL/g (McKinley and Scholtis, 1993). For L-Bar, a Kd value of 10 mL/g is conservatively assumed.

A-4.2.8 Selenium

Selenium is known to adsorb to mineral surfaces. However, because they form negatively charged aqueous species, their Kd values are low in comparison to radium, thorium, and nickel at neutral to high pH values. For selenium, the Kd values used in performance assessment for soil/surface sediment range from 1 to 8 mL/g (McKinley and Scholtis, 1993). A value of 5 mL/g has been applied for L-Bar.

A-4.2.9 Antimony

Like selenium, antimony occurs in groundwater as a negatively charged species. As a result, it does not adsorb strongly to mineral surfaces which are also predominantly negatively charged. Though no elevated concentrations of antimony are observed in groundwater samples near the dam, nor has it been detected in the tailings fluid, a Kd value of 0 mL/g is conservatively assumed for the site. However, since it has not been identified as a constituent in the contaminant source, it is unlikely to affect groundwater quality at L-Bar.

A-4.2.10 Nitrate

Under oxidizing conditions and in the absence of vegetation, nitrate migrates in groundwater without retardation (Drever, 1988). Groundwater samples at L-Bar show that elevated nitrate concentrations occur over the same distance that elevated chloride concentrations occur. Thus, the Kd value for nitrate at the site is set at 0 mL/g.

A-5 CONCLUSIONS

The fluid beneath the surface of the tailings impoundment has a pH of around 2 and an estimated acidity of 0.68 M. Contributing to this acidity are dissolved aluminum (0.37 M), ferric iron (0.24 M), ammonium (0.05 M), and hydrogen ion (0.01 M). The total volume of this tailings fluid is estimated to be 65,500,000 gallons (INTERA, 1996); therefore, the total amount of acidity remaining in the fluids is approximately 170,000,000 moles.

The alluvium, Mancos shale, and First Tres Hermanos formations beneath the impoundment contain abundant calcite for acid neutralization. When contacted by acid, calcite dissolves producing free calcium ion (Ca^{2+}) and carbonic acid ($H_2CO_3^0$). The high sulfate concentrations in the tailings fluid combine with calcium to precipitate gypsum while carbonic acid slowly degasses as carbon dioxide.

The alluvium and Mancos shale have calcite contents of approximately 20%. As a result, approximately 820,000 ft^3 of alluvium or Mancos shale are needed to neutralize the acidity of the remaining tailings fluid. This volume translates to a depth of contact of about 0.2 feet over the approximate 110 acre tailings basin.

The First Tres Hermanos has a calcite content of around 2%; thus 8,200,000 ft^3 of First Tres Hermanos sandstone would be needed to neutralize the acidity of the remaining tailings fluid, should the full strength tailings fluid come into direct contact with the sandstone. Although this is highly unlikely to occur, the required volume of First Tres Hermanos sandstone for neutralization of all tailings fluid, given no buffering in the alluvium or Mancos Shale, is equivalent to approximately 2 feet depth over the area of the tailings basin.

Based on the small volume of formation required to neutralize the acidity of the remaining tailings fluid relative to the size of the tailings impoundment, the acid zone will never likely extend a considerable distance from the base of the tailings impoundment. In fact, much if not all, of the neutralization is expected to occur in the vadose zone between the base of the tailings and the groundwater. Based on observed neutral pH from wells completed in the sandstone directly beneath the impoundment, it appears that the acid front has not reached the groundwater in the FTH sandstone. Therefore, it is assumed that all migration of contaminants beyond the aerial boundaries of the tailings impoundment occurs only after tailings fluid has passed through the acid and neutralization zones and into the transport zone. In the transport zone, the pH is above 6 and no reactions other than adsorption occur.

The geochemical controls on contaminant migration in the transport zone are solubility and adsorption. Solubility controls the source concentration of a constituent entering the transport zone and adsorption controls the rate at which the constituent travels in the transport zone. The constituents of regulatory concern at the site are U, Th-230, Ra-226, Ra-228, pH, Ni, Se, Sb, NO_3, Cl, and SO_4.

The source concentration is limited by the tailings fluid concentration or by the minimum solubility encountered within the neutralization zone or transport zone. Analysis of field data, MINTEQA2 solubility calculations, and literature solubility data indicate or suggest that Th-230, Ra-226, Ra-228, Ni, and Cl are not limited by solubility at the site. Therefore, source concentrations for the transport zone are assumed to equal concentrations in the tailings fluid for these constituents. Uranium solubility is predicted by MINTEQA2 calculations to be limited within the neutralization zone between pH 5 and 6. Field data indicate the solubility limit in this zone, and thus the source concentration, is approximately 3 mg/L. MINTEQA2 calculations suggest a slightly higher minimum solubility (13 mg/L). For conservatism, the theoretical solubility is chosen as the source concentration for the transport zone. For pH, PHREEQM calculations and field observations suggest that its source value for the transport zone should be around 6.5. This pH value results from pH buffering by the carbonate system. Sulfate source concentrations in the transport zone are limited to 10,000 mg/L. PHREEQM calculations indicate that this limit results from the precipitation of gypsum. Se and Sb source concentrations also appear to be limited by solubility. Field data indicate source concentrations for these components are 6 mg/L and 0.05 mg/L, respectively. Finally, field data indicate an approximate source concentration for nitrate of around 285 mg/L. The likely explanation for the appearance of nitrate in the transport zone is that it is produced from ammonium as the tailings fluid encounters nitrifying bacteria (Chapelle, 1993).

Adsorption to mineral surfaces will retard the transport of several of the regulated constituents in the transport zone. Based on field data and the literature, those that are not appreciably adsorbed are Cl, SO_4, NO_3, Sb, and pH (around 6.5). In contrast, thorium, radium, and nickel are strongly adsorbed. Kd values assigned to these elements are 100 mL/g for thorium and 10 mL/g for radium and nickel. Less pronounced adsorption is predicted for Se, with a Kd of 5 and U with a Kd of 0.1. All these Kd values are considered conservative.

A-6. REFERENCES

Allison, J.D., D.S. Brown, and K.J. Nove-Gradac, 1991. MINTEQA2/PRODEFA2, a Geochemical Assessment Model for Environmental Systems: Version 3.0 User's Manual. Environmental Research Laboratory, Office of Research and Development, U.S. EPA, Athens, GA, 30613, EPA/600/3-91/021.

Appelo, C.A.J., P.R. Nienhuis, P.M.H. Smit, and A. Willemsen, 1993. PHREEQM Software. A.A. Balkama Publishers, Rotterdam, Netherlands.

BGW, 1997, Projected Long-Term Flow and Quality of Groundwater at the L-Bar, New Mexico, Uranium Site, Albuquerque, New Mexico, report for Kennecott Energy Company.

Brookins, D.G., 1988. *Eh-pH Diagrams for Geochemistry*. Springer-Verlag, New York.

Brookins, D.G., B.M. Thomson, P.A. Longmire, and P.G. Eller, 1993. Geochemical Behavior of Uranium Mill Tailings Leachate in the Subsurface. *Radioactive Waste Management and the Nuclear Fuel Cycle*, 17(3-4), pp. 269-287.

Bryson H.C, K. Bostick, P. Longmire, UMTRA Hydrology Group, 1988. *In Proceedings*: FOCUS Conference on Southwestern Ground Water Issues. National Water Well Association, Dublin, OH.

Chapelle, F.H., 1993. *Ground-Water Microbiology and Geochemistry*. John Wiley & Sons, Inc., New York.

Copenhaver, S.A., S. Krishnaswami, K.K. Turekian, N. Epler, and J.K. Cochran, 1993. Retardation of ^{238}U and ^{232}Th Decay Chain Radionuclides in Long Island and Connecticut Aquifers. *Geochimica et Cosmochimica Acta*, Vol. 57, pp. 597-603.

Drever, J.I., 1988. *The Geochemistry of Natural Waters*. Prentice Hall, Englewood Cliffs, NJ, 437 pp.

Duff, M.C., and C. Amrhein, 1996. Uranium (VI) Adsorption on Goethite and Soil in Carbonate Solutions. *Soil Sci. Soc. Am. J.*, Vol. 60, pp. 1393-1400.

Dzombak, D.A., and F.M.M. Morel, 1990. *Surface Complexation Modeling. Hydrous Ferric Oxide*. John Wiley & Sons, New York.

Hodge, V.F., K.H. Johannesson, and K.J. Stetzenbach, 1996. Rhenium, Molybdenum, and Uranium in Groundwater from the Southern Great Basin, USA: Evidence for Conservative Behavior. *Geochimica et Cosmochimica Acta*, 60(17), pp. 3197-3214.

INTERA, 1996. *Final Report: Hydrogeology Investigation of the L-Bar Uranium Mill Tailings Pile Cibola County, New Mexico,* report prepared for Kennecott Corporation on behalf of SOHIO Western Mining Company.

Langmuir, D., and J.S. Herman, 1980. The Mobility of Thorium in Natural Waters at Low Temperatures. *Geochimica et Cosmochimica Acta,* Vol. 44, pp. 1753-1766.

Langmuir, D., and A.C. Riese, 1985. The Thermodynamic Properties of Radium. *Geochimica et Cosmochimica Acta,* Vol. 49, pp. 1593-1601.

Lemire, R.J., and F. Garisto, 1989. The Solubility of U, Np, Pu, Th, and Tc in a Geological Disposal Vault for Used Nuclear Fuel. Atomic Energy of Canada Limited, Whiteshell Nuclear Research Establishment, Pinawa, Manitoba, ROE 1LO, AECL-10009.

Longmire, P.A., and D.G. Brookins, 1982. Geochemical Studies of Discharge Water From a Uranium Acid-Leach Process. New Mexico Society Guidebook, 33rd Field Conference, Albuquerque Country II.

McKinley, I.G., and A. Scholtis, 1993. A Comparison of Radionuclide Sorption Databases Used in Recent Performance Assessments. *J. Contam. Hydrology,* Vol. 13, pp. 347-363.

Moench, Robert H. and John S. Schlee, 1967. Geology and Uranium Deposites of the Laguna District, New Mexico, U.S. Geological Survey Prof. Paper 519, 117 pp.

Murray, J.W., and B.R. Coughlin, 1992. Competitive Adsorption: The Effect of Carbonate Alkalinity on the Adsorption of Lead, Thorium and Plutonium by Goethite (3αFeOOH). In: *Water Rock Interaction,* Kharaka & Maest (eds.), Balkema, Rotterdam.

Nordstrom, D.K., and J.L. Munoz, 1986. *Geochemical Thermodynamics.* Blackwell Scientific Publications, Palo Alto, CA.

Osthols E., 1995. Thorium Sorption on Amorphous Silica. *Geochimica et Cosmochimica Acta,* 59(7), pp. 1235-1249.

Parkhurst, D.L., D.C. Thorstenson, and L.N. Plummer, 1980. PHREEQE - A Computer Program for Geochemical Calculations. USGS/WRI-80-96., U.S. Geological Survey, Water Resources Division.

Pacific Northwest Laboratory (PNL), 1986. Predictive Geochemical Modeling of Contaminant Concentrations in Laboratory Columns and in Plumes Migrating from Uranium Mill Tailings Waste Impoundments. NUREG/CR-4520, U.S. Nuclear Regulatory Commission.

Pacific Northwest Laboratories (PNL), 1990. Mobilization and Transport of Uranium at Uranium Mill Tailings Disposal Sites: Application of a Chemical Transport Model. NUREG/CR-5169, U.S. Nuclear Regulatory Commission.

Righetto, L., G. Bidoglio, B. Marcandalli, and I.R. Bellobono, 1988. Surface Interactions of Actinides with Alumina Colloids. *Radiochimica Acta*, Vol. 44/45, pp. 73-75.

Schlee, J.S. and R.H. Moench, 1963. Geologic Map of the Moquino Quadrangle, New Mexico, U.S. Geological Survey, GQ-209.

Shepard, T.A., and S.E. Brown, 1982. A Generic Model of Contaminant Migration from Uranium Tailings Impoundments. Symposium on Uranium Mill Tailings Management, Fort Collins, Colorado, December 9-10, 1982, Geotechnical Engineering Program, Civil Engineering Department, Colorado State University.

Stollenwerk, K.G., 1994. Geochemical Interactions Between Constituents in Acidic Groundwater and Alluvium in an Aquifer near Globe, Arizona. *Applied Geochemistry*, Vol. 9, pp. 353-369.

van Geen, A., A.P. Robertson, and J.O. Leckie, 1994. Complexation of Carbonate Species at the Goethite Surface: Implications for Adsorption of Metal Ions in Natural Waters. *Geochimica et Cosmochimica Acta*, 58(9), pp. 2073-2086.

Waite, T.D., J.A. Davis, T.E. Payne, G.A. Waychunas, and N. Xu, 1994. Uranium(VI) Adsorption to Ferrihydrite: Application of a Surface Complexation Model. *Geochimica et Cosmochimica Acta*, 58(24), pp. 5465-5478.

White, A.F., J.M. Delany, T.N. Narasimhan, and A. Smith, 1984. Groundwater Contamination From an Inactive Uranium Mill Tailings Pile, 1. Application of a Chemical Mixing Model. *Water Resources Research*, 20(11), pp. 1743-1752, November 1984.

FIGURES

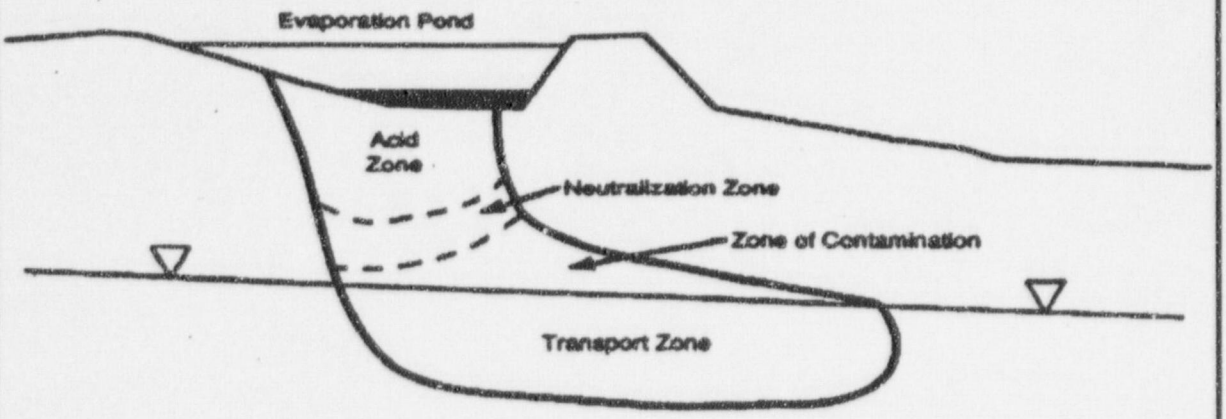

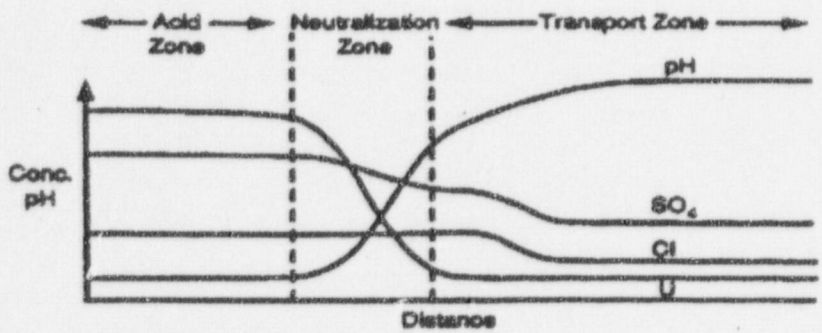

DATE: 6/22/98	Generic Uranium Mill Tailings Model (Sheppard and Brown, 1982)	
REF: 00137.00.0001.00.00005		
FILE: Genemod2.PPT		
DE&S Duke Engineering & Services	KENNECOTT-LBar	Figure A-3.1

Model Initial Background Ground Water Composition

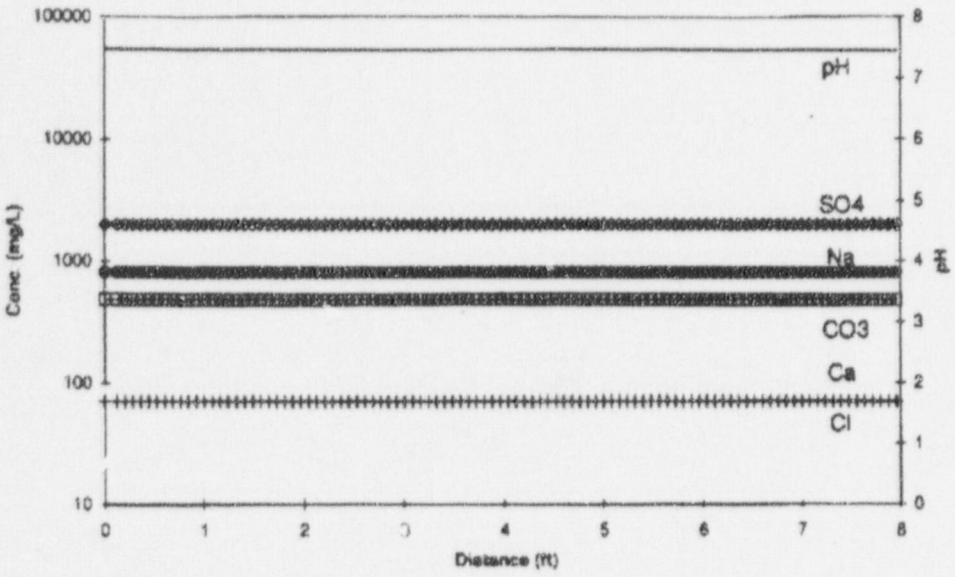

Model Initial First Tres Hermanos Mineral Concentrations

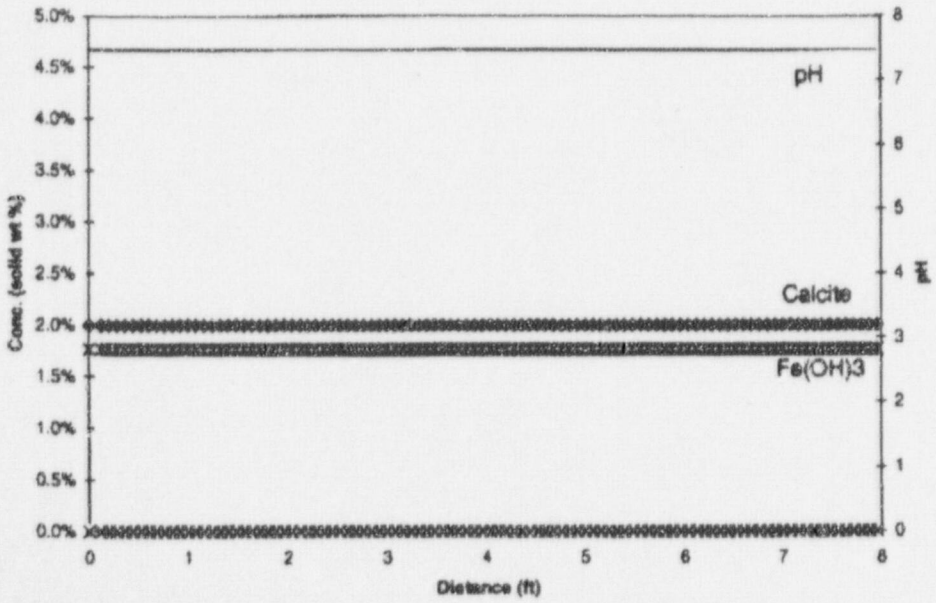

DATE: 6/22/98	Initial Mineral Concentrations	
REF: 00137.00.0001.00.00005		
FILE: Genemod2.PPT		
DE&S Duke Engineering & Services	KENNECOTT-LBar	Figure A-3.4.2.1

Simulation of 1996 Tailings Fluid Migration in First Tres Hermanos
(assumes 2% calcite in aquifer, 0.75 ft/yr gw velocity)
Aqueous Concentrations at 2 yrs

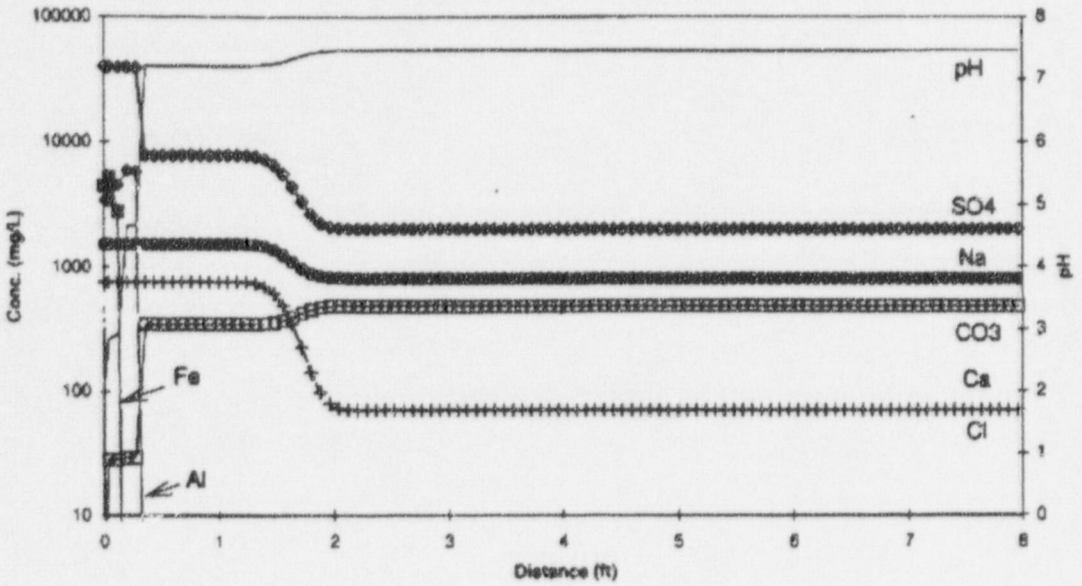

Mineral Concentrations at 2 yrs

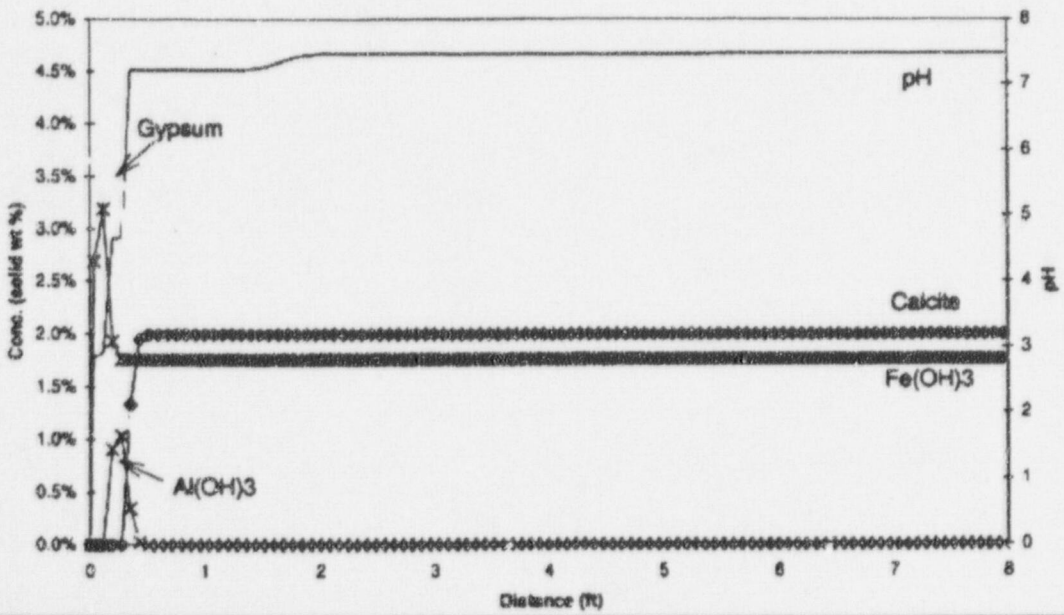

DATE: 6/22/98	Mineral Concentrations at 2 years	
REF: 00137.00.0001.00.00005		
FILE: Genemod2.PPT		
DE&S Duke Engineering & Services	KENNECOTT-LBar	Figure A-3.4.2.2

Simulation of 1996 Tailings Fluid Migration in First Tres Hermanos
(assumes 2% calcite in aquifer, 0.75 ft/yr gw velocity)
Aqueous Concentrations at 4 yrs

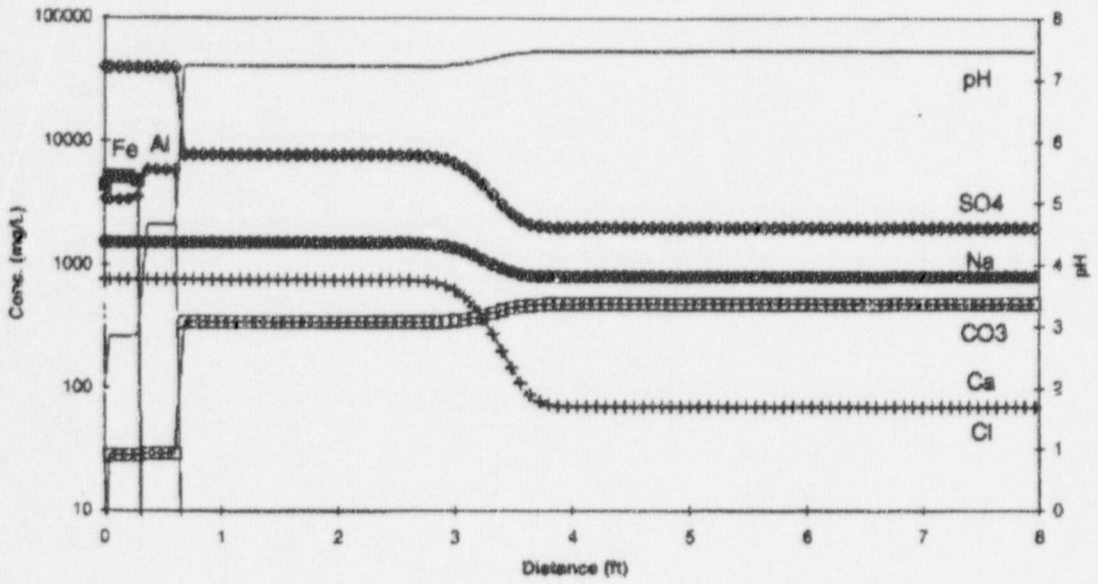

Mineral Concentrations at 4 yrs

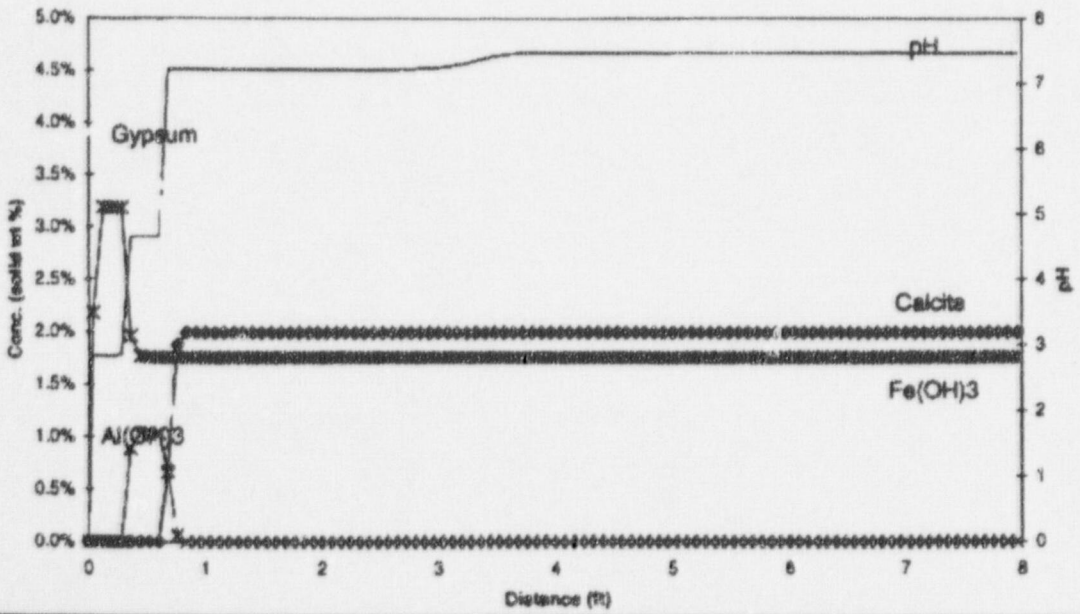

DATE: 6/22/98	Mineral Concentrations at 4 years	
REF: 00137.00.0001.00.00005		
FILE: Genemod2.PPT		
DE&S Duke Engineering & Services	KENNECOTT-LBar	Figure A-3.4.2.3

Simulation of 1990 Tailings Fluid Migration in [illegible] Tree Hermanos
(assuming 5% calcite in aquifer, 0.75 ft/yr gw velocity)
Aqueous Concentrations at 6 yrs

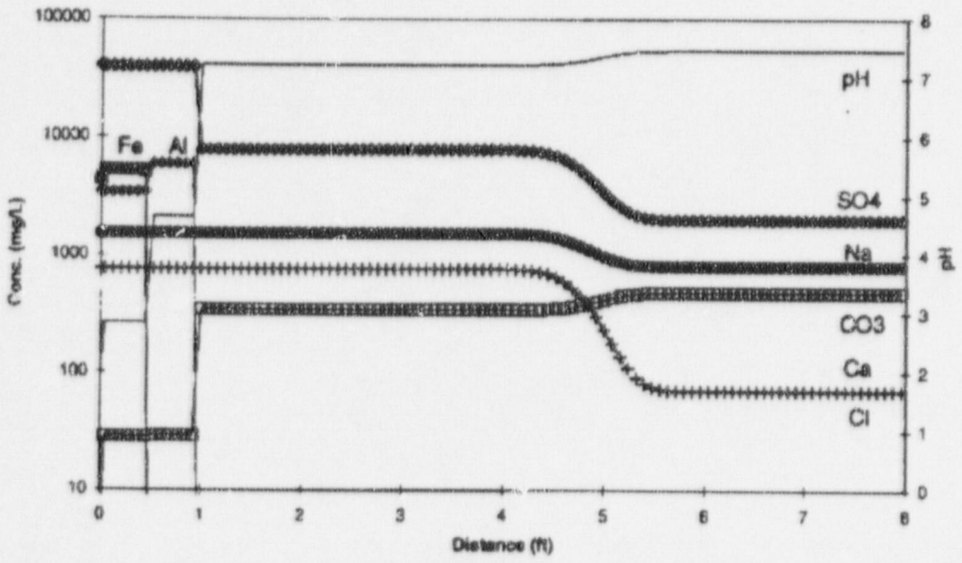

Mineral Concentrations at 6 yrs

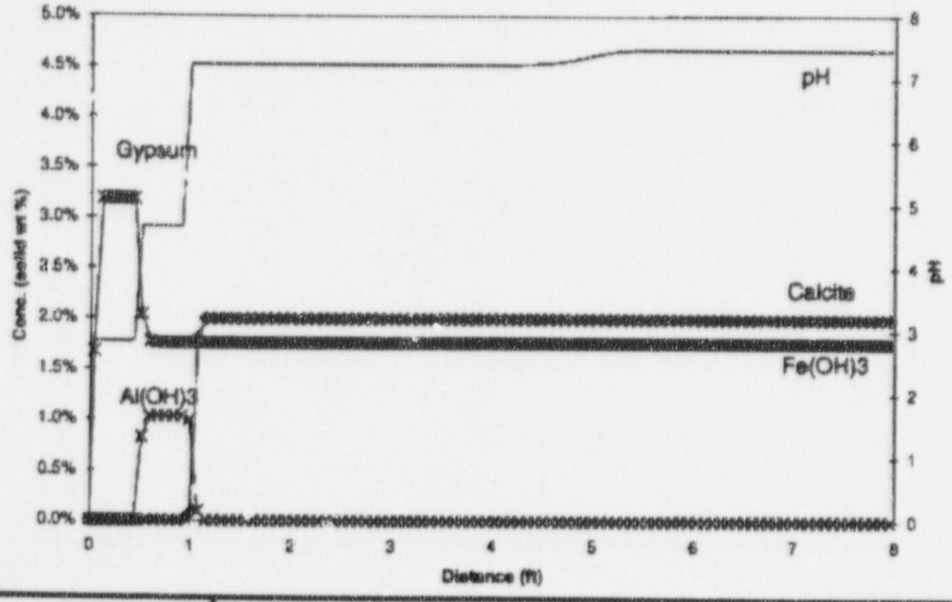

DATE: 6/22/98	Mineral Concentrations at 6 years
REF: 00137.00.0001.00.00005	
FILE: Genemod2.PPT	
DE&S Duke Engineering & Services	KENNECOTT-LBar
	Figure A-3.4.2.4

Simulation of 1996 Tailings Fluid Migration in First Tres Hermanos
(assumes 2% calcite in aquifer, 0.75 ft/yr gw velocity)
Aquesous Concentrations at 8 yrs

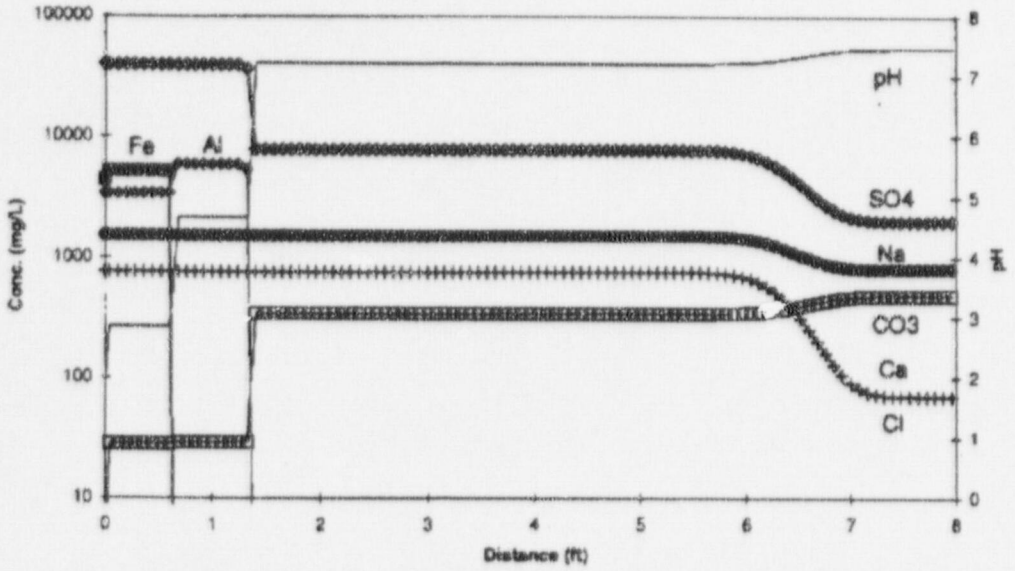

Mineral Concentrations at 8 yrs

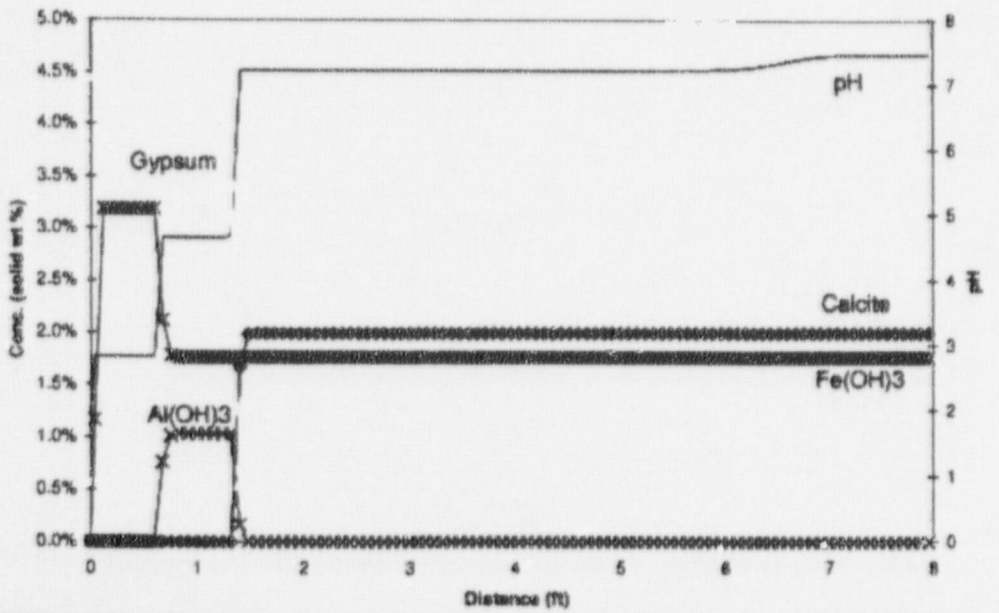

DATE: 6/22/98	Mineral Concentrations at 8 years	
REF: 00137.00.0001.00.00005		
FILE: Genemod2.PPT		
DE&S Duke Engineering & Services	KENNECOTT-LBar	Figure A-3.4.2.5

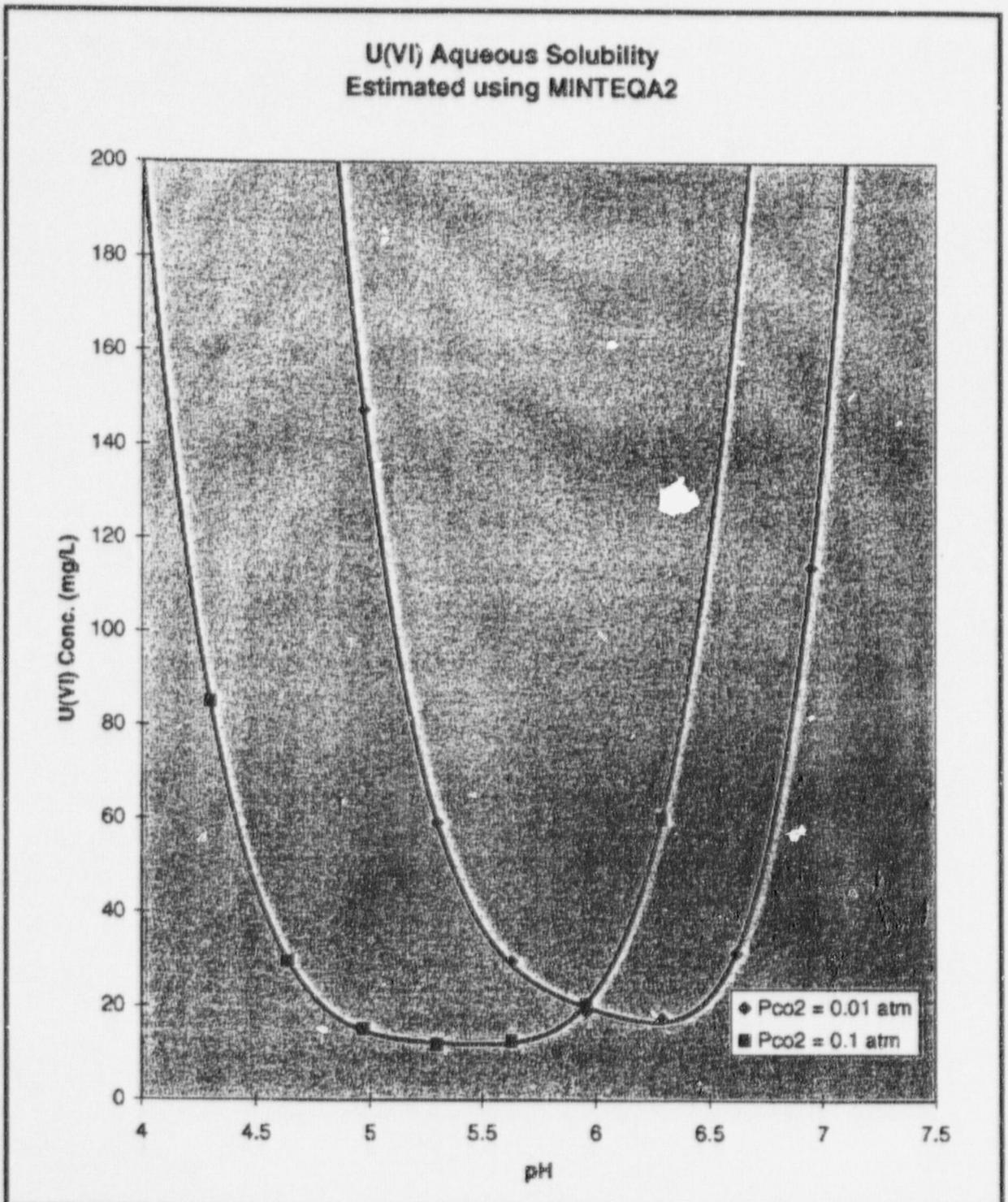

DATE: 6/22/98	Uranium Aqueous Solubility	
REF: 00137.00.0001.00.00005		
FILE: Genemod2.PPT		
DE&S Duke Engineering & Services	KENNECOTT-LBar	Figure A-4.1.1.1

APPENDIX A-1

MINERAL ANALYSIS REPORT

DE&S
Duke Engineering & Services

The Mineral Lab, Inc.
2700 Youngfield Suite 105
Lakewood, CO 80215
(303) 232-8708

October 4, 1996
Lab no. 960453

Mr. Andrew Backus
INTERA, Inc
6850 Austin Center Boulevard
Suite 300
Austin, Texas 78731

Dear Mr. Backus:

Enclosed are the x-ray fluorescence (XRF) and x-ray diffraction (XRD) analytical results and a sample index for 30 of the "L-Bar Project" samples received last week. The XRD results will be telefaxed to Ron Schott at DCM Science and the entire report will be telefaxed to you, as requested.

Twenty-two of the samples were too large as received to grind in our swing mill so were crushed to -1/4" size before grinding. A representative portion of each sample was ground to approximately -400 mesh in a steel swing mill and then analyzed by our standard "XRF-powder" procedure for 31 major, minor and trace elements. The relative precision/accuracy for this procedure is ~5-10% for major-minor elements and ~10--15% for trace elements (those elements listed in ppm) at levels greater than twice the detection limit in samples of average geologic composition. Two replicate samples and a standard reference material ("SY3", a Canadian standard rock) were analyzed with the samples to demonstrate analytical reproducibility for your samples and analytical accuracy for a geologic standard, respectively. The accepted ("known") values for the standard are listed with the XRF results.

A representative portion of each ground sample was packed into a well-type plastic holder and then scanned with the diffractometer over the range, 3-61° 2θ using Cu-Kα radiation. The samples were also prepared as "oriented mounts" by drawing a mixture of distilled water and ground sample onto a filter and rolling the filtrate onto a glass disk. Each oriented mount was scanned over the range, 2-22° 2θ, treated with glycol and then rescanned over the range, 2-15°. Analysis of oriented mounts aids in the identification of clay minerals. Estimates of mineral concentrations were made using our XRF--determined elemental compositions and the relative peak heights/areas on the XRD scans. The detection limit for an average mineral in these samples is ~1-3% (somewhat higher for clay minerals) and the analytical reproducibility is approximately equal to the square root of the amount. "Unidentified" accounts for that portion of the XRD scan which could not be resolved and a "?" indicates doubt in both mineral identification and amount.

Thank you for the opportunity to be of continuing service to INTERA.

Sincerely,

Peggy Dalheim

PD/ka

Peggy Dalheim

INTERA, Inc
Sample Identification Index for "L-Bar Project" Samples

October 4, 1996
Lab no. 960453

Sample Number	INTERA Sample Identification			
1	MW 106	50.0	53.5	WEATH. MANCOS
2	MW 106	53.5	55.0	TAN WEATH. FTH
3	MW 106	65.0	66.7	TAN FTH
4	MW 106	67.0	68.5	GREY FTH
5	MW 106	90.0	95.0	GREY FTH
6	MW 107	16.0	20.0	ALLUV.
7	MW 107	23.0	24.0	ALLUV.
8	MW 107	31.5	32.4	WEATH. MANCOS
9	MW 107	36.0	40.5	WEATH. MANCOS
10	MW 107	64.0	69.0	MANCOS
11	MW 107	77.5	80.5	GREY FTH
12	MW 107	90.5	95.5	GREY FTH
13	MW 107	104.0	109.0	GREY FTH
14	MW 107	115.5	120.5	GREY FTH
15	MW 108	21.0	23.0	ALLUV.
16	MW 108	31.0	32.0	SLIGHTLY WEATH. MA.
17	MW 108	49.0	51.0	MANCOS
18	MW 108	52.0	54.0	TAN FTH
19	MW 108	89.3	94.3	GREY FTH
20	MW 109	46.5	48.5	TAN FTH
21	MW 109	80.5	85.8	GREY FTH
22	FTH-SS EAST 1	TAN - WEATH FTH		
23	FTH-SS EAST 2	"		
24	FTH-SS WEST 1	"		
25	WEATH. MANCOS NORTH			
26	ALLUVIUM NORTH			
27	WEATH. MANCOS EAST			
28	ALLUVIUM EAST			
29	WEATH. MANCOS SOUTH			
30	ALLUVIUM SOUTH			

OUT OF RESPECTIVE DIVERSION CHANNELS.

Analysis performed by The Mineral Lab, Inc.

INTERA, Inc
Sample Identification Index for "L-Bar Project" Samples

October 4, 1996
Lab no. 960453

Sample Number	INTERA Sample Identification		
1	MW 106	50.0 -	53.5
2	MW 106	53.5 -	55.0
3	MW 106	65.0 -	66.7
4	MW 106	67.0 -	68.5
5	MW 106	90.0 -	95.0
6	MW 107	16.0 -	20.0
7	MW 107	23.0 -	24.0
8	MW 107	31.5 -	32.4
9	MW 107	36.0 -	40.5
10	MW 107	64.0 -	69.0
11	MW 107	77.5 -	80.5
12	MW 107	90.5 -	95.5
13	MW 107	104.0 -	109.0
14	MW 107	115.5 -	120.5
15	MW 108	21.0 -	23.0
16	MW 108	31.0 -	32.0
17	MW 108	49.0 -	51.0
18	MW 108	52.0 -	54.0
19	MW 108	89.3 -	94.3
20	MW 109	46.5 -	48.5
21	MW 109	80.5 -	85.8
22	FTH-SS EAST 1		
23	FTH-SS EAST 2		
24	FTH-SS WEST 1		
25	WEATH. MANCOS NORTH		
26	ALLUVIUM NORTH		
27	WEATH. MANCOS EAST		
28	ALLUVIUM EAST		
29	WEATH. MANCOS SOUTH		
30	ALLUVIUM SOUTH		

Analysis performed by The Mineral Lab, Inc.

INTERA, INC.
XRF-POWDER RESULTS FOR, "L-BAR PROJECT" SAMPLES.

OCTOBER 4, 1996
LAB NO. 960453

	WT %												
IDENT	Na2O	MgO	Al2O3	SiO2	P2O5	S	Cl	K2O	CaO	TiO2	MnO	Fe2O3	BaO
1	0.51	3.05	18.1	50.8	0.15	1.53	<0.02	2.71	8.64	0.68	0.02	4.61	0.04
2	0.42	2.88	6.84	74.7	0.06	<0.05	<0.02	1.22	5.13	0.27	0.02	2.07	0.02
3	0.27	0.77	2.80	92.7	<0.05	<0.05	<0.02	0.64	0.52	0.12	<0.01	1.02	0.01
4	0.34	1.55	4.47	86.1	<0.05	0.22	<0.02	0.91	1.91	0.18	0.01	1.27	0.01
5	0.25	1.73	4.66	82.9	0.05	0.30	<0.02	1.05	2.47	0.17	0.01	1.98	0.01
6	0.57	2.43	16.0	55.1	0.10	0.62	<0.02	2.23	2.63	0.82	0.05	6.04	0.05
7	0.44	1.81	10.7	35.9	0.15	2.51	0.03	1.48	19.7	0.52	0.05	5.76	0.03
8	0.31	2.09	10.9	36.4	0.09	0.86	<0.02	1.77	24.1	0.46	0.04	3.94	0.02
9	0.32	2.10	10.6	36.3	0.10	0.22	<0.02	1.66	26.1	0.42	0.04	4.09	0.01
10	0.39	2.60	15.0	47.9	0.11	0.30	<0.02	2.56	13.9	0.55	0.02	3.75	0.03
11	0.32	2.07	8.45	70.6	0.06	0.32	<0.02	1.38	6.30	0.32	0.02	2.27	0.02
12	0.27	1.06	3.22	87.3	<0.05	0.15	<0.02	0.73	1.37	0.16	0.01	1.29	0.01
13	0.21	1.58	5.43	77.2	0.06	0.40	<0.02	1.01	5.23	0.22	0.02	2.14	0.01
14	0.26	1.71	5.30	83.8	0.06	0.30	<0.02	1.11	1.36	0.18	<0.01	1.90	0.01
15	0.31	1.91	10.5	38.1	0.08	0.51	<0.02	1.51	19.3	0.48	0.09	4.94	0.06
16	0.12	1.97	11.0	34.1	0.12	0.22	<0.02	1.37	25.2	0.36	0.03	3.14	0.03
17	0.20	3.18	16.1	50.9	0.15	0.16	<0.02	2.80	8.34	0.66	0.03	4.35	0.03

ANALYSIS PERFORMED BY THE MINERAL LAB, INC.

OCTOBER 4, 1996
LAB NO. 960453

	WT %												
IDENT	Na2O	MgO	Al2O3	SiO2	P2O5	S	Cl	K2O	CaO	TiO2	MnO	Fe2O3	BaO
18	0.20	0.95	3.25	83.8	<0.05	0.20	<0.02	0.69	3.73	0.13	0.02	1.74	0.01
19	0.23	1.75	4.85	81.4	0.07	0.31	<0.02	1.05	1.83	0.19	0.01	2.26	<0.01
20	0.21	0.52	2.43	89.8	<0.05	0.21	<0.02	0.56	0.58	0.14	0.01	1.47	<0.01
21	0.19	1.31	4.02	75.7	0.07	0.25	<0.02	0.99	7.93	0.15	0.04	1.93	0.01
22	0.30	0.46	3.38	86.2	<0.05	<0.05	<0.02	0.89	2.19	0.09	<0.01	1.28	0.03
23	0.26	0.38	4.02	89.4	<0.05	<0.05	<0.02	0.84	0.10	0.11	0.01	1.27	0.02
24	0.13	0.38	3.05	89.5	<0.05	<0.05	<0.02	0.60	0.47	0.15	0.01	1.18	0.01
25	0.34	2.42	15.1	49.4	0.05	2.07	<0.02	2.05	6.77	0.64	0.03	5.96	0.02
26	0.43	2.10	14.9	54.5	0.11	0.78	<0.02	2.27	3.76	0.67	0.03	4.57	0.04
27	0.34	2.16	12.3	39.3	0.13	0.47	<0.02	1.77	20.0	0.48	0.04	4.47	0.02
28	0.29	2.23	14.6	49.8	0.09	0.76	<0.02	2.14	8.38	0.72	0.05	5.48	0.05
29	0.16	1.54	8.83	30.9	0.06	0.70	<0.02	1.57	24.4	0.37	0.03	3.46	<0.01
30	0.23	2.23	14.3	44.1	0.08	1.07	<0.02	1.84	8.28	0.57	0.03	4.32	0.02
QUALITY CONTROL - REPLICATE (R) SAMPLES AND STANDARD REFERENCE MATERIAL (SY3) ANALYZED WITH SA[illegible]3													
1(R)	0.45	2.85	16.2	46.5	0.13	1.33	<0.02	2.49	7.99	0.63	0.02	4.33	0.03
15(R)	0.30	1.91	10.3	37.5	0.08	0.50	<0.02	1.49	19.0	0.47	0.09	4.90	0.06
SY3-XRF	3.99	2.60	11.9	57.5	0.71	<0.05	<0.02	4.20	7.93	0.12	0.30	6.29	0.05
SY3-known	4.15	2.67	11.8	59.7	0.54	0.05	0.014?	4.20	8.26	0.15	0.32	6.45	0.05

ANALYSIS PERFORMED BY THE MINERAL LAB, INC.

INTERA, INC.
XRF-POWDER RESULTS FOR, "L-BAR PROJECT" SAMPLES.

OCTOBER 4, 1996
LAB NO. 960453

	PPM												
IDENT	V	Cr	Co	Ni	W	Cu	Zn	As	Sn	Pb	Mo	Sr	U
1	119	75	<10	31	<10	11	113	<20	98	14	<10	301	10
2	29	45	<10	11	<10	<10	30	<20	52	<10	<10	93	20
3	15	67	<10	12	<10	<10	<10	<20	<50	<10	<10	31	<10
4	19	54	<10	10	<10	<10	16	<20	<50	<10	<10	45	<10
5	20	65	<10	14	<10	<10	18	<20	<50	<10	<10	76	<10
6	123	63	<10	32	<10	15	89	<20	123	<10	<10	369	63
7	321	65	<10	32	<10	37	82	<20	96	10	<10	593	65
8	122	41	<10	25	<10	16	84	<20	67	13	<10	809	<10
9	114	37	<10	23	<10	16	76	<20	62	11	<10	644	<10
10	111	73	<10	29	<10	<10	75	<20	76	<10	<10	409	<10
11	52	69	<10	16	<10	<10	29	<20	60	<10	<10	122	<10
12	14	73	<10	14	<10	<10	11	<20	<50	<10	<10	39	<10
13	27	64	<10	11	<10	<10	19	<20	<50	<10	<10	151	<10
14	24	50	<10	11	<10	<10	15	<20	<50	<10	<10	52	<10
15	87	41	<10	26	<10	<10	68	<20	106	<10	<10	493	<10
16	74	44	<10	11	<10	<10	44	<20	75	15	<10	778	16
17	124	82	<10	20	<10	14	105	<20	95	<10	<10	250	<10

ANALYSIS PERFORMED BY THE MINERAL LAB, INC.

ANTERA, INC.
XRF-POWDER RESULTS FOR, "L-BAR PROJECT" SAMPLES.

OCTOBER 4, 1996
LAB NO. 960453

	PPM												
IDENT	V	Cr	Co	Ni	W	Cu	Zn	As	Sn	Pb	Mo	Sr	U
18	17	72	<10	13	<10	<10	10	<20	<50	<10	<10	85	<10
19	22	80	<10	15	<10	<10	19	<20	56	<10	<10	54	<10
20	13	102	<10	17	<10	<10	<10	<20	<50	<10	<10	32	<10
21	22	65	<10	11	<10	<10	15	<20	76	<10	<10	164	<10
22	11	76	<10	12	<10	<10	<10	<20	<50	<10	<10	64	<10
23	13	71	<10	16	<10	<10	10	<20	<50	<10	<10	27	<10
24	15	66	<10	11	<10	<10	<10	<20	<50	<10	<10	30	<10
25	115	57	<10	28	<10	20	90	<20	108	<10	<10	234	<10
26	87	51	<10	25	<10	12	74	<20	98	<10	<10	251	13
27	103	42	<10	20	<10	16	78	<20	83	11	<10	696	<10
28	103	59	<10	27	<10	19	89	<20	112	<10	<10	500	<10
29	105	27	<10	21	<10	11	74	<20	99	<10	<10	759	<10
30	85	54	<10	26	<10	<10	79	<20	100	<10	<10	733	<10
QUALITY CONTROL													
1(R)	108	71	<10	29	<10	12	106	<20	90	10	<10	280	<10
15(R)	86	37	<10	25	<10	<10	67	<20	94	<10	<10	474	<10
SY3-XRF	47	<10	<10	12	59	18	265	20	<50	162	<10	324	551
SY3-known	51	10	12	11	--	16	250	20	--	130	--	306	650

ANALYSIS PERFORMED BY THE MINERAL LAB, INC.

INTERA, INC.
XRF-POWDER RESULTS FOR, "L-BAR PROJECT" SAMPLES.

OCTOBER 4, 1996
LAB NO. 960453

	PPM				
IDENT	Th	Nb	Zr	Rb	Y
1	36	15	159	105	47
2	25	<10	297	39	28
3	20	<10	193	21	17
4	<10	<10	194	28	18
5	<10	<10	138	28	18
6	<10	15	216	85	54
7	<10	12	138	68	45
8	<10	<10	93	70	32
	<10	<10	93	63	29
10	<10	11	126	91	31
11	<10	<10	301	41	28
12	15	<10	264	22	14
13	11	<10	270	28	23
14	<10	<10	119	30	17
15	<10	<10	180	56	28
16	<10	11	96	40	30
17	29	11	159	106	44

ANALYSIS PERFORMED BY THE MINERAL LAB, INC.

OCTOBER 4, 1996
LAB NO. 960453

	PPM				
IDENT	Th	Nb	Zr	Rb	Y
18	<10	<10	178	17	16
19	<10	<10	121	32	16
20	<10	<10	245	11	16
21	11	<10	114	30	24
22	<10	<10	91	27	10
23	<10	<10	77	24	13
24	<10	<10	216	16	10
25	<10	<10	137	99	44
26	<10	12	255	82	43
27	<10	<10	110	65	32
28	<10	11	209	90	47
29	<10	<10	76	56	22
30	<10	10	142	83	36
QUALITY CONTROL					
1(R)	<10	12	149	88	39
15(R)	17	<10	183	60	37
SY3-XRF	866	152	326	177	686
SY3-known	990	145	320	208	740

ANALYSIS PERFORMED BY THE MINERAL LAB, INC.

INTERA, Inc
XRD Results for "L-Bar Project" Samples

October 4, 1996
Lab no. 960453

Mineral	Approx Wt % 1	2	3	4	5	6	7	8	9	10
Quartz	26	60	88	77	74	25	10	8	16	17
Plagioclase feldspar	<5	<5	<5	<5	<3	5	<5	<5?	<5	<3?
K-feldspar	<5	<5	<5	<5	<5	<5	<5	--	<3?	<5
Kaolinite	24	9	<5	8	7	6	--	--	13	10
Mica/illite	14	--	--	<5	<5	--	<5?	5	<5	12
Smectite	--	--	--	--	--	54	37	37	12?	30
Illite-smectite*	--	<10?	--	--	--	--	--	--	--	--
Chlorite	<5	--	--	--	--	--	--	--	--	--
Palygorskite	--	--	--	--	--	--	--	--	--	--
Calcite	7	3	--	<3	<3	--	25	35	40	20
Dolomite	7	12	<5	<5	<5	--	--	<3?	<3	<5
Gypsum	8	--	--	--	--	3	10	5	<3	--
Jarosite	--	--	--	--	--	--	<5	--	--	--
Pyrite	--	--	--	<1	<1	--	--	--	--	<1
Scawtite	--	--	--	--	--	--	--	--	<3?	--
"Unidentified"	<5	<5	<5	<5	<5	<5	<5	<5	<5	<5

*Mixed-layer clay?

Analysis performed by The Mineral Lab, Inc.

INTERA, Inc
XRD Results for "L-Bar Project" Samples

October 4, 1996
Lab no. 960453

	Approx Wt %									
Mineral	**11**	**12**	**13**	**14**	**15**	**16**	**17**	**18**	**19**	**20**
Quartz	55	80	68	75	20	10	27	80	75	86
Plagioclase feldspar	<3	<5	<3	<3	<3	--	<5	<3	<3	<3
K-feldspar	<5	<5	<5	<5	<3	<3?	<3?	<3	<3	<3
Kaolinite	12	7	8	8	5	<5	14	<5	7	5
Mica/illite	7	--	<5?	<5	<5	<5	20	<3	5	--
Smectite	--	--	--	--	28	36	<10?	--	--	--
Illite-smectite*	--	--	--	--	--	--	--	--	--	--
Chlorite	--	--	--	--	--	--	<5	--	--	--
Palygorskite	<10?	--	--	--	--	--	--	--	--	--
Calcite	8	<2	7	<1	33	40	12	5	<2	--
Dolomite	<5	<5	<5	<5	--	--	<5	<3	<5	<3
Gypsum	--	--	--	--	<3	<3	<1	--	--	--
Jarosite	--	--	--	--	--	--	--	--	--	--
Pyrite	<1	<1	<1	<1	--	--	--	--	<1	--
Scawtite	--	--	--	--	--	--	--	--	--	--
"Unidentified"	<5	<5	<5	<5	<5	<5	<5	<5	<5	<5

*Mixed-layer clay?

Analysis performed by The Mineral Lab, Inc.

October 4, 1996
Lab no. 960453

Approx Wt %

Mineral	21	22	23	24	25	26	27	28	29	30
Quartz	66	81	83	85	11	22	12	17	11	15
Plagioclase feldspar	<3	<5	<3	<3	<3	5	<3	<3	<3	5
K-feldspar	<5	<5	5	<5	<3	<5	<3	<3	<3	5
Kaolinite	7	6	7	7	<5	8	<5	5	<5	16
Mica/illite	--	--	--	--	--	<5	<5	<5	--	<5?
Smectite	--	--	--	--	63	45	40	52	33	33
Illite-smectite*	--	--	--	--	--	--	--	--	--	--
Chlorite	--	--	--	--	--	--	<5	--	--	--
Palygorskite	<5?	--	--	--	--	--	--	--	--	--
Calcite	12	3	--	<1	<5	4	34	12	41	9
Dolomite	<5	<1?	--	--	<5	<3?	--	--	--	<5
Gypsum	--	--	--	--	11	4	<3	4	4	6
Jarosite	--	--	--	--	--	--	--	--	--	--
Pyrite	<1	--	--	--	--	--	--	--	--	--
Scawtite	--	--	--	--	--	--	--	--	--	--
"Unidentified"	<5	<5	<5	<5	<5	<5	<5	<5	<5	<5

*Mixed-layer clay?

Analysis performed by The Mineral Lab, Inc.

The Mineral Lab, Inc.
2700 Youngfield Suite 105
Lakewood, CO 80215
(303) 232-8708

November 15, 1996
Lab no. 960519

Mr. Andrew H. Backus
Intera, Inc
6850 Austin Center Blvd
Suite 300
Austin, Texas 78731

Dear Mr. Backus:

Enclosed are the x-ray fluorescence (XRF) and x-ray diffraction (XRD) analytical results for the nine "L-Bar Project, Fracture Filling" samples received last week.

A representative portion of each sample was ground to approximately -400 mesh in a steel swing mill and then analyzed by our standard "XRF-powder" procedure for 31 major, minor and trace elements. The relative precision/accuracy for this procedure is ~5-10% for major-minor elements and ~10–15% for trace elements (those elements listed in ppm) at levels greater than twice the detection limit in samples of average geologic composition. A replicate sample and a standard reference material ("SY3", a Canadian standard rock) were analyzed with the samples to demonstrate analytical reproducibility for your samples and analytical accuracy for a geologic standard, respectively. The accepted ("known") values for the standard are listed with the XRF results.

A representative portion of each ground sample was packed into a well-type plastic holder and then scanned with the diffractometer over the range, 3-61° 2θ using Cu-Kα radiation. All of the samples were also prepared as "oriented mounts" by drawing a mixture of distilled water and ground sample onto a filter and rolling the filtrate onto a glass disk. Each oriented mount was scanned over the range, 2-40° 2θ, treated with glycol and then rescanned over the range, 2-22°. Analysis of oriented mounts aids in the identification of clay minerals. Estimates of mineral concentrations were made using our XRF–determined elemental compositions and the relative peak heights/areas on the XRD scans. The detection limit for an average mineral in these samples is ~1-3% (somewhat higher for clay minerals) and the analytical reproducibility is approximately equal to the square root of the amount. "Unidentified" accounts for that portion of the XRD scan which could not be resolved and a "?" indicates doubt in both mineral identification and amount.

Thank you for the opportunity to be of continuing service to Intera.

Sincerely,

Peggy Dalheim

PD/ka

INTERA, INC
XRF-POWDER RESULTS FOR "L-BAR PROJECT, FRACTURE FILLING SAMPLES"

NOVEMBER 14, 1996
LAB NO. 960519

	WT %												
IDENT	Na2O	MgO	Al2O3	SiO2	P2O5	SO3	Cl	K2O	CaO	TiO2	MnO	Fe2O3	BaO
MW106 50.5	0.12	0.60	3.13	10.6	<0.05	37.4	<0.02	0.54	27.6	0.15	0.01	0.83	0.02
MW106 53.0	0.30	1.54	13.8	26.6	0.06	26.1	<0.02	1.27	18.0	0.43	0.02	2.55	0.03
MW107 36.5	0.14	0.77	4.22	14.4	<0.05	28.2	<0.02	0.65	32.8	0.16	0.02	1.04	<0.01
MW107 46.3	0.30	2.14	14.7	28.7	0.12	19.3	<0.02	0.79	20.5	0.29	0.02	3.67	0.02
MW107 48.3	0.11	0.64	3.77	8.07	<0.05	34.8	<0.02	0.18	33.5	0.15	0.02	1.21	0.01
MW107 55.2	0.21	1.30	6.68	21.1	0.07	23.2	<0.02	1.17	30.1	0.25	0.02	2.09	0.01
MW108 40.8	0.09	1.20	9.52	22.8	<0.05	30.1	<0.02	1.18	21.8	0.33	0.01	2.56	0.04
MW108 48.5	0.06	0.53	3.03	9.98	<0.05	39.3	<0.02	0.55	29.0	0.12	0.06	0.85	<0.01
MW108 51.6	<0.05	0.31	1.98	6.17	<0.05	43.5	<0.02	0.35	30.5	0.08	<0.01	0.58	<0.01
QUALITY CONTROL - REPLICATE (R) SAMPLE AND STANDARD REFERENCE MATERIAL (SY3) ANALYZED WITH SAMPLES													
MW106 50.5(R)	0.13	0.60	3.12	10.5	<0.05	37.3	<0.02	0.54	27.5	0.14	<0.01	0.83	0.02
SY3-XRF	4.36	2.70	13.0	60.7	0.71	0.05	<0.02	4.50	8.16	0.12	0.30	6.33	0.05
SY3-known	4.15	2.67	11.8	59.7	0.54	0.12	0.014?	4.20	8.26	0.15	0.32	6.45	0.05

ANALYSIS PERFORMED BY THE MINERAL LAB, INC.

INTERA, INC
XRF-POWDER RESULTS FOR "L-BAR PROJECT, FRACTURE FILLING SAMPLES"

NOVEMBER 14, 1996
LAB NO. 960519

	PPM												
IDENT	V	Cr	Co	Ni	W	Cu	Zn	As	Sn	Pb	Mo	Sr	U
MW106 50.5	45	51	<10	14	<10	<10	<10	20	136	<10	<10	597	<10
MW106 53.0	67	36	<10	13	<10	<10	66	<20	111	<10	<10	444	<10
MW107 36.5	57	43	<10	11	<10	<10	30	<20	83	<10	<10	684	<10
MW107 46.3	80	20	<10	12	<10	<10	66	21	93	34	<10	458	10
MW107 48.3	40	37	<10	<10	<10	<10	31	25	120	<10	<10	391	<10
MW107 55.2	71	45	<10	14	<10	12	31	<20	87	17	<10	603	<10
MW108 40.8	73	41	<10	16	<10	<10	55	34	111	<10	<10	542	11
MW108 48.5	43	47	22	19	<10	<10	13	21	111	<10	<10	425	<10
MW108 51.6	37	43	<10	<10	<10	<10	<10	25	113	<10	<10	454	13
JALITY CONTROL													
.W106 50.5(R)	41	52	<10	13	<10	<10	<10	<20	132	<10	<10	595	<10
SY3-XRF	48	<10	<10	11	52	19	265	24	<50	144	<10	349	599
SY3-known	51	10	12	11	--	16	250	20	--	130	--	306	650

ANALYSIS PERFORMED BY THE MINERAL LAB, INC.

INTERA, INC
"-POWDER RESULTS FOR "L-BAR PROJECT, FRACTURE FILLING SAMPLES"
AGE 3 OF 3

NOVEMBER 14, 1996
LAB NO. 960519

	PPM				
IDENT	Th	Nb	Zr	Rb	Y
MW106 50.5	<10	<10	34	22	17
MW106 53.0	15	10	108	53	27
MW107 36.5	<10	<10	40	27	25
MW107 46.3	25	13	160	28	30
MW107 48.3	<10	<10	58	14	13
MW107 55.2	<10	<10	57	44	31
MW108 40.8	12	<10	86	43	29
MW108 48.5	<10	<10	37	28	10
MW108 51.6	<10	<10	31	16	19
QUALITY CONTROL					
MW106 50.5(R)	<10	<10	33	23	12
r3-XRF	945	171	323	200	738
SY3-known	990	145	320	208	740

ANALYSIS PERFORMED BY THE MI[illegible]RAL LAB, INC.

Intera, Inc
XRD Results for "L-Bar Project, Fracture Filling Samples"

November 15, 1996
Lab no. 960519

Mineral	MW106 50.5	MW106 53.0	MW107 36.5	MW107 46.3	Approx Wt % MW107 48.3	MW107 55.2	MW108 40.8	MW108 48.5	MW108 51.6
Gypsum	75	54	60	38	72	50	64	82	>85
Bassanite	<5	--	--	--	--	--	--	--	<3?
Anhydrite	--	--	--	--	--	--	--	<3	<3?
Quartz	8	8	8	5	<3	12	10	7	<5
Calcite	<5	--	20	11	15	24	--	--	--
Kaolinite	--	30	<3	20	<5	<5	14	<5	<5
Smectite	--	<5?	<5	22	<10	<5?	<10	--	--
Mica/illite	<5	--	<3	<3	<3?	<5	<3	<3	<3?
Chlorite	<5?	--	--	--	--	<3?	--	<5	--
K-feldspar	<3?	<3	<3?	<3?	--	<3?	--	--	--
Plagioclase feldspar	--	--	--	--	--	<3	--	--	--
"Unidentified"	<5	<5	<5	<5	<5	<5	<5	<5	<5

Analysis performed by The Mineral Lab, Inc.

DCM SCIENCE LABORATORY, INC.
PETROGRAPHIC ANALYSIS

REPORTING DATE:	OCTOBER 7, 1996
CLIENT:	INTERA, INC.
CLIENT JOB NO.:	NONE GIVEN
PROJECT TITLE:	NONE GIVEN
DCMSL PROJECT NO.:	INTERA4

The purpose of this analysis is to perform a petrographic examination of sixteen sedimentary rock samples. The sample group consists of four suites of samples as well as three additional samples. One thin-section per sample was analyzed by polarized light microscopy (PLM). Mineral concentrations were quantified by a 500 point count modal analysis performed on each thin section. Photomicrographs are included for documentation.

Summary

Additional Samples

The three rock samples are fine grained sandstones that represent an exposed outcrop. The samples are texturally and mineralogically similar. Diagenic processes are evident subsequent to deposition. Sediment compaction is low and lithification is primarily by quartz overgrowth cementation. Sample no. FTH-SS East 1 contains small, irregular patches of secondary calcite and dolomite. Due to weathering, the carbonate is severely corroded and has weak contacts with quartz-feldspathic clasts. Overall, the rocks are soft, have high porosity and are friable. Feldspar contained in the samples shows extremes in alteration ranging from minor corrosion to complete dissolution and clay formation. Detrital clay coats many of the clasts with higher concentrations along bedding planes. These features are attributed to fluid movement through the sediment during deposition. Some pores, however, contain delicate structures and vermicular kaolinite, indicating that a portion of the clay is authigenic. Green glauconite pellets are also present in trace amounts.

Suite MW106

The four samples in this suite encompass depths between 53.5' to 93.2' and show some differences in lithology and diagenesis. Sample no. MW106 53.5'-54.0' and sample no. MW106 92.9'-93.2' are carbonate cemented. The first sample has a high dolomite content and shows etching and dissolution along calcite cleavage planes, giving the matrix a granular appearance in thin section. In contrast, the calcite matrix seen in the later sample doesn't appear to have interacted with acidic pore fluids as indicated by its fresh and unaltered appearance. These samples are hard and non-friable. Samples no. MW106 66.5'-66.8' and MW106 67.0'-67.3' are situated between the carbonate samples and are silica cemented. Some minor dolomite and calcite are present and show minor dissolution. All the samples have feldspar in various stages of alteration. Some grains show minor etching while, in contrast, some clasts show extreme dissolution and clay formation. Detrital and authigenic clays are also present.

Suite MW107

The five borings in this suite encompass depths between 77.5' to 120' of drill core material. The sediment at the top of the suite (sample no. MW107 77.5'-78.5') and core sample (sample no. MW107 109.5') are carbonate cemented. The sample at the top of the suite contains dolomite and calcite as the cementing matrix. Quartz grains rarely show overgrowths and feldspar alteration is minor, suggesting the influx of carbonate took place shortly after deposition. The carbonate is fresh and shows no indication of leaching. Sample no. MW107 109.5' contains sparry calcite as the cementing agent. Some dolomite is present, but is restricted to the biogenic structures. Like the first sample, carbonate precipitation appears to have taken place soon after deposition, as feldspar alterations are minor and quartz overgrowths are uncommon. The carbonate shows no indication of leaching or dissolution. Biogenic structures contained in this rock have good porosity, little carbonate, high clay content and show some diagenetic effects due to fluid migration. The feldspars show greater alteration and patches of chert have precipitated, engulfing quartz-feldspathic grains. The remaining samples in the suite are consolidated primarily by quartz overgrowth cementation. Some small patches of calcite and dolomite cement some grains but is insignificant. When next to open pore space, the calcite retains sharp angular faces, indicating no alteration after deposition. Feldspar, detrital clay, glauconite, chert, authigenic kaolinite and pyrite are common constituents.

Suite MW108

The samples in suite MW108 encompass depths between 51.9' to 90.3' of drill core material. Samples between the depths of 65.2' and 68.0' were not evaluated by petrographic analysis.

When compared, the sedimentary samples at the top and the bottom of the suite show extremes in diagenesis. The upper specimen has a high clay content, an unsorted assemblage of mineral grains and is texturally immature. Clay coats most grains and forms fine clay bridges in pore space between grains. Some pores are filled with authigenic kaolinite. Thick accumulations of clay in some areas promote minor lithification. Quartz overgrowths are not present. More significantly, consolidation is due to a patchwork of gypsum mixed with dolomite. When adjoining pore space, the gypsum shows corrosion along edges and cleavage planes.

In contrast, the sample at the bottom of the suite is well sorted, texturally mature and cemented by quartz overgrowths. Authigenic kaolinite is seen in some pore space, but quartz-feldspathic grains lack clay skins. Glauconite rich bedding planes mixed with authigenic pyrite are a conspicuous feature.

Suite MW109

The samples in suite MW109 encompass depths between 47.5' and 81.8' of drill core material. Cores between the depths of 62.2' and 66.5' were not evaluated by petrographic analysis.

The sediments at the top and bottom of the suite analyzed petrographically exhibit good sorting of mineral clasts and are texturally and mineralogically

mature. The sample at the top of the suite is a fined grained sandstone cemented by quartz overgrowths, followed by inconsistent gypsum cementation. Pitting and corrosion of the gypsum are common. Trace amounts of dolomite showing minor corrosion are also present. The sample at the bottom of the suite is a medium to coarse grained, silica cemented sandstone containing no secondary gypsum. Dark green glauconite and small areas of authigenic kaolinite are scattered throughout. Both samples contain some detrital clay mixed with dark organic material and minor dolomite. Feldspars show varying degrees of alteration.

Petrographic and Modal Analyses

CLIENT SAMPLE NO.: FTH-SS EAST 1
DCMSL SAMPLE NO. INTERA4-1

Hand Specimen Description

In hand specimen sample no. FTH-SS EAST 1 is a tan sedimentary rock showing moderate uniformity in grain size. The rock contains sedimentary features in the form of weakly pronounced bedding planes, has well developed porosity and is moderately friable. Based on the following petrographic and modal analyses, the rock is classified as a fine grained, calcite/silica cemented subarkose.

Microscopic Description

The rock is primarily composed of quartz, feldspar, minor clay and carbonate cement. Grain size measurements fall between 0.06mm to .25mm. The grains are angular to subround and moderately sorted, indicating the rock is texturally submature. In thin section, diagenic processes are evident subsequent to deposition. Grain to grain contact is low and porosity is well developed, indicating compaction of the sediment is low. Consolidation of the grains is due to quartz overgrowth cementation and secondary carbonate. Most of the quartz grains show early stage overgrowths, which promotes minor cementation when in contact with other grains. Calcite weakly joins grains in small areas throughout the section. At one time it may have been a significant cementing agent, but due to leaching, most has been removed. The small patchy areas that remain are severely corroded and have weak intergranular contacts. Trace amounts of corroded dolomite are also present but do not appear to significantly aid in cementation.

The feldspar contained in the sample is predominantly grid twinned microcline in addition to minor amounts of plagioclase. The potassium feldspar grains show various stages of preservation with the majority of grains showing minor alteration. In contrast some grains show evidence of dissolution with corroded edges and intraparticle porosity. Plagioclase is seen altering to clay and sericite.

Clay contained in the sample is minor and appears to be deposited by fluids moving through the sediment and diagenic processes. Clay is generally seen coating grains, but small masses of clay marginal to pores have a vermicular and radial growth pattern into the pore spaces, indicating an authigenic origin. Trace amounts of green glauconite clasts are also present.

Modal Analysis

Quartz	73.4
K-Feldspar	6.0
Plagioclase	0.2
Clay (Undifferentiated)	3.0
Calcite	6.0
Chert	0.4
Pore Space	11.0
Dolomite	<0.2
Mica	<0.2
Glauconite	<0.2

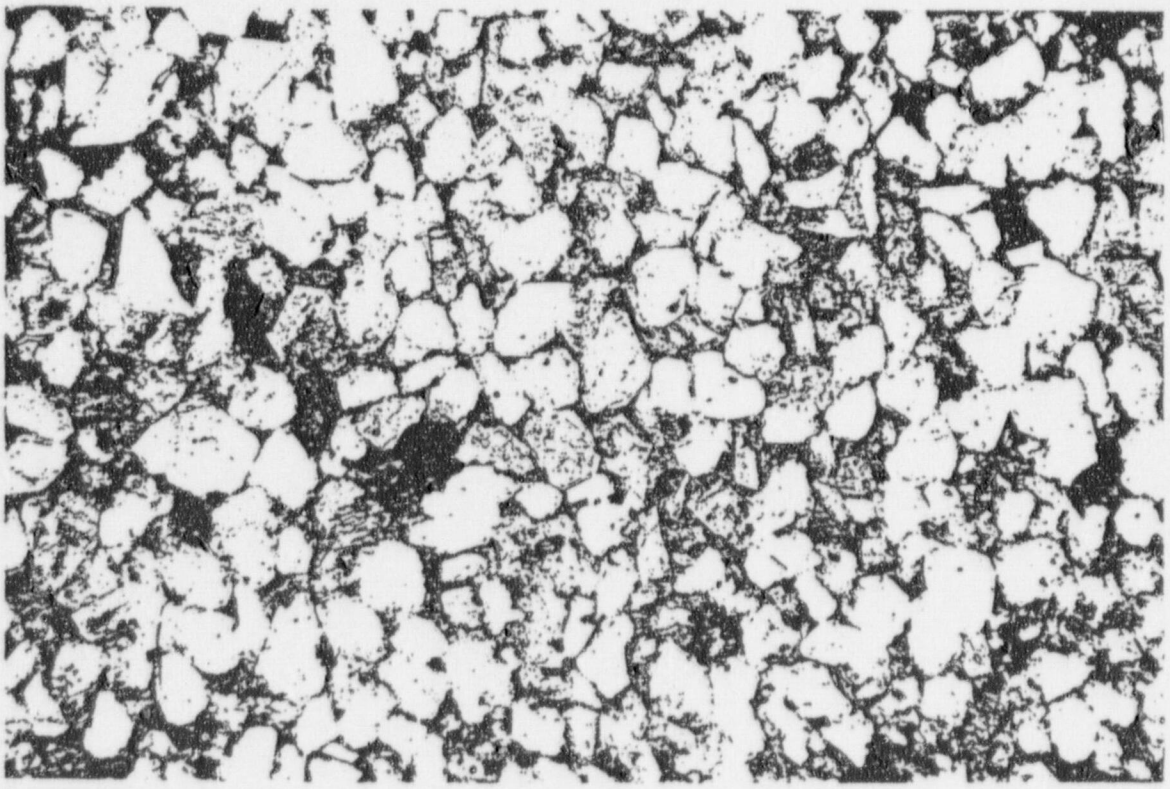

Photo 1: Photomicrograph showing distribution of grains and pore space (blue). Some of the quartz (clear) show idiomorphic outlines due to overgrowths. Yellow clasts are stained K-feldspar. Plane polarized light - 40X.

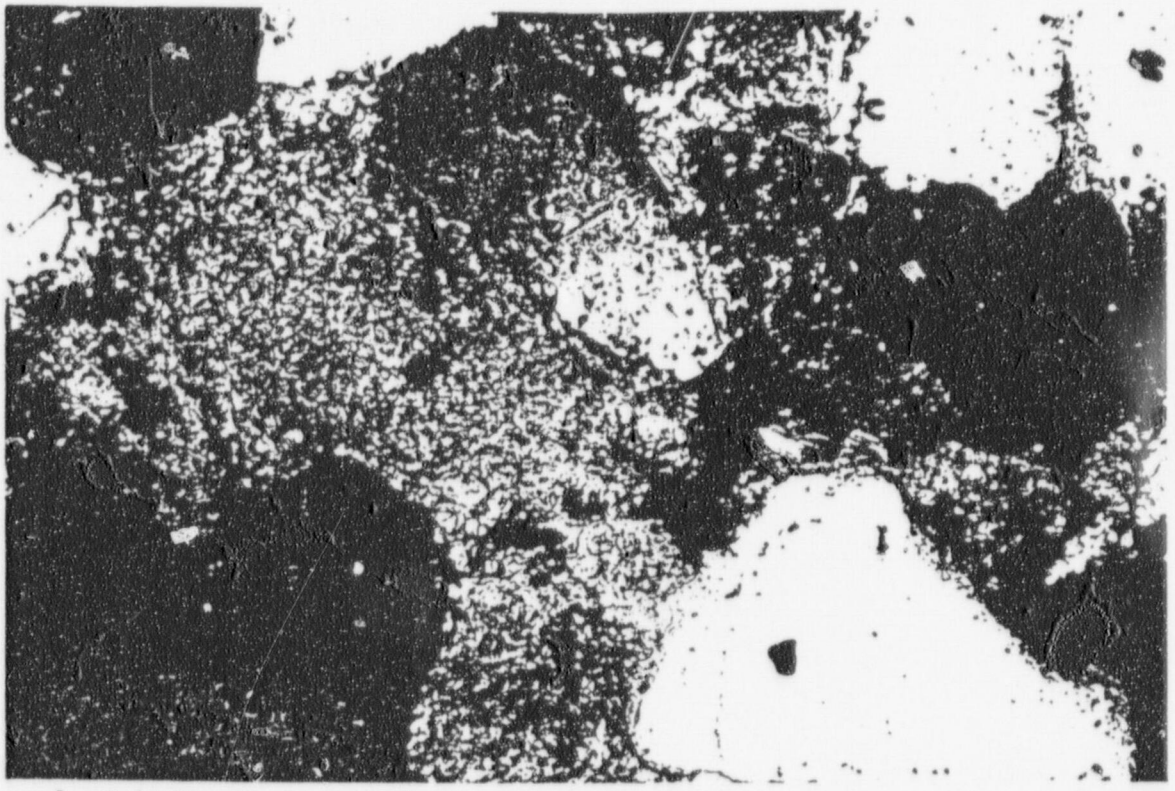

Photo 2: Calcite showing high interference colors and signs of corrosion weakly joins quartz grains. Crossed polarized light - 250X.

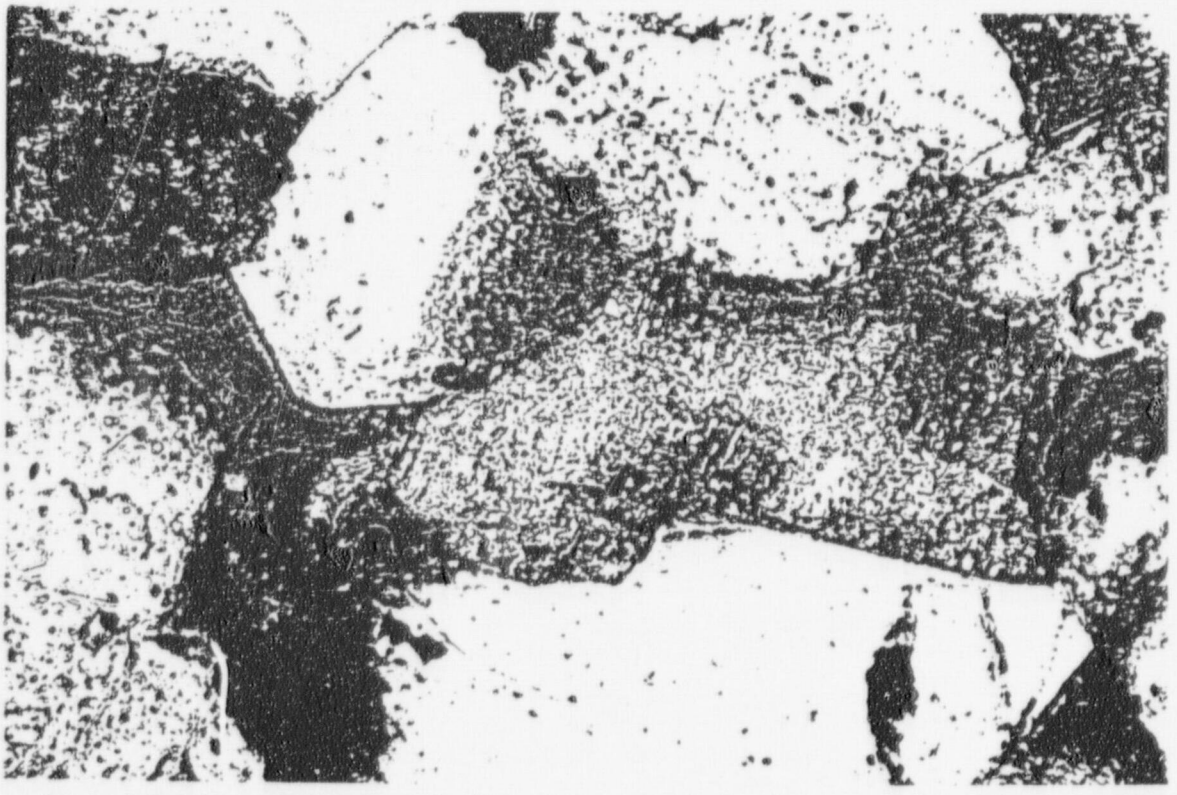

Photo 3: K-feldspar clast (stained yellow) shows severe dissolution with corroded margins and intraparticle porosity. Detrital clay and quartz are also pictured. Plane polarized light - 250X.

CLIENT SAMPLE NO.: FTH-SS EAST 2
DCMSL SAMPLE NO. INTERA4-2

Hand Specimen Description

In hand specimen sample no. FTH-SS EAST 2 is a tan sedimentary rock showing moderate uniformity in grain size. In cross section, the rock shows sedimentary structures in the form of weak bedding planes. The sample is soft, friable and has high porosity. Based on the following petrographic and modal analyses, the rock is classified as a fine grained, silica cemented subarkose.

Microscopic Description

Primary constituents include quartz, feldspar, clay minerals and minor chert. Individual grains are angular to subround and have grain sizes ranging from 0.08mm to 0.3mm. Texturally and mineralogically the rock is submature. Grain to grain contact is low, indicating compaction was not a significant factor in sediment consolidation. Induration is due to minor quartz overgrowth cementation. Silica overgrowths observed on grain boundaries are very early stage. Not all grains show overgrowth boundaries and idiomorphic overgrowths are uncommon.

Feldspar is primarily grid twinned microcline and plagioclase. The feldspars show extremes in alteration. Many of the microcline clasts show minimal weathering, while some show corrosion along cleavage planes to complete dissolution. Alteration is most severe with the plagioclase where it has been replaced with clay and sericite.

Excluding grain contacts, many of the quartz-feldspathic grains have minor thin clay films on the surface, indicating clay infiltration by fluid movement. More significant are small, occluded pores showing radial and vermicular growths of kaolinite, indicating some of the clay is authigenic. Some glauconite is also present. Minor amounts of chert and biotite mica are present with biotite showing minor chloritization along cleavage planes.

Modal Analysis

Quartz	75.8
K-Feldspar	4.2
Plagioclase	2.4
Clay (Undifferentiated)	1.4
Void	15.6
Chert	0.6
Glauconite	<0.2

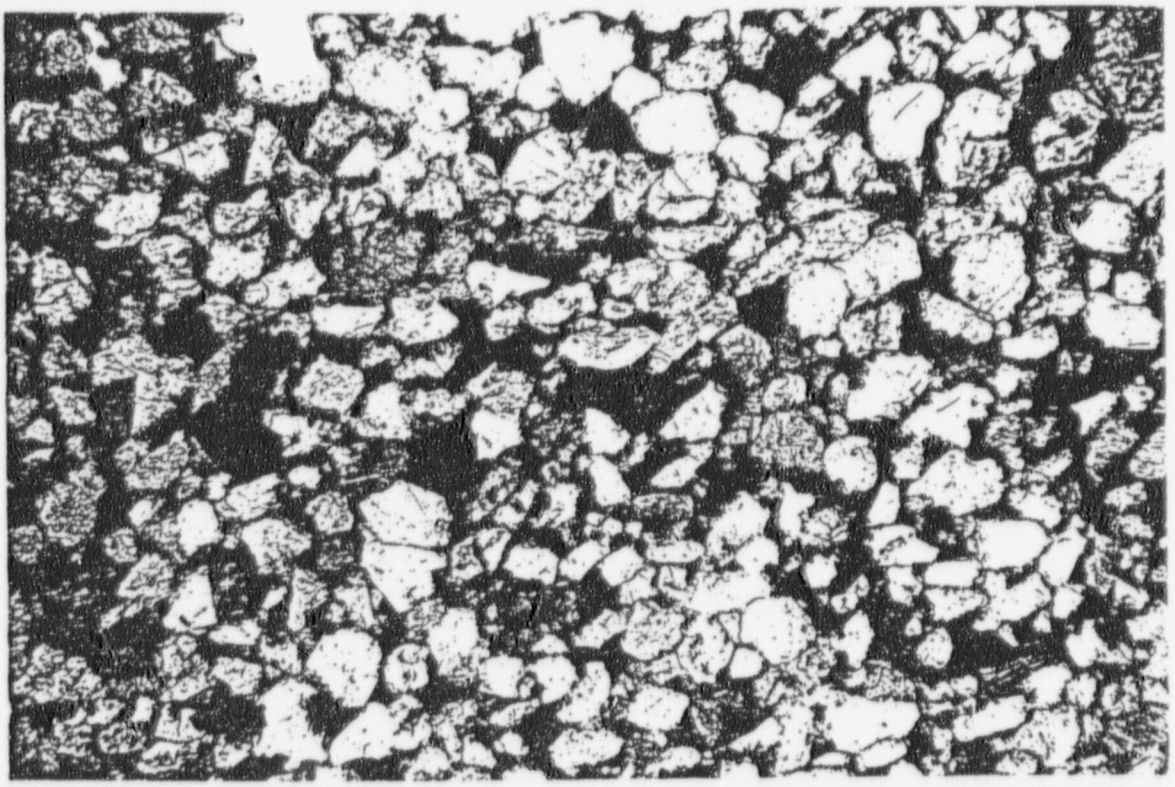

Photo 1: Photomicrograph showing distribution of grains and pore space (blue). Quartz overgrowths are seen on some grains. Yellow clasts are stained K-feldspar Plane polarized light - 40X.

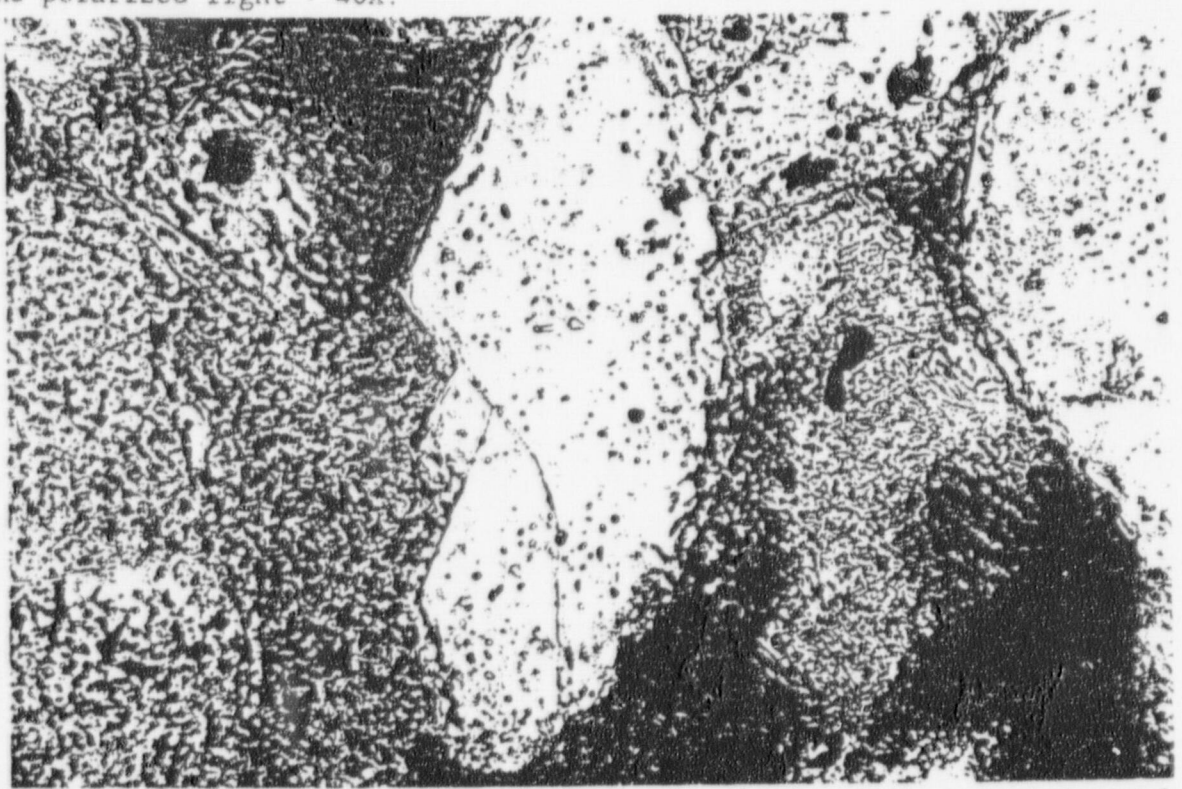

Photo 2: K-feldspar clast (yellow) shows dissolution with corroded margins. Quartz grains show idiomorphic overgrowths. Kaolinite (K) fills a small pore. Plane polarized light - 250X.

CLIENT SAMPLE NO.: FTH-SS WEST 1
DCMSL SAMPLE NO. INTERA4-3

Hand Specimen Description

In hand specimen sample no. FTH-SS WEST 1 is a tan sedimentary rock exhibiting moderate uniformity in mineralogic grain size. The rock shows no visible sedimentary structures, has well developed porosity and is friable. Based on the following petrographic and modal analyses, the rock is classified as a silica cemented quartzarenite.

Microscopic Description

Detrital grains contained in the rock are primarily quartz with minor amounts of feldspar and some clay. Grain size measurements fall between .1mm to .25mm. The grains are angular to subrounded and are moderately sorted, indicating a submature bordering mature texture. Boundaries between grains show little effect due to compaction. Consolidation of the grains is accomplished by quartz overgrowth cementation. Many of the grains have well developed, idiomorphic overgrowths. The overgrowth is early to intermediate, as indicated by the remaining primary porosity.

Feldspar grains are primarily microcline with some plagioclase, and exhibit various stages of alteration. Some of the microcline clasts show little diagenic alteration, while others are severely corroded and pitted. This is particularly significant with the plagioclase, which is often seen altering to clay and sericite.

Excluding point of grain contact, clay skins are visible on many of the boundaries and may have infiltrated by fluid movement. In addition some of the small pore space contains vermicular kaolinite and radial clay growth, indicating an authigenic origin. Trace amounts of muscovite and biotite are also present. Minor chloritization of the biotite is present.

Modal Analysis

Quartz	84.4
K-Feldspar	1.6
Plagioclase	0.2
Clay (Undifferentiated)	2.0
Void	11.8
Mica	<0.2
Chert	<0.2

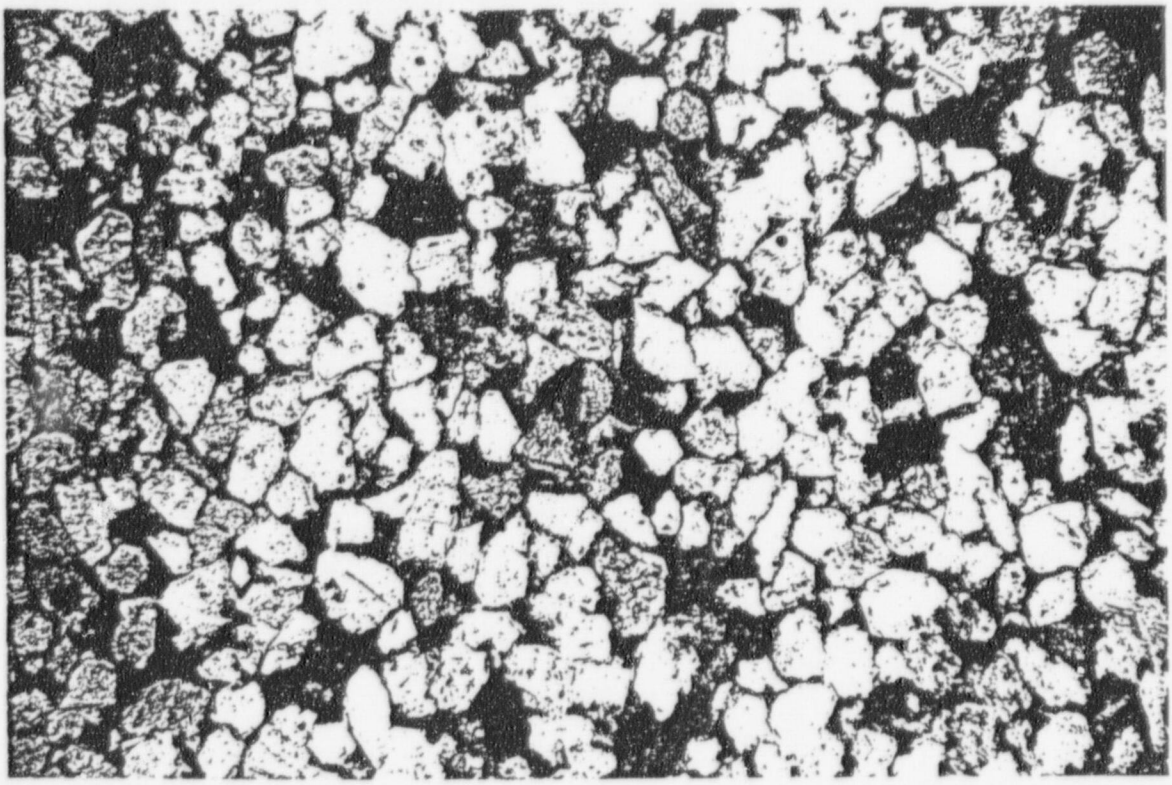

Photo 1: Photomicrograph showing distribution of grains and pore space (blue). Clear grains are quartz, some showing overgrowth outlines. Yellow clasts are stained K-feldspar. Plane polarized light - 40X.

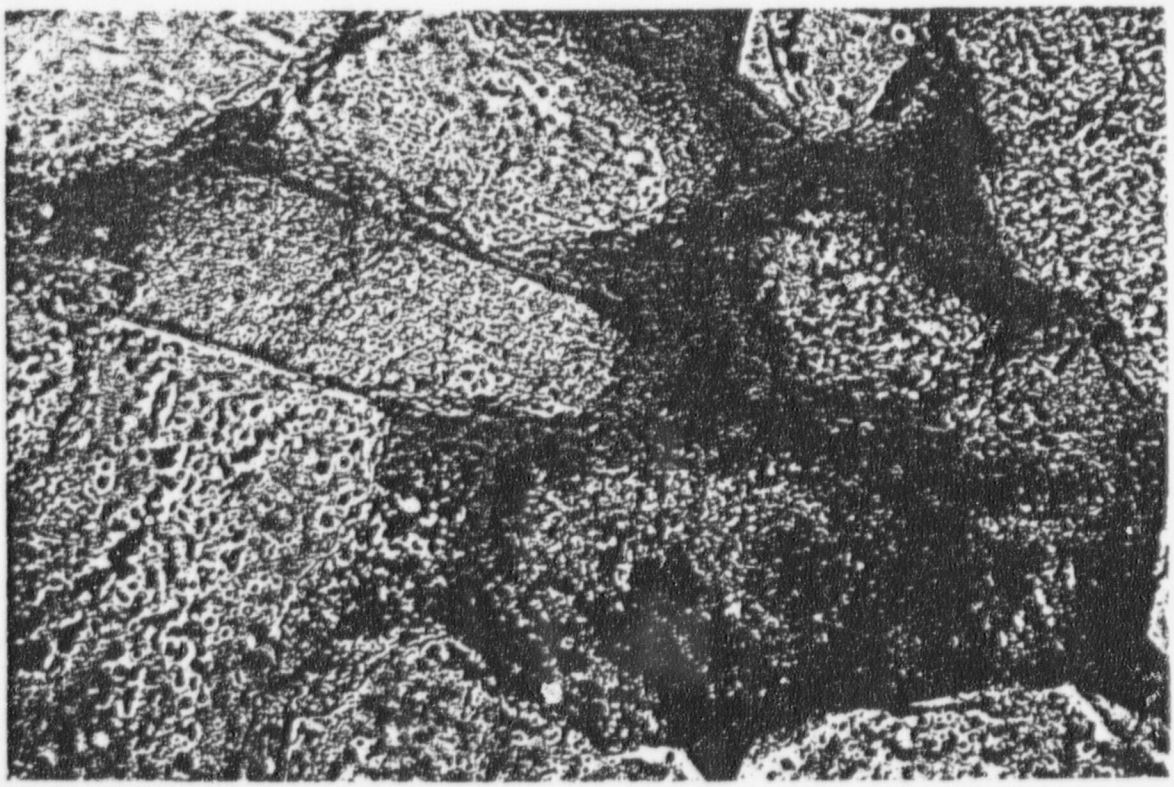

Photo 2: K-feldspar (yellow) showing intraparticle porosity and corroded margins due to dissolution. Feldspar in upper left shows little or no alteration. Clear quartz grains with clay skins are also pictured. Plane polarized light - 250X.

CLIENT SAMPLE NO. MW106 53.5'-54.0'
DCMSL SAMPLE NO. INTERA4-4

Hand Specimen Description

Sample no. MW106 53.5'-54.0' is a light tan colored sandstone showing poor uniformity in grain size. In cross section, the core shows wavy, clay-rich lenses and is mottled due to bioturbation. The rock has poor porosity and is non-friable due to a calcite matrix. Based on the following petrographic and modal analyses, the rock is classified as a fine grained carbonate cemented subarkose.

Microscopic Description

Primary constituents include quartz, feldspar, carbonate and clay. Individual grains vary greatly from angular to well rounded. Grain size measurements range from .05mm to .5mm, indicating the rock is poorly sorted and texturally immature. Contacts between quartz-feldspathic grains are low. Consolidation of the grains is achieved by a matrix of calcite and dolomite. Overgrowths on quartz grains are rare. More significantly, the anhedral calcite that precipitated in the pore space has, in some cases, etched and dissolved parts of the quartz grains, giving them irregular shapes. Calcite also shows evidence of dissolution and leaching. Some areas contain patches of carbonate, showing corrosion and pitting along cleavage planes and giving the carbonate a granular, sieve-like appearance. This is most prominent around biogenic structures where fluids have a route of migration. Dolomite is present in the form of euhedral crystals that are generally seen enclosed by calcite, indicating dolomite crystallization was first.

Feldspar contained in the rock is predominantly microcline and perthite with minor amounts of plagioclase. With minor exceptions, the more stable potassium feldspar grains show little alteration or dissolution. Clasts that have altered are sometimes seen replaced by calcite. The plagioclase is commonly altered to clay and sericite.

Clay is not seen on grain boundaries. Rather, it is seen filling pore space or veinlets, either by itself or intermixed with carbonate and organic material. In places clay marginal to pore space shows delicate radial growths indicating some is authigenic. Most significant are large pores, patches and veinlets containing well crystallized, vermicular kaolinite. Minor amounts of chert, glauconite and biotite mica are also present. Most of the biotite shows alteration to chlorite.

Modal Analysis

Quartz	48.2
K-Feldspar	6.2
Plagioclase	0.4
Clay (undifferentiated)	4.4
Calcite	34.2
Dolomite	6.2
Chert	0.4
Mica	<0.2
Clauconite	<0.2

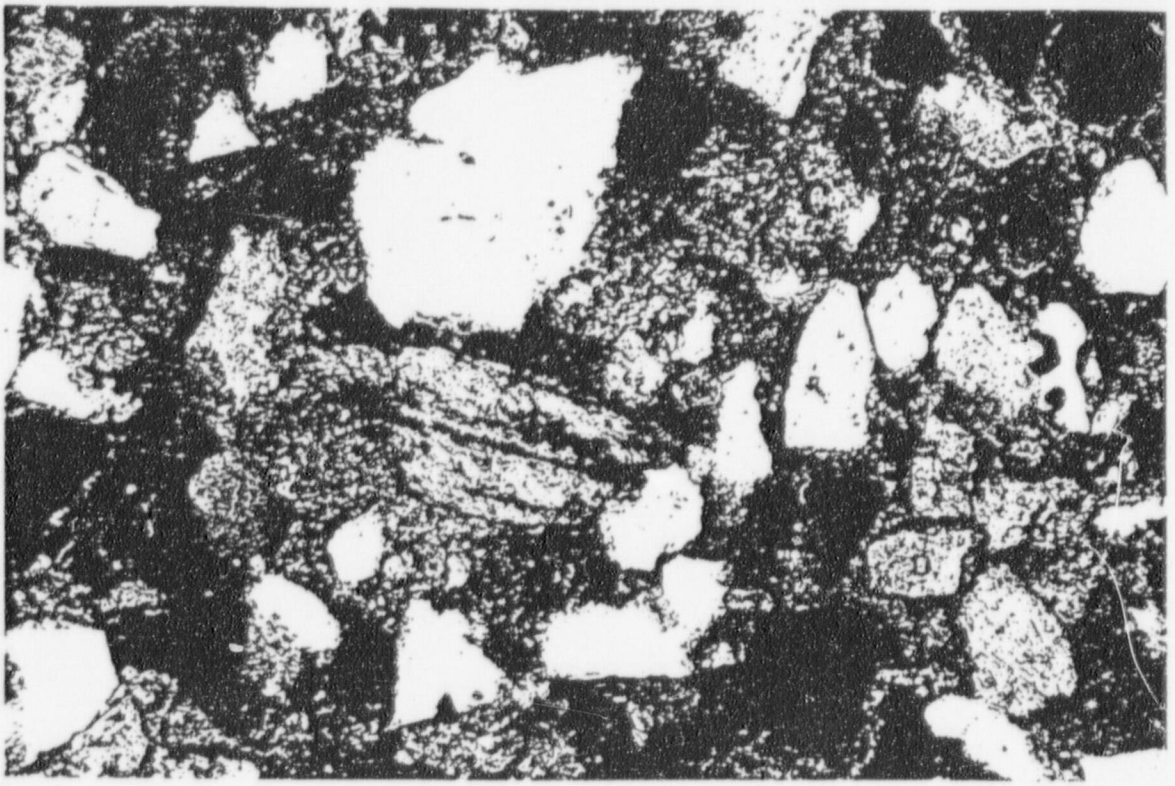

Photo 1: Photomicrograph showing distribution of grains and carbonate cement. Some of the calcite (C) has a granular appearance due to dissolution. Subhedral dolomite (D), K-feldspar (yellow) and quartz (white/grey) are also pictured. Crossed polarized light - 100X.

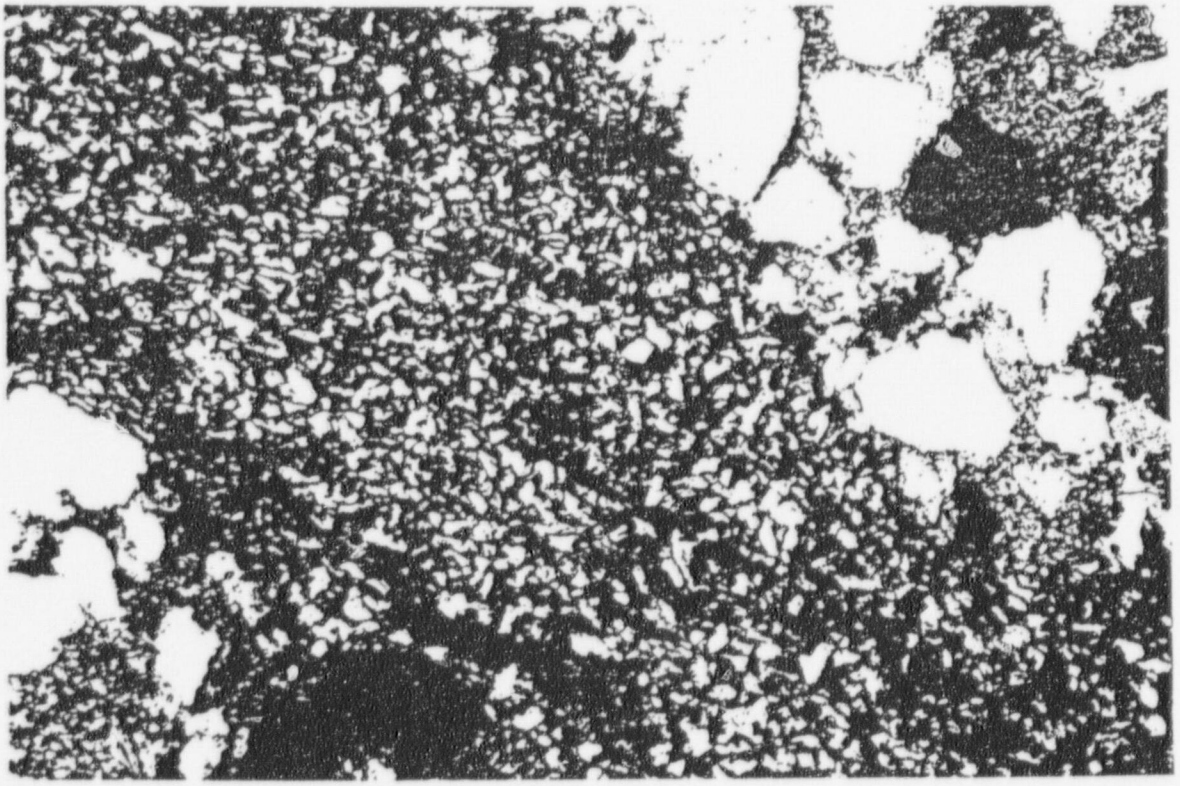

Photo 2: Vermicular kaolinite filling a thin veinlet. Quartz and calcite are also pictured at upper right and lower left corners. Crossed polarized light - 100X.

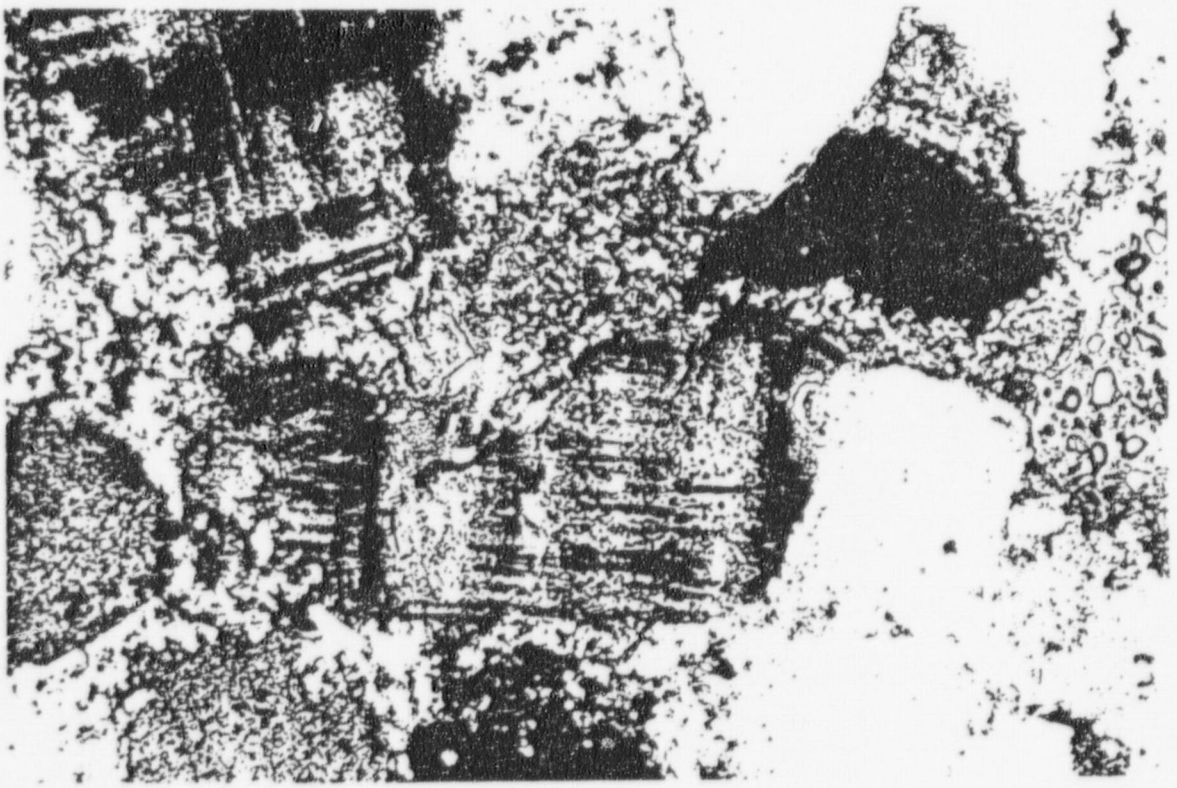

Photo 3: Calcite partially replacing microcline feldspar. Crossed polarized light - 250X.

CLIENT SAMPLE NO.: MW106 66.5'-66.8'
DCMSL SAMPLE NO. INTERA4-5

Hand Specimen Description

In hand specimen sample no. MW106 66.5'-66.8' is a tan sandstone showing fairly uniform grain size. In cross section, the rock shows sedimentary features including weakly defined bedding planes. Some bioturbation is present giving the rock a mottled and streaked look. Some thin argillaceous laminae are present. The rock has well developed porosity and is moderately friable. Based on the following petrographic and modal analyses, the rock is classified as a fine grained, silica cemented quartzarenite.

Microscopic Description

The primary constituent of the rock is quartz in addition to minor chert, feldspar, dolomite, clay and mica. The grains are angular to subrounded and grain size measurements range from 0.1mm to 0.21mm. The rock is well sorted texturally and mineralogically mature. Grain boundaries between quartz-feldspathic grains are low and show little effect from compaction. The consolidating agent is quartz overgrowth cementation. The overgrowths are early to intermediate stage, as indicated by the moderate amount of primary porosity retained in the rock. Some granular masses and euhedral dolomite are present, but are insignificant as cementing agents. The carbonate shows dissolution along edges and cleavage planes, giving it a corroded and pitted appearance.

The sample contains grid twinned microcline, perthite and plagioclase feldspar, which exhibits various stages of chemical attack. Some of the potassium feldspar shows alterations in the form of corroded boundaries to complete dissolution, but most show little effect. Plagioclase shows the most alteration with grains weathering to clay and coarse sericite.

The quartz-feldspathic clasts have little or no clay coatings. More commonly, clay is present as authigenic pore filling, where fine radial growths join grains. Some detrital clay is also present in thin veinlets where it is mixed with organic material. Minor glauconite and biotite mica are also present. Biotite shows alteration to chlorite.

Modal Analysis

Quartz	81.4
K-Feldspar	2.2
Plagioclase	0.4
Clay (Undifferentiated)	2.2
Void	11.6
Chert	0.8
Dolomite	1.4
Mica	<0.2
Calcite	<0.2

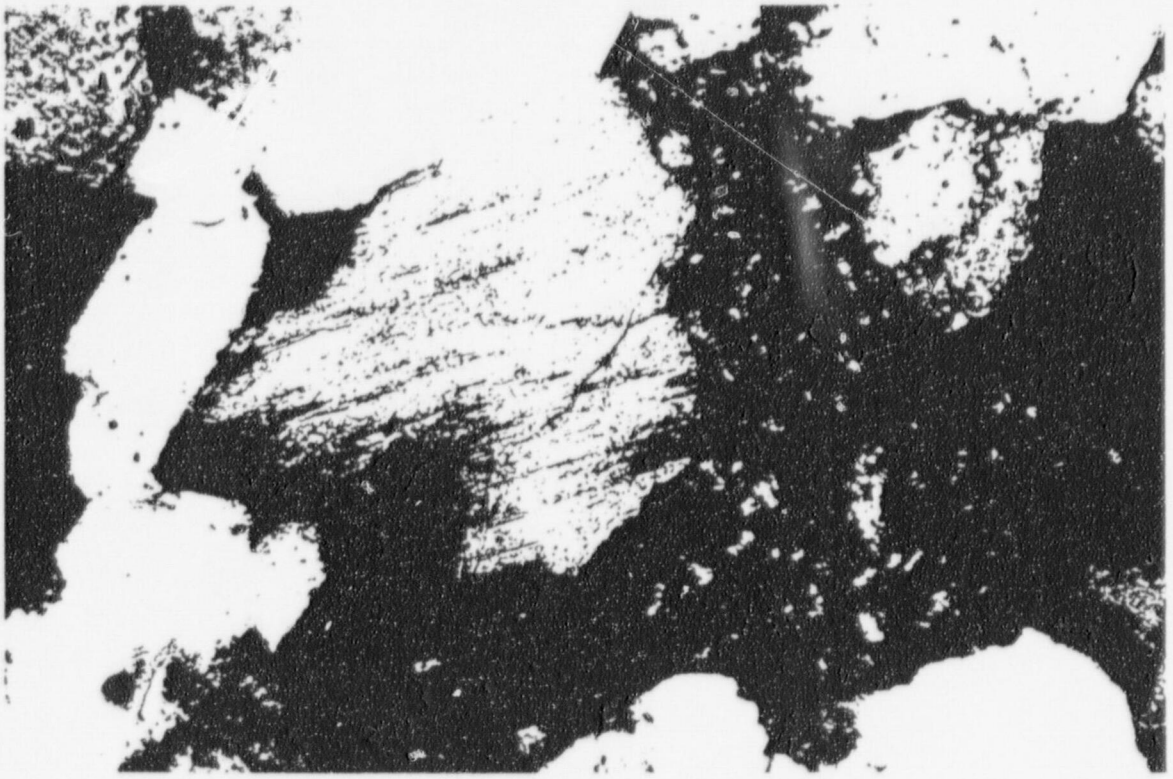

Photo 1: K-feldspar (yellow) showing partial dissolution around edges and cleavage planes. To the right is a small patch of authigenic kaolinite showing a vermicular habit. Quartz (white/grey) is also pictured. Crossed polarized light - 250X.

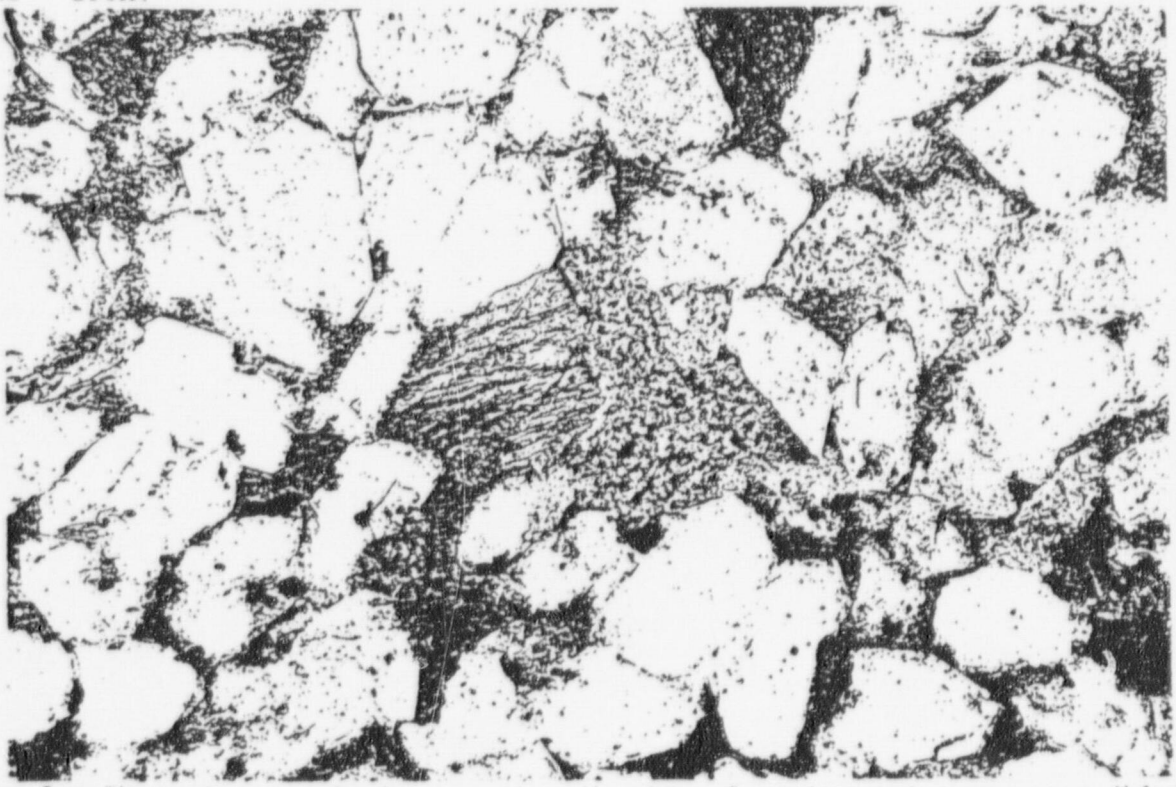

Photo 2: Photomicrograph showing distribution of grains and pore space (blue). K-feldspar (yellow) and quartz showing overgrowths make up the rock framework. Plane polarized light - 100X.

CLIENT SAMPLE NO.: MW106 67.0'-67.3'
DCMSL SAMPLE NO. INTERA4-6

Hand Specimen Description

Sample no. MW106 67.0'-67.3' is a light grey sandstone showing uniformity in grain size. In cross section, the rock has sedimentary structures in the form of very weak bedding planes cut by bioturbation. Some thin clay lenses and voids are present due to biogenic disturbance. The rock has well developed porosity and low to moderate friability. Based on the following petrographic and modal analyses, the rock is classified as a fine grained, silica cemented quartzarenite.

Microscopic Description

Quartz, feldspar, minor clay and carbonate are the main constituents. Grain size measurements of 0.1mm to 0.25mm indicate the rock is composed of fine sand grains that are angular to subrounded. The rock is texturally and mineralogically mature. Grain boundary contacts are low to moderate and clasts show no signs of deformation, suggesting compaction after deposition was minimal. Induration of the rock is primarily the result of quartz overgrowth cementation. Most grains show idiomorphic outlines, indicating intermediate stage cementation. In some places, the overgrowths choke off the porosity, but is not a common feature. Small patches of calcite act as a cementing agent, but are insignificant. Trace amounts of euhedral dolomite are also present. The carbonate shows little corrosion, indicating limited fluid interaction after deposition.

Grid twinned microcline and perthite are the most abundant feldspar as well as minor amounts of plagioclase. Chemical attack is seen on some of the K-feldspar in the form of corrosion along cleavage planes to complete dissolution. Most, however, show little or no alteration. Plagioclase shows the least resistance to chemical attack. Most grains exhibit alteration to white mica (sericite) or are cloudy due to clay formation.

The quartz-feldspathic grains have little or no clay coatings. Detrital clay is restricted to voids produced by biogenic activity where it is mixed with dark organic matter. Delicate growths of vermicular kaolinite fill some pores and thin veinlets. Chert clasts, mica, green glauconite and authigenic pyrite are also present. The biotite displays alteration to chlorite.

Modal Analysis

Quartz	81.2
K-Feldspar	3.6
Plagioclase	1.0
Clay (Undifferentiated)	2.0
Void	10.6
Calcite	1.2
Dolomite	0.2
Chert	0.2
Mica	<0.2
Glauconite	<0.2

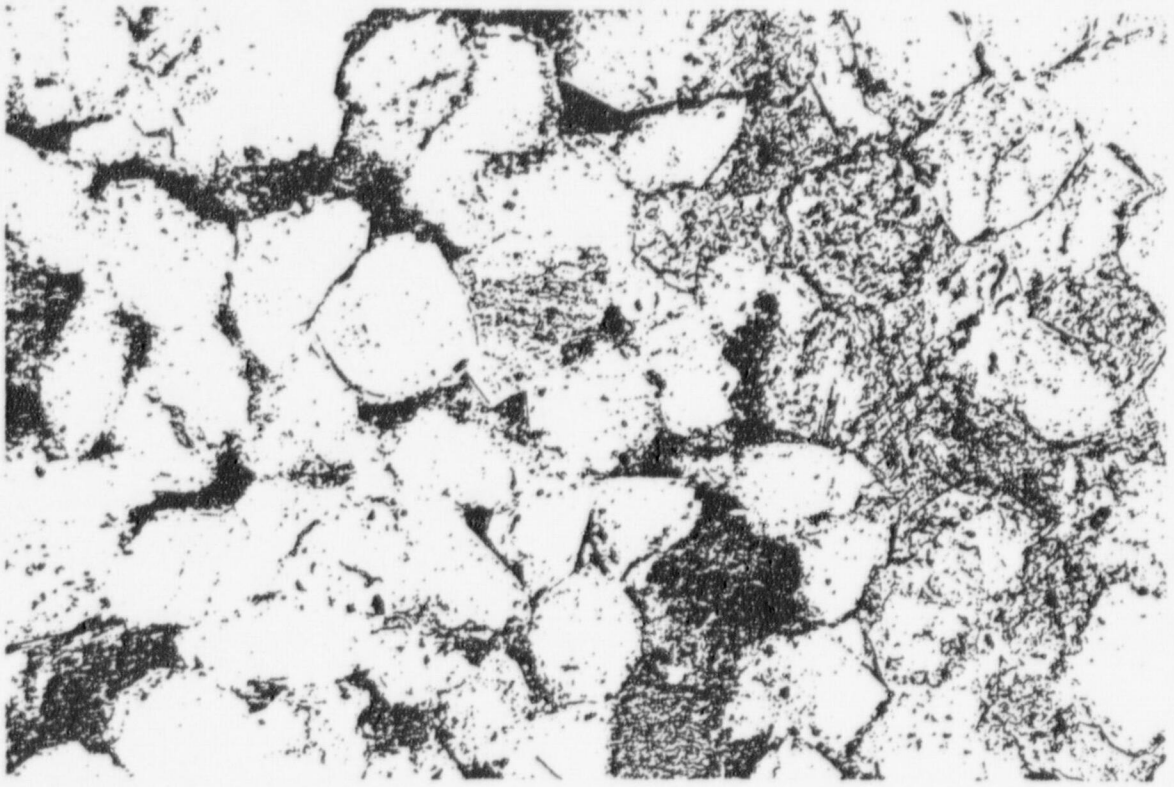

Photo 1: Photomicrograph showing grain distribution and pore space (blue). To the right is a small patch of sparry calcite (light pink) cementing grains. Feldspar (yellow) is also present. Plane polarized light - 100X.

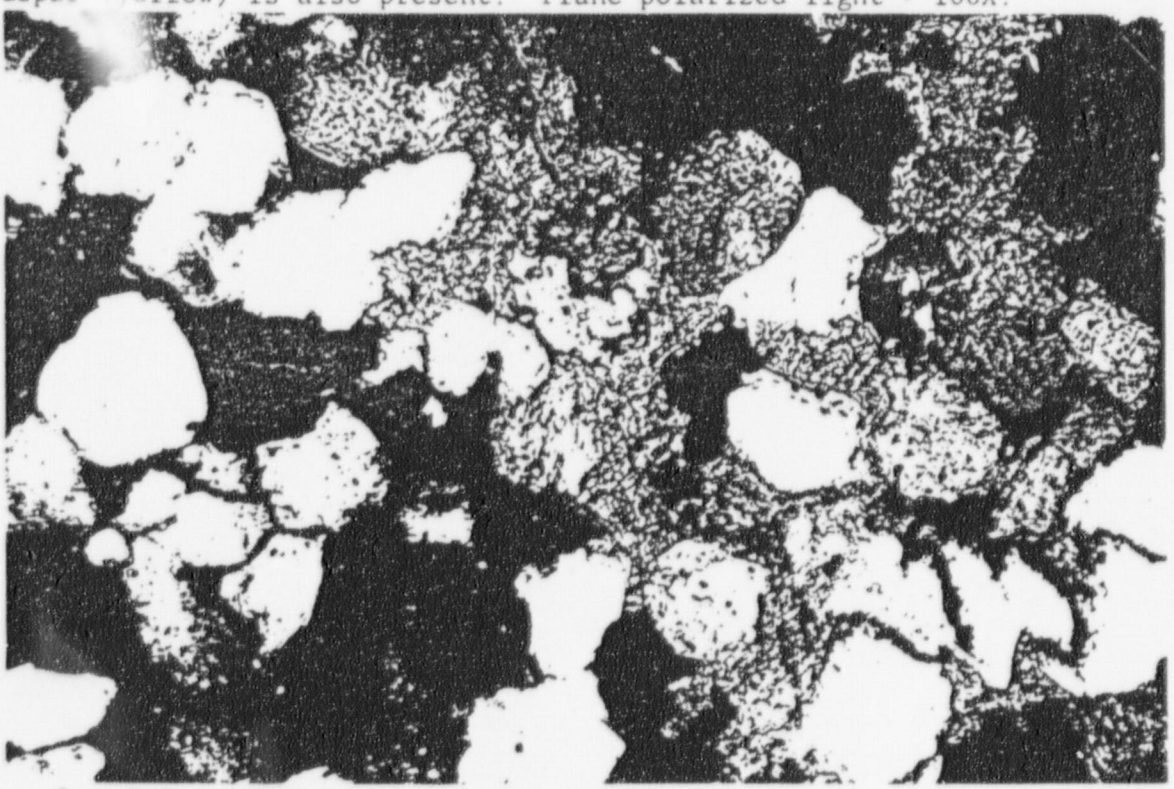

Photo 2: Calcite showing high interference colors cements quartz-feldspathic grains. Crossed polarized light - 100X.

CLIENT SAMPLE NO.: MW106 92.9'-93.2'
DCMSL SAMPLE NO. INTERA4-7

Hand Specimen Description

Client sample no. MW106 92.9'-93.2' is a grey sandstone showing moderate uniformity in mineralogic grain size. In cross section, the rock has very weak bedding planes crosscut by biogenic structures. Pellets of dark green glauconite are scattered throughout. Due to a carbonate matrix, the rock contains little porosity and is hard, dense and nonfriable. Based on the following petrographic and modal analyses, the sample is classified as a medium to coarse grained, calcite cemented quartzarenite.

Microscopic Description

The rock's primary constituents include quartz, feldspar, chert and glauconite locked in a sparry calcite matrix. The grains are subangular to rounded and vary in size from .2mm to .55mm. The rock is well sorted, texturally and mineralogically mature. Contact between quartz-feldspathic grain boundaries is low, indicating there was little effect from compaction. Consolidation of the grains is of chemical origin and occurred in two episodes. First stage grain cementation is due to quartz overgrowths. Nearly all quartz grains show overgrowths and many are idiomorphic in outline. Subsequent to quartz overgrowth is the precipitation of coarse grained calcite. The carbonate has completely occluded and choked all pore space. Calcite precipitation has etched and dissolved parts of many quartz grains, giving them irregular shapes. Additionally there is evidence that calcite cement precipitated at relatively shallow depths. In some areas large patches of calcite harbor individual grains that do not contact one another, suggesting the pressure exerted by the growing calcite crystals forced apart the quartz framework.

Microcline and perthite are the most abundant feldspar in addition to minor plagioclase. With the exception of minor carbonate replacement, the feldspar species represented are rarely altered, suggesting that the influx of carbonate cut off the porosity of the rock early after deposition.

Detrital grains of dark green glauconite are scattered throughout the rock. The clasts are rounded to irregular in shape and have some minor, secondary porosity around their margin due to shrinkage. Authigenic pyrite is common along these margins. Other detrital clay is rare and is restricted to biogenic structures where it is mixed with dolomite and dark organic material. Some chert and fibrous chalcedony are also present.

Modal Analysis

Quartz	66.8
K-Feldspar	2.4
Plagioclase	0.2
Clay (Undifferentiated)	0.4
Void	0.4
Calcite	23.8
Dolomite	0.2
Glauconite	3.8
Chert	1.8
Chalcedony	0.2

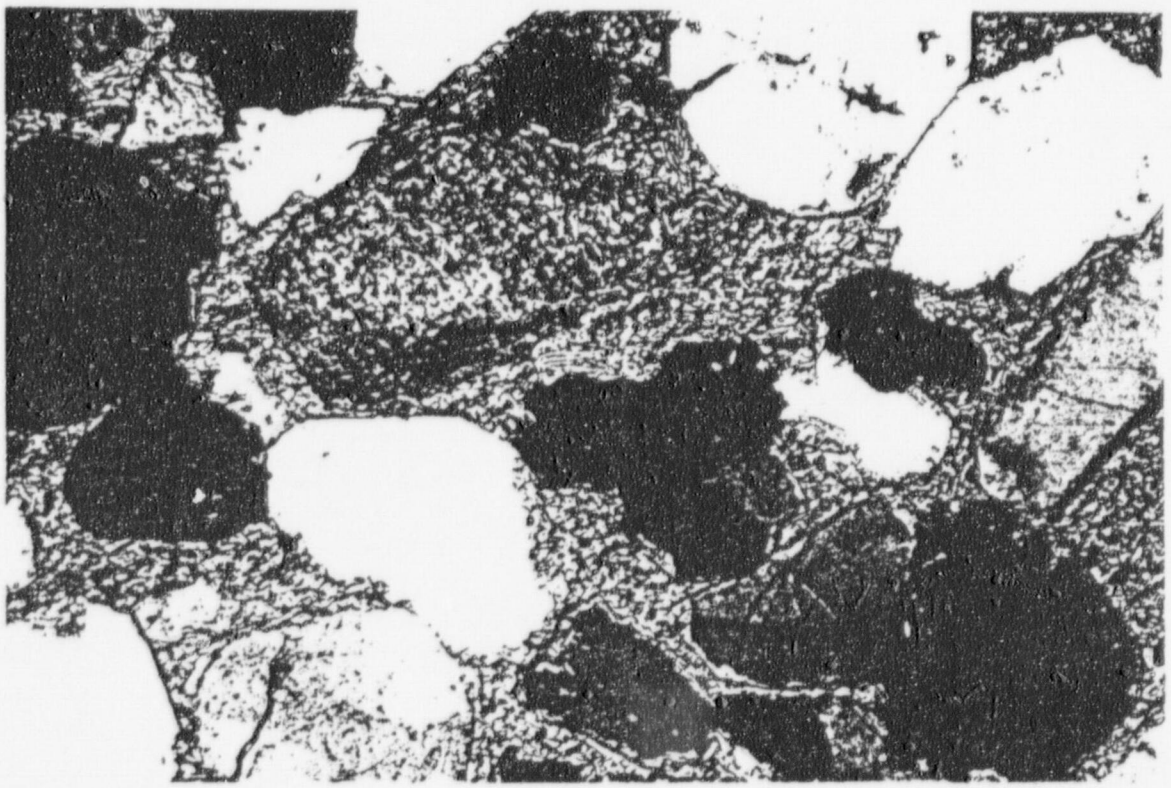

Photo 1: Quartz grains (white/grey) and K-feldspar (yellow) cemented by calcite. Quartz shows some corrosion along grain boundaries due to carbonate precipitation. Crossed polarized light - 250X.

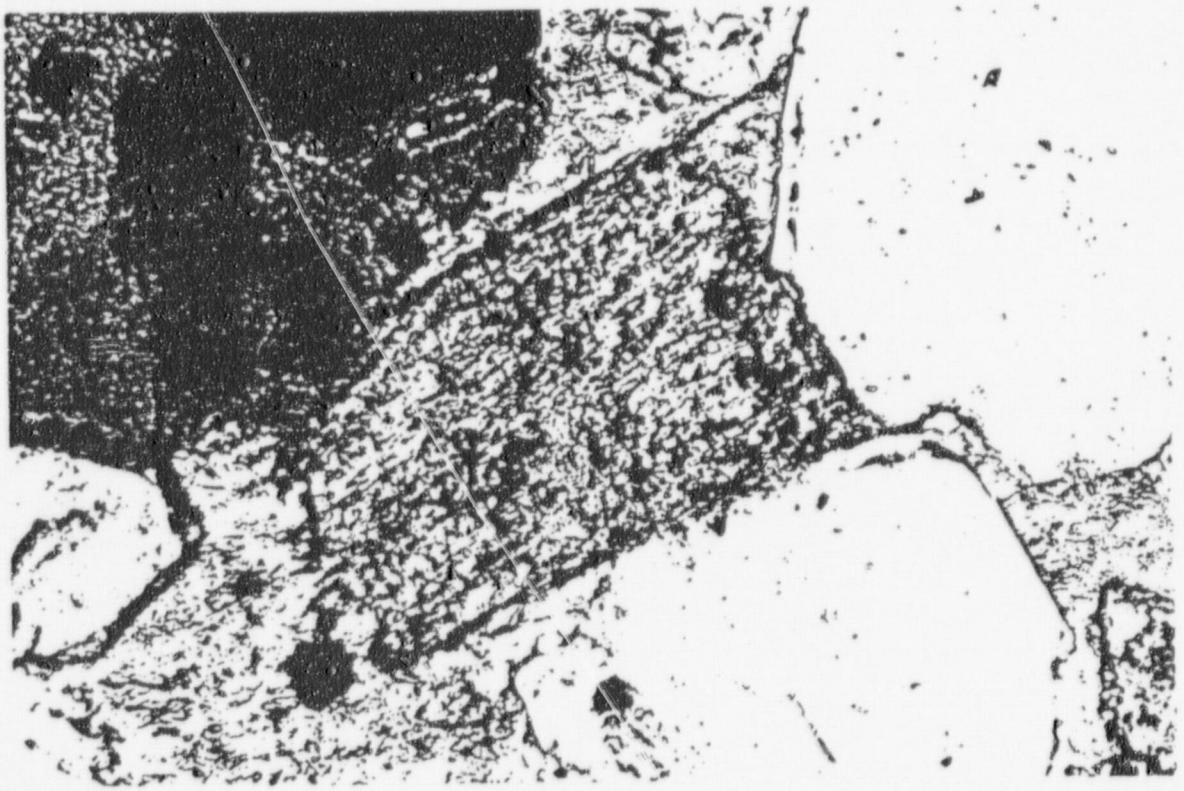

Photo 2: Center grain is K-feldspar replaced by calcite (pink). Outline of feldspar grain and some small remnants (yellow) are all that remain. Glauconite (upper left) and quartz with idiomorphic outline are also pictured. Plane polarized light - 250X.

CLIENT SAMPLE NO.: MW107 77.5'-78.5'
DCMSL SAMPLE NO. INTERA4-8

Hand Specimen Description

Client sample no. MW107 77.5'-78.5' is a grey colored sedimentary rock showing poor uniformity in grain size. In cross section, the rock contains numerous wavy lenses composed of clay and organic rich material because of severe bioturbation of the sediment before consolidation. Due to a carbonate matrix, the rock has little porosity, is dense, hard and nonfriable. Based on the following petrographic and modal analyses, the rock is classified as a very fine to fine grained, calcite cemented subarkose.

Microscopic Description

The rock's primary constituents are quartz, feldspar and carbonate. Individual quartz-feldspathic grains vary greatly from angular to well rounded. The well rounded grains are large and indicate a mixing of sediments from biogenic activity. Grain size measurements range from 0.05mm to 0.55mm. The rock is poorly sorted and texturally immature. Contacts between quartz-feldspathic grains are low. Consolidation of the clasts is the result of chemically precipitated calcite and dolomite. Quartz grains show virtually no overgrowths. In some areas pressure exerted from the growing calcite crystals has forced apart the grains' framework in addition to etching and corroding some quartz. Euhedral dolomite is also present and is seen enclosed by calcite, indicating it crystallized first. Overall, the carbonate is fresh and shows no indication of leaching.

Feldspar contained in the rock is primarily microcline, perthite and some plagioclase. Feldspar alteration is minor, suggesting that porosity in this rock has been relatively low and the influx of carbonate probably took place soon after deposition.

Clay contained in the rock consists of minute patches of authigenic kaolinite and some detrital clay mixed with dark organic material is present in biogenic structures. Trace amounts of rounded glauconite pellets are also present.

Modal Analysis

Quartz	56.0
K-Feldspar	4.8
Plagioclase	0.6
Clay (Undifferentiated)	1.6
Void	-
Calcite	32.6
Dolomite	3.4
Chert	0.8
Glauconite	0.2

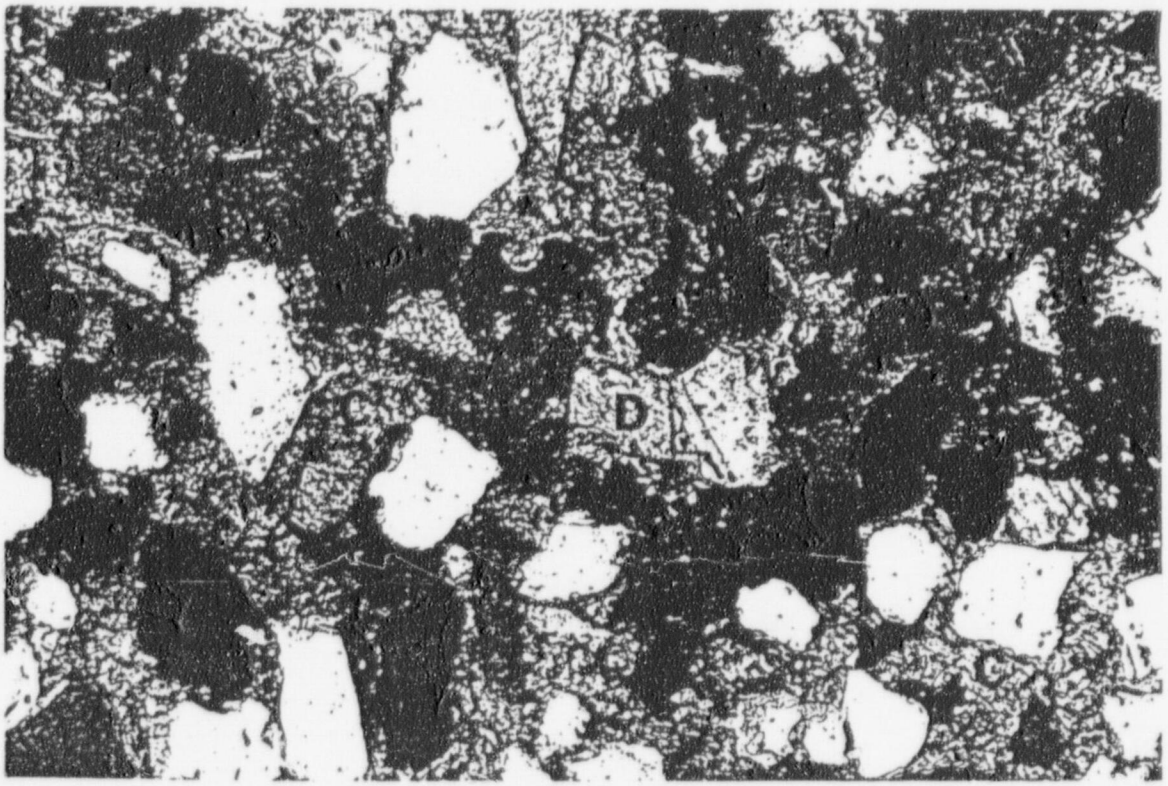

Photo 1: Quartz grains (white/grey) and K-feldspar (yellow stained) are cemented by calcite (C) and dolomite (D). Crossed polarized light - 100X.

Photo 2: Biogenic structure showing clay mixed with organic material, porosity (blue) and quartz grains (white/grey). Crossed polarized light - 100X.

CLIENT SAMPLE NO.: MW107 91.25'-91.5'
DCMSL SAMPLE NO. INTERA4-9

Hand Specimen Description

Client sample no. MW107 91.25'-91.5' is a grey sedimentary rock showing uniformity in grain size. In cross section, the rock has wavy, clay/organic rich laminae and numerous biogenic structures. Some dark green glauconite is also present. The rock has well developed porosity and is low to moderately friable. Based on the following petrographic and modal analyses, the rock is classified as a fine grained, silica cemented quartzarenite.

Microscopic Description

The primary constituents of the core are quartz, minor feldspar, carbonate and some clay. The quartz feldspathic grains are angular to subrounded and vary in size from 0.1mm to 0.2mm. The rock is texturally and mineralogically mature. Contacts between grains boundaries are low to moderate and show little effect due to compaction. More significantly, consolidation of the quartz grains is by quartz overgrowths. The overgrowths are intermediate stage as most quartz grains have well developed idiomorphic outlines. Some pore space has been filled by the overgrowths. Small random areas contain calcite and dolomite that act as a cementing agent, but are insignificant due to their low volume. Carbonate, when adjacent to pore space, exhibits euhedral features indicating no chemical attack.

Feldspar contained in the sample is microcline and plagioclase, with the potassium type as the most abundant. All show various stages of alteration. Microcline is the least altered with minor corrosion along cleavage planes. The plagioclase is frequently seen weathering to clay and sericite.

Detrital clay is restricted to biogenic structures where it is mixed with dolomite and dark organic material. Minor authigenic kaolinite occludes some pore space and rounded, dark green glauconite is also present.

Modal Analysis

Quartz	81.8
K-Feldspar	3.0
Plagioclase	1.2
Clay (Undifferentiated)	2.8
Void	8.6
Dolomite	0.8
Calcite	0.8
Chert	1.0
Glauconite	<0.2

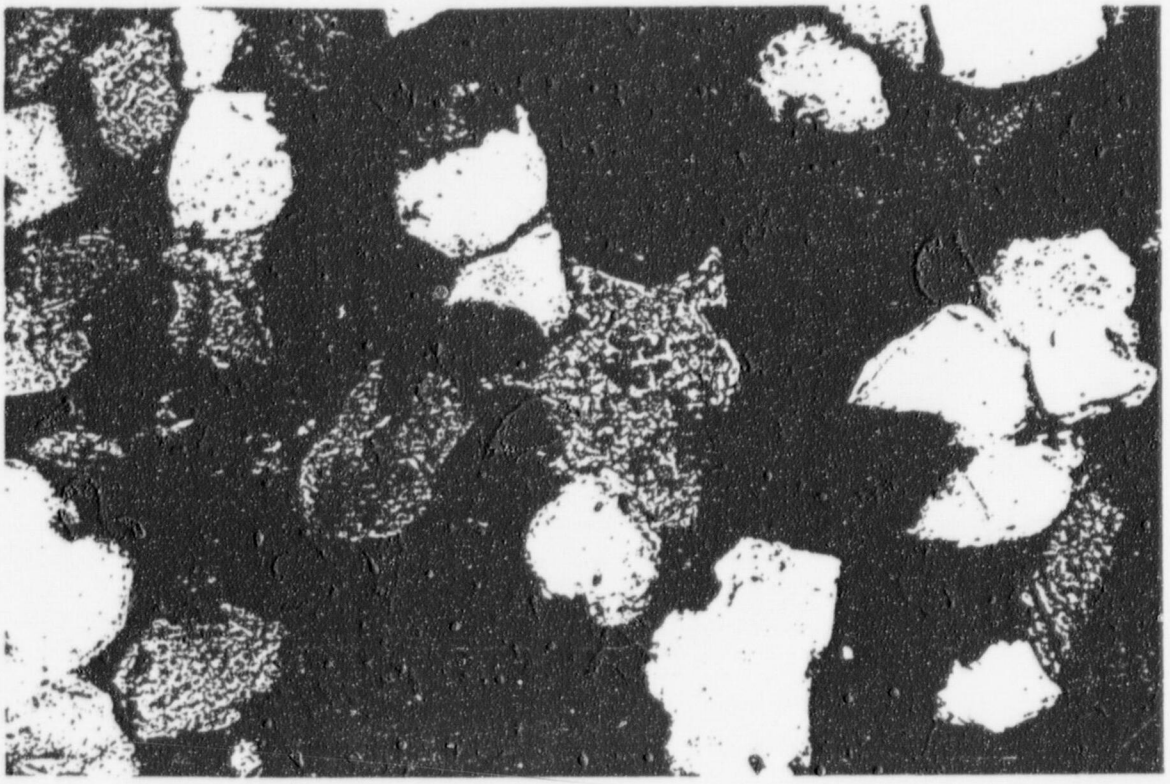

Photo 1: Small patch of calcite cements some quartz grains. K-feldspar is pictured in lower right corner. Crossed polarized light - 100X.

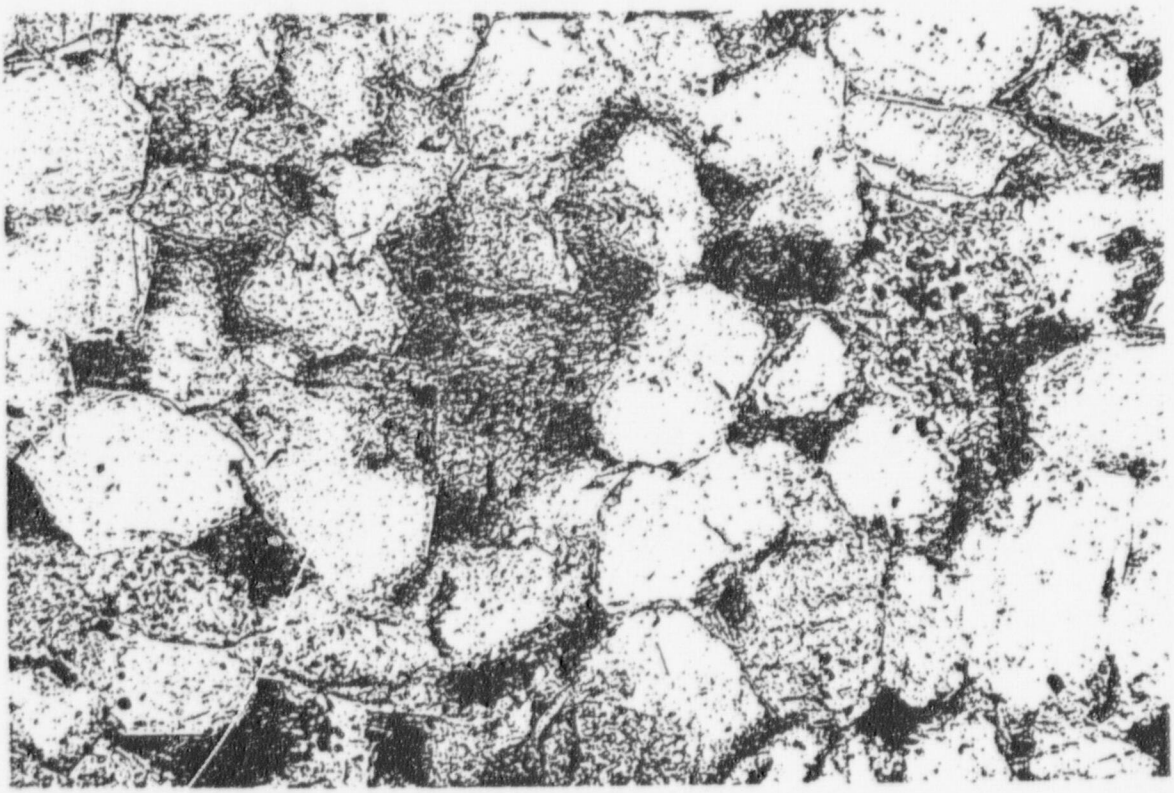

Photo 2: Area photomicrograph showing grain distribution and pore space. K-feldspar in the center exhibits dissolution and quartz grains show idiomorphic overgrowths. Plane polarized light - 100X.

CLIENT SAMPLE NO.: MW107 104'-105'
DCMSL SAMPLE NO. INTERA4-10

Hand Specimen Description

Client sample no. MW107 104'-105' is a grey sedimentary rock showing uniformity in mineralogic grain size. In cross section, the rock shows wavy clay/organic rich lenses and stringers due to biogenic activity. Some dark green, rounded glauconite is present. The rock has well developed porosity and is low to moderately friable. Based on the following petrographic and modal analyses, the rock is classified as a fine grained, silica cemented quartzarenite.

Microscopic Description

Texturally and lithologically, the rock is very similar to sample no. MW107 91.25'-91.5'. The primary constituent is quartz with minor amounts of feldspar, carbonate and some clay. The quartz-feldspathic grains are angular to subrounded and have grain sizes between 0.1mm and 0.25mm. The rock is texturally and mineralogically mature. Grain to grain contact is low to moderate and shows little effect from compaction. Consolidation of the rock is accomplished by quartz overgrowth cementation. The overgrowths are intermediate stage with many grains showing idiomorphic outlines. In some small areas, overgrowths have filled or restricted pore space. Calcite and dolomite are present, but are insignificant as cementing agents. The carbonate retains sharp outlines indicating no alteration.

Microcline and plagioclase show various stages of weathering ranging from minor corrosion in potassium feldspar to clay and sericite formation in the plagioclase. Detrital clay is present and is generally restricted to biogenic material, dolomite and silt. Authigenic, vermicular kaolinite is seen filling some pores. Microcrystalline chert, fibrous chalcedony and dark green glauconite are included as minor constituents.

Modal Analysis

Quartz	83.2
K-Feldspar	2.2
Plagioclase	0.2
Clay (Undifferentiated)	2.8
Void	7.8
Dolomite	<0.2
Calcite	1.6
Chert	1.2
Glauconite	1.0

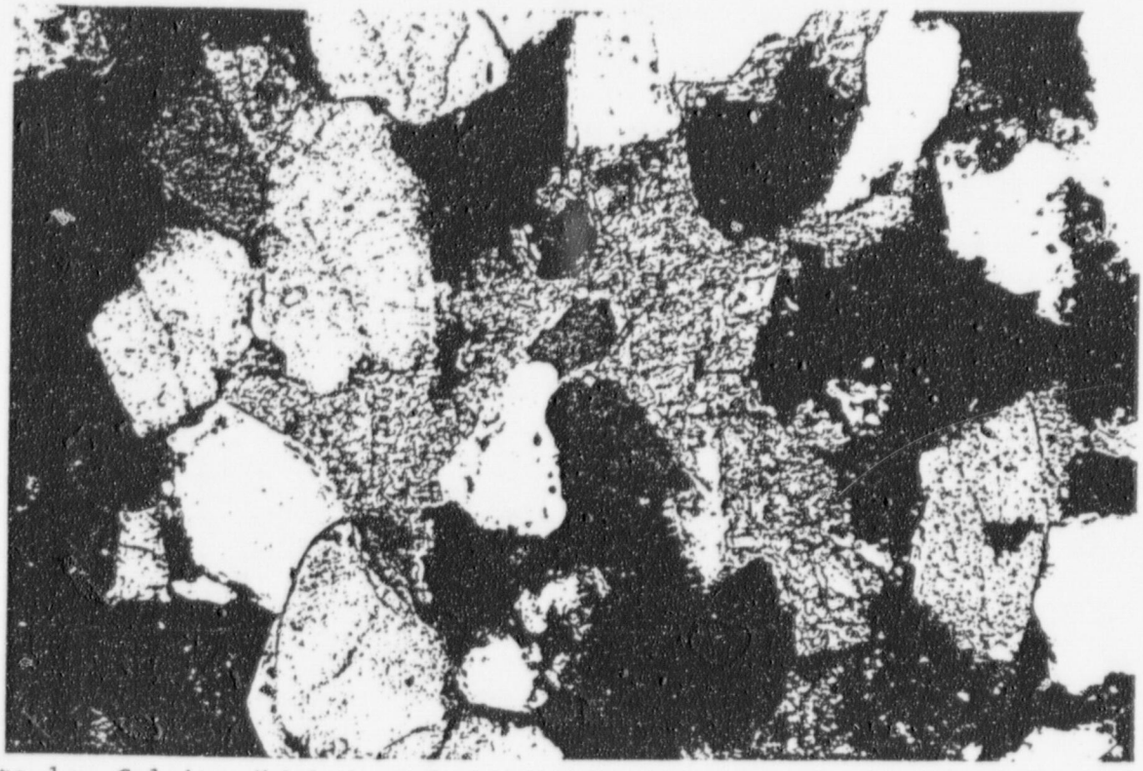

Photo 1: Calcite (high interference colors) cements quartz grains. Crossed polarized light - 100X.

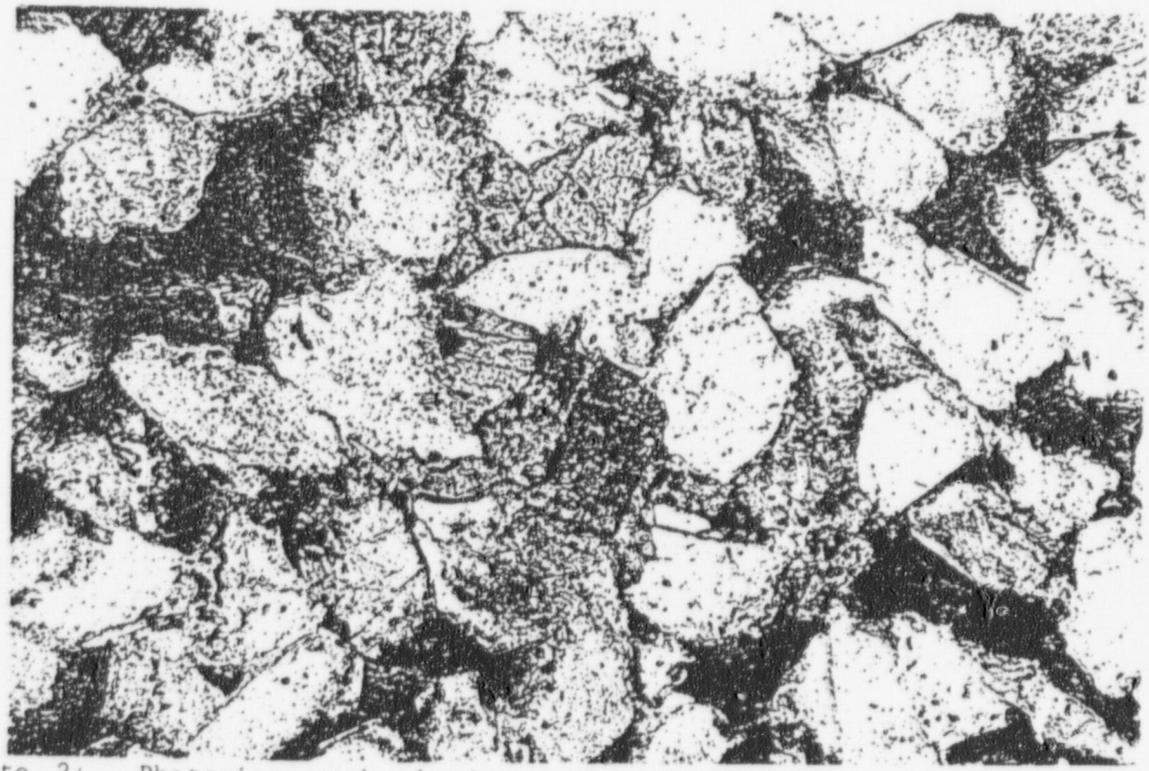

Photo 2: Photomicrograph showing grain distribution and porosity (blue). Calcite (light pink) partially replaces K-feldspar (yellow). Remainder of grains is quartz with some exhibiting idiomorphic outlines.

CLIENT SAMPLE NO.: MW107 109.5'
DCMSL SAMPLE NO. INTERA4-11

Hand Specimen Description

Client sample no. MW107 109.5' is a grey sedimentary rock showing significant variation in mineralogic grain size. In cross section, the rock shows evidence of severe bioturbation in the form of burrows and borings. The biogenic structures have moderate porosity, abundant clay mixed with dark organic material, glauconite and some authigenic pyrite. The rock surrounding the structures has little or no porosity and is non-friable due to a dense carbonate matrix. Based on the following petrographic and modal analyses, the rock is classified as a medium to coarse grained, calcite cemented subarkose.

Microscopic Description

The mineralogy of the rock is primarily quartz, chert, chalcedony, feldspar, calcite and glauconite. The grains are angular to well rounded. Grain size measurements are extreme, ranging from 0.05mm (coarse silt) to 1.00mm (coarse sand). The poor sorting and textural immaturity indicate a textural inversion from mixing and reworking of older sediments by biogenic activity. Contacts between quartz-feldspathic grains are low. Excluding the biogenic structures, lithification of the grains is due to sparry calcite. Additionally most of the quartz present shows little or no quartz overgrowths, suggesting calcite precipitated soon after deposition. Some minor dolomite is also present. The carbonate matrix is fresh and unaltered.

Biogenic structures (burrows) contain little carbonate, have good porosity and show some diagenic effects due to pore fluid migration. The rock in general contains numerous chert and fibrous chalcedony clasts, but the burrows contain large patches of chert that appear to have precipitated in site. The patches conform to the geometry of the larger voids and in some cases, engulf quartz-feldspathic grains. Additionally, the feldspars present show a greater degree of dissolution with most grains showing corroded boundaries, pitting, intraparticle porosity and alteration to clay. Feldspar contained in the carbonate matrix shows some calcite replacement but overall, little alteration is indicated.

Detrital clay mixed with dark organic material, small occluded pores containing authigenic, vermicular kaolinite, authigenic pyrite and glauconite are also common features in the structures. Glauconite contained in the carbonate shows shrinkage around grain boundaries, accounting for some minor secondary porosity.

Modal Analysis

Quartz	58.4
K-Feldspar	3.0
Plagioclase	0.2
Clay (Undifferentiated)	5.8
Void	9.2
Dolomite	0.2
Calcite	10.6
Chert/Chalcedony	9.0
Glauconite	3.6

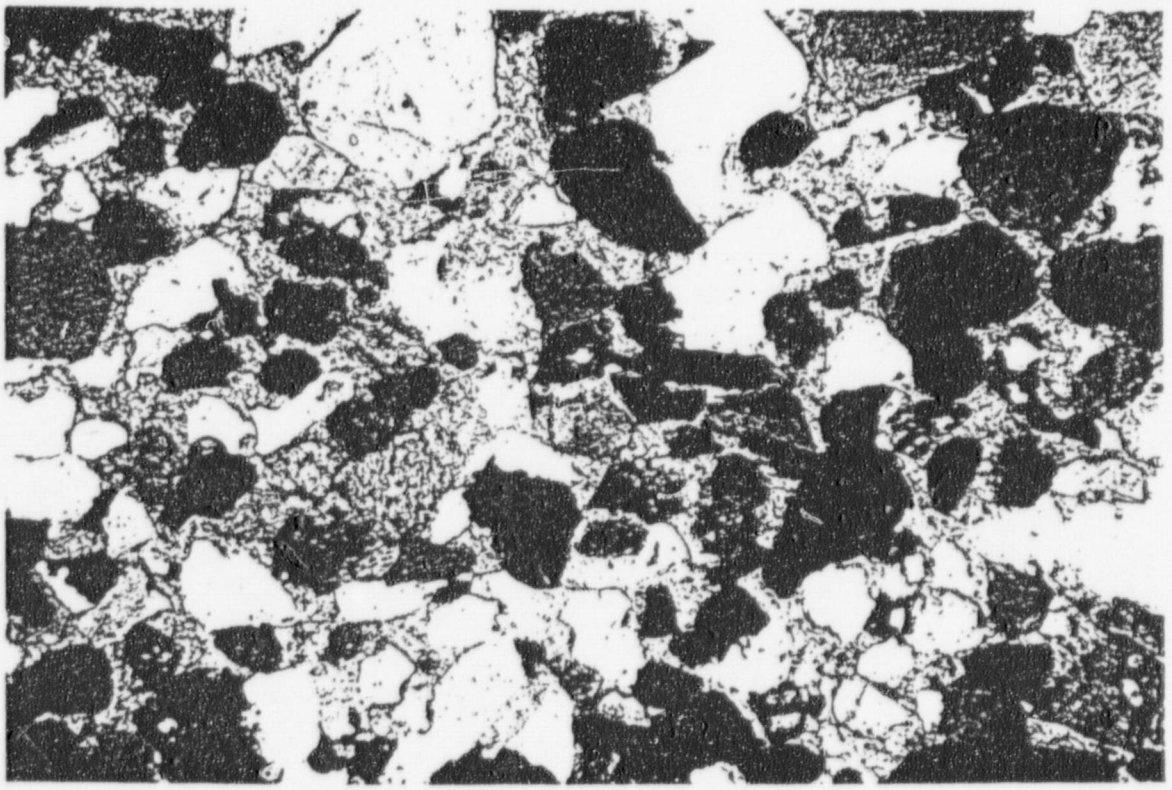

Photo 1: Poorly sorted quartz (grey/white) and K-feldspar (yellow) cemented by sparry calcite. Crossed polarized light - 40X.

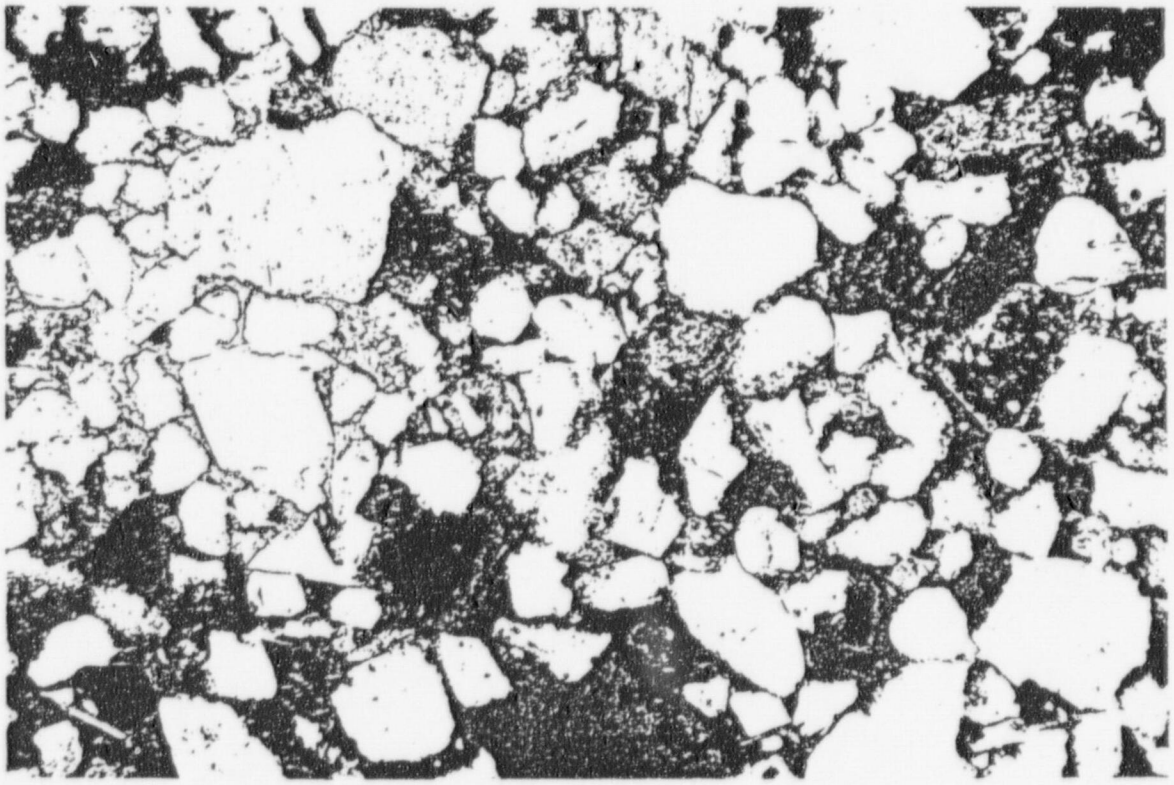

Photo 2: Area photo of biogenic structure showing high porosity, green glauconite, K-feldspar (yellow) and poorly sorted quartz. Plane polarized light - 40X.

CLIENT SAMPLE NO.: MW107 120'
DCMSL SAMPLE NO. INTERA4-12

Hand Specimen Description

Client sample no. MW107 120' is a grey sedimentary rock showing moderate variation in mineralogic grain size. In cross section, the rock shows thin, wavy laminae composed of clay mixed with dark organic material and numerous biogenic structures (burrows). Dark green glauconite and clay occluded voids are common. Excluding areas of patchy carbonate cement, the rock has well developed porosity and is moderately soft and friable. Based on the following petrographic and modal analyses, the rock is classified as a fine to medium grained, silica/calcite cemented subarkose.

Microscopic Description

Framework of the sandstone is primarily made of quartz, chert, feldspar and glauconite pellets. Included in the matrix is clay and secondary carbonate. Quartz-feldspathic grains are angular to rounded and have measurements between 0.1mm and 0.5mm, indicating the rock is moderately sorted and texturally submature. Some coarse silt size particles are also present but are restricted to biogenic structures. Contact between grain boundaries is low and porosity is well developed, indicating little effect from compaction. Lithification is achieved by quartz overgrowth cementation followed by secondary calcite. Many of the grains show idiomorphic outlines and when in contact promote minor cementation.

Calcite cement is random and consists of small patches. When next to open pore space, the carbonate shows a partial, euhedral outline with a fresh, unaltered appearance. This suggests spasmodic precipitation where periods of growth were interrupted by a period of non-deposition. Minor dolomite is also present but appears to be confined to the biogenic structures.

Feldspar contained in the rock is primarily microcline along with minor amounts of plagioclase. Both species show various stages of alteration. Microcline is altered the least with minor corrosion along cleavage planes. Rarely, some clasts show replacement by calcite. Plagioclase is frequently seen altering the clay and sericite.

Excluding glauconite pellets, detrital clay is restricted to biogenic features and voids where it promotes very minor cementation. Some small pores are occluded with fine grained vermicular kaolinite. Dark green glauconite pellets are randomly scattered throughout and are associated with authigenic pyrite.

Modal Analysis

Quartz	74.4
K-Feldspar	3.6
Plagioclase	0.8
Clay (Undifferentiated)	4.6
Void	7.4
Dolomite	0.4
Calcite	3.0
Chert	2.2
Glauconite	3.6

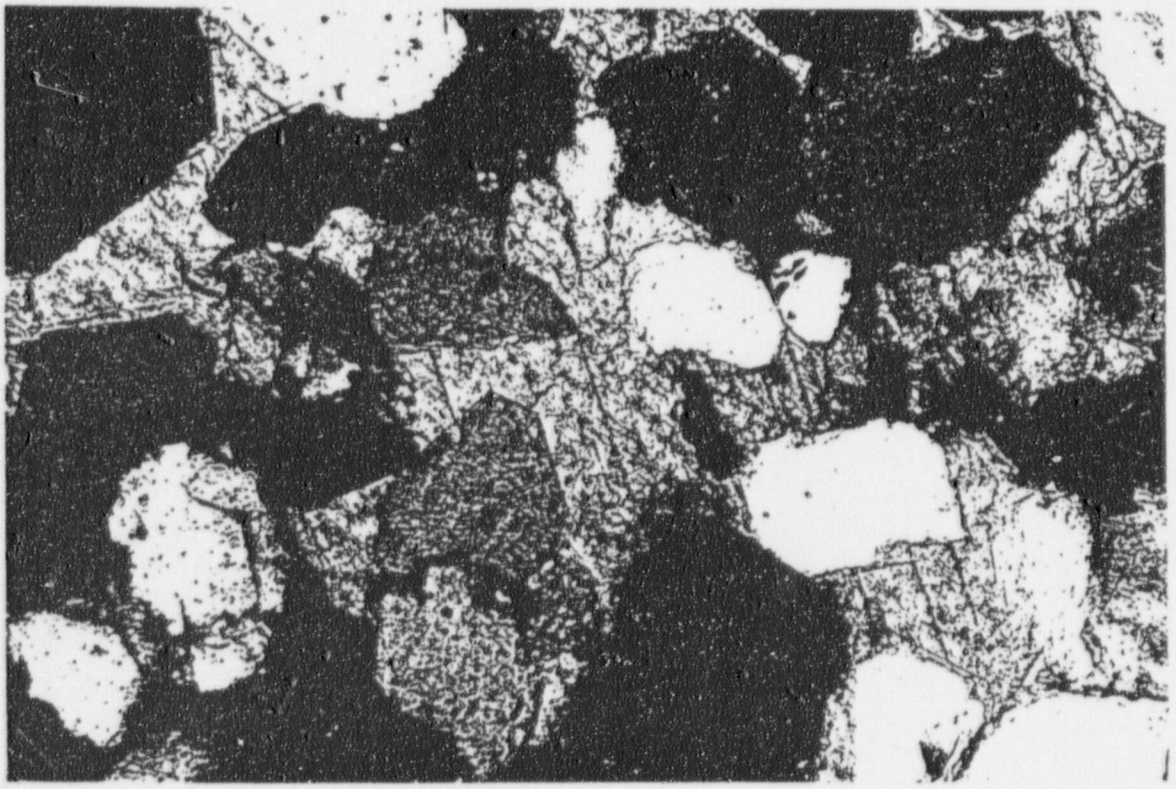

Photo 1: Coarse grained calcite (high interference colors) cement quartz (white/grey) and K-feldspar (yellow). Crossed polarized light - 100X.

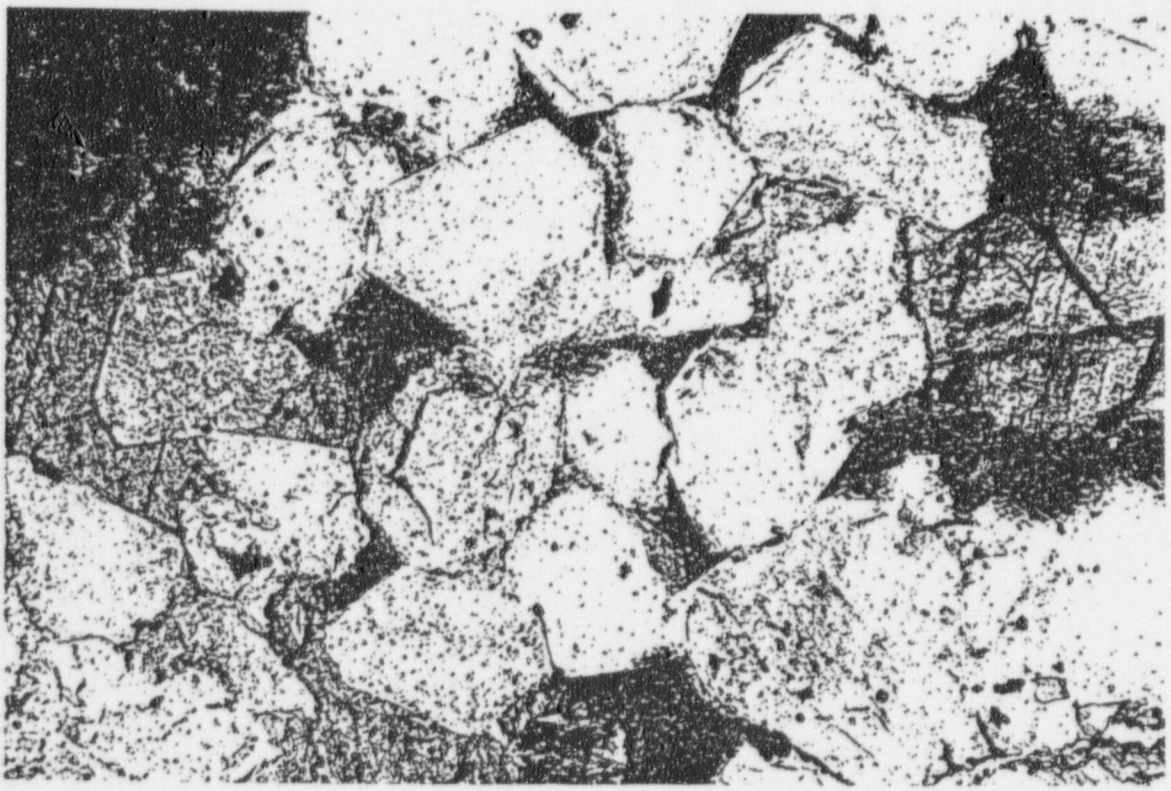

Photo 2: Clear quartz showing idiomorphic outlines. Pictured to the right is K-feldspar showing some dissolution and intraparticle porosity. Green glauconite is at the upper left hand corner and calcite (light pink) is to the left and lower left. Porosity is blue. Plane polarized light - 100X.

Modal Analysis

Quartz	74.4
K-Feldspar	3.6
Plagioclase	0.8
Clay (Undifferentiated)	4.6
Void	7.4
Dolomite	0.4
Calcite	3.0
Chert	2.2
Glauconite	3.6

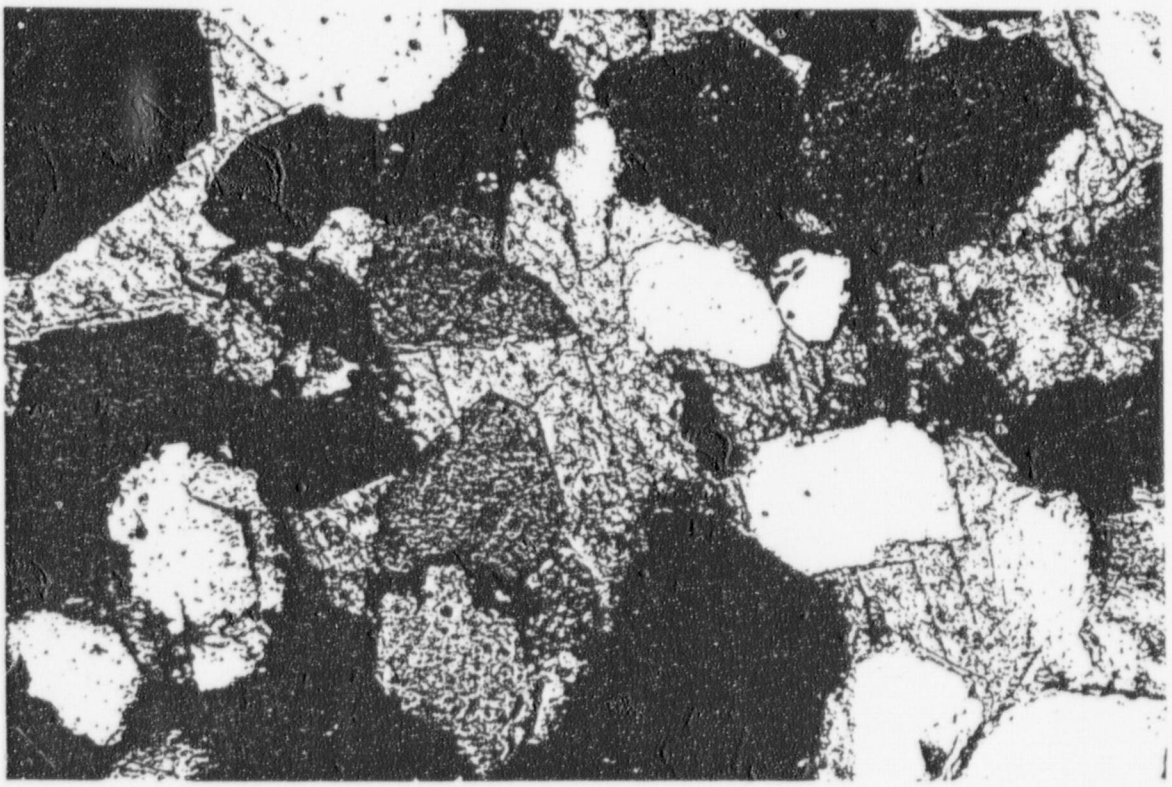

Photo 1: Coarse grained calcite (high interference colors) cement quartz (white/grey) and K-feldspar (yellow). Crossed polarized light - 100X.

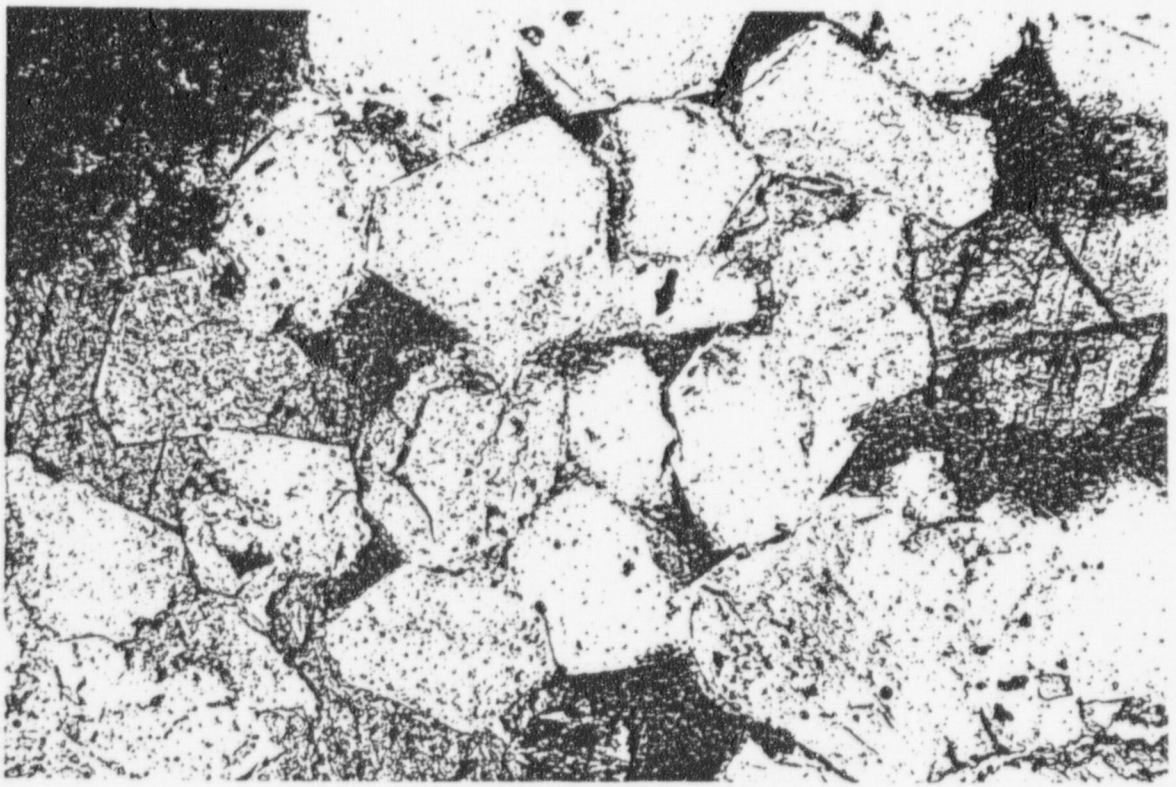

Photo 2: Clear quartz showing idiomorphic outlines. Pictured to the right is K-feldspar showing some dissolution and intraparticle porosity. Green glauconite is at the upper left hand corner and calcite (light pink) is to the left and lower left. Porosity is blue. Plane polarized light - 100X.

CLIENT SAMPLE NO.: MW108 51.9'-52.2'
DCMSL SAMPLE NO. INTERA4-13

Hand Specimen Description

Client sample no. MW108 51.9'-52.2' is a tan colored sedimentary rock showing great variation in mineralogic grain size. In cross section the rock has no bedding planes, but shows the effects of bioturbation in the form of borings and clay/organic rich, wavy laminae. Clay, carbonate and patchy gypsum occlude some pore space, but porosity is well developed and the rock is moderately soft and friable. Based on the following petrographic and modal analyses, the rock is classified as a poorly sorted, very fine to medium grained, gypsum/dolomite cemented subarkose.

Microscopic Description

The sample consists of very fine to medium grained quartz, chert and feldspar in a patchy matrix of clay, gypsum and dolomite. Clasts possess a wide range of grain size from 0.05mm (coarse silt) to 0.45mm (medium sand) and retain angular to subrounded shapes, indicating a poorly sorted and texturally immature sediment. Contacts between quartz-feldspathic grains are low and overgrowths are rarely present on quartz. Consolidation of the sediment is the result of secondary gypsum, dolomite and the infiltration of clay. Cementation by gypsum and dolomite is patchy and inconsistent. Many times, euhedral dolomite is surrounded by gypsum, indicating it crystallized first. When adjacent to open pore space, both cements show signs of dissolution, suggesting that at least some of the rock's porosity is secondary.

Clay coats many of the grains, but more significantly, it is seen occluding pore space and as thin lenses where it is mixed with silt, dolomite and dark organic material. In areas of high concentration, the clay promotes some minor cementation. Clay marginal to and filling pore space commonly shows radial and vermicular growth, indicating some of the clay is authigenic. Some minor glauconite is also present.

Feldspar is primarily microcline as well as minor plagioclase. Alteration of plagioclase to clay and sericite is common. Microcline shows various stages of alteration ranging from minor corrosion to complete dissolution. Some grains have minor carbonate replacement. Microcrystalline chert, fibrous chalcedony and biotite mica are also contained in the sample. Some of the biotite shows alteration to chlorite.

Modal Analysis

Quartz	63.2
K-Feldspar	3.6
Plagioclase	1.4
Clay (Undifferentiated)	14.6
Void	7.0
Gypsum	4.2
Dolomite	4.8
Chert	1.2
Glauconite	<0.2

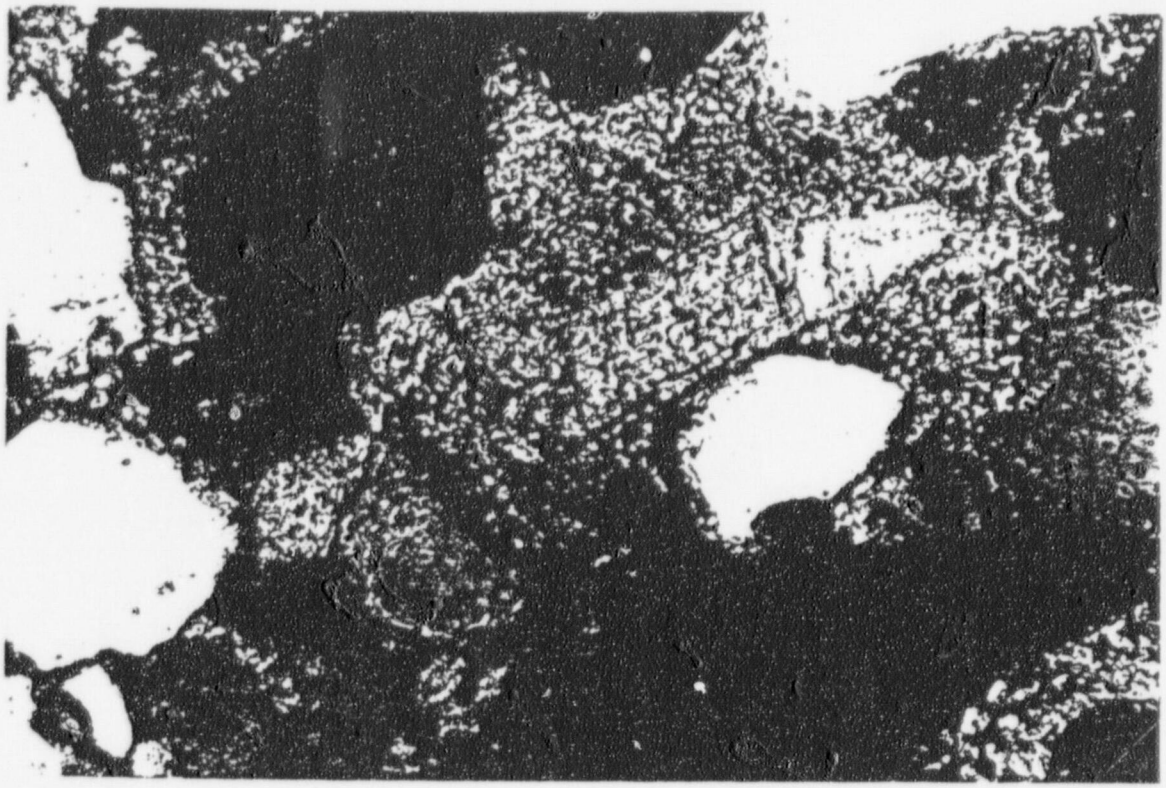

Photo 1: Photomicrograph of gypsum (G) cementing quartz grains (white/grey) and including an euhedral grain of dolomite. Mass of clay mixed with dark organic material is pictured at the bottom. Crossed polarized light - 250X.

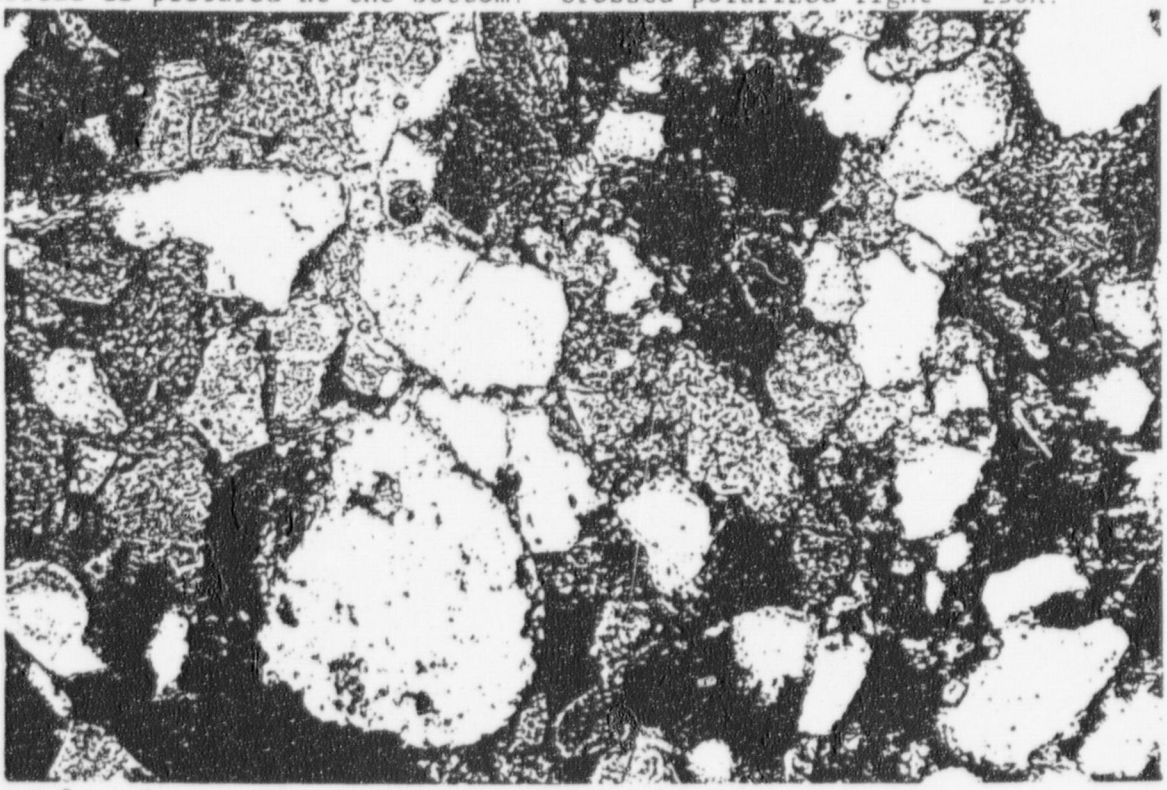

Photo 2: Gypsum (G) cementing quartz (white/grey) is adjacent to area of porosity (blue). A grain of K-feldspar (yellow) is also pictured. Slightly uncrossed polarized light - 100X.

CLIENT SAMPLE NO.: MW108 90.0'-90.3'
DCMSL SAMPLE NO. INTERA4-14

Hand Specimen Description

Client sample no. MW108 90.0'-90.3' is a light grey colored sedimentary rock showing moderate uniformity in grain size. In cross section, the rock has well-developed bedding planes that change in composition. Dark thin beds of predominantly glauconite mixed with quartz and authigenic pyrite alternate with thicker beds of quartz feldspathic sandstone. The sample has well developed porosity and is moderately soft and friable. Based on the following petrographic and modal analyses, the rock is classified as a medium to coarse grained, silica cemented subarkose.

Microscopic Description

The sample consists of medium to coarse grained quartz, feldspar and green glauconite. The clasts range in size from 0.25mm to 0.75mm and are subangular to rounded, indicating a well sorted and texturally mature sandstone. Overall, quartz-feldspathic grain contacts are low and porosity is well developed. Consolidation of the clasts is primarily due to intermediate stage quartz overgrowths. Most of the quartz clasts show idiomorphic outlines. Minor effects from compaction can be seen in the glauconite rich lenses where the softer glauconite is squeezed and deformed. When squeezed into adjoining pore space, the glauconite promotes minor lithification.

Microcline, perthite and trace amounts of plagioclase are present. Most of the potassium feldspar clasts show minor dissolution particularly at edges and cleavage planes. The plagioclase is altered to clay and sericite. Delicate, vermicular kaolinite is seen in some pores and detrital clay is seen mixed with dolomite and dark organic material. Euhedral cubes of authigenic pyrite are associated with the glauconite.

Modal Analysis

Quartz	68.0
K-Feldspar	4.0
Plagioclase	<0.2
Clay (Undifferentiated)	1.8
Void	9.4
Pyrite	1.4
Glauconite	12.2
Chert	3.2

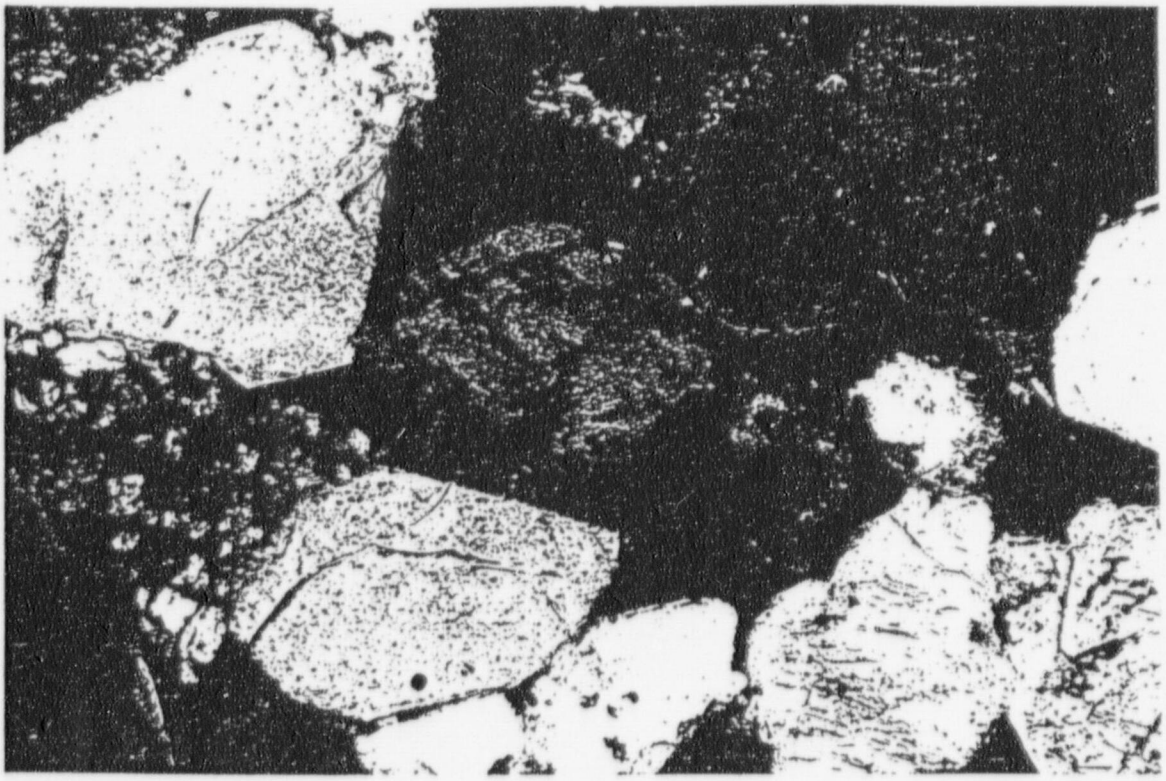

Photo 1: Pictured is quartz (white/grey) showing idiomorphic outlines, K-feldspar in the center exhibiting intraparticle porosity and corrosion due to dissolution and porosity (blue). Crossed polarized light - 250X.

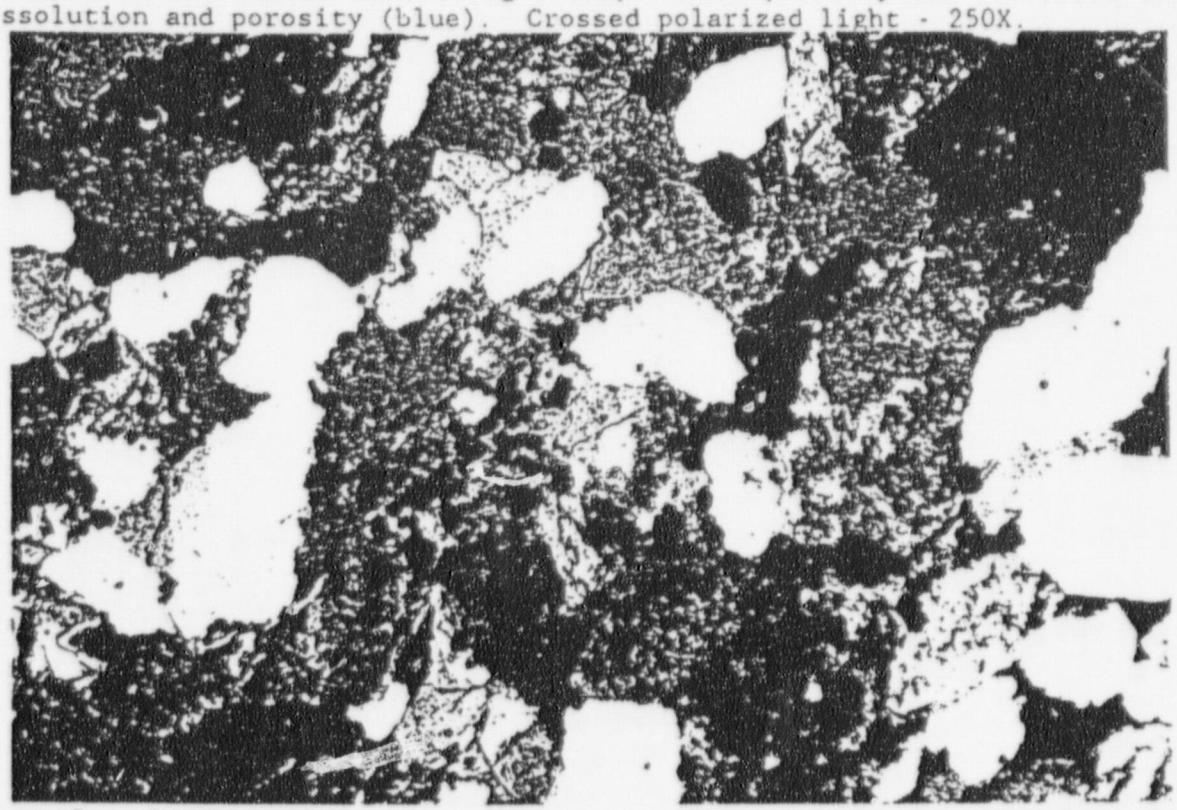

Photo 2: Bedding plane showing concentration of green glauconite cementing quartz grains (white/grey) and chert (C). Euhedral cubes of opaque pyrite are scattered throughout. Crossed polarized light - 100X.

CLIENT SAMPLE NO.: MW109 47.5'-47.8'
DCMSL SAMPLE NO. INTERA4-15

Hand Specimen Description

Sample no. MW109 47.5'-47.8' is a light tan colored fine grained sedimentary rock showing moderate uniformity in mineralogic grain size. In cross-section the sample has weak bedding planes and some evidence of light bioturbation. The rock has well developed porosity and exhibits low to moderate friability. Based on the following petrographic and modal analyses, the rock is classified as a fine grained, silica/gypsum cemented subarkose.

Microscopic Description

In thin section, the rock's clasts are primarily quartz and feldspar with minor amounts of clay, dolomite and gypsum. The clasts range in size from 0.12mm to 0.25mm, are subangular to rounded indicating a well sorted and texturally mature sandstone. The majority of quartz-feldspathic grains shows low contact between grain boundaries. The effects of sediment compaction are insignificant. Lithification was a two stage process in which quartz overgrowth cementation was followed by minor gypsum precipitation. Most of the quartz grains show early to intermediate overgrowths with some having well developed idiomorphic outlines. Subsequent to quartz overgrowths, secondary gypsum precipitates and promotes some cementation. Its occurrence, however, is patchy and irregular. When adjacent to pore space, the gypsum shows signs of dissolution along edges and cleavage planes. Many places show complete removal and the formation of secondary porosity. Minor amounts of secondary dolomite are also present, but are insignificant as a cementing agent.

Feldspar clasts include grid twinned microcline and plagioclase. The more stable microcline shows some dissolution along cleavage planes. In contrast, the plagioclase has altered to clay and sericite. Detrital clay is present but uncommon and delicate vermicular kaolinite occludes some pores.

Modal Analysis

Quartz	83.4
K-Feldspar	3.2
Plagioclase	1.4
Clay (Undifferentiated)	1.6
Void	8.4
Gypsum	1.0
Dolomite	0.8
Chert	0.2

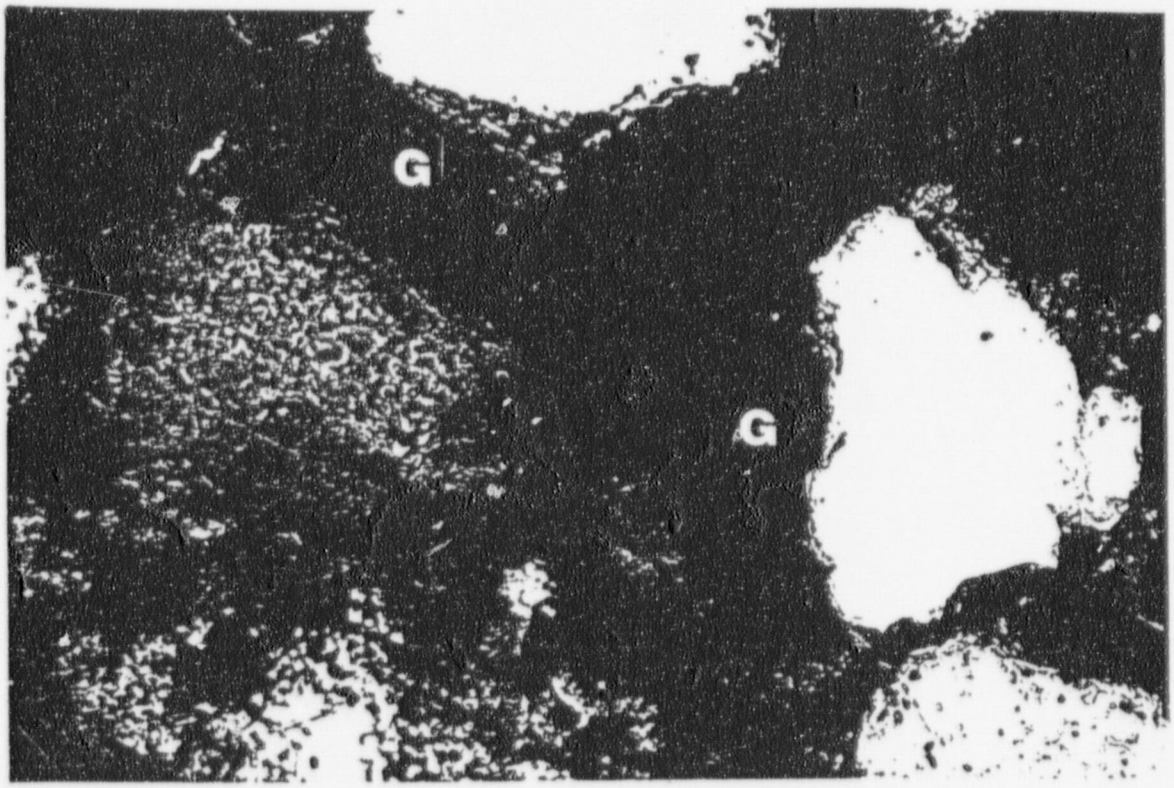

Photo 1: Gypsum (G) cements quartz grains (white/grey) and K-feldspar (yellow). Crossed polarized light - 250X.

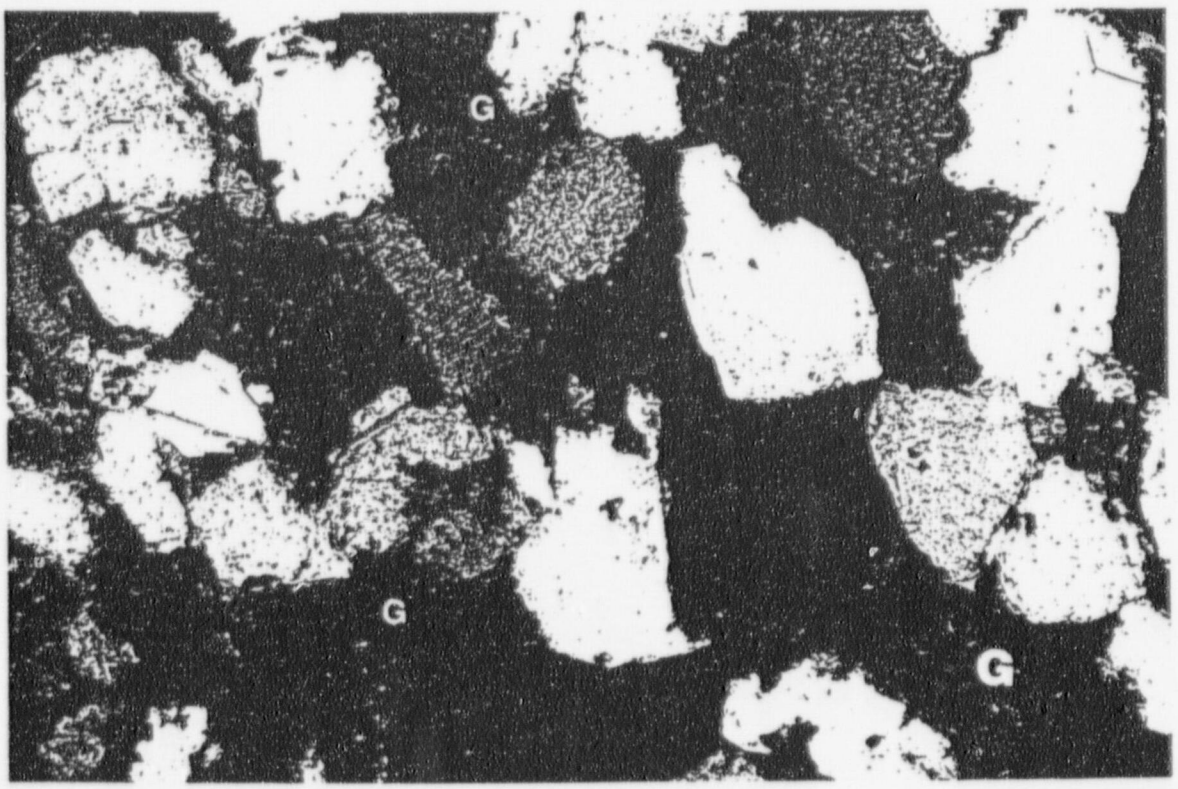

Photo 2: Gypsum (G) cementing quartz grains adjacent to area of porosity (blue). Crossed polarized light - 100X.

CLIENT SAMPLE NO.: MW109 81.4'-81.8'
DCMSL SAMPLE NO. INTERA4-16

Hand Specimen Description

Client sample no. MW109 81.4'-81.8' is a grey sedimentary rock showing uniformity in mineralogic grain size. In cross section the rock shows sedimentary structures that include bedding planes and some minor bioturbation. Green glauconite pellets are scattered throughout and some pores and voids are occluded with detrital clay. The rock has well developed porosity and is moderately soft and friable. Based on the following petrographic and modal analyses, the rock is classified as a medium to coarse grained, silica cemented subarkose.

Microscopic Description

The sample consists of medium to coarse grained quartz, feldspar and glauconite pellets. The clasts range from 0.25mm to 0.50mm and are subangular to rounded, indicating a well sorted and texturally mature sediment. Compaction of the sediment is low as indicated by low quartz-feldspathic grain contact, well developed porosity and presence of large voids. Lithification is achieved by quartz overgrowth cementation. Most grains show idiomorphic outlines, indicating overgrowths are of intermediate stage.

Feldspar is primarily microcline and perthite with minor showing of plagioclase. The feldspar is in various stages of alteration. Although some of the potassium feldspar grains show minor corrosion to nearly complete dissolution, most are fresh and unaltered. Alteration is most severe in plagioclase where it has been replaced with sericite and clay.

Clay contained in the sample is generally restricted to bedding planes and biogenic structures where it is mixed with silt, organic matter and dolomite grains. Some small pores are filled with authigenic, vermicular kaolinite. Green detrital glauconite is randomly scattered throughout the rock. In some cases it has formed secondary and intraparticle porosity due to shrinkage.

Modal Analysis

Quartz	75.2
K-Feldspar	3.4
Plagioclase	0.8
Clay (Undifferentiated)	2.8
Void	10.4
Dolomite	0.8
Glauconite	3.6
Chert	3.0

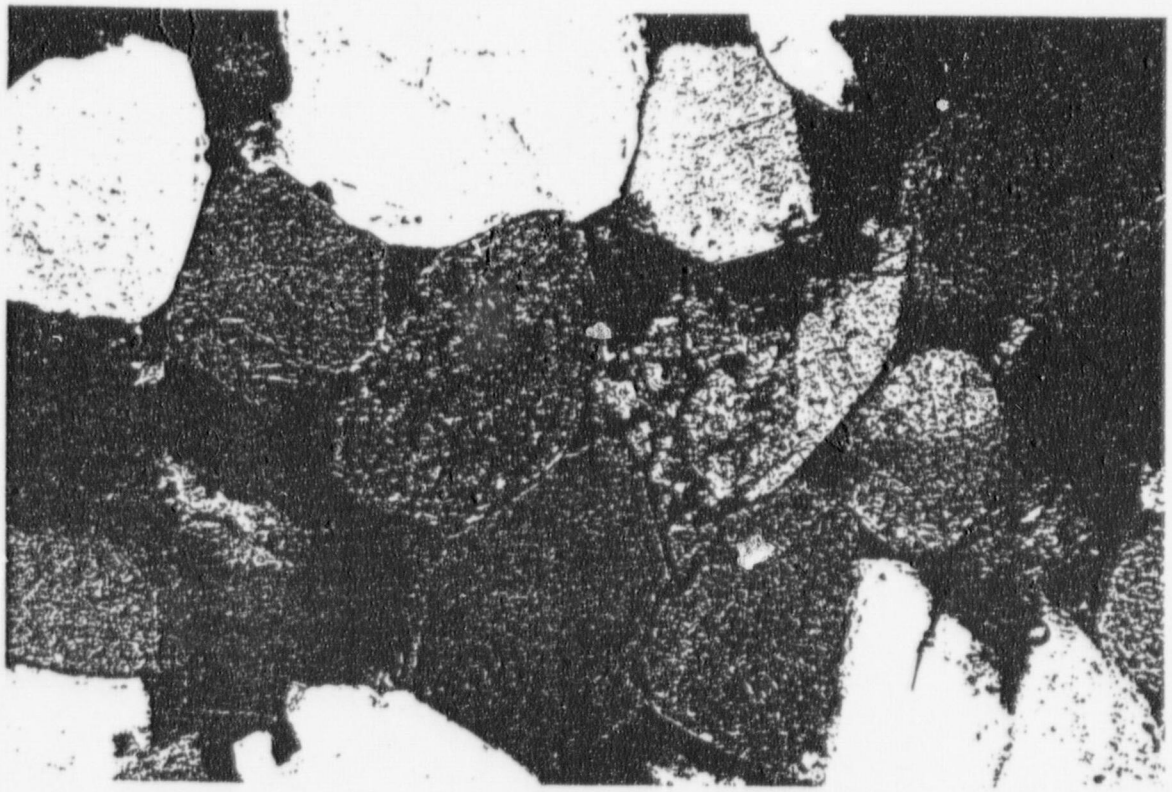

Photo 1: Quartz grains (white/grey) show well developed idiomorphic outlines. In the center, a well rounded glauconite pellet (green) adjacent to a K-feldspar clast shows the effects of dissolution. Crossed polarized light - 100X.

Don L. Mott
ANALYST

APPENDIX A-2

ACIDITY AND ACID-NEUTRALIZATION CALCULATIONS

Estimated Acidity of Tailings Fluid

1996 Tailings Fluid Volume $Vtail := 65.5 \cdot 10^{6} \cdot gal$

Acidity To Be Neutralized

H+ in fluid (pH 2.03): $Ah := \left(\frac{10^{-2.03}}{0.764} \cdot \frac{mole}{liter}\right) \cdot Vtail$ $Ah = 3.0 \cdot 10^{6} \cdot mole$ $\frac{Ah}{Vtail} = 0.012 \cdot \frac{mole}{liter}$

Al+3 in fluid: Al+3 + 3 H2O ==> Al(OH)3 (s) + 3 H+

or: 2 Al+3 + 2 H4SiO4(aq) + H2O ==> Al2(Si2O5)(OH)4(s) + 6 H+

$Aal := \frac{3370 \cdot mg \cdot liter^{-1}}{27 \cdot gm \cdot mole^{-1}} \cdot \left(\frac{3 \cdot mole}{1 \cdot mole}\right) \cdot Vtail$ $Aal = 9.3 \cdot 10^{7} \cdot mole$ $\frac{Aal}{Vtail} = 0.374 \cdot \frac{mole}{liter}$

Fe+3 in fluid: Fe+3 + 3 H2O ==> Fe(OH)3 (s) + 3 H+

$Afe := \frac{4390 \cdot mg \cdot liter^{-1}}{55.85 \cdot gm \cdot mole^{-1}} \cdot \left(\frac{3 \cdot mole}{1 \cdot mole}\right) \cdot Vtail$ $Afe = 5.8 \cdot 10^{7} \cdot mole$ $\frac{Afe}{Vtail} = 0.236 \cdot \frac{mole}{liter}$

NH4+ in fluid: NH4+ + 2 O2 (g) ==> NO3- + H2O + 2 H+

or NH4+ ==> NH3(g) + H+

$Anh4 := \frac{650 \cdot mg \cdot liter^{-1}}{18 \cdot gm \cdot mole^{-1}} \cdot \left(\frac{1.5 \cdot mole}{1 \cdot mole}\right) \cdot Vtail$ $Anh4 = 1.3 \cdot 10^{7} \cdot mole$ $\frac{Anh4}{Vtail} = 0.054 \cdot \frac{mol}{liter}$

Total acidity: $Atot := Ah + Aal + Afe + Anh4$ $Atot = 1.68 \cdot 10^{8} \cdot mole$ $\frac{Atot}{Vtail} = 0.677 \cdot \frac{mole}{liter}$

Stratigraphic Acid-Neutralizing Capacity

Alluvium or Mancos Shale:

Porosity: $por := 0.3$

Dry bulk density: $dbdens := (1 - por) \cdot 2.6 \cdot \frac{kg}{liter}$

$dbdens = 1.82 \cdot gm \cdot mL^{-1}$

Mineral Content:

$Fcalcite := 20 \cdot \%$

Acidity Neutralization (>99 % acidity is neutralized as pH increases to 6):

$CaCO3 + 2\,H+ \Longrightarrow Ca+2 + H2CO3(aq) + H2O$

$MWcalcite := 100 \cdot gm \cdot mole^{-1}$

Volume of formation needed for neutralization:

$$Vf := \frac{Atot}{dbdens \cdot \left(2 \cdot \frac{mole}{mole} \cdot \frac{Fcalcite}{MWcalcite}\right)}$$

$Vf = 8.1 \cdot 10^{5} \cdot ft^{3}$

$Vf = 2.3 \cdot 10^{7} \cdot liter$

First Tres Hermanos Formation:

Porosity: $por := 0.3$

Dry bulk density: $dbdens := (1 - por) \cdot 2.6 \cdot \frac{kg}{liter}$

$dbdens = 1.82 \cdot gm \cdot mL^{-1}$

Mineral Content:

$FTHcalcite := 2 \cdot \%$

$FTHkaol := 7 \cdot \%$

Acidity Neutralization (>99% acidity is neutralized as pH increases to 6):

$CaCO3 + 2\,H+ \Longrightarrow Ca+2 + H2CO3(aq) + H2O$

$MWcalcite := 100 \cdot gm \cdot mole^{-1}$

Volume of FTH for neutralization:

$$Vfth := \frac{Atot}{dbdens \cdot \left(2 \cdot \frac{mole}{mole} \cdot \frac{FTHcalcite}{MWcalcite}\right)}$$

$Vfth = 8.1 \cdot 10^{6} \cdot ft^{3}$

$Vfth = 2.3 \cdot 10^{8} \cdot liter$

Prepared for
KENNECOTT ENERGY COMPANY
Gillette, Wyoming

PROJECTED LONG-TERM FLOW AND QUALITY OF GROUNDWATER AT THE L-BAR, NEW MEXICO, URANIUM SITE

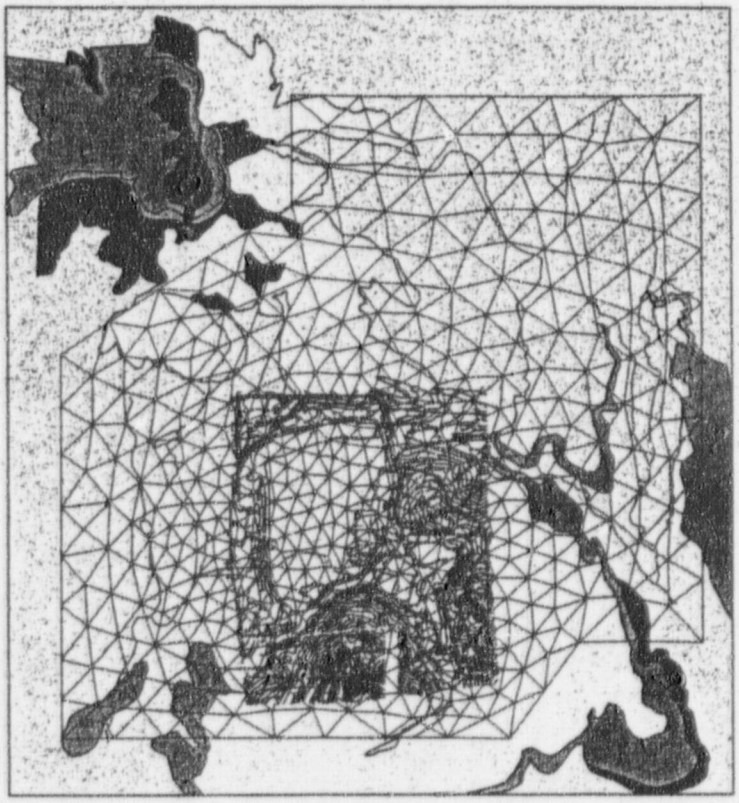

JULY 1997

BALLEAU GROUNDWATER, INC.
901 Rio Grande Boulevard NW, Suite F-242
Albuquerque, New Mexico 87104
(505) 247-2000

Prepared for
KENNECOTT ENERGY COMPANY
Gillette, Wyoming

Projected Long-Term Flow and Quality of Groundwater at the L-Bar, New Mexico, Uranium Site

BALLEAU GROUNDWATER, INC.
901 Rio Grande Blvd. NW, Suite F-242
Albuquerque, New Mexico 87104
(505) 247-2000

Nabil G. Shafike, Ph.D.

W. Peter Balleau, CPG, P.Hg.

Date July 25, 97

PROJECTED LONG-TERM FLOW AND QUALITY OF GROUNDWATER AT THE L-BAR, NEW MEXICO, URANIUM SITE

TABLE OF CONTENTS

SUMMARY 1
INTRODUCTION 2
HISTORY OF THE TAILINGS RESERVOIR 5
GEOLOGIC SETTING 7
MODEL STRUCTURE 7
BOUNDARY CONDITIONS 19
HYDROLOGIC PARAMETERS 23
TRANSIENT RUN SCHEDULE 27
RESULTS AND ANALYSIS 27
- Steady State 27
- Transient Simulation 27
- Head 32
- Concentration 42
- Future Prediction 46

CONCLUSIONS 51
REFERENCES 52

LIST OF TABLES

		Page
Table 1.	Tailings Reservoir Water Levels	6
Table 2.	Calibrated Hydrologic Parameters for Model Materials	26
Table 3.	Schedule of the Transient Model Run	28
Table 4.	Observed and Simulated Steady-State Head	30
Table 5.	Steady-State Recharge and Discharge	31
Table 6.	The Simulated Flow Components of the System	34

LIST OF FIGURES

		Page
Figure 1.	Location Map	3
Figure 2.	Generalized Stratigraphic Column of the L-Bar Mine Area	8
Figure 3.	Surface Geology of the L-Bar Site	9
Figure 4.	Location of Well Columns and Control Points Used to Define Model Structure	10
Figure 5.	East-West Model Cross Section	12
Figure 6.	North-South Model Cross Section	13
Figure 7.	Specified Thickness of the Tailings	14
Figure 8a.	Specified Elevation of the Alluvium	15
Figure 8b.	Specified Thickness of the Alluvium	16
Figure 9.	Specified Thickness of the Weathered Mancos Shale	17
Figure 10.	Specified Thickness of the Mancos Shale	18
Figure 11a.	Specified Elevation of the Top of the First Tres Hermanos Sandstone	20
Figure 11b.	Specified Thickness of the First Tres Hermanos Sandstone	21
Figure 12.	Model Boundary Conditions	22

Figure 13.	Location of Simulated Recovery System Features	24
Figure 14.	Pre-Tailings Steady-State Head Contours	29
Figure 15.	Correlation of Observed and Simulated Head for Year 1996	33
Figure 16.	Trend of Observed Versus Simulated Water Levels at Well PZ-4	35
Figure 17.	Trend of Observed Versus Simulated Water Levels at Well PZ-10	36
Figure 18.	Trend of Observed Versus Simulated Water Levels at Well MW-109	37
Figure 19.	Trend of Observed Versus Simulated Water Levels at Well MW-2A	38
Figure 20.	Trend of Observed Versus Simulated Water Levels at Well MW-3A	39
Figure 21.	Trend of Observed Versus Simulated Water Levels at Well MW-17	40
Figure 22.	Trend of Observed Versus Simulated Water Levels at Well MW-50	41
Figure 23.	Simulated Total Head in First Tres Hermanos Aquifer at Year 1996	43
Figure 24.	Observed and Simulated Chloride Concentrations in the FTH Aquifer at Year 1996	44
Figure 25.	Simulated and Observed Chloride Concentration at Well MW-69	45
Figure 26.	Simulated 200-Year Total Head at Year 2196 in the First Tres Hermanos Aquifer	47
Figure 27.	Simulated 1000-Year Total Head at Year 2996 in the First Tres Hermanos Aquifer	48
Figure 28.	Simulated 200-Year Average Concentration in the FTH Aquifer at Year 2196	49
Figure 29.	Simulated 1000-Year Average Concentration in the FTH Aquifer at Year 2996	50

PROJECTED LONG-TERM FLOW AND QUALITY OF GROUNDWATER AT THE L-BAR, NEW MEXICO, URANIUM SITE

SUMMARY

Sohio Western Mining Company authorized Balleau Groundwater, Inc. to provide an evaluation of the hydrologic conditions at the L-Bar Uranium mill site tailings located in Cibola County about 47 miles west of Albuquerque, New Mexico. The milling activities began during 1976 and ceased in 1981. A groundwater-recovery system consisting of pumping wells northeast and west of the tailings reservoir was installed in 1981 to capture seepage from the tailings. Recovered groundwater is routed to evaporation ponds near the southeast corner of the tailings reservoir.

A three-dimensional finite-element model that simulates the flow and transport in saturated and unsaturated conditions was developed to aid in understanding and planning the tailings management operation. The model was checked against the historical conditions (1977 through 1996) and then run for 1000 years of predictions.

The results indicated that the model can be used for decisions about managing the hydrologic conditions in the tailings area. Soil moisture trends in the tailings area indicate that the tailings will drain to unsaturated conditions by the year 2010.

The model simulates the advective and dispersive movement of constituents in the tailings area. The future projections indicate that constituent concentration above one percent of the source concentrations will reach no further than 2500 feet southwest of the tailings after 1000 years.

INTRODUCTION

Sohio Western Mining Company (Sohio) owns the L-Bar Uranium site (the site) located in Cibola County, New Mexico. The site is about 47 miles west of Albuquerque, New Mexico, and about ten miles north of Laguna Pueblo as shown in Figure 1. Mining and milling activities at the site began during 1976 and continued until 1981 when milling ceased. Reclamation of the site, including the tailings impoundment, was completed in 1989.

Sohio authorized Balleau Groundwater, Inc. (BGW) to model the history of hydrogeologic conditions in the tailings reservoir and the surrounding areas for projecting future conditions. The purpose of this report is to provide a summary of the modeling process and to illustrate the model results.

The flow system in the tailings site is controlled by the geologic structure and the hydrologic properties of the tailings area. BGW investigated the available codes that simulate three-dimensional movement of flow and transport under variably-saturated conditions. The code selection process reviewed the Los Alamos National Laboratory code FEHMN (Los Alamos National Laboratory, 1996), the Lawrence Berkeley Laboratory code TOUGH2 (Pruess, 1991), and the version of FEMWATER (Lin et al., 1996) prepared for the U.S. Environmental Protection Agency (EPA). TOUGH2 simulates only advective transport, therefore, it was excluded. Both FEHMN and FEMWATER simulate the geologic conditions and transport processes that are of interest in the L-Bar site, such as advection, dispersion, diffusion, adsorption, decay and source/sink. Both models are capable of addressing the objectives of the study. BGW selected FEMWATER because of its history of use by the EPA and the advanced graphical interface developed for the U.S. Department of Defense (Boss International, 1996). The automatic graphical interface was essential in developing the model and the three-dimensional finite-element grid.

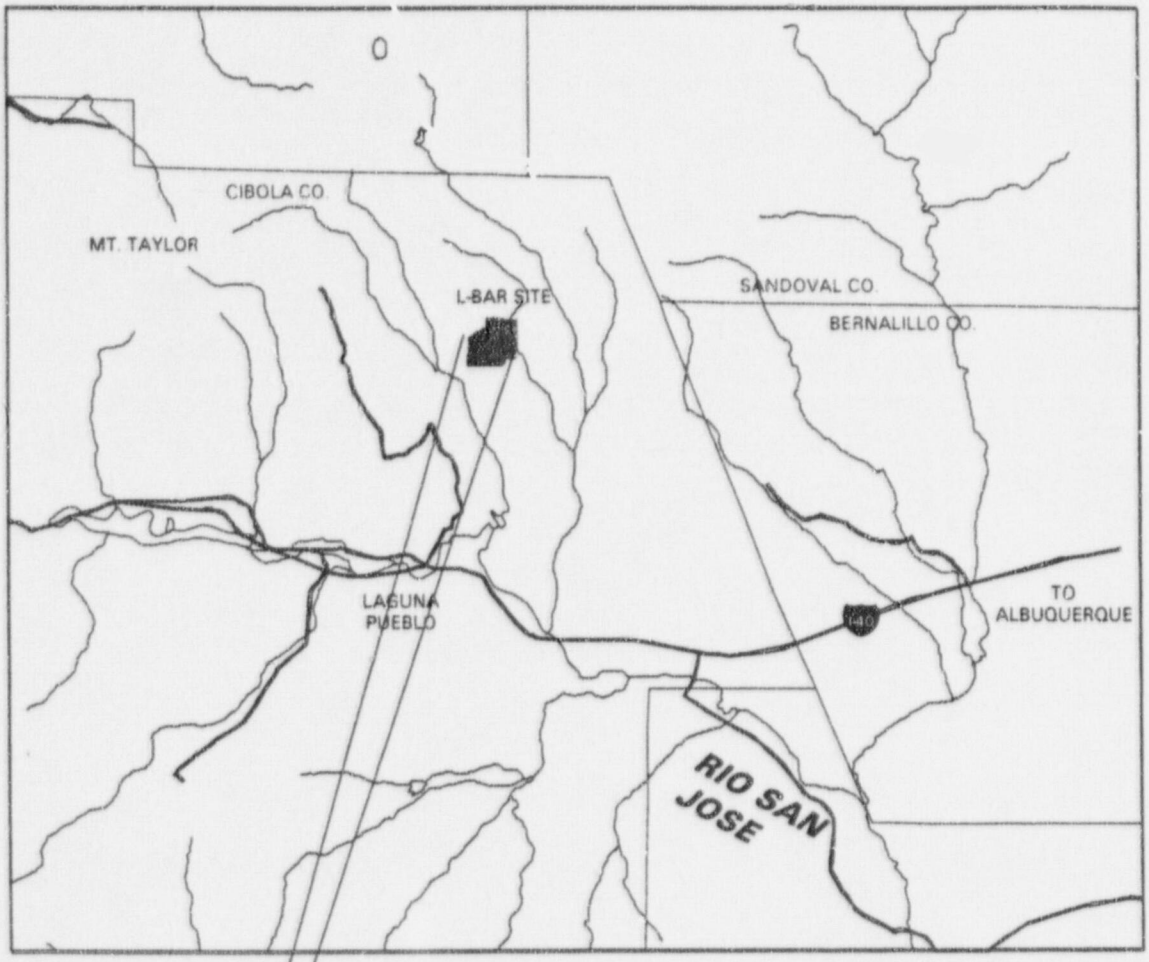

5 0 5 10 Miles

N

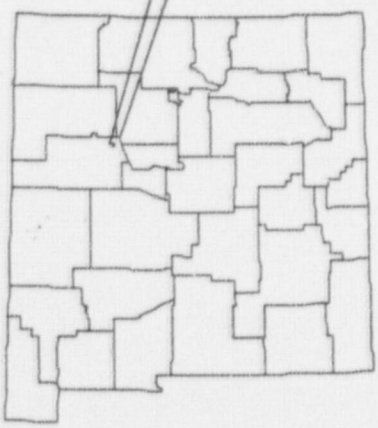

SOHIO WESTERN MINING COMPANY/ L-BAR MINE

LOCATION MAP

Date: 06/14/96 Produced By: BEB Checked By: WPB File Name: FIG1.SMF	**FIGURE 1**	BGW

BALLEAU GROUNDWATER, INC.

The objectives of the modeling investigations were to:

1. Characterize the hydrologic conditions prior to construction of the tailings reservoir.
2. Characterize the historical change in the hydrogeologic system in and around the tailings reservoir.
3. Project the hydrologic conditions after the existing groundwater-recovery system is shutdown.
4. Characterize the movement over time of tailings fluid and constituents through variably-saturated conditions to estimate the extent of groundwater impacted by tailings fluid after the groundwater-recovery system is shutdown.

The modeling work in this study consisted of:

1. Constructing a hydrologic database that includes structural elevations for each geologic formation, formation thickness, water levels, hydrologic parameters, well locations and pumping rates, and water-quality data.
2. Assessing and selecting the modeling techniques and tools that are suitable for characterizing the site hydrological conditions.
3. Developing a three-dimensional finite-element model to simulate the variably-saturated groundwater flow and transport in the tailings area.
4. Calculating steady-state conditions to represent the hydrologic conditions prior to constructing the tailings reservoir.
5. Simulating the hydrologic response to:

    a. Construction and filling of the tailings reservoir from 1976 to 1981.
    b. Implementing the groundwater-recovery system from 1981 to 1989, when the tailings cover was put in place.
    c. Extension of the groundwater-recovery system until 1996.
    e. A prediction period of 1000 years from 1996 to 2996.

The transient model simulation used the calibrated steady-state heads as initial conditions and the calculated transient water levels then were compared to the observed water levels. For the transport runs, advection and dispersion are the transport processes used in simulating the movement of the tailings constituents.

HISTORY OF THE TAILINGS RESERVOIR

The tailings reservoir was constructed during 1976 to contain the tailings fluid by building a dam from local clay soils. The material for the starter dam was obtained by excavating the southwest corner of the existing tailings area. A minimum of five feet of Mancos Shale was left as a cover for the sandstone aquifer below the tailings. As the size of the tailings reservoir increased, a saddle dam was constructed across a topographic divide at the northeast corner of the tailings reservoir.

During the period from fall 1976 to 1981, tailings were conveyed to the tailings disposal reservoir. During 1981, the mine and mill were closed. A groundwater-recovery system was installed west of the dam and east of the saddle dam to prevent the spread of tailings contaminants. The recovered water was pumped back to two evaporation ponds located near the southeast corner of the tailings area. The groundwater-recovery system has been operating 16 years, from 1981 to the present time. The reported tailings pond water levels were used to represent tailings groundwater levels for the period from 1977 to 1989.

Water levels in the tailings pond increased gradually from about 6180 feet above mean sea level (ft msl) during 1977 to about 6196 ft msl during 1981. After mining operations ceased and after implementation of the groundwater-recovery system, water levels in the tailings pond dropped six feet to a level of 6190 ft msl. During 1989, the ponded water was evaporated and cover material consisting of waste rock with a clay cap was placed on top of the tailings. The cover pressurized the tailings and resulted in an increase in tailings water levels to 6200 ft msl in the saturated tailings. Table 1 illustrates

TABLE 1
TAILINGS RESERVOIR WATER LEVELS

YEAR	ELEVATION
	(ft msl)
1977	6180
1978	6184
1979	6188
1980	6192
1981	6196
1982	6196
1983	6195
1984	6194
1985	6193
1986	6192
1987	6191
1988	6190
1989	6200

the record of water levels in the tailings pond from 1977 to 1989 when the surface ponds were reclaimed. After 1989, tailings piezometer water levels are used in calibration.

GEOLOGIC SETTING

The geology of the mine area was used in developing the conceptual groundwater-flow model. The tailings reservoir is located southeast of Mount Taylor in the San Juan Basin. The formations in the vicinity of the mine are the Morrison Formation, Dakota Sandstone, the Mancos Shale, Tertiary igneous intrusives and Quaternary Alluvium, as shown in the geologic column in Figure 2 (Intera, Inc., 1996). The Mancos Shale is considered the upper-most bedrock layer with only its lower part present in the mine area. The lower part of the Mancos Shale consists of alternating units of sandstone and shale. The uppermost three sandstone units locally are referred to, from youngest to oldest, as First, Second and Third Tres Hermanos sandstones. The surface geology of the mine area indicates that alluvium/colluvium materials cover most of the area, except where the First Tres Hermanos (FTH) sandstone aquifer crops out as shown in Figure 3.

The conceptual model was designed to simulate the flow system through the alluvium, shale and the FTH sandstone aquifer. The FTH is underlain by about 100 feet of Mancos Shale, which is considered an impermeable boundary.

MODEL STRUCTURE

The model was constructed using data from 70 well bores and control points in and around the tailings area, as shown in Figure 4. A three-dimensional mesh module was used to generate the finite-element mesh. Each element is represented by six nodes (prism elements). The model grid covers a horizontal area of about two miles by two miles. The grid dimension is about 300 feet in the tailings area and about 1000 feet at the model edges.

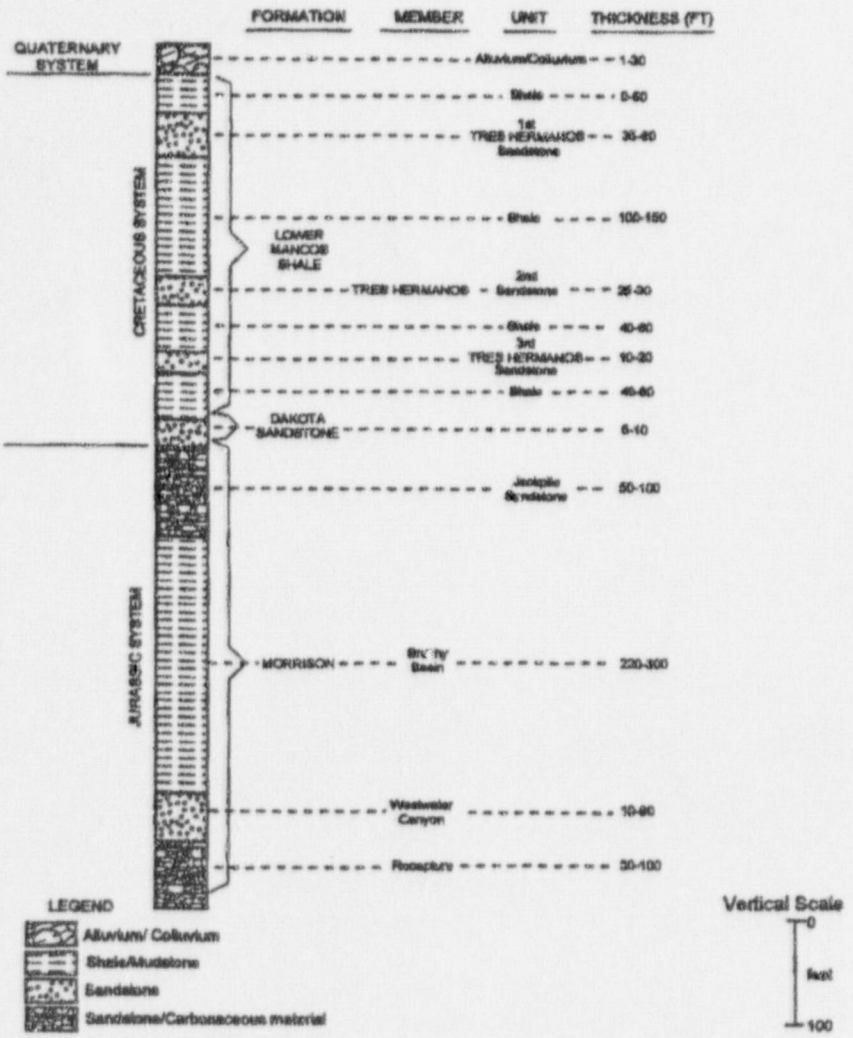

ADAPTED FROM INTERA, INC., 1996

SOHIO WESTERN MINING COMPANY/
L-BAR MINE

GENERALIZED STRATIGRAPHIC COLUMN OF THE L-BAR MINE AREA

Date: 08/04/98 Produced By: SEB Checked By: WPB File Name: FIG2.SMF	**FIGURE 2**	BGW

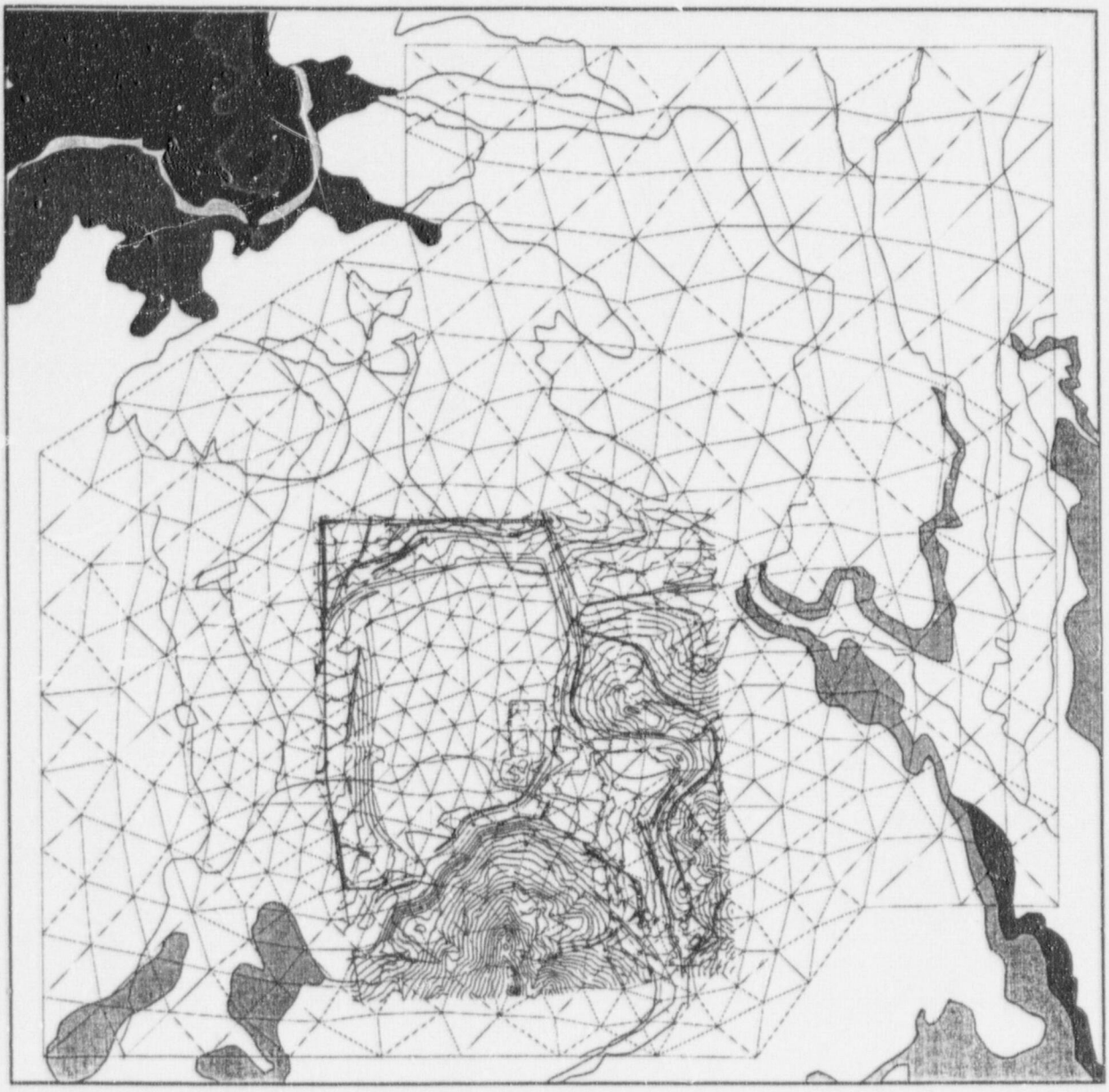

2000 0 2000 4000 Feet

SITE TOPOGRAPHY
WATER COURSE
FIRST TRES HERMANOS SANDSTONE
DILCO
GALLUP SANDSTONE
MANCOS SHALE
EOLIAN AND ALLUVIAL DEPOSITS
BASALT UNDIFFERENTIATED
COLLUVIAL DEPOSITS

N

SOHIO WESTERN MINING COMPANY/
L-BAR MINE

SURFACE GEOLOGY OF THE L-BAR SITE

Date: 5/5/93	
Produced By: SHS	
Checked By: WPB	**FIGURE 3**
File Name: GEO.apr	

BGW

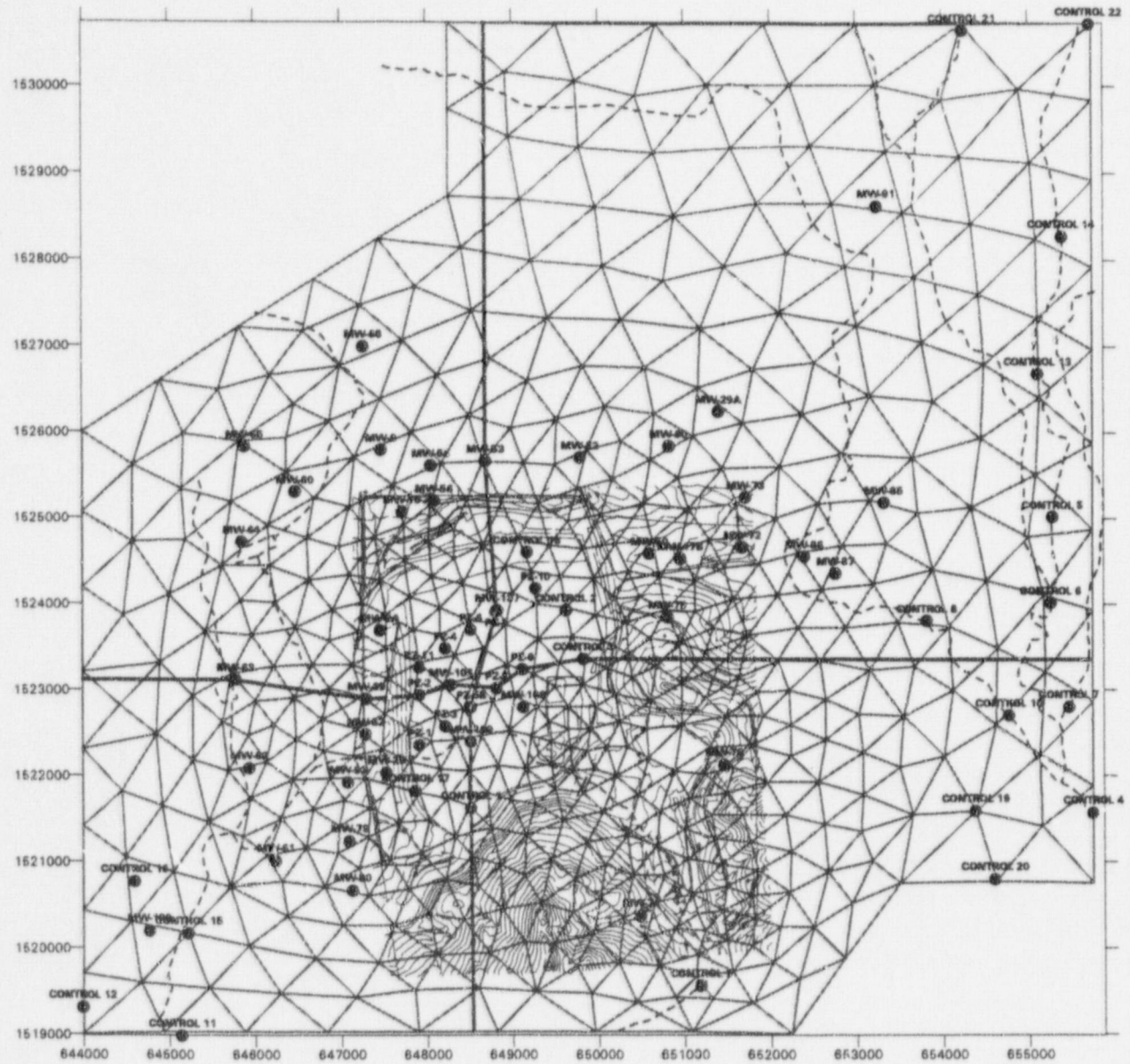

1" = 2000 FEET

0 2000 4000 6000 8000

------ WATERCOURSE
——— TAILINGS TOPOGRAPHY
——— LINE OF SECTION (FIGURE 5)
——— LINE OF SECTION (FIGURE 6)

SOHIO WESTERN MINING COMPANY/
L-BAR MINE

LOCATION OF WELL COLUMNS AND CONTROL POINTS USED TO DEFINE MODEL STRUCTURE

Date:
Produced By:
Checked By:
File Name: ELEVAT.SRF

FIGURE 4

BALLEAU GROUNDWATER, INC.

The model grid consists of 7365 nodes and 13,118 elements. In the vertical dimension, the grid, of 14 layers, varies according to the top and the bottom of each material. Figures 5 and 6 show east-west and north-south cross sections in the model grid.

Six materials are represented in the model grid, from top to bottom; tailings cover material, tailings material, colluvium, weathered Mancos Shale, Mancos Shale and FTH sandstone. The FTH has three zones of different hydrologic properties. Other units' properties are characterized by a single value. The model simulates flow through unsaturated and saturated conditions in three dimensions.

The elevation of the top of the tailings cover is 6200 ft msl and its thickness varies from four feet to about ten feet. The thickness of the tailings cover material was represented in the model with uniform thickness of five feet. Two model layers were used to represent this material.

The top elevation of the tailings material is about 6195 ft msl and its thickness varies from ten feet at the northeast corner of the tailings to about 40 feet close to the dam (Figure 7). Four model layers were used to represent this material.

The colluvial material covers the study area except in the east area where the FTH crops out. Figure 8a shows the top elevation of the alluvium. The thickness of the alluvium cover (Figure 8b) varies from one foot to 30 feet and about ten feet below the tailings reservoir. Eight model layers were used to represent the alluvial material.

The weathered Mancos Shale is present with significant thickness only below and north of the tailings. Its thickness is about five feet below and about 40 feet north of the tailings. Figure 9 shows the contour lines for the thickness of the weathered Mancos Shale. Two model layers were used to represent this material.

The Mancos Shale is present with large thickness in the north and northwest of the tailings reservoir. Figure 10 illustrates the contour lines for the thickness of the Mancos Shale. Below the tailings, the thickness of the Mancos Shale varies from five feet at the

WEST

EAST

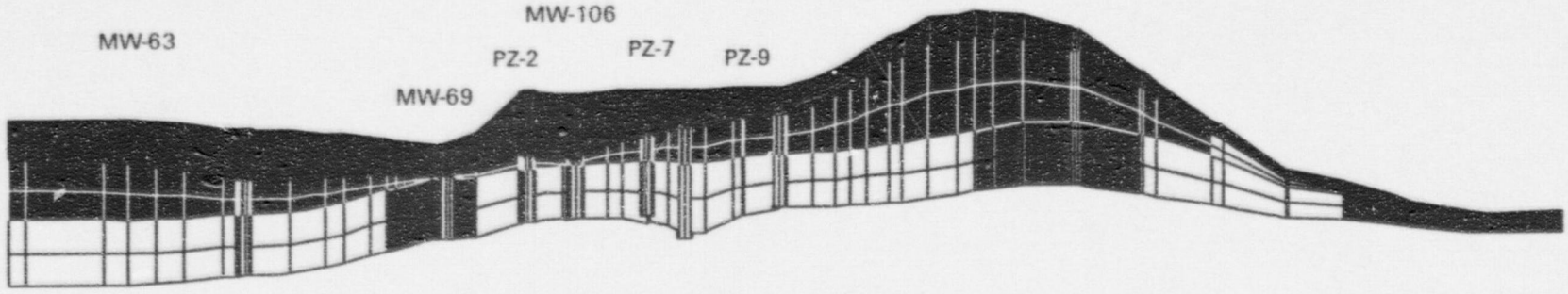

1 " = 1250 FEET

0 1250 2500 3750 5000

Materials

- *Alluvium*
- *Clay_Cover*
- *FTH_High*
- *FTH_Low*
- *First_Tres_Hermanos*
- *Mancos*
- *Mancos*
- *Tailings*
- *Weathered_Mancos*

NOTE: SEE FIGURE 4 FOR LINE OF SECTION
VERTICAL SCALE IS TEN TIMES HORIZONTAL SCALE

SOHIO WESTERN MINING COMPANY/
L-BAR MINE

EAST-WEST MODEL CROSS SECTION

Date: 08/04/98
Produced By: SSB
Checked By: WPB
File Name: FIG5.SHF

FIGURE 5

BGW

BALLEAU GROUNDWATER, INC.

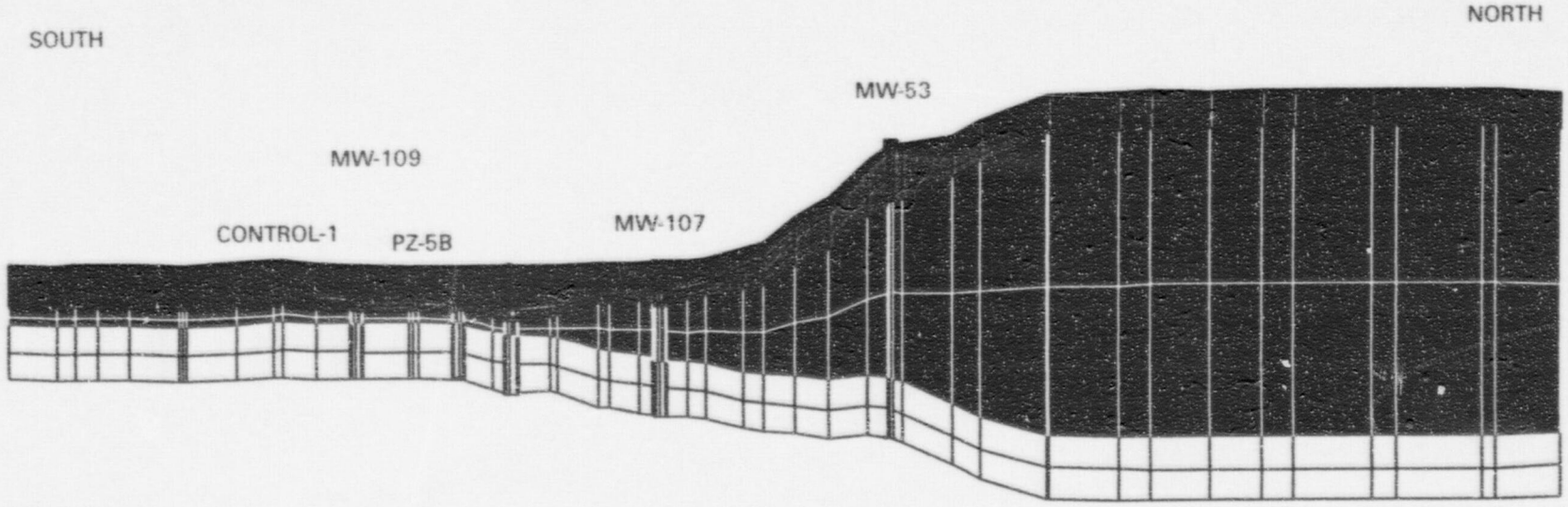

Materials

- *Alluvium*
- *Clay_Cover*
- *FTH_High*
- *FTH_Low*
- *First_Tres_Hermanos*
- *Mancos*
- *Mancos*
- *Tailings*
- *Weathered_Mancos*

1 " = 1250 FEET

0 1250 2500 3750 5000

NOTE: SEE FIGURE 4 FOR LINE OF SECTION
VERTICAL SCALE IS TEN TIMES HORIZONTAL SCALE

SOHIO WESTERN MINING COMPANY/
L-BAR MINE

NORTH-SOUTH MODEL CROSS SECTION

Date: 06/04/98
Produced By: SES
Checked By: WPB
File Name: FIG6.SRF

FIGURE 6

BGW

BALLEAU GROUNDWATER, INC.

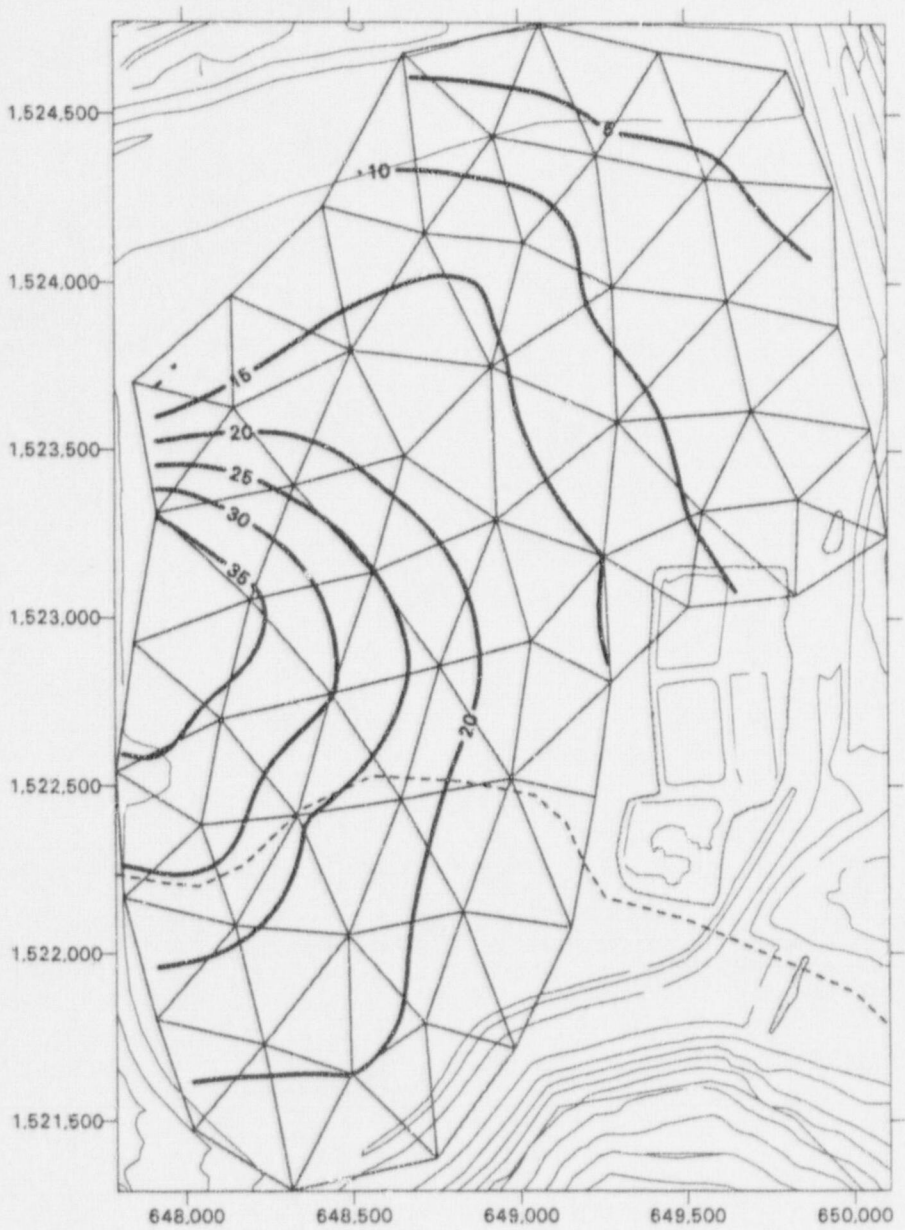

0 500 1,000 1,500 2,000

1" = 500 FEET

CONTOUR LINE OF TAILINGS THICKNESS (FEET)
WATER COURSES
SITE TOPOGRAPHY

SOHIO WESTERN MINING COMPANY/
L-BAR MINE

SPECIFIED THICKNESS OF THE TAILINGS

Date: 09/04/90	**FIGURE 7**
Produced By: BGW	
Checked By: WPH	
File Name: FIG7.SRF	

BGW

BALLEAU GROUNDWATER, INC.

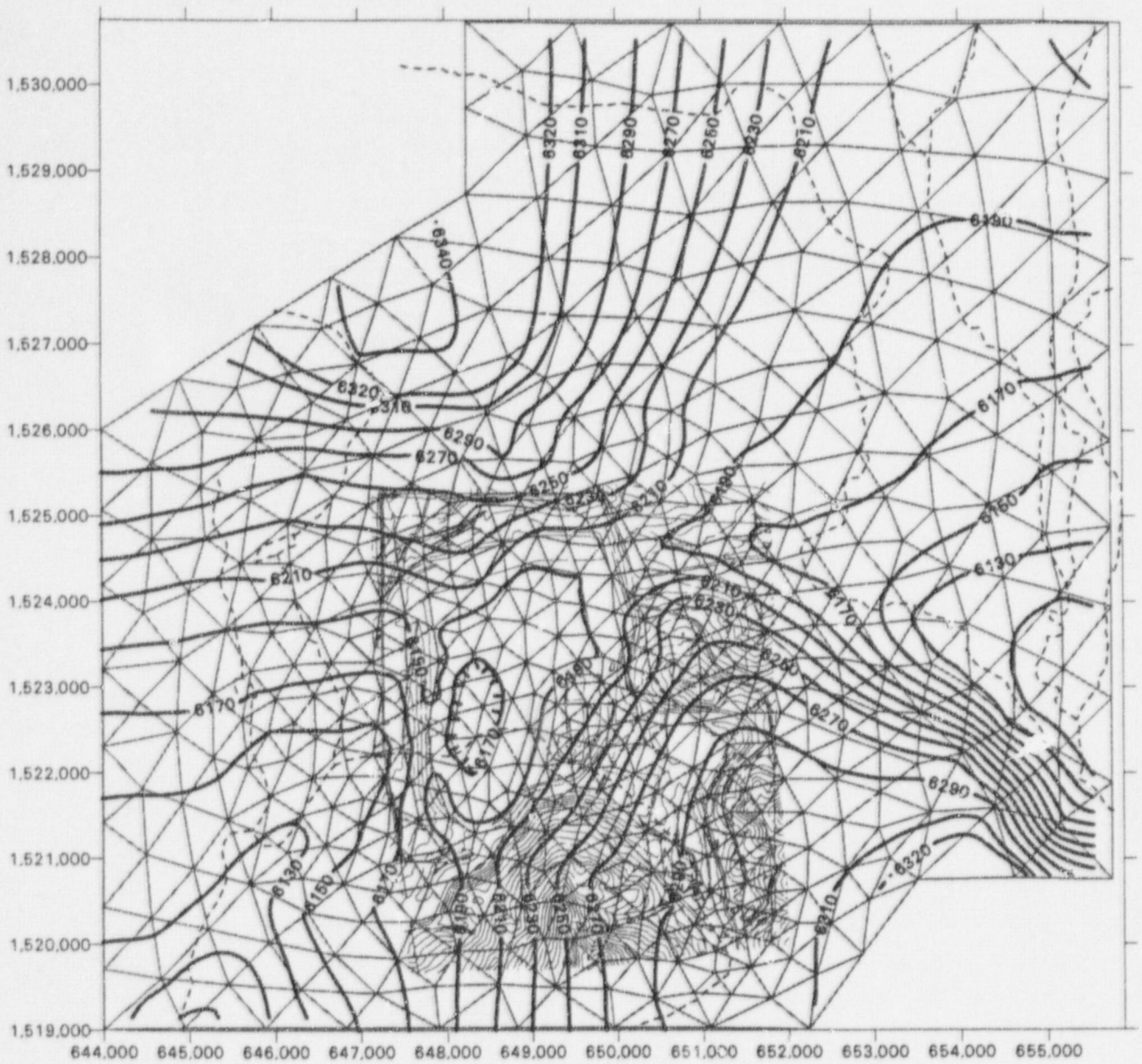

CONTOUR LINE OF ALLUVIUM ELEVATION (FEET MSL)
WATER COURSES
SITE TOPOGRAPHY

SOHIO WESTERN MINING COMPANY/
L-BAR MINE

SPECIFIED ELEVATION OF THE ALLUVIUM

Date
05/04/98
Produced By:
SEB
Checked By:
WTB
File Name:
F8C8A.SRF

FIGURE 8A

BALLEAU GROUNDWATER, INC.

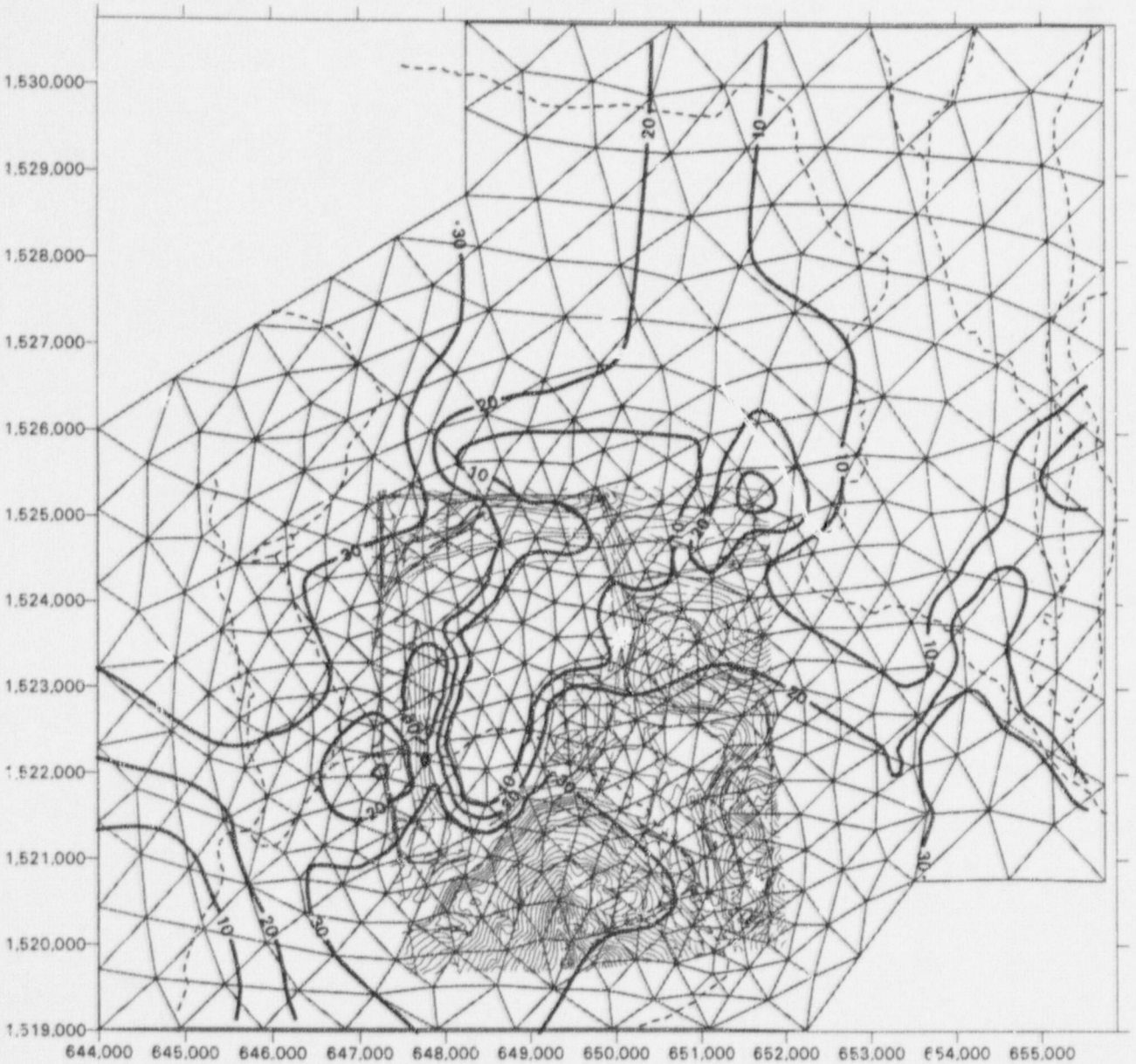

CONTOUR LINE OF ALLUVIUM THICKNESS (FEET)
WATER COURSES
SITE TOPOGRAPHY

SOHIO WESTERN MINING COMPANY/
L-BAR MINE

SPECIFIED THICKNESS OF THE ALLUVIUM

Date
06/04/98
Produced By:
MEB
Checked By:
WPB
File Name:
FIG8B.MXD

FIGURE 8B

BALLEAU GROUNDWATER, INC.

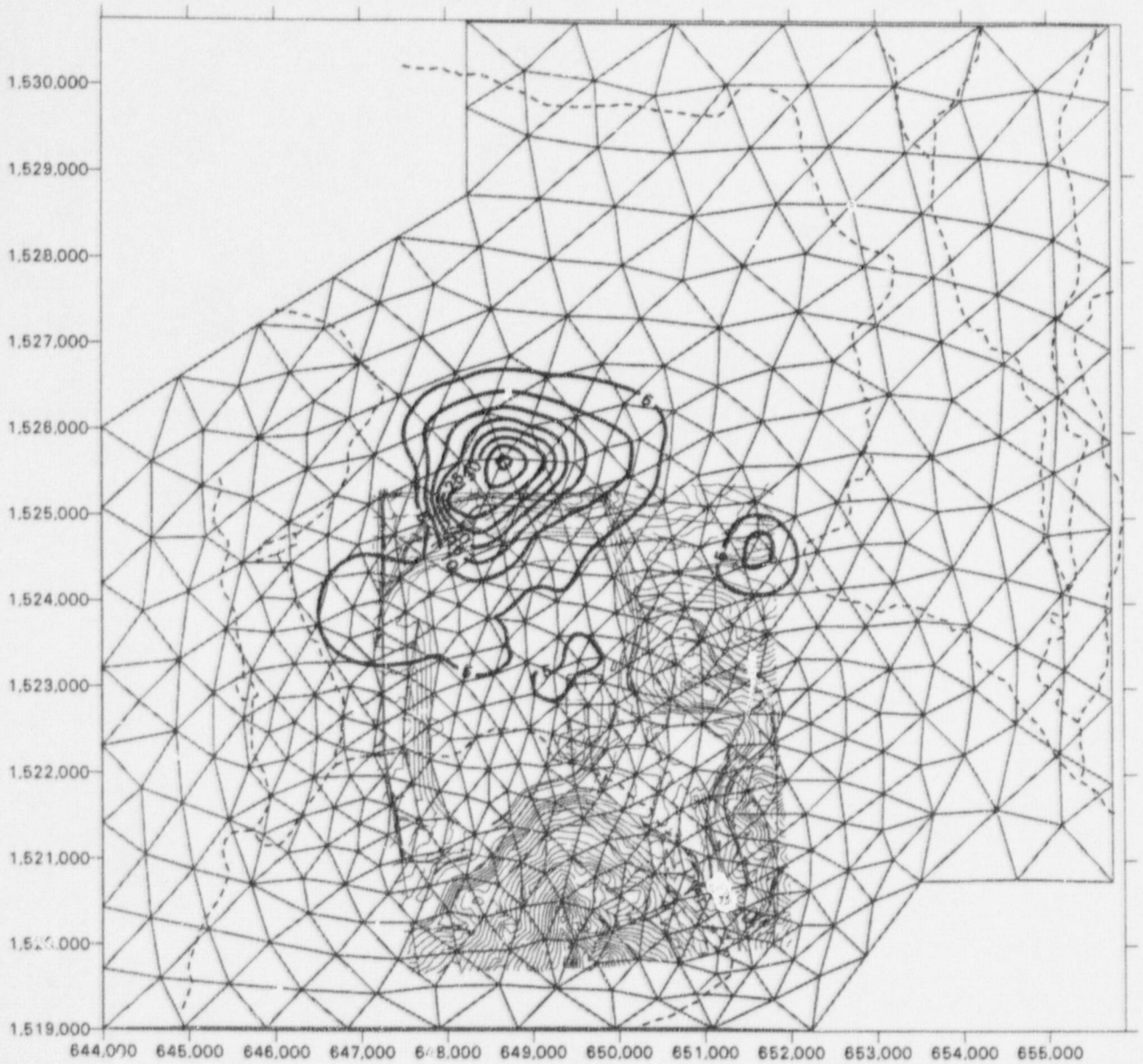

CONTOUR LINE OF WEATHERED MANCOS SHALE THICKNESS (FEET)

WATER COURSES

SITE TOPOGRAPHY

SOHIO WESTERN MINING COMPANY/
L-BAR MINE

SPECIFIED THICKNESS OF THE WEATHERED MANCOS SHALE

FIGURE 9

BALLEAU GROUNDWATER, INC.

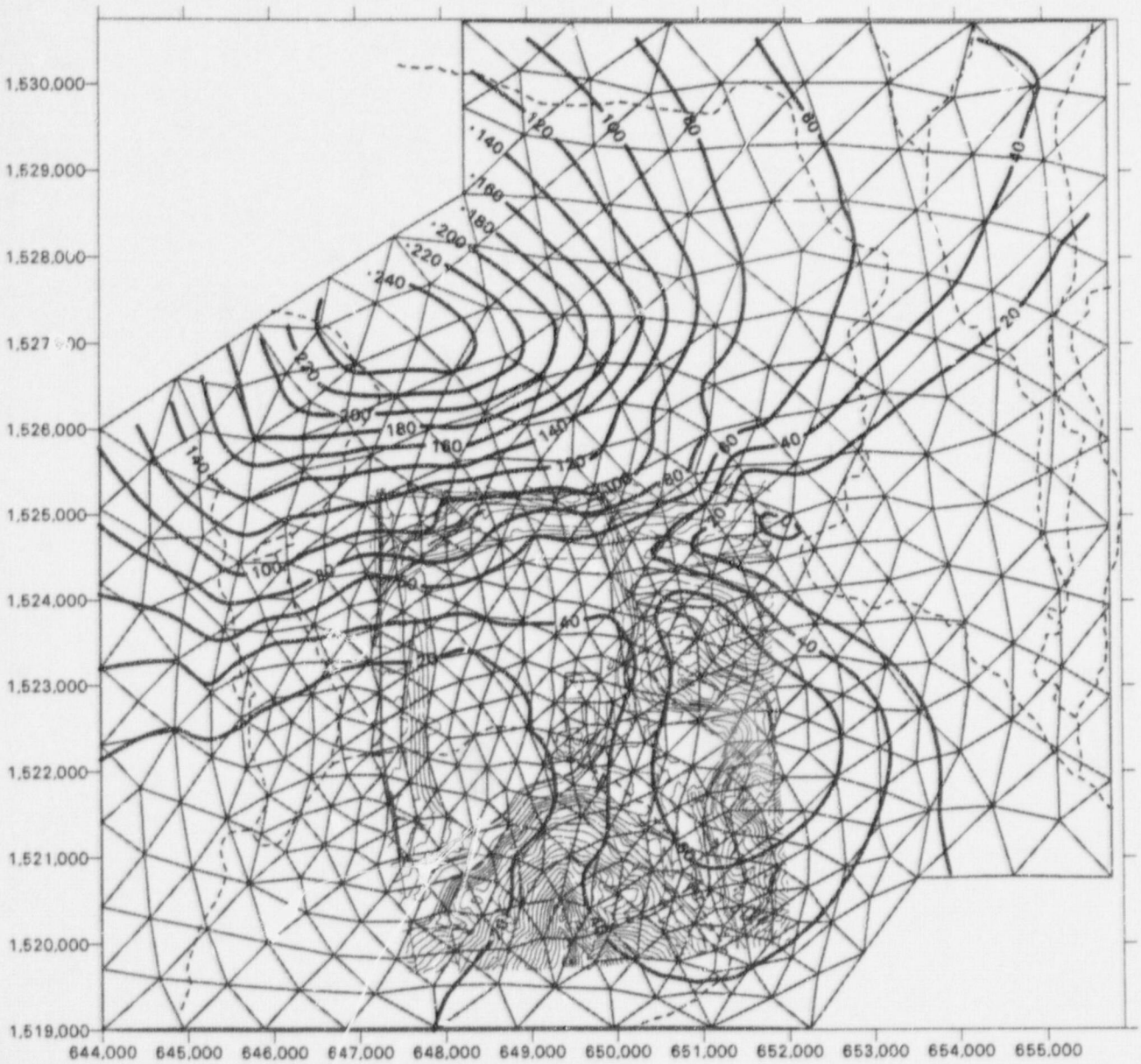

SOHIO WESTERN MINING COMPANY/
L-BAR MINE

SPECIFIED THICKNESS OF THE MANCOS SHALE

Date: 08/06/98
Produced By: SES
Checked By: WPB
File Name: FIG10.SRF

FIGURE 10

BALLEAU GROUNDWATER, INC.

southwest corner of the tailings to about 60 feet in the northern part of the tailings. Two model layers were used to represent the Mancos Shale in the model.

The upper 40 feet of the FTH is the monitored aquifer in the study area. Figure 11a illustrates the contour lines of the top elevation of the FTH, which dips gently to the northwest. The thickness of the FTH is a few feet in the east and southwest where it crops out and 40 feet below the tailings (Figure 11b). Two model layers represent the FTH.

BOUNDARY CONDITIONS

Regional groundwater-flow patterns are from the northern recharge area associated with Mount Taylor to arroyo-bed discharge areas southwest and southeast of the study area. The model is recharged from the north and northwest boundaries. Phreatophytic areas indicate the locations of the discharge areas. Two discharge areas are in the study area; one is east of the tailings and the other is southwest of the tailings as shown in Figure 12. The tailings reservoir is located in a groundwater divide between the two discharge areas. Recharge and discharge areas were represented as constant-head boundary conditions. The constant head in the recharge area varies from 6140 ft msl at the northern corner of the study area to 6120 ft msl in the west boundary interpreted from the head in outlying monitor wells. The constant head at the discharge areas was represented as ten feet to 15 feet below the ground surface. A stock pond to the east of the tailings reservoir was represented as a small source of recharge.

Natural areal recharge and evaporation was not simulated in the study area based on the assumption that soil moisture added from precipitation will equal soil moisture lost by evaporation. We interpret the net soil flux to be negative such that evaporation reduces soil moisture at the L-Bar site. Representing areal soil moisture flux throughout the model would add a major numerical burden to the model. By not including that feature, the model overstates the down-gradient movement of tailings fluid. Where the water table is

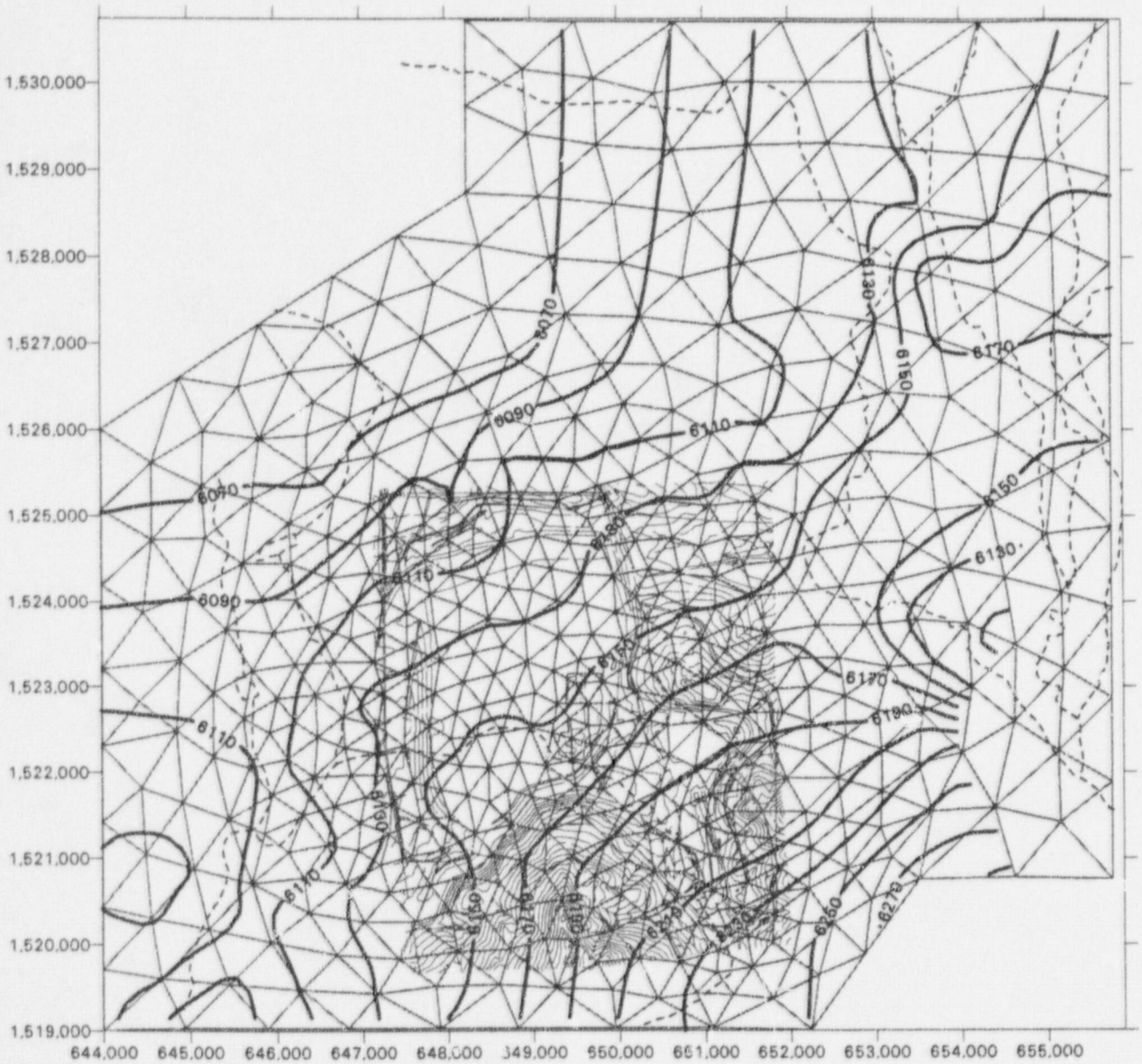

CONTOUR LINE OF THE TOP OF FTH SANDSTONE ELEVATION (FEET MSL)

WATER COURSES

SITE TOPOGRAPHY

SOHIO WESTERN MINING COMPANY/
L-BAR MINE

SPECIFIED ELEVATION OF THE TOP OF THE FIRST TRES HERMANOS SANDSTONE

Date: 08/04/00	
Produced By: SES	
Checked By: WPB	
File Name: FIG11A.SRF	

FIGURE 11A

BGW

BALLEAU GROUNDWATER, INC.

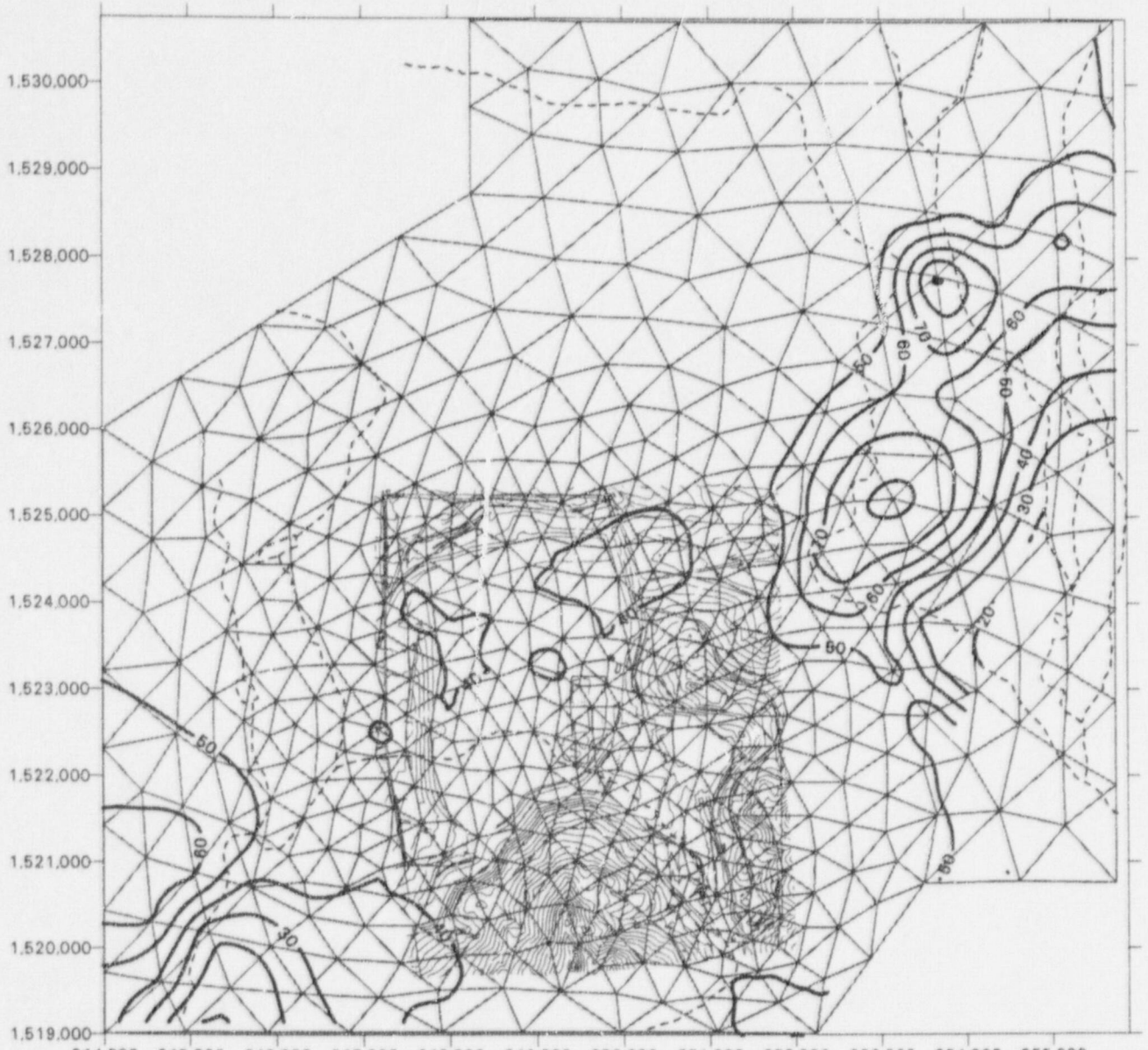

SOHIO WESTERN MINING COMPANY/
L-BAR MINE

SPECIFIED THICKNESS OF THE FIRST TRES HERMANOS SANDSTONE

Date: 09/04/98	**FIGURE 11B**
Produced By: JGS	
Checked By: WPB	
File Name: FIG11B.SRF	

BGW

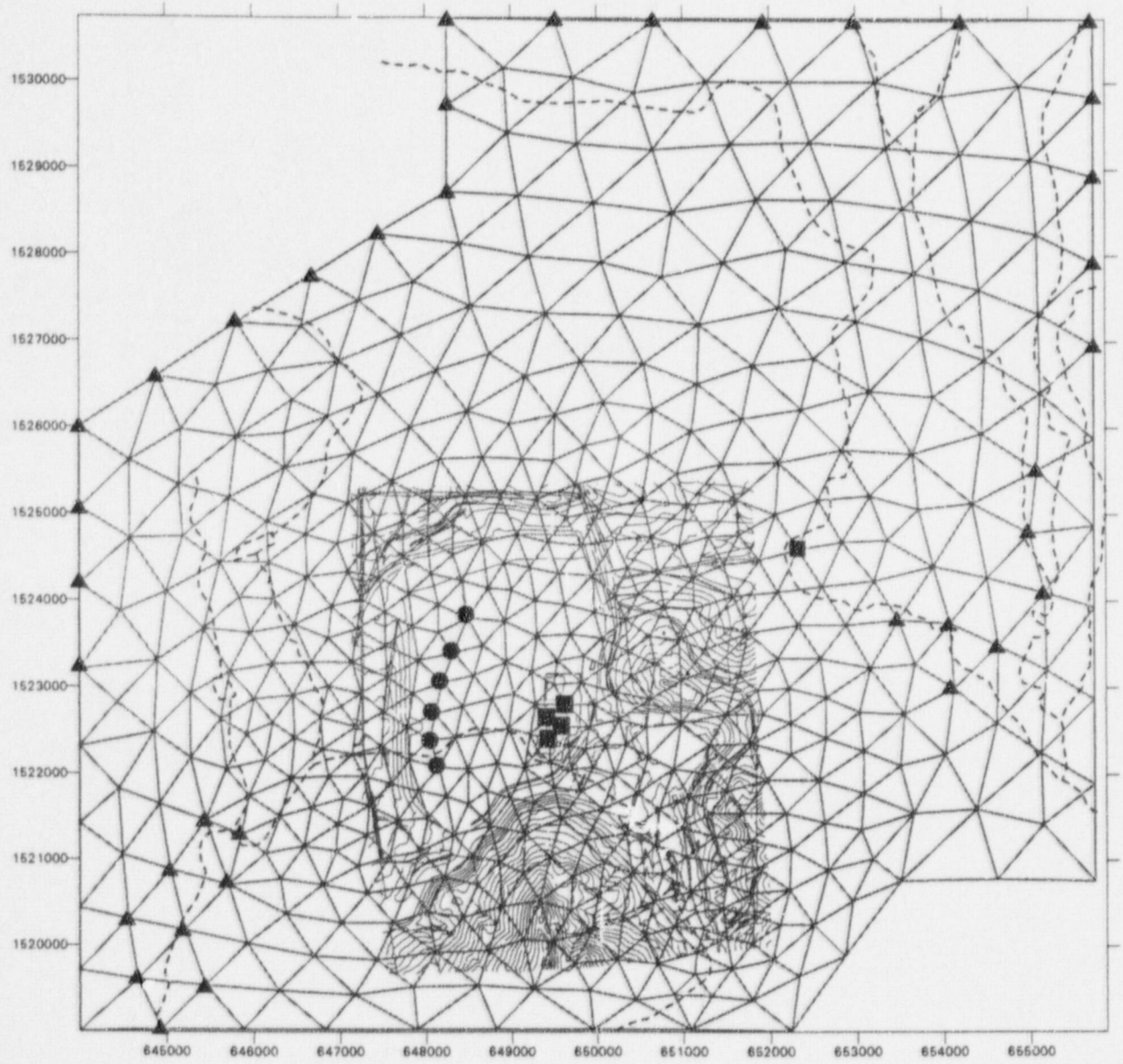

1" = 2000 FEET

0 2000 4000 6000 8000

- RECHARGE BOUNDARY
- STOCK POND (RECHARGE)
- DISCHARGE BOUNDARY
- EVAPORATION PONDS (DISCHARGE)
- TOE DRAINS (DISCHARGE)
- WATERCOURSE
- TAILINGS TOPOGRAPHY

SOHIO WESTERN MINING COMPANY/
L-BAR MINE

MODEL BOUNDARY CONDITIONS

Date: 06/05/86 Produced By: SEB Checked By: WTB File Name: FIG12.MOF	**FIGURE 12**	BGW

closer to the ground surface (less than 20 feet), however, evapotranspiration was represented in the model at the discharge areas (east and west discharge areas). Evapotranspiration was not represented in the tailings itself, which also is a conservative approach.

The elevation of water in the tailings reservoir was represented as a variable-head boundary condition. The head within the tailings varies with the tailings reservoir elevation. The groundwater-recovery system was represented as a well system discharging from the saturated part of the FTH. For wells that lie inside an element, the pumping rate was proportioned using the distance between the well point and each node. The location of the groundwater-recovery system is shown in Figure 13. The evaporation ponds were represented as a constant head at an elevation of 6194 ft msl. These ponds evaporate pump-back water. Concentrations of tailings constituents increase in the ground due to seepage from the ponds. A system of toe drains in the dam was active during the years 1989 to 1996 and is represented in the model as constant head at the drain elevation during that period.

A groundwater mound is present northeast of the tailings area close to wells MW-17B and MW-50. Chemical analysis of this water mound indicated that it has a high nitrate concentration. The results of an isotope analysis (Drimmie, 1995) indicated that the nitrate in this location has a different character than the nitrate of the tailings fluid. The source of this nitrate is not defined. This nitrate plume is simulated in the model as a small rate of recharge at nodes close to wells MW-17B and MW-50.

HYDROLOGIC PARAMETERS

The model simulates flow through unsaturated and saturated conditions in three dimensions. In the northern part of the study area, the FTH and part of the Mancos Shale are saturated. Water levels decrease gradually to the southwest and to the southeast where only the FTH is saturated. All model layers in the south part of the study area are

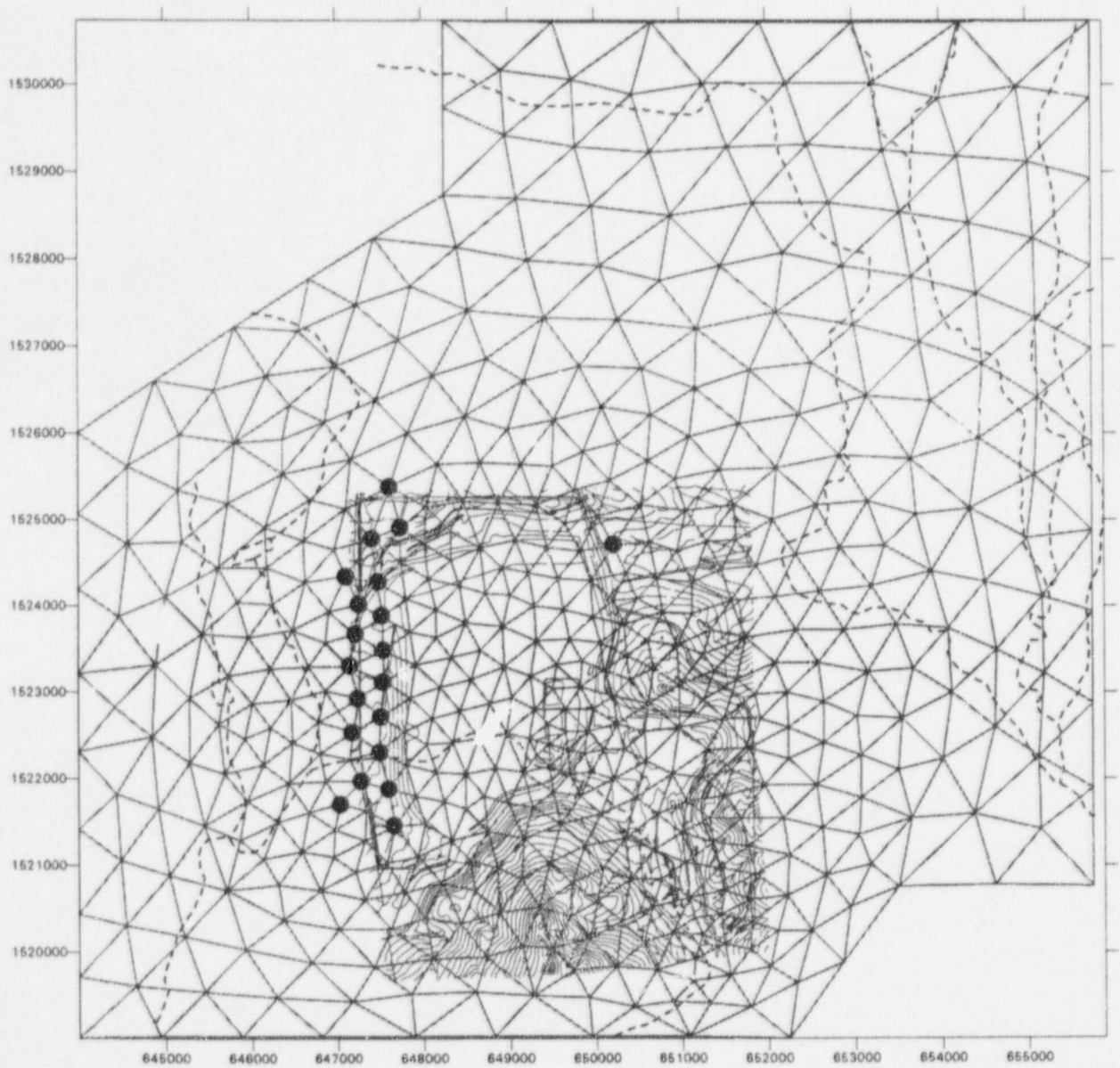

1" = 2000 FEET

0 2000 4000 6000 8000

● NODES REPRESENTING THE RECOVERY SYSTEM WELLS
------ WATERCOURSE
——— TAILINGS TOPOGRAPHY

SOHIO WESTERN MINING COMPANY/
L-BAR MINE

LOCATION OF SIMULATED RECOVERY SYSTEM FEATURES

Date: 09/05/89	**FIGURE 13**
Produced By: SES	
Checked By: WPB	
File Name: ELEVAT.SRF	

BALLEAU GROUNDWATER, INC.

unsaturated. In unsaturated-flow conditions, the hydraulic conductivity and pressur ' ad depend on the moisture conditions of the soil. The van Genuchten (van Genuchten, 1980) relations were used to simulate the unsaturated conditions in the study area.

The hydrologic parameters for each material type are the satur ated hydraulic conductivity tensor, saturated moisture content, residual moisture content, soil moisture characteristic curve, relative hydraulic conductivity curve and the water-capacity curve. Table 2 illustrates the calibrated hydrologic parameters used for each material type in the study area.

All the materials are considered isotropic in the horizontal plane. An anisotropy ratio of 0.1 was used in the vertical direction. Fracture flow has been interpreted as affecting some wells on the site, such as well MW-2A. No information is available on the orientation or properties of discrete fractures. Discrete fracture flow is not represented, but the effect of random fractures is treated by calibration of the specific discharge and dispersive properties of the model. Based on the previous analysis of pumping tests performed west of the dam and northeast of the tailings, three zones were simulated in the FTH aquifer; a zone west of the dam with saturated horizontal hydraulic conductivity (k) of 1.0 foot per day ft/day, a low permeability zone northeast of the tailings of k=0.02 ft/day and the regional FTH zone of k=0.1 ft/day. All other material types are simulated as homogeneous and anisotropic soils.

The numerical model simulated advective and dispersive transport constituents. The irreducible numerical dispersion (estimated at 100 feet of dispersivity) associated with the numerical model was corrected by adding a more characteristic hydrodynamic dispersion to the convective (50 percent) isosurface using an analytical solution. The longitudinal dispersivity used in the analytical solution is 50 feet based on calibration to the spread of observed concentrations through 1996. Therefore, the numerical model provided the advective front and velocity field for transport of dissolved constituents, but numerically overstated dispersion. Dispersion was corrected outside the FEMWATER code.

SOHIO WESTERN MINING COMPANY

L-BAR MINE

TABLE 2
CALIBRATED HYDROLOGIC PARAMETERS FOR MODEL MATERIALS

MATERIAL	SATURATION MOISTURE CONTENT	RESIDUAL MOISTURE CONTENT	EFFECTIVE POROSITY	SATURATED HORIZONTAL HYDRAULIC CONDUCTIVITY	SATURATED VERTICAL HYDRAULIC CONDUCTIVITY
	(ft^3/ft^3)	(ft^3/ft^3)	(ft^3/ft^3)	(ft/d)	(ft/d)
Tailings Cover	0.38	0.13	0.25	0.5	0.5/0.05
Tailings	0.38	0.18	0.2	0.5/0.1[1]	.5/.01
Colluvium	0.43	0.07	0.36	0.1	0.01
Weathered Mancos	0.38	0.13	0.25	1	0.1
Mancos	0.38	0.2	0.18	0.001	0.0001
First Tres Hermanos	0.25[2]	0.1	0.15	0.1	0.01
First Tres Hermanos High	0.25[2]	0.1	0.15	1	0.1
First Tres Hermanos Low	0.25[2]	0.1	0.15	0.02[3]	0.002

Saturated properties - Intera, Inc., 1996, "Hydrogeology Investigations of the L-Bar Uranium Mill Tailings Pile, Cibola County, New Mexico."

Unsaturated properties - D.B. Stephens, 1996, "Unsaturated Hydrology."

1. Layer 4 in the tailings adjusted from 0.1 to 0.01.
2. Adjusted from 0.40 to 0.25.
3. Adjusted from 0.05 to 0.02.

TRANSIENT RUN SCHEDULE

The steady-state pressure head distribution was used as initial conditions for starting the transient simulation. The transient run started at 1977, simulated the historical conditions until the end of 1996 and was extended to 1000 years of future prediction. Table 3 illustrates the schedule of the simulated events.

RESULTS AND ANALYSIS

One objective of the modeling studies is to provide an understanding of the hydrologic system after constructing the tailings reservoir. The model is calibrated to reproduce the historical water levels and the movement of non-reactive constituents. That understanding is the basis for projecting future transport of constituents.

Steady State

The steady-state water-level map represents hydrologic conditions prior to the tailings reservoir. The water levels at wells far from the tailings reservoir were used as a guide for the simulated steady-state water levels. The simulated steady-state water levels are illustrated in Figure 14. Table 4 illustrates observed versus simulated steady-state head at selected wells far from the tailings. The characteristic hydraulic conductivity of the FTH implies that the total flow through the study area is about 1.44 gallons per minute (gpm) entering through the north and northeast boundaries. The west discharge area discharges about 0.7 gpm and the east discharges about 0.48 gpm as shown in Table 5.

Transient Simulation

The historical period of tailings operations from fall 1976 to 1996 was divided into three annualized sub-periods as follows:

TABLE 3
SCHEDULE OF THE TRANSIENT MODEL RUN

YEARS	FEATURES
1/1977 - 12/1981	Start of the Tailings Reservoir + Northeast Recharge
1/1982 - 12/1989	Recovery Wells + Northeast Recharge + Decrease Tailings Reservoir Level
1/1990 - 12/1996	Recovery Wells + Toe Drains + Evaporation Pond + Decrease Northeast Recharge
1996 - 2996	No Action

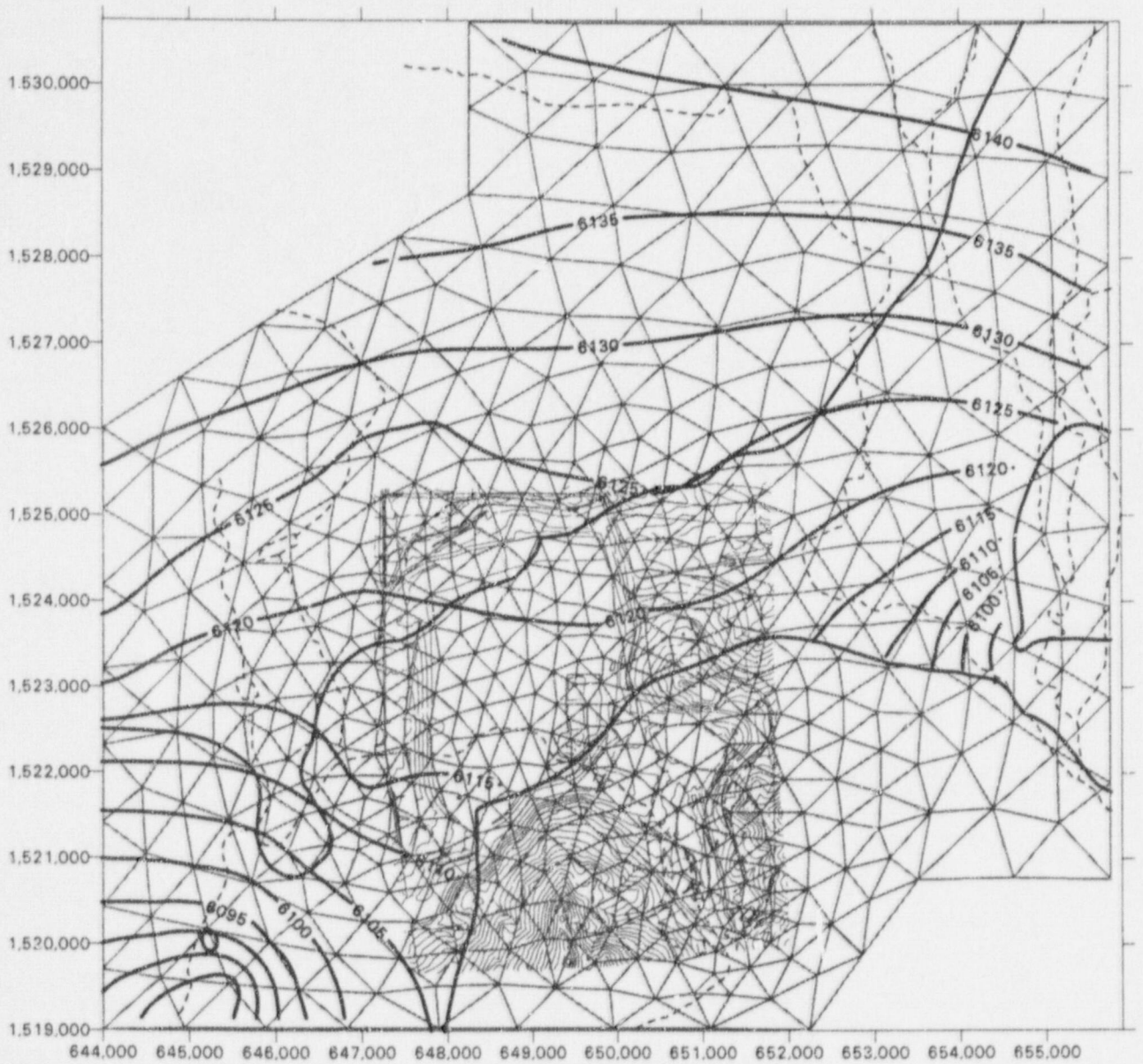

1" = 2000 FEET

0 2,000 4,000 6,000 8,000

CONTOUR OF HEAD (FEET)
LINE OF FULL FTH SATURATION
LINE OF UNSATURATED FTH (DRY LINE)

SOHIO WESTERN MINING COMPANY
L-BAR MINE

PRE-TAILINGS STEADY-STATE HEAD CONTOURS

Date: 09/04/90	
Produced By: SEB	
Checked By: WPB	
File Name: FIG14.SRF	

FIGURE 14

BGW

BALLEAU GROUNDWATER, INC.

TABLE 4
OBSERVED AND SIMULATED STEADY-STATE HEAD

WELL NUMBER	OBSERVED HEAD	SIMULATED HEAD
	(ft msl)	(ft msl)
MW-91	6135	6136
MW-29A	6136	6127
MW-68	6120	6130
MW-65	6117	6127
MW-100	6088	6090
MW-85	6128	6120
MW-87	6125	6117

TABLE 5
STEADY-STATE RECHARGE AND DISCHARGE

NORTH AND NORTHWEST BOUNDARY RECHARGE	EAST DISCHARGE AREA	WEST DISCHARGE AREA	IMBALANCE
(gpm)	(gpm)	(gpm)	(gpm)
1.44	0.48	0.7	0.26

1. 1977-1981 represents the time when the tailings reservoir was being filled and the northeast recharge was active. Tailings-pond water-level records begin in 1977.
2. 1981-1989 represents the start of the groundwater-recovery system and continuation of the northeast recharge.
3. 1990-1996 represents continuing the groundwater-recovery system, activating the toe drains, and decreasing the amount of northeast recharge.

Head

Figure 15 illustrates the 1996 correlation between the observed and the simulated water levels in selected wells. The correlation coefficient is 0.95 and the root mean square of the error is 9.23 feet, which indicates the model is able to simulate observed water levels in the tailings site.

Table 6 illustrates the simulated inflow to the tailings reservoir, the northeast recharge, the pumping rate for the groundwater-recovery system, the flow out of the tailings bottom and the toe drain flow for the period from 1977 to 1996. The results indicate that the model is able to simulate observed flow rates and volumes at the tailings site. Observed tailings water levels are declining at about one foot per year. About 300 acre feet of water is still present in the tailings, but largely in unsaturated conditions seeping downward at a slow rate.

Figures 16 to 22 illustrate the water-level hydrographs for wells PZ-4, PZ-10, MW-2A, MW-3A, MW-109, MW-17B and MW-50. Well PZ-4 is located close to the tailings dam and well PZ-10 is located in the northeast corner of the tailings reservoir. These hydrographs indicate that the model is able to simulate the decline of the water level in the tailings reservoir for the historical period. Well MW-109 was drilled in 1996 in the FTH aquifer below the tailings reservoir. Only one reading was available for that well. The model simulated the water level within acceptable error, which indicates that the model simulation of the groundwater mound in the FTH is acceptable.

FIGURE 15
CORRELATION OF OBSERVED AND SIMULATED HEAD FOR YEAR 1996

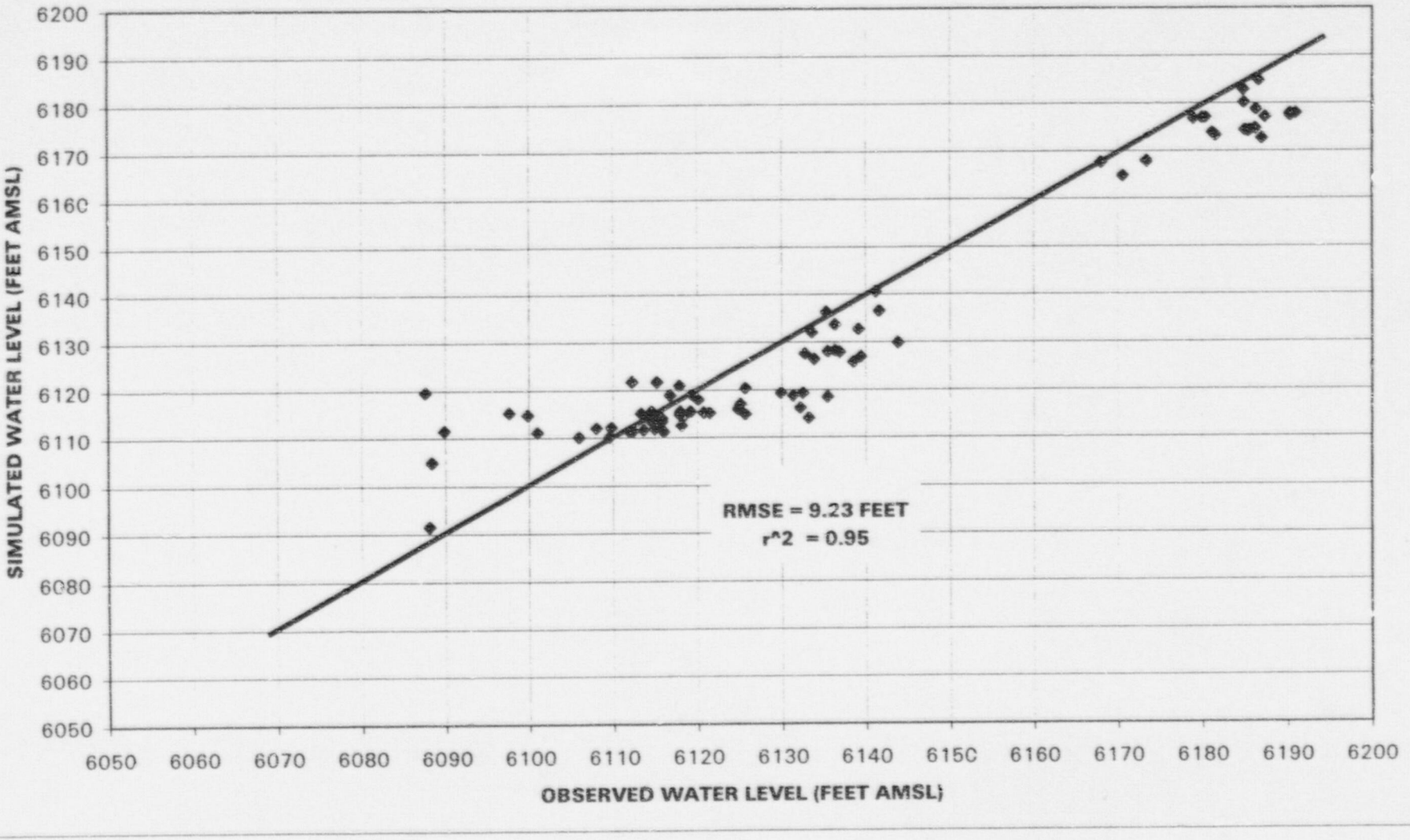

8/5/98
SES
FIG15.xls

TABLE 6

THE SIMULATED FLOW COMPONENTS OF THE SYSTEM

YEAR	FLOW TO THE TAILINGS	NORTHEAST AREA RECHARGE	WELL FLOW	FLOW OUT OF THE TAILINGS BOTTOM	TOE DRAINS FLOW
	(gpm)	(gpm)	(gpm)	(gpm)	(gpm)
1976	0	0.0	0.0	0	0
1977	192	1.15	0.0	-33.1	0
1978	102	1.15	0.0	-35.0	0
1979	49	1.15	0.0	-38.4	0
1980	44	1.15	0.0	-45.2	0
1981	43	1.15	0.0	-49.9	0
1982	23	1.15	-9.9	-36.4	0
1983	22	1.15	-9.9	-20.5	0
1984	21	1.15	-9.9	-19.1	0
1985	19	1.15	-9.9	-17.9	0
1986	17	1.15	-9.9	-16.8	0
1987	16	1.15	-9.9	-15.9	0
1988	14	1.15	-9.9	-15.1	0
1989	31	1.15	-9.9	-18.2	0
1990	0	1.15	-8.1	-13.2	-1.70
1991	0	0.99	-7.2	-4.2	-0.61
1992	0	0.73	-6.6	-3.5	-0.35
1993	0	0.52	-6.5	-3.1	-0.21
1994	0	0.31	-5.4	-2.8	-0.12
1995	0	0.10	-5.1	-2.6	-0.05
1996	0	0.00	-5.1	-2.5	0.00
HISTORY VOLUME (AF)	**955**	**30**	**-198**	**-635**	**-5**
2001	0	0	0	-2.12	0
2006	0	0	0	-1.70	0
2011	0	0	0	-1.41	0
2016	0	0	0	-1.18	0
2021	0	0	0	-0.98	0
2026	0	0	0	-0.82	0
2031	0	0	0	-0.68	0
2036	0	0	0	-0.57	0
2041	0	0	0	-0.47	0
2046	0	0	0	-0.39	0
2196	0	0	0	-0.19	0
2496	0	0	0	-0.02	0
2596	0	0	0	-0.01	0
2696	0	0	0	-0.01	0
2796	0	0	0	-0.01	0
2896	0	0	0	-0.01	0
2996	0	0	0	-0.01	0
TOTAL VOLUME (AF)	**955**	**30**	**-198**	**-785**	**-5**

SOHIO WESTERN MINING COMPANY

L-BAR MINE

FIGURE 16
TREND OF OBSERVED VERSUS SIMULATED WATER LEVELS AT WELL PZ-4

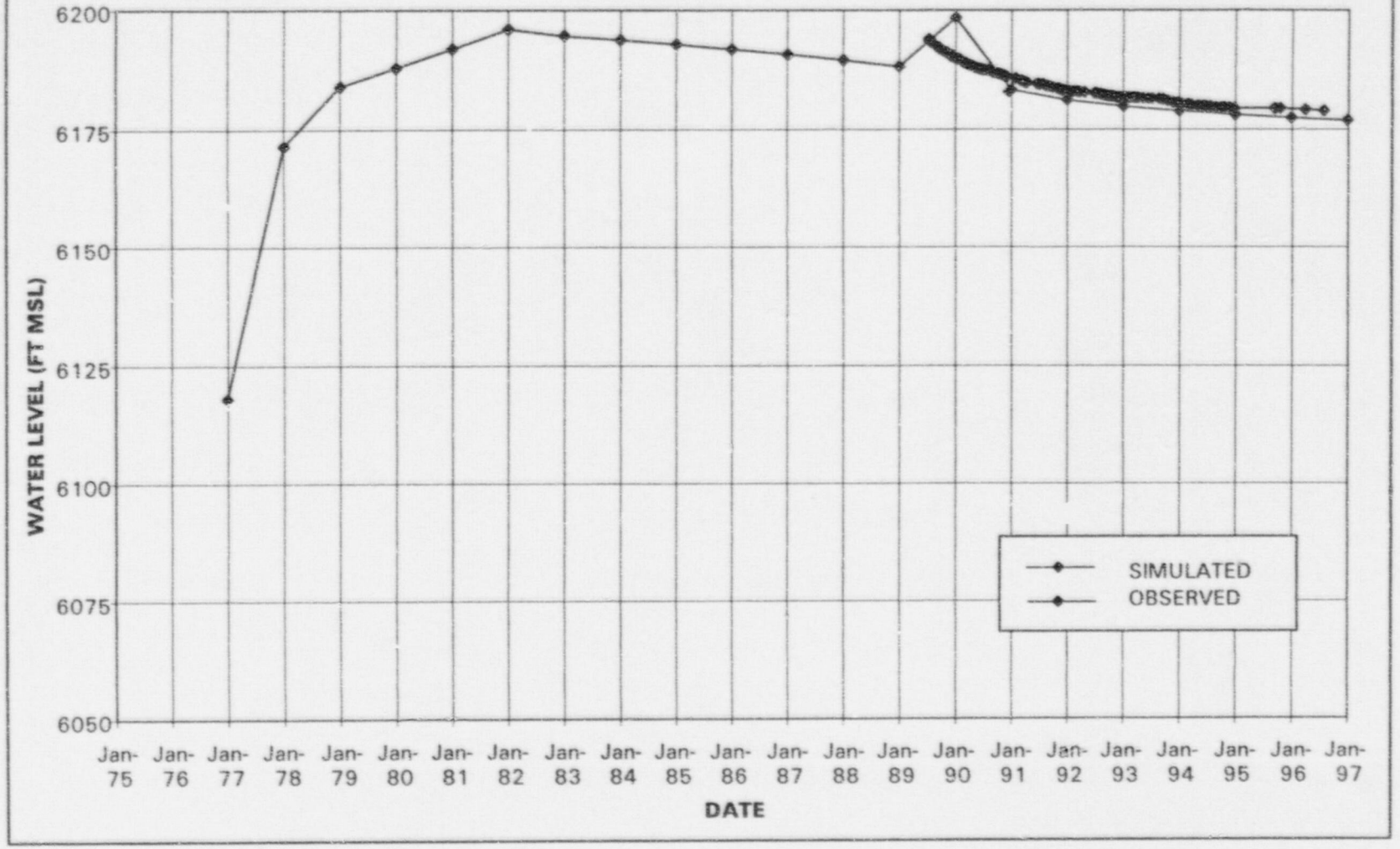

7/14/97
SES
FIG.PPT

BALLEAU GROUNDWATER, INC.

SOHIO WESTERN MINING COMPANY

L-BAR MINE

FIGURE 17

TREND OF OBSERVED VERSUS SIMULATED WATER LEVELS AT WELL PZ-10

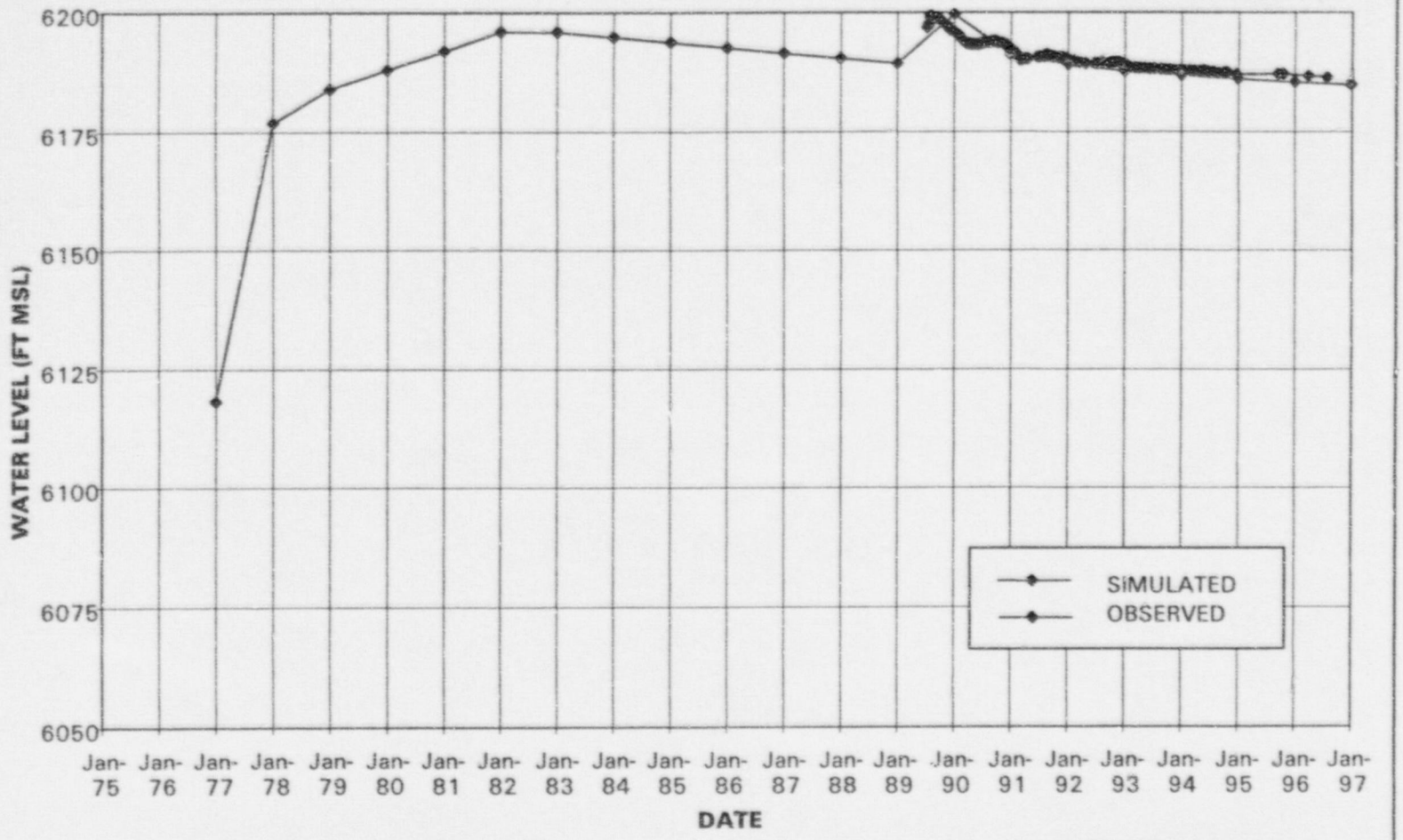

7/14/97
SES
FIG.PPT

BALLEAU GROUNDWATER, INC.

SOHIO WESTERN MINING COMPANY

L-BAR MINE

FIGURE 18
TREND OF OBSERVED VERSUS SIMULATED WATER LEVELS AT WELL MW-109

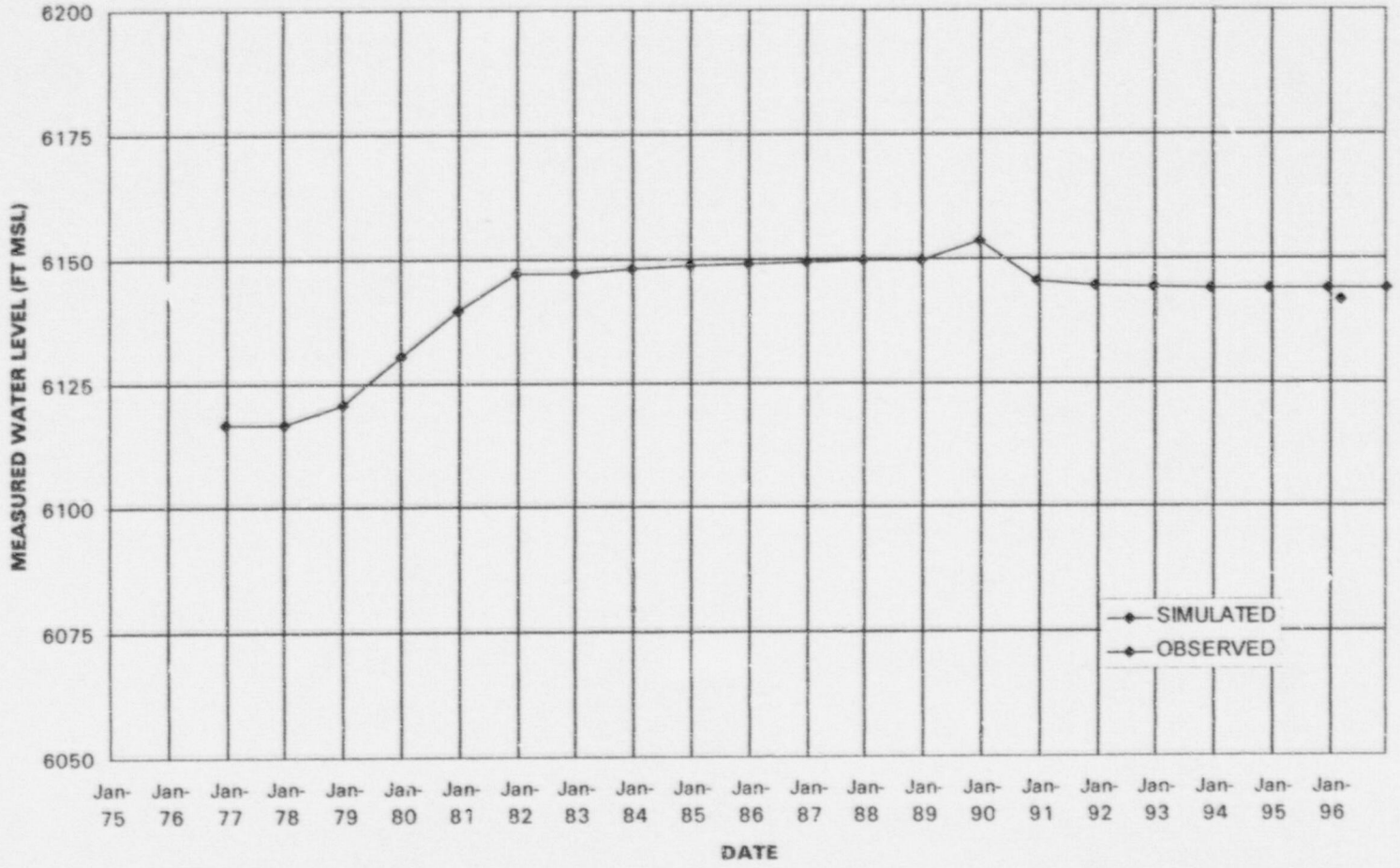

7/14/97
CN
BALLEAU.PPT

BALLEAU GROUNDWATER, INC.

SOHIO WESTERN MINING COMPANY

L-BAR MINE

FIGURE 19
TREND OF OBSERVED VERSUS SIMULATED WATER LEVELS AT WELL MW-2A

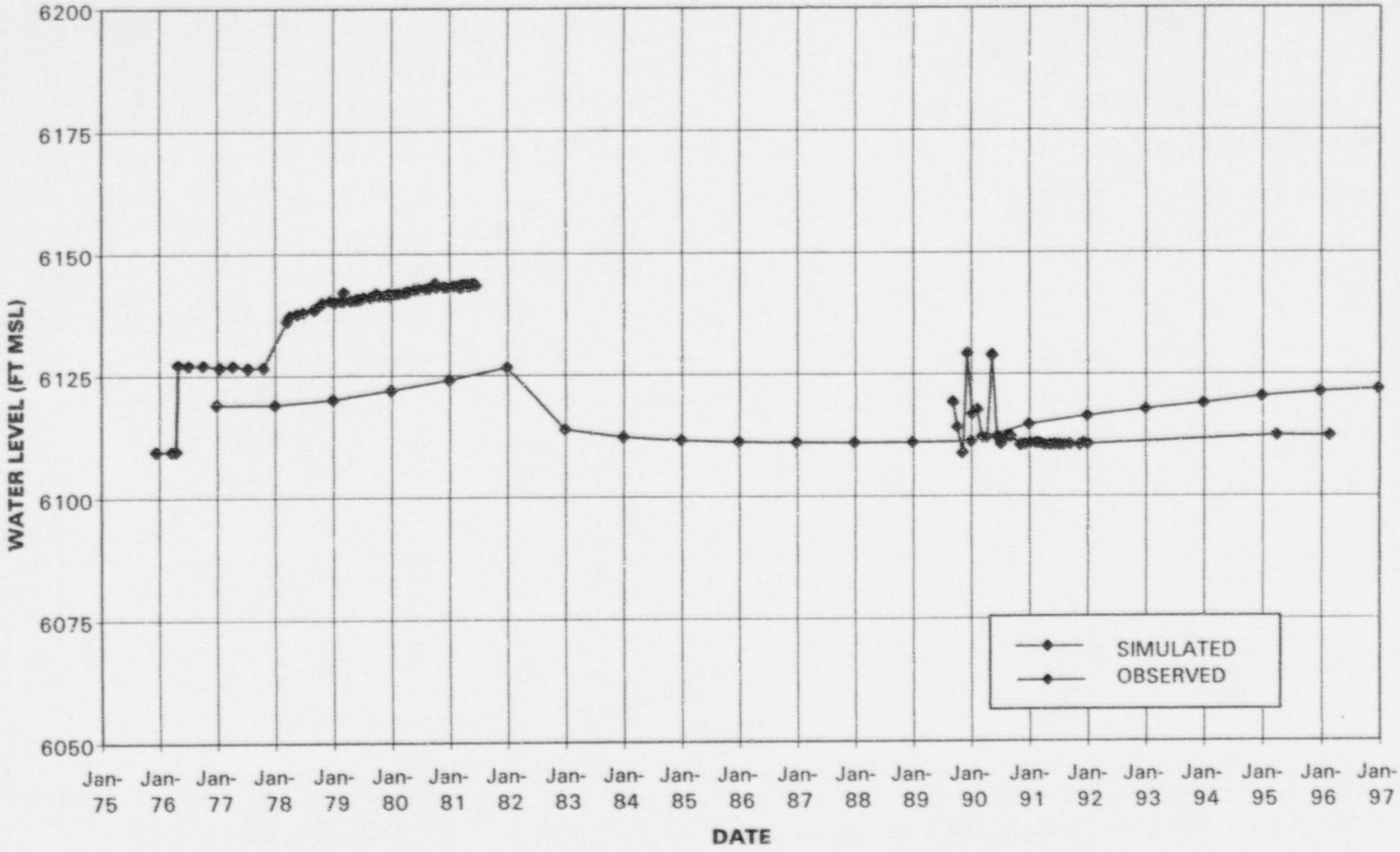

7/14/97
CN
BALLEAU.PPT

BALLEAU GROUNDWATER, INC.

SOHIO WESTERN MINING COMPANY

L-BAR MINE

FIGURE 20
TREND OF OBSERVED VERSUS SIMULATED WATER LEVELS AT WELL MW-3A

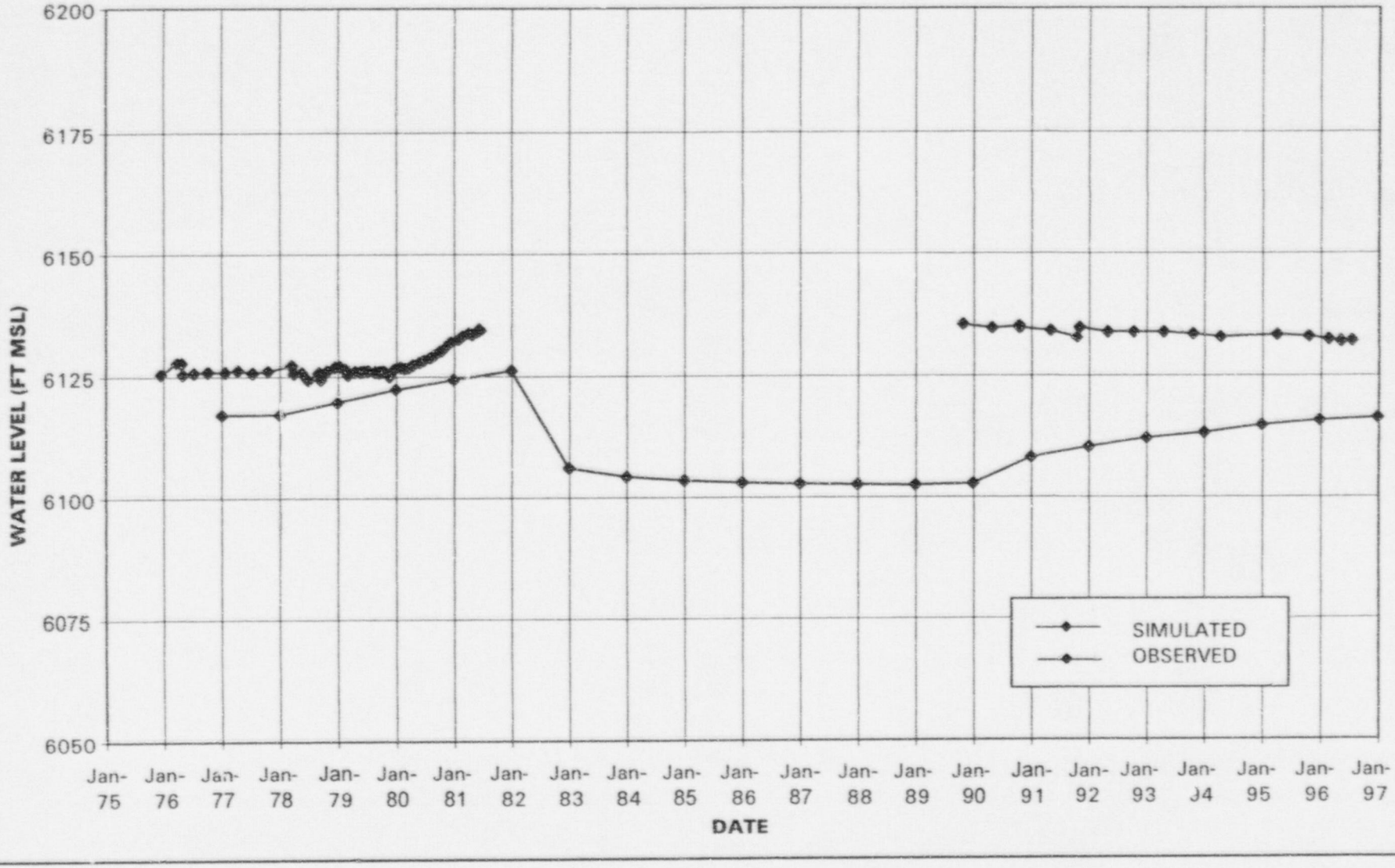

7/14/97
CN
BALLEAU.PPT

BALLEAU GROUNDWATER, INC.

SOHIO WESTERN MINING COMPANY

L-BAR MINE

FIGURE 21
TREND OF OBSERVED VERSUS SIMULATED WATER LEVELS AT WELL-17B

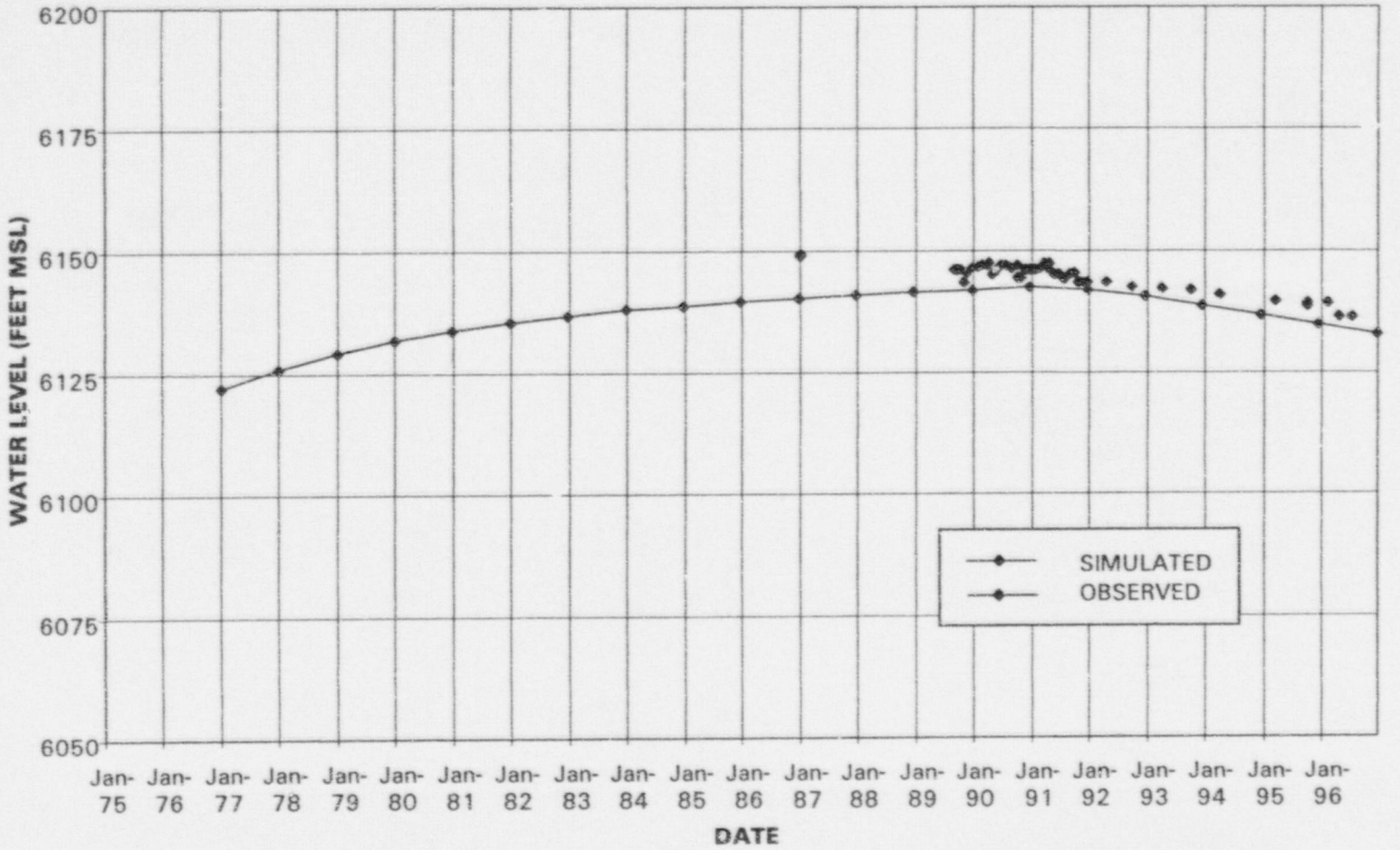

8/5/98
CN/SE9
FIG2.PPT

BALLEAU GROUNDWATER, INC.

SOHIO WESTERN MINING COMPANY

L-BAR MINE

FIGURE 22
TREND OF OBSERVED VERSUS SIMULATED WATER LEVELS AT WELL MW-50

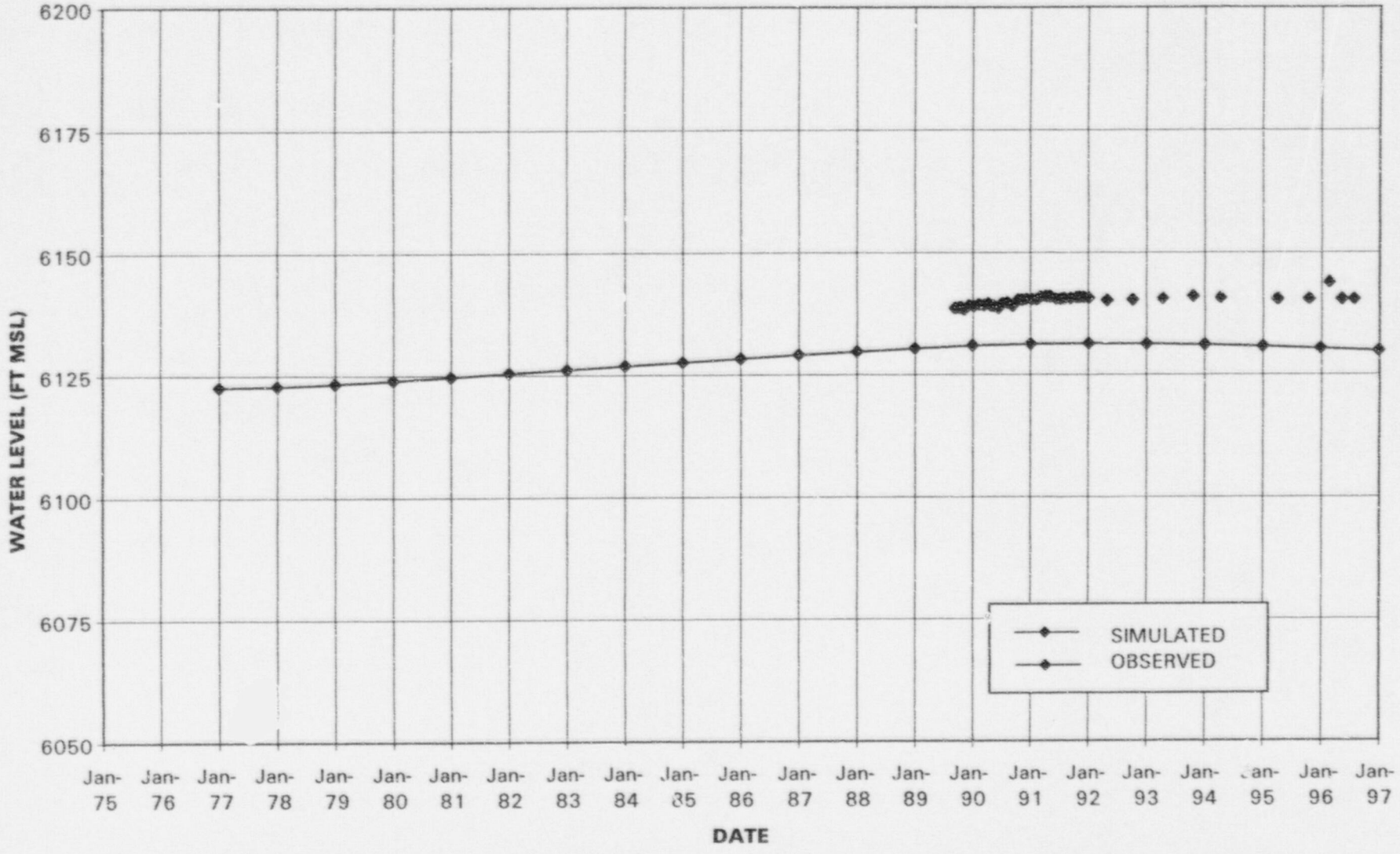

BALLEAU GROUNDWATER, INC.

7/14/97
CN
BALLEAU.PPT

Well MW-2A is located northwest of the dam. Its water level rose about 20 feet during the active period of the mine. The model simulated only ten feet of water-level rise during the same period. By the end of 1996, the simulated water level was close to the observed water level. Well MW-3A is located just west of the middle of the tailings dam and displayed ten feet of water-level rise by the end of mining activities. The model simulated about the same water-level rise.

Wells MW-17B and MW-50 are located northeast of the tailings reservoir within the nitrate plume area. The simulated build-up and decline of water levels in this area are close to the observed water levels, which indicate that the annual amount of the northeast recharge is appropriate.

Figure 23 illustrates the resulting groundwater mound in the FTH aquifer due to seepage from the tailings reservoir. At 1996, the observed water level at the FTH below the tailings was about 6140 ft msl as the model simulated (well MW-109).

Concentration

The model currently simulates the advective and dispersive movement of a non-reactive constituent. For example, the observed versus simulated chloride concentration is illustrated in Figure 24, based on a tailings chloride concentration of 2000 mg/l. The background chloride concentration is 100 mg/l. The model simulates the increments of concentration added to background conditions, therefore, model results are superimposed on a chloride value of 100 mg/l. The results illustrate the correlation between the observed and simulated chloride concentration. The adsorption and decay facilities of the program currently are not applied.

Figure 25 illustrates the observed versus the simulated chloride concentration at MW-69. At 1996, the model predicts, based on a chloride source concentration of 2000 mg/l, and background chloride concentration of 100 mg/l, chloride concentrations of 620 mg/l in well MW-69, compared to an observed concentration of 681 mg/l.

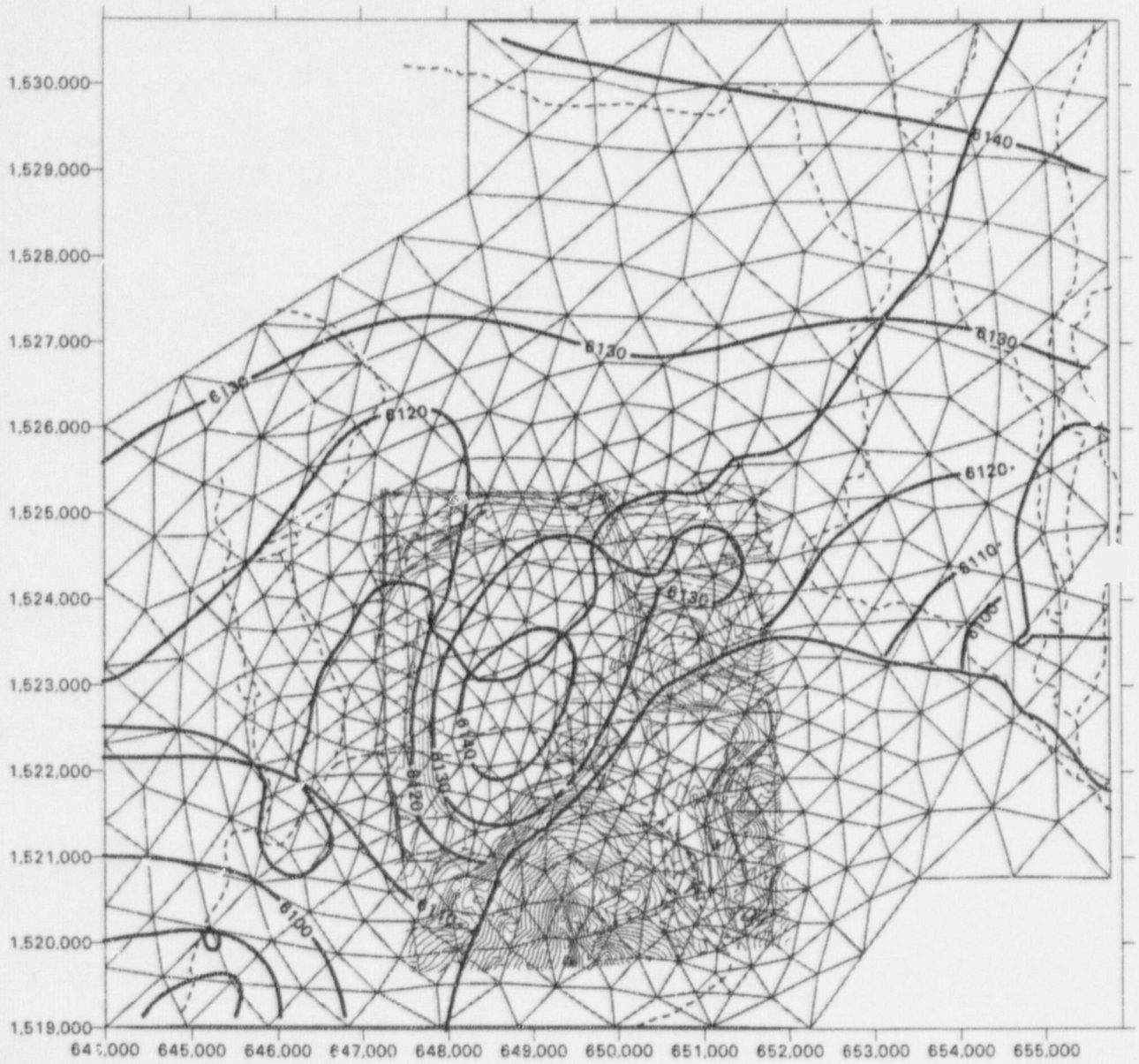

CONTOUR OF HEAD (FEET MSL)
LINE OF FULL FTH SATURATION
LINE OF UNSATURATED FTH (DRY LINE)

SOHIO WESTERN MINING COMPANY
L-BAR MINE

SIMULATED TOTAL HEAD IN FIRST TRES HERMANOS AQUIFER AT YEAR 1996

Date: 09/04/96	**FIGURE 23**
Produced By: SES	
Checked By: WPJ	
File Name: ELEVAT.SHP	

BALLEAU GROUNDWATER, INC.

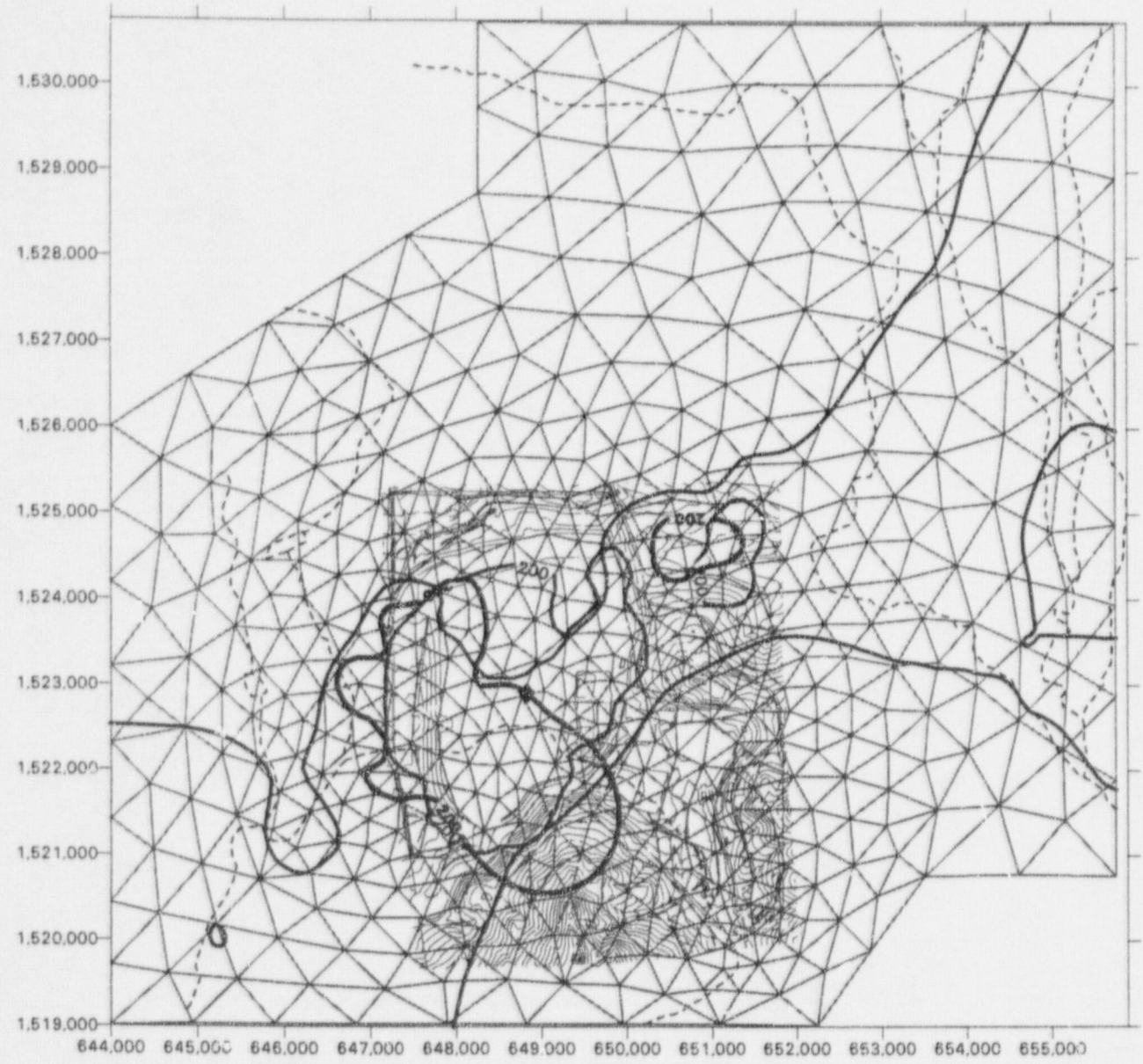

OBSERVED 1996 CHLORIDE CONCENTRATION (MG/L)

SIMULATED 1996 AVERAGE FIRST TRES HERMANOS CHLORIDE CONCENTRATION (MG/L)

LINE OF FULL FTH SATURATION
LINE OF UNSATURATED FTH (DRY LINE)

SOHIO WESTERN MINING COMPANY/ L-BAR MINE

OBSERVED AND SIMULATED CHLORIDE CONCENTRATIONS IN THE FTH AQUIFER AT YEAR 1996

Date: 06/04/98	**FIGURE 24**
Produced By: SEB	
Checked By: WPB	
File Name: FIG24.SRF	

BALLEAU GROUNDWATER, INC.

SOHIO WESTERN MINING COMPANY/
L-BAR MINE

FIGURE 25
OBSERVED AND SIMULATED CHLORIDE CONCENTRATION AT MW-69

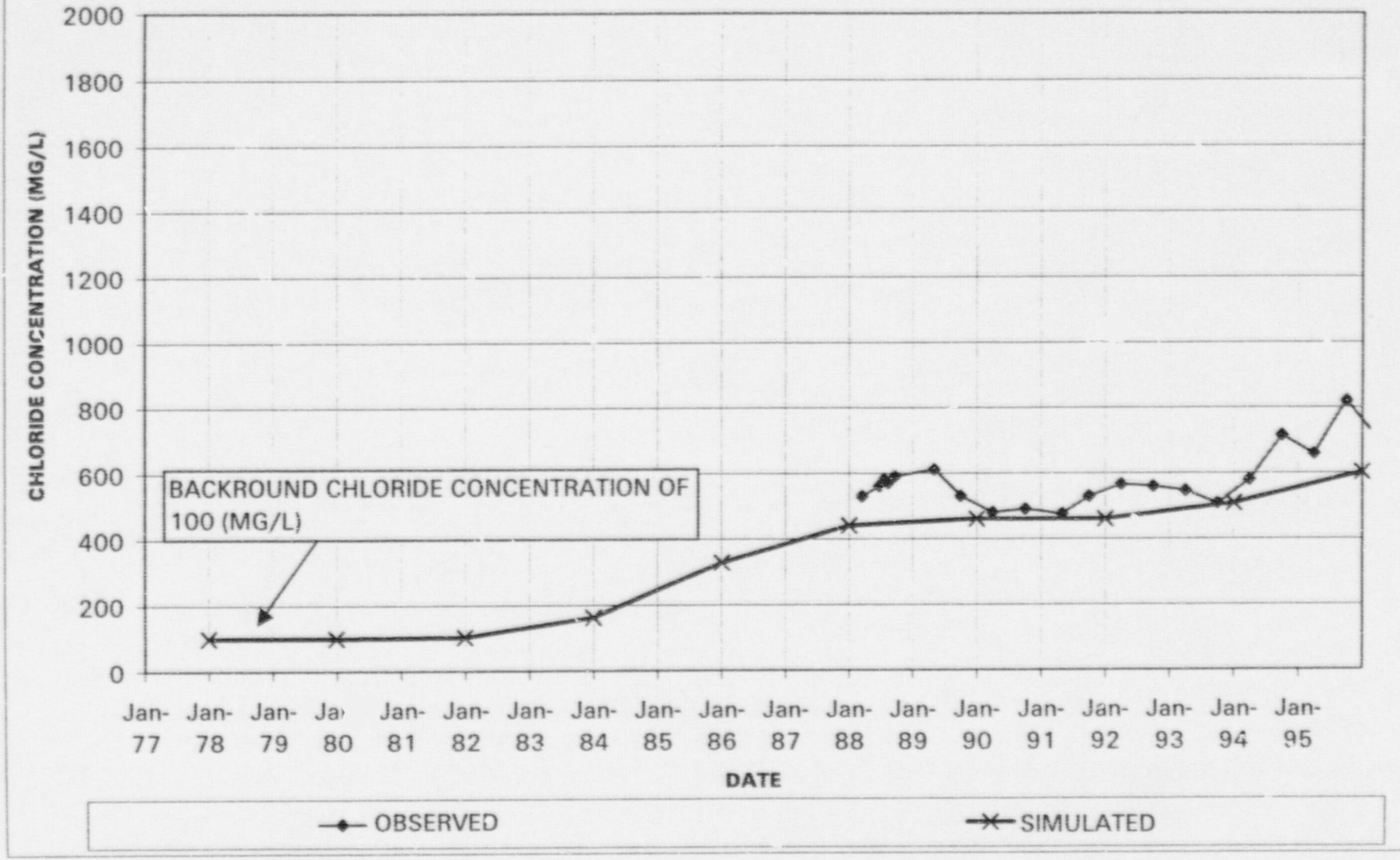

mw69.xls
SES
8/5/98

BALLEAU GROUNDWATER, INC.

Future Prediction

The model was run for 1000 years from 1996 with the groundwater-recovery system shut off. Figures 26 and 27 illustrate water levels in the FTH aquifer after 200 years and 1000 years. The levels in the FTH below the tailings are expected to drop 15 feet after 1000 years leaving a groundwater mound of about five feet in height in the FTH aquifer.

The results of the constituents transport are represented as a percentage of the source concentration. The source concentration is estimated to be 2000 mg/l for chloride. Figures 28 and 29 illustrate the contour lines of equal percentage of the source concentration after 200 and 1000 years. It is expected that after 1000 years, one percent of the source concentration (i.e., 20 mg/l of chloride) will reach no further than 2500 feet west of the dam.

The model also may be used to simulate transport of regulated constituents such as antimony, cyanide, nickel, selenium, radium-226 and -228, thorium-230 and uranium. For those constituents that behave as non-reactive tracers, the observed concentration profile for each constituent will be used to calibrate the model and to estimate the source concentration (as for chloride, 2000 mg/l). Source concentrations for reactive constituents will be estimated by geochemical models. Source concentrations of these constituents will be considered to be downstream of the zone of neutralization. For those constituents that decay or precipitate, the concentration profile for each constituent will be used to determine the decay coefficient and distribution coefficient associated with each constituent, allowing quantitative future projections to be made of constituent transport.

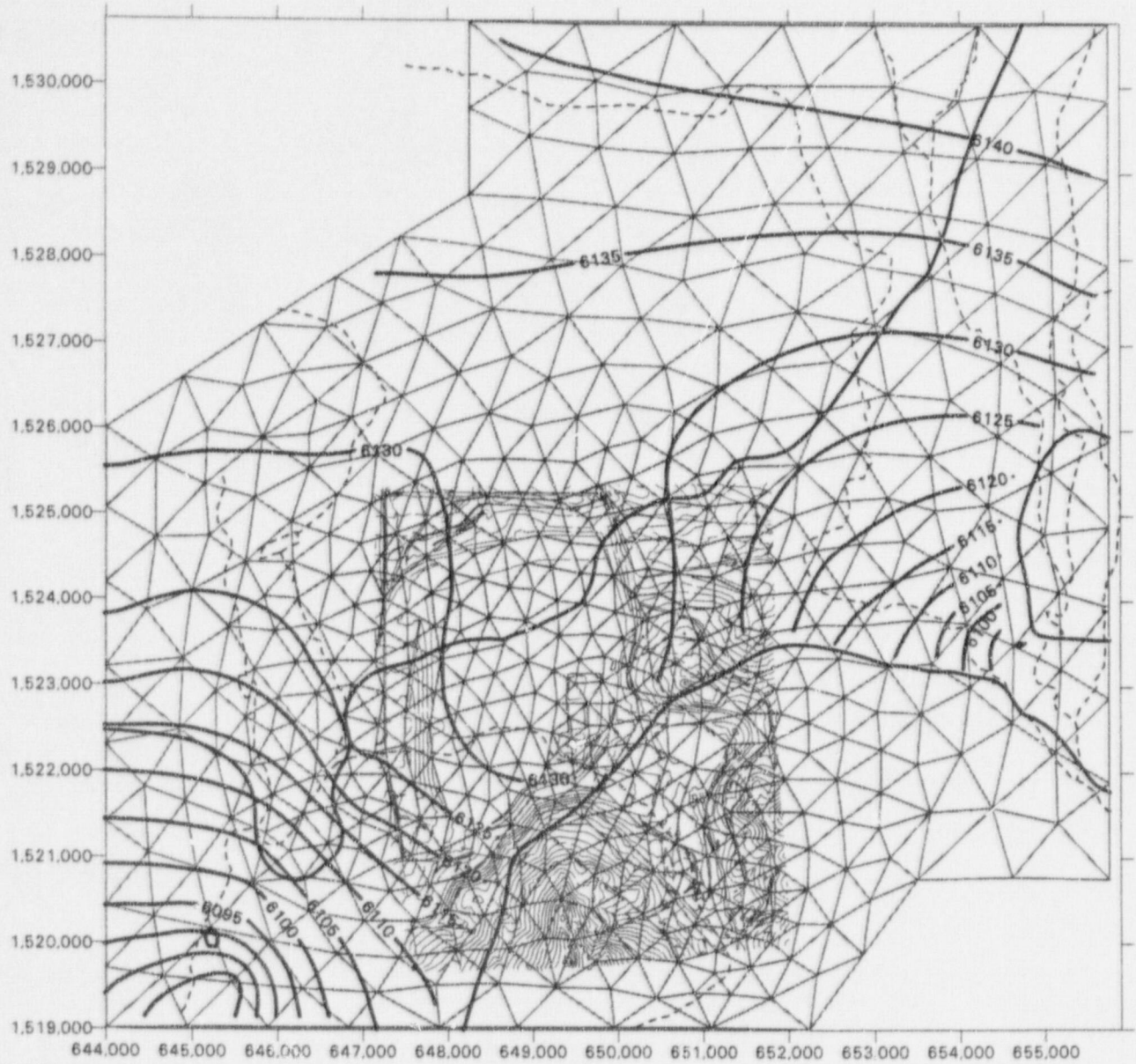

CONTOUR OF HEAD (FEET)
LINE OF FULL FTH SATURATION
LINE OF UNSATURATED FTH (DRY LINE)

SOHIO WESTERN MINING COMPANY/
L-BAR MINE

SIMULATED 200-YEAR TOTAL HEAD AT YEAR 2196 IN THE FIRST TRES HERMANOS AQUIFER

Date: 09/04/96	**FIGURE 26**
Produced By: SGS	
Checked By: WTH	
File Name: FIG26.SGO	

BALLEAU GROUNDWATER, INC.

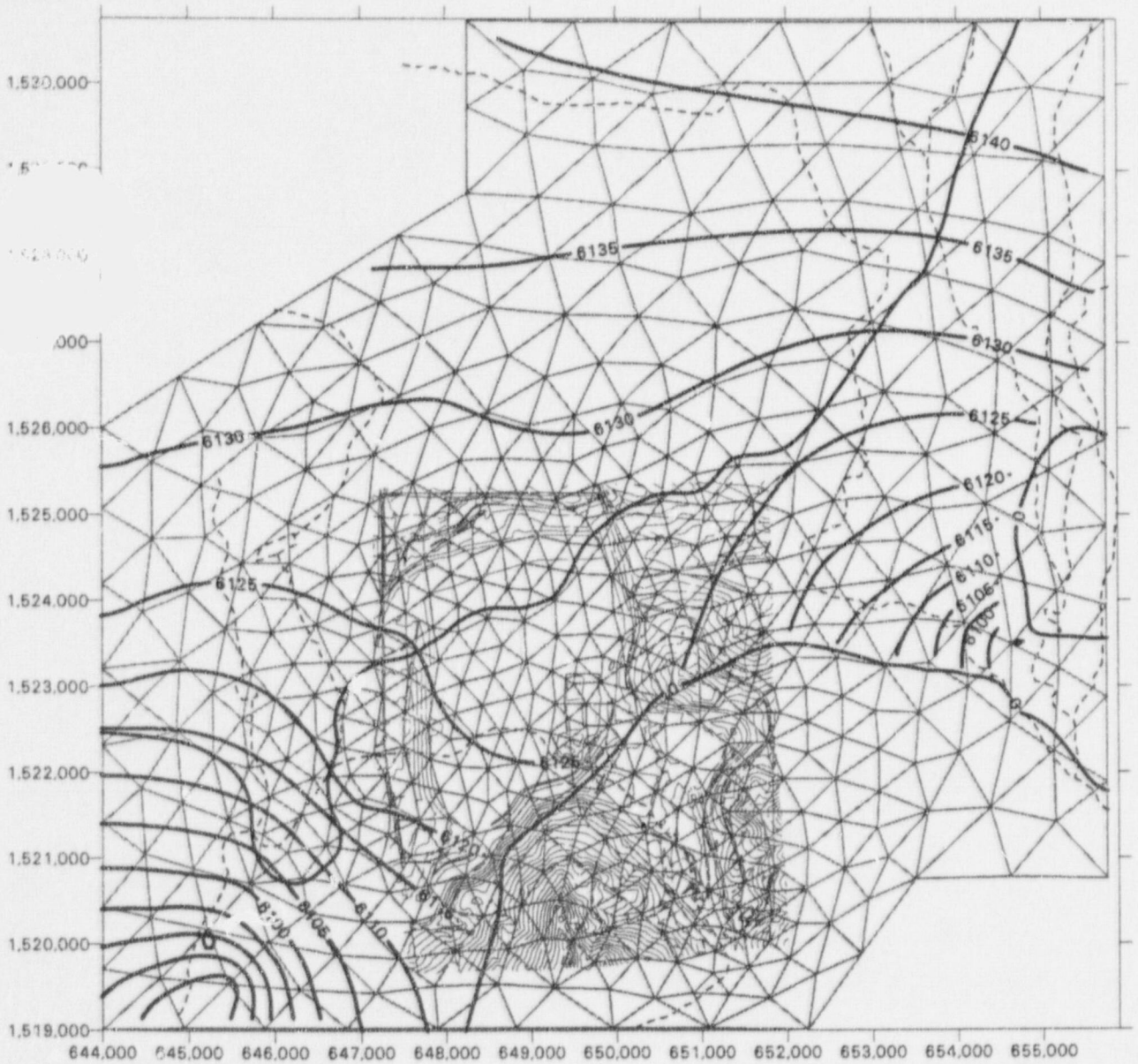

1" = 2000 FEET

0 2,000 4,000 6,000 8,000

CONTOUR OF HEAD (FEET)
LINE OF FULL FTH SATURATION
LINE OF UNSATURATED FTH (DRY LINE)

SOHIO WESTERN MINING COMPANY
L-BAR MINE

SIMULATED 1000-YEAR TOTAL HEAD AT YEAR 2996 IN THE FIRST TRES HERMANOS AQUIFER

Date: 08/04/98	**FIGURE 27**
Produced By: SGS	
Checked By: WPB	
File Name: FIG26.SRF	

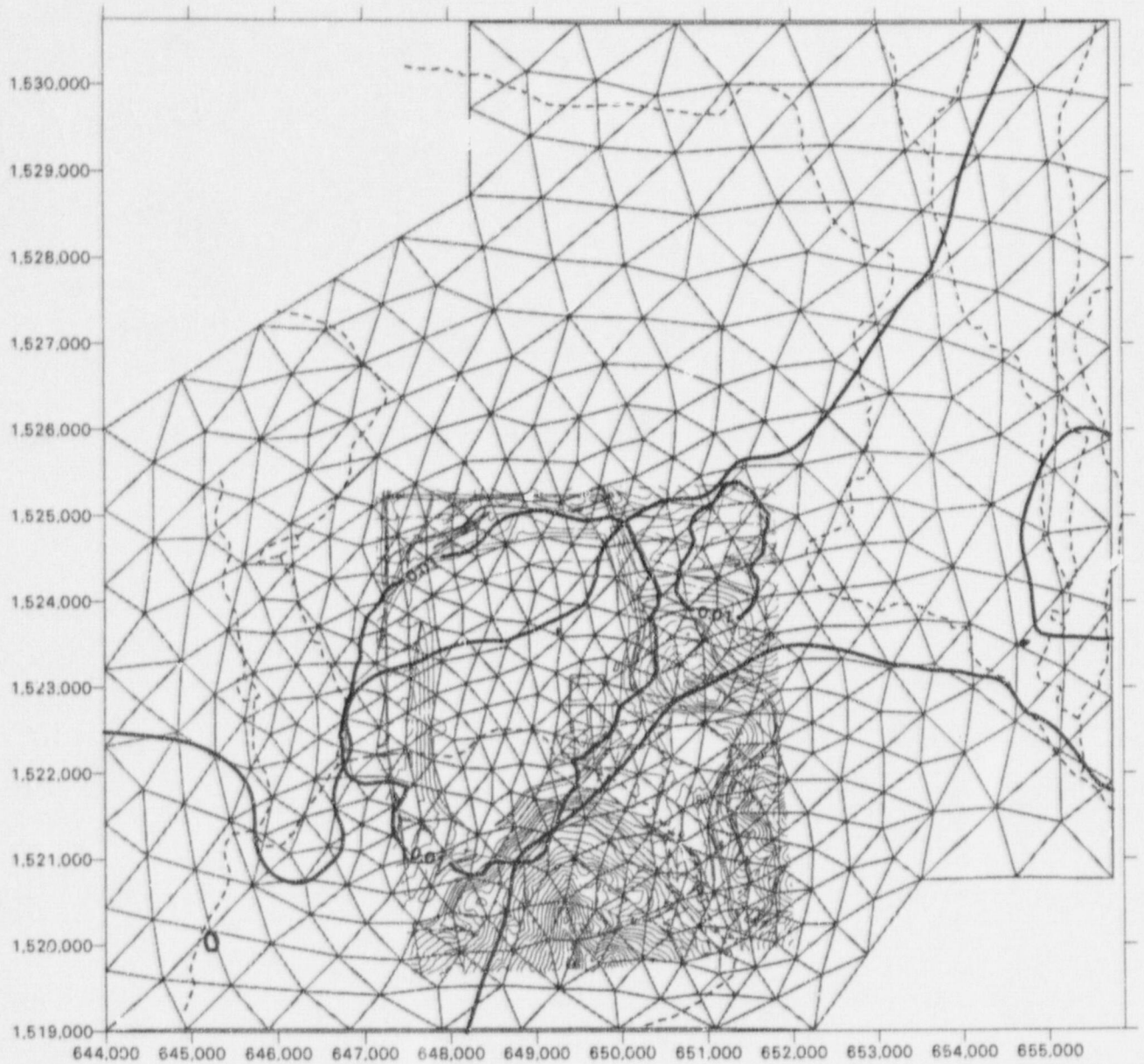

1" = 2000 FEET

0 2,000 4,000 6,000 8,000

RELATIVE CONCENTRATION OF 1%
FTH FULL SATURATION
FTH DRY LINE

SOHIO WESTERN MINING COMPANY/
L-BAR MINE

SIMULATED 200 YEAR AVERAGE CONCENTRATION IN THE FTH AQUIFER AT YEAR 2196

Date
Produced By:
Checked By:
File Name:

FIGURE 28

BGW

BALLEAU GROUNDWATER, INC.

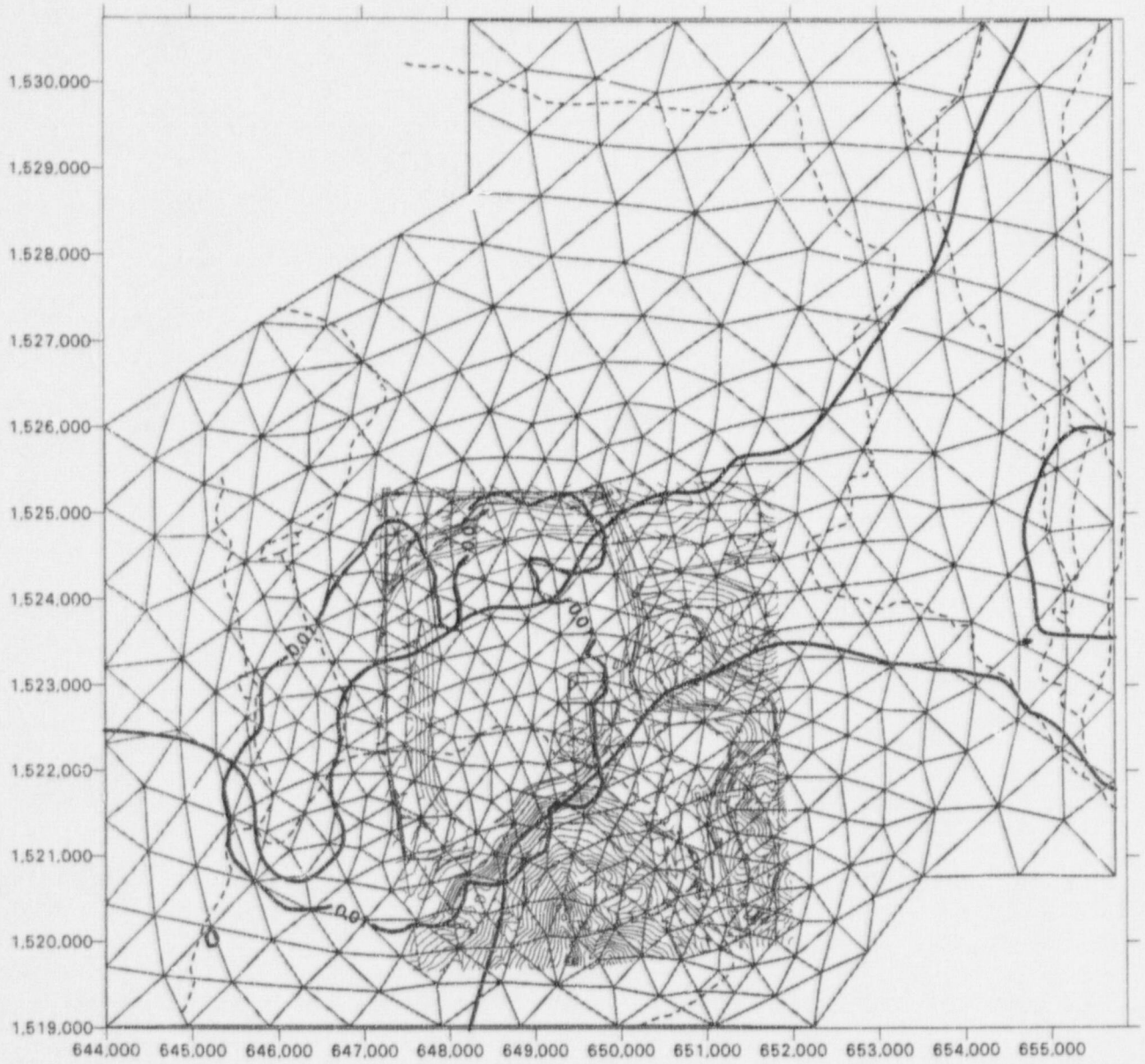

1" = 2000 FEET

0 2,000 4,000 6,000 8,000

RELATIVE CONCENTRATION OF 1%
FTH FULL SATURATION
FTH DRY LINE

SOHIO WESTERN MINING COMPANY/
L-BAR MINE

SIMULATED 1000 YEAR AVERAGE CONCENTRATION IN THE FTH AQUIFER AT YEAR 2996

Date: 08/04/98 Produced By: SEB Checked By: WPB File Name: FIG26.SRF	**FIGURE 29**	BGW

CONCLUSIONS

The hydrologic system in the L-Bar Uranium Mine mill tailings was investigated using a three-dimensional finite-element model. The model simulates the flow and dispersive transport in saturated and unsaturated conditions. The conclusions of the modeling are:

1. The model results indicated that the model is capable of simulating the hydrologic system in and around the tailings area.

2. Seepage through the tailings reservoir created a 20-foot groundwater mound in the FTH by year 1996. After 1000 years, the groundwater mound is expected to decay to about five feet.

3. Observed soil-moisture trends and projections indicate that the tailings are draining at a slow rate and will become entirely unsaturated by year 2010.

4. Through 1000 years (year 2996), the constituent concentration zones greater than one percent of the source concentrations will be contained in a 2500-foot distance west of the dam. Future model projections will allow quantitative conclusions to be made about constituent transport.

REFERENCES

Boss International , 1996, "BOSS GMS User's Manual," with Brigham Young University

Drimmie, R.J., 1995, "Report of Isotope and Selected Chemistry Results for the L-Bar Mine Tailings Pond, L-Bar Uranium Mine, Cibola County, New Mexico, Results from Stable Isotope Sampling Program October 1994," unpublished consultant's report to Intera, Inc.

Intera, Inc., 1996, "Final Report: Hydrogeology Investigation of the L-Bar Uranium Mill Tailings Pile Cibola County, New Mexico," consultants report to Kennecott Corporation.

Lin, H.C.J., Richards, D.R., Yeh, G.T., Cheng, J.R., Cheng, P.H. and Jones, N.L., 1996, "FEMWATER: A Three-Dimensional Finite Element Computer Model for Simulating Density Dependent Flow and Transport," U.S. Environmental Protection Agency, Technical Report HL-96.

Los Alamos National Laboratory, 1996, "FEHMN: Finite Element Heat and Mass Transfer Code."

Pruess, K., 1991, "TOUGH2 - A General-Purpose Numerical Simulator for Multiphase Fluid and Heat Flow," Lawrence Berkeley Laboratory, Earth Sciences Division, LGL-29400.

van Genuchten, M.T., 1980, "A Closed-Form Equation for Predicting the Hydraulic Conductivity of Unsaturated Soils," in Soil Science Society Journal, Vol. 44.

APPENDIX C

Corrective Action Program Summary

TABLE OF CONTENTS

C-1.0 Introduction C-2
C-2.0 Description of the Corrective Action Program C-2
C-3.0 Chronology C-2
C-4.0 Barrier System Performance C-3
Table C-4.1 Barrier Well Production Summary – 1991 through 1997 ..... C-4
C-5.0 Point-of-Compliance Monitoring C-5
Table C-5.1 Summary of L-Bar Compliance Monitoring C-7
Constituent Concentrations When Detected: 03/88 to 10/97 ..... C-7
Table C-5.1 (Cont.) C-8
C-6.0 Summary C-12

FIGURES

Figure C-1 Concentrations at Point of Compliance Well MW-1A
Figure C-2 Concentrations at Point of Compliance Well MW-17B
Figure C-3 Concentrations at Point of Compliance Well MW-29A
Figure C-4 Concentrations at Point of Compliance Well MW-69
Figure C-5 Concentrations at Point of Compliance Well MW-81

C-1.0 INTRODUCTION

The Groundwater Corrective Action Program (CAP) at the L-Bar tailings site has been fully operational since July 1, 1990. The NRC was notified in writing on this date to fulfill the requirements of License Condition 31A. Since the CAP became fully operational, the L-Bar Nuclear Regulatory Commission (NRC) Source Material License SUA-1472 has required the submittal of an annual groundwater corrective action program review report that describes the progress toward attaining Groundwater Protection Standards. Each year, beginning in 1990, a Corrective Action Program Report has been submitted to the NRC.

C-2.0 DESCRIPTION OF THE CORRECTIVE ACTION PROGRAM

The CAP at L-Bar was designed to recover contaminated groundwater as well as control and minimize the spread of tailings seepage. The CAP captures seepage waters from the two main flow paths, the northeastern and the southwestern flow paths. The design of the CAP relied upon recovering contaminated waters from these flow paths and the tailings impoundment, returning the seepage water and dissolved constituents to a sump, and then pumping the fluid to evaporation cells. This process was adaptable to the work that was being undertaken on the tailings impoundment, and gathered valuable data on the rate and direction of groundwater flow as well as on the concentrations of constituents in the groundwater. The combination of tailings dewatering, contaminant recovery, and enhanced evaporation proved to be an effective CAP.

C-3.0 CHRONOLOGY

The first Corrective Action Program Review Report, submitted in March 1990, described the corrective action program and presented groundwater modeling results demonstrating the program's effectiveness. A June 28, 1990 addendum to the report updated the observed water quality at point-of-compliance wells, discussed how the addition of two pumpback wells to the barrier system could increase effectiveness, and calculated the amount of residual mass of hazardous constituents remaining in the tailings impoundment.

The second annual groundwater corrective action program review, submitted in February 1991, discussed the status of the program at the L-Bar site and provided an update to the 1990 report. The specific points discussed in the report included the installation of two additional barrier wells, the performance of the barrier well system for the previous year, the concentrations of regulated constituents at the point of compliance wells, and the performance of the toe drain system in collecting and removing tailings fluid from the system.

The third through seventh annual groundwater corrective action program reviews described the status of the program at the L-Bar site between 1992 and 1996. Operations and conditions at the site during those periods changed very little after the 1990 report.

An extensive characterization of the tailings pile and the underlying aquifer was initiated in late 1995 and completed in 1996. This involved an extensive cone penetrometer survey of the tailings, the installation of wells and piezometers in the tailings and in the underlying aquifer, hydraulic testings of the wells, core samples of the formations under the tailings and their characterization, and tailings and radon barrier sampling and characterization. These tests allowed evaluation of the settlement status of the tailings, the amount and quality of remaining tailings fluid, the impact of tailings on water levels and water quality under the tailings, and an evaluation of geochemical and geotechnical characteristics of tailings, radon barrier, underlying Mancos Shale and the First Tres Hermanos sandstone aquifer. These sample results, characterizations and interpretations have been compiled in a report entitled Hydrogeology Investigation of the L-Bar Uranium Mill Tailings Pile, Cibola County, New Mexico which was submitted to the NRC on December 19, 1996 (Mr. Joseph Holonich, Docket 40-8904).

In addition, an extensive ground water flow, contaminant transport and geochemical modeling study was initiated in 1996 and was completed in 1997. The report for this modeling, entitled Projected Long-term Flow and Quality of Ground Water at L-Bar, New Mexico Uranium Site, was submitted to the USNRC in July 1997. The report provided an extensive and thorough review of the ground water situation at the L-Bar site. The report supplemented historical reports by documenting and baselining the ground water quality at the POCs and the barrier system performance for 1997.

The eighth annual groundwater Corrective Action Program Review described operations which took place during 1997. The characteristics described in the 1997 review report are representative of current conditions. Changes to the site during 1997 include discontinuing the toe drains. The water levels in the wells and piezometers located at the toe of the dam were closely monitored during and after the toe drains were turned off in July 1997. No significant change was observed in the wells and piezometers that were in closest proximity and would most likely be affected by the toe drain system being shut down.

C-4.0 BARRIER SYSTEM PERFORMANCE

The barrier system located west of the former tailings impoundment, consisting of a series of eleven pumpback wells, continues to intercept seepage resulting from consolidation and drainage of the tailings pile. The initial system has been in operation since 1981. The enhanced system, which includes wells 101 and 102, has been fully operational since September 1990. All pumpback wells are completed in the First

Tres Hermanos sandstone. A seepage-collection trench completed in the First Tres Hermanos also intercepts seepage from the former tailings impoundment area. Discharge from the pumpback wells and the trench is collected in a sump at the bottom of the trench. The cumulative discharge is pumped from the sump to two evaporation cells located on the east portion of the property. All pumpback wells are equipped with switches that control intermittent pumping. Pumping cycles in most of these wells occur every fifteen minutes. Pumpback well 102 pumps less frequently, with cycles occurring every 2 hours. Table C-4.1 shows the cumulative amounts of fluid collected annually from the barrier wells and the seepage collection trench from 1991 through 1997. The mean pumping rates for each well in the barrier system are submitted annually in the Corrective Action Program Summary Report.

Table C-4.1 Barrier Well Production Summary – 1991 through 1997

Year	Barrier Well System Annual Production (gallons)	Tailings Fluid Collected (gallons)
1991	3,778,227	1,616,324
1992	3,486,191	1,301,470
1993	3,405,857	1,054,220
1994	2,851,430	881,854
1995	2,680,686	691,085
1996	2,664,085	386,000*
1997	2,525,839	*
TOTAL	**21,392,315**	**5,930,953**

* Toe Drains turned off on July 23, 1996, the 1996 total provided is for the year up to July 23, 1996.

The barrier system on the east side of the former tailings impoundment consists of pumpback well 89, which is also equipped with a switch to control intermittent pumping on a fifteen minute cycle. The purpose of this well is to recover groundwater that may be affected by seepage to the northeast. This water is pumped directly to the evaporation ponds. Past water-level data collected on a monthly basis indicate that pumpback well 89 is effectively producing a capture zone and eliminating any further eastward migration of seepage beyond point-of-compliance well MW-17B.

C-5.0 POINT-OF-COMPLIANCE MONITORING

Four point-of-compliance (POC) wells and one background well, as designated by Condition 31.A of License SUA-1472, are used to evaluate the water quality over time. These POC wells are: MW-1A to the northwest of the former tailings impoundment, MW-69 directly west of the former tailings impoundment, MW-81 to the southwest of the former tailings impoundment, and MW-17B to the northeast of the former tailings impoundment. The background well, MW-29A, is northeast of MW-17B.

As part of the groundwater compliance monitoring program at the L-Bar tailings site, POC wells are sampled and analyzed for nickel, combined radium-226 and radium-228, selenium, thorium-230, and uranium. Amendment 28 to the license was issued on June 30, 1998 accepting the request to delete antimony and cyanide from the list of hazardous constituents at the L-Bar site. Table C-5.1 summarizes the L-Bar compliance monitoring results when constituents are found at or above laboratory minimum detection levels. The historical behavior of each constituent of concern is described below.

Nickel (Ni). License SUA-1472 was amended in 1992 to change the GPS for nickel to 0.05 mg/l from the earlier GPS of 0.001 mg/l. Nickel was not detected in any POC well at the laboratory detection limit of 0.04 mg/l in 1992. However, laboratory results for the April 1993 sampling showed significantly elevated nickel concentrations in three POC wells, MW-17B (0.22 mg/l), MW-69 (0.25 mg/l), and MW-81 (0.13 mg/l). These reported results were over an order of magnitude higher than the highest previous reported nickel concentration for each of the wells. A laboratory check discovered no problems with the analysis or concentration calculations and no apparent source of nickel contamination was found. The results for wells MW-1A and MW-29A during the same period showed no nickel detected at the 0.04 mg/l detection limit. The results for the October 1993 sampling period reported non-detects for nickel in all POC wells except MW-17B, which showed a nickel concentration at the detection limit of 0.04 mg/l. The elevated nickel concentrations reported for the April 1993 sampling period are viewed as suspect due to the large difference between historical well concentrations and the April 1993 results and because the results were not repeated during the October 1993 sampling period or during the 1994, 1995, 1996, or 1997 sampling periods. Nickel was not detected in any of the POC wells or the background well during 1994, 1995, 1996, or 1997.

Selenium (Se). was detected above the GPS of 0.01 mg/l in POC wells MW-81 and MW-17B. Selenium was not detected above the GPS in any POC well during 1996. However, selenium was detected above the GPS (0.01 mg/l) in MW-17B (0.366 mg/l), MW-69 (0.012 mg/l), and MW-81 (0.23 mg/l) in April 1995. Selenium was not detected in any POC wells or the background well in October 1995. In 1994, selenium was not detected in any monitor well. However, selenium was detected above the GPS of 0.01 mg/l in three wells in 1993: MW-17B (0.014mg/l), MW-69 (0.02 mg/l), and MW- 81

(0.16 mg/l). Although not consistent, historically MW-17B, MW-69, and MW-81 have had results detected above the GPS for selenium.

Combined Radium-226 (Ra-226) and **Radium-228 (Ra-228)** continue to be found in all POC wells and the background well at levels just above or just below the GPS of 5.0 pCi/l.

Thorium-230 (Th-230) continues to be found in all POC wells and the background well at levels above the GPS of 0.13 pCi/l.

Uranium (U) was again only detected above the GPS of 0.50 mg/l in MW-69 in 1997. The uranium concentration in MW-69 was above the GPS for both sampling periods as has been the case for most sampling periods since 1988. Uranium concentrations are consistently below the GPS in all other POC wells.

Table C-5.1 Summary of L-Bar Compliance Monitoring
Constituent Concentrations When Detected: 03/88 to 10/97

POC WELL	CONSTITUENT CONCENTRATIONS WHEN DETECTED						
	Sb (0.2 mg/l)	Ni (0.05 mg/l)	Se (0.01 mg/l)	U (0.5 mg/l)	Ra226 + Ra228 (5 pCi/l)	Th230 (0.13 pCi/l)	CN (0.01)
1A	0.02 (10/93)	0.006 (03/88)	0.009 (07/88)	0.002 (05/91)	0.30 (06/88)	0.20 (07/88)	----------
		0.004 (07/88)	0.0038 (10/89)	0.001 (10/91)	0.17 (07/88)	0.07 (05/89)	
		0.005 (08/88)	0.002 (05/96)	0.001 (04/92)	0.80 (08/88)	0.07 (04/90)	
		0.0064 (10/89)	0.005 (10/96)	0.002 (10/92)	0.26# (05/89)	4.20 (10/90)	
		0.0041 (10/90)		0.003 (04/93)	0.13# (10/89)	0.70 (05/91)	
				0.002 (10/93)	6.37 (04/90)	22.8 (10/91)	
				0.002 (04/94)	0.40 (10/90)	4.5 (10/92)	
				0.001 (10/94)	10.3 (05/91)	0.5 (04/93)	
				0.002 (05/97)	0.9 (10/91)	0.4 (10/93)	
				0.002 (10/97)	1.6 (04/92)	0.6 (04/94)	
					2.6 (10/92)	2.8 (10/94)	
					3.9 (04/93)	0.4 (04/95)	
					2.9 (10/93)	0.3 (10/95)	
					0.6 (04/94)	1.4 (05/96)	
					0.5 (10/94)	0.8 (10/96)	
					1.6 (04/95)	0.9 (05/97)	
					0.9 (10/95)	1.7 (10/97)	
					0.9 (05/96)		
					1.3 (10/96)		
					0.3 (05/97)		
					0.1 (10/97)		

Table C-5.1 (Cont.)

	Sb (0.2 mg/l)	Ni (0.05 mg/l)	Se (0.01 mg/l)	U (0.5 mg/l)	Ra226 + Ra228 (5 pCi/l)	Th230 (0.13 pCi/l)	CN (0.01)
17B	0.24 (06/88)	0.011 (03/88)	0.33 (01/88)	2.0 (05/89)	1.10 (03/88)	0.82 (03/88)	0.10 (06/88)
	0.29 (10/89)	0.016 (06/88)	0.41 (03/88)	0.025 (05/91)	1.00 (06/88)	0.30 (06/88)	0.07 (07/88)
	0.10 (05/91)	0.007 (07/88)	0.46 (06/88)	0.028 (10/91)	19.6 (07/88)	0.30 (07/88)	0.20 (08/88)
	0.011 (10/92)	0.011 (08/88)	0.50 (07/88)	0.036 (04/92)	0.90 (08/88)	0.02 (08/88)	0.03 (05/89)
	0.006 (04/94)	0.007 (09/88)	0.42 (08/88)	0.032 (10/92)	0.70# (05/89)	0.10 (05/89)	0.38 (10/89)
	0.006 (10/94)	0.010 (05/89)	0.35 (09/88)	0.030 (04/93)	0.77# (10/89)	0.31 (10/89)	0.024 (10/90)
		0.012 (10/89)	0.27 (05/89)	0.035 (10/93)	4.00 (04/90)	0.04 (04/90)	0.05 (10/96)
		0.016 (04/90)	0.28 (10/89)	0.036 (04/94)	6.70 (10/90)	3.40 (10/90)	
		0.026 (10/90)	0.27 (04/90)	0.030 (10/94)	3.40 (05/91)	1.0 (05/91)	
		0.04 (10/91)	0.17 (10/90)	0.036 (04/95)	3.70 (10/91)	0.9 (10/91)	
		0.22 (04/93)	0.40 (05/91)	0.037 (10/95)	4.7 (04/92)	0.9 (04/92)	
		0 04 (10/93)	0.30 (10/91)	0.0345 (05/96)	5.2 (10/92)	0.4 (10/92)	
			0.40 (04/92)	0.032 (10/96)	5.0 (04/93)	0.2 (04/93)	
			0.014 (04/93)	0.039 (05/97)	1.9 (10/93)	0.8 (10/93)	
			0.366 (04/95)	0.041 (10/97)	3.5 (04/94)	0.3 (04/94)	
			0.006 (05/96)		5.0 (10/94)	3.2 (10/94)	
			0.012 (10/97)		5.4 (05/96)	0.5 (10/96)	
					13.7 (10/96)	3.7 (05/97)	
					5.2 (05/97)	1.2 (10/97)	
					8.5 (10/97)		

Table C-5.1 (Cont.)

	Sb (0.2 mg/l)	Ni (0.05 mg/l)	Se (0.01 mg/l)	U (0.5 mg/l)	Ra226 + Ra228 (5 pCi/l)	Th230 (0.13 pCi/l)	CN (0.01)
69	0.27 (06/88)	0.011 (03/88)	0.020 (03/88)	1.10 (06/88)	2.30 (07/88)	0.13 (07/88)	----------
	0.25 (07/88)	0.010 (06/88)	0.012 (08/88)	1.10 (07/88)	1.22 (08/88)	0.45 (08/88)	
	0.39 (10/89)	0.016 (07/88)	0.020 (05/89)	0.93 (08/88)	0.45# (05/89)	0.20 (05/89)	
	0.005 (04/94)	0.011 (08/88)	0.0066 (10/89)	2.50 (05/89)	0.39# (10/89)	0.2 (10/89)	
		0.006 (09/88)	0.02 (10/93)	1.0 (10/89)	6.40 (04/90)	0.04 (04/90)	
		0.012 (05/89)	0.012 (04/95)	0.68 (04/90)	7.30 (10/90)	9.80 (10/90)	
		0.016 (10/89)	0.008 (05/97)	0.492 (05/91)	7.20 (05/91)	8.5 (05/91)	
		0.0063 (04/90)		0.641 (10/91)	3.50 (10/91)	1.3 (10/91)	
		0.010 (10/90)		0.506 (04/92)	8.1 (04/92)	0.4 (10/92)	
		0.070 (05/91)		0.63 (10/92)	10.5 (10/92)	0.2 (04/93)	
		0.25 (04/93)		0.691 (04/93)	11.6 (04/93)	0.6 (10/93)	
				0.539 (10/93)	8.9 (10/93)	0.5 (04/94)	
				0.526 (04/94)	8.8 (04/94)	2.8 (10/94)	
				1.51 (10/94)	1.3 (10/94)	0.9 (05/96)	
				0.892 (04/95)	7.8 (04/95)	0.4 (10/96)	
				1.9 (10/95)	4.6 (10/95)	0.7 (05/97)	
				1.28 (05/96)	6.7 (05/96)	0.8 (10/97)	
				0.91 (10/96)	13.2 (10/96)		
				0.865 (05/97)	9.4 (05/97)		
				3.13 (10/97)	1.6 (10/97)		

DE&S Duke Engineering & Services

Table C-5.1 (Cont.)

	Sb (0.2 mg/l)	Ni (0.05 mg/l)	Se (0.01 mg/l)	U (0.5 mg/l)	Ra226 + Ra228 (5 pCi/l)	Th230 (0.13 pCi/l)	CN (0.01)
81	0.005(10/92)	0.017 (06/88)	0.0061 (04/90)	0.9 (05/89)	0.60 (06/88)	0.06 (06/88)	----------
	0.01 (10/93)	0.004 (07/88)	0.10 (05/91)	0.005 (05/91)	0.60 (07/88)	0.12 (05/89)	
		0.005 (08/88)	0.03 (04/92)	0.009 (10/91)	0.60 (08/88)	0.03 (10/89)	
		0.004 (05/89)	0.003 (04/93)	0.008 (04/92)	1.10# (05/89)	0.06 (04/90)	
		0.0059(10/89)	0.16 (10/93)	0.004 (10/92)	0.63# (10/89)	1.80 (10/90)	
		0.0032 (10/90)	0.23 (04/95)	0.009 (04/93)	5.40 (04/90)	2.3 (05/91)	
		0.13 (04/93)	0.01 (05/96)	0.011 (10/93)	9.00 (10/90)	0.2 (10/91)	
			0.002 (10/96)	0.020 (04/94)	4.4 (05/91)	0.6 (10/92)	
			0.066 (05/97)	0.014 (10/94)	5.9 (10/91)	0.4 (04/93)	
				0.022 (10/95)	8.0 (04/92)	1.0 (10/93)	
				0.0166 (05/96)	10.0 (10/92)	0.6 (04/94)	
				0.012 (10/96)	7.7 (04/93)	3.9 (10/94)	
				0.018 (05/97)	7.8 (10/93)	20.5 (10/95)	
				0.021 (10/97)	6.4 (04/94)	1.0 (05/96)	
					8.1 (10/94)	0.6 (10/96)	
					7.7 (04/95)	1.6 (05/97)	
					8.9 (10/95)	1.0 (10/97)	
					8.1 (05/96)		
					11.1 (10/96)		
					6.6 (05/97)		

Table C-5.1 (Cont.)

	Sb (0.2 mg/l)	Ni (0.05 mg/l)	Se (0.01 mg/l)	U (0.5 mg/l)	Ra226 + Ra228 (5 pCi/l)	Th230 (0.13 pCi/l)	GN (0.01)
29A	0.009(04/95)	0.010 (04/90)	0.003 (10/96)	0.001 (05/91)	4.20 (06/88)	0.07 (06/88)	----------
(Back-				0.003 (04/93)	2.90 (07/88)	0.21 (07/88)	
Ground)				0.001 (04/94)	3.20 (08/88)	0.01 (05/89)	
				0.002 (10/94)	1.39# (05/89)	0.02 (10/89)	
				0.001 (05/97)	0.68# (10/89)	0.06 (04/90)	
					5.90 (04/90)	2.60 (10/90)	
					5.00 (10/90)	0.5 (05/91)	
					3.5 (05/91)	1.4 (10/91)	
					3.4 (10/91)	0.1 (10/92)	
					5.6 (04/92)	0.6 (04/93)	
					6.3 (10/92)	0.6 (10/93)	
					7.1 (04/93)	0.9 (04/94)	
					5.9 (10/93)	4.7 (10/94)	
					4.5 (04/94)	0.2 (04/95)	
					5.6 (10/94)	0.9 (05/96)	
					5.6 (04/95)	0.2 (10/96)	
					9.9 (10/95)	0.6 (05/97)	
					4.7 (05/96)	0.8 (10/97)	
					11.5 (10/96)		
					5.3 (05/97)		
					5.6 (10/97)		

Only analyzed for radium 226

C-6.0 SUMMARY

The groundwater protection program at the L-Bar Uranium Mine continues to operate as designed. The system was enhanced on the west side in 1990 with the addition of two pumping wells, bringing the total pumping wells on the west side to twelve. Since then, one very low productivity well (MW-05) has been removed from service, leaving eleven wells on the west side in service. The drawdown experienced in the pumping and neighboring wells has indicated that the system is providing an effective barrier to further downstream transport of contaminants.

Semi-annual sampling at point-of-compliance wells continues at the site. The concentrations of regulated constituents are reported for each of the point-of-compliance wells for 1997 and preceding years.

The toe drain system at the site has been taken out of operation as it no longer contributes significantly to tailings drainage or groundwater protection.

A significant tailings characterization study was completed in 1996 and this report has been submitted to NRC. The Corrective Action Program or CAP has been successful in reducing the amount of tailings fluid drainage from the tailings pile and preventing contaminants from migrating off-site.

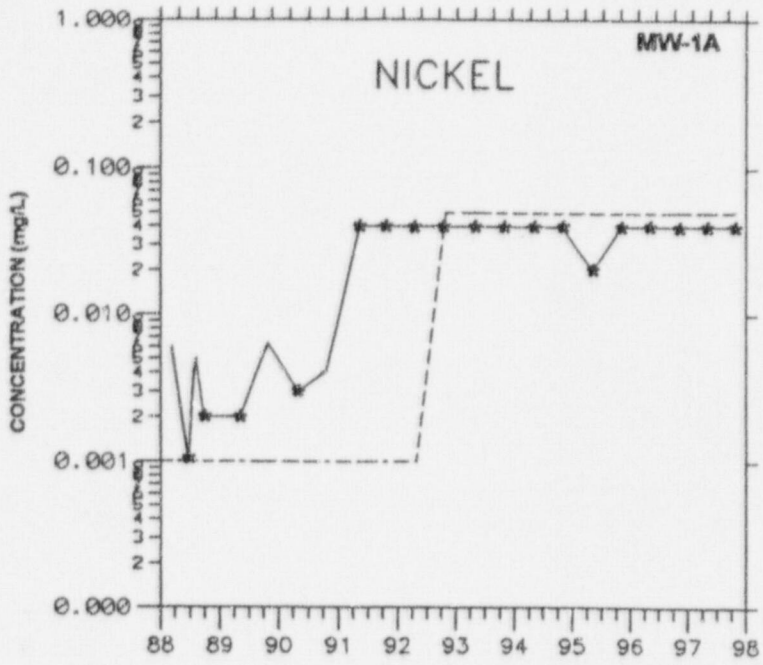

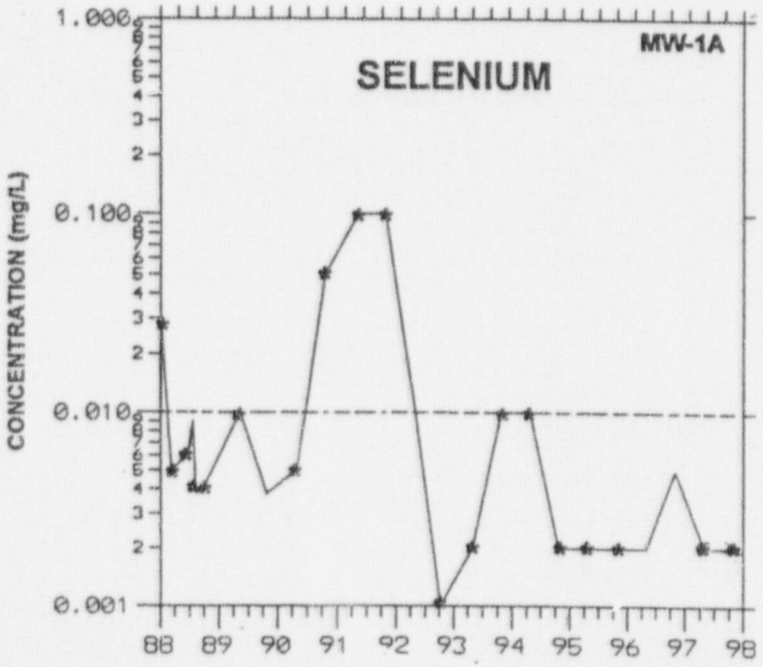

- - - Groundwater Protection Standard

★ Not Detected, Value Plotted is Method Detection Limit

▣ Only Analyzed for Ra226

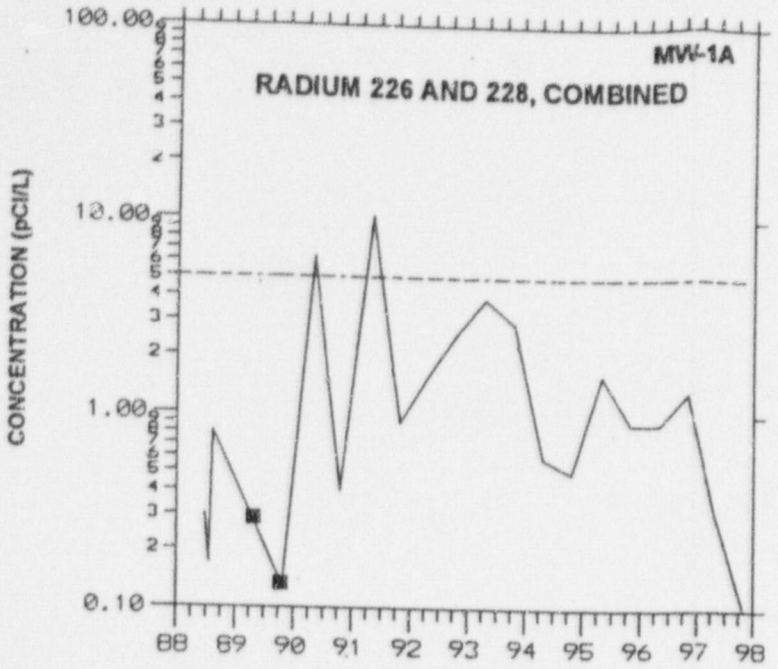

APERTURE CARD
Also Available on Aperture Card

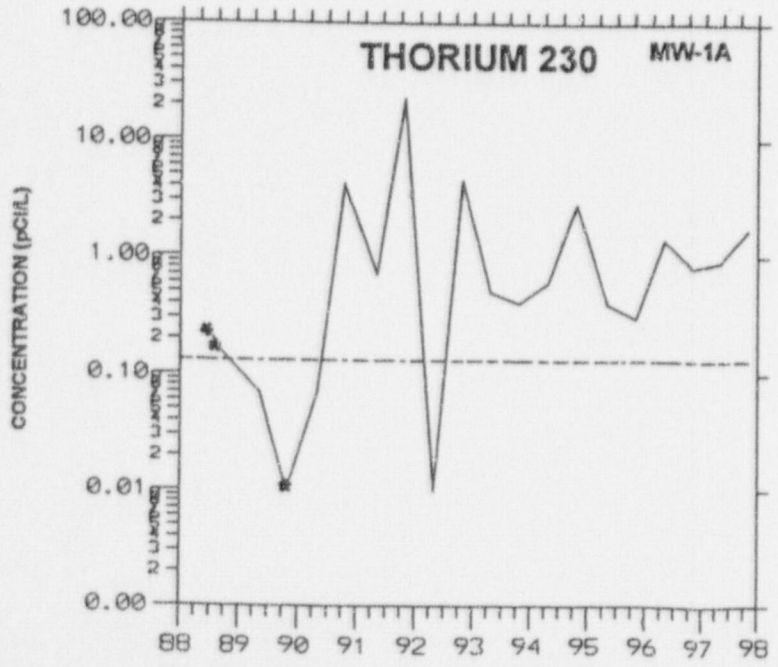

9903120203-01

DATE: 2/98	Concentrations at Point of Compliance Well MW-1A
REF: TKE 101	
DE&S Duke Engineering & Services	Figure C-1

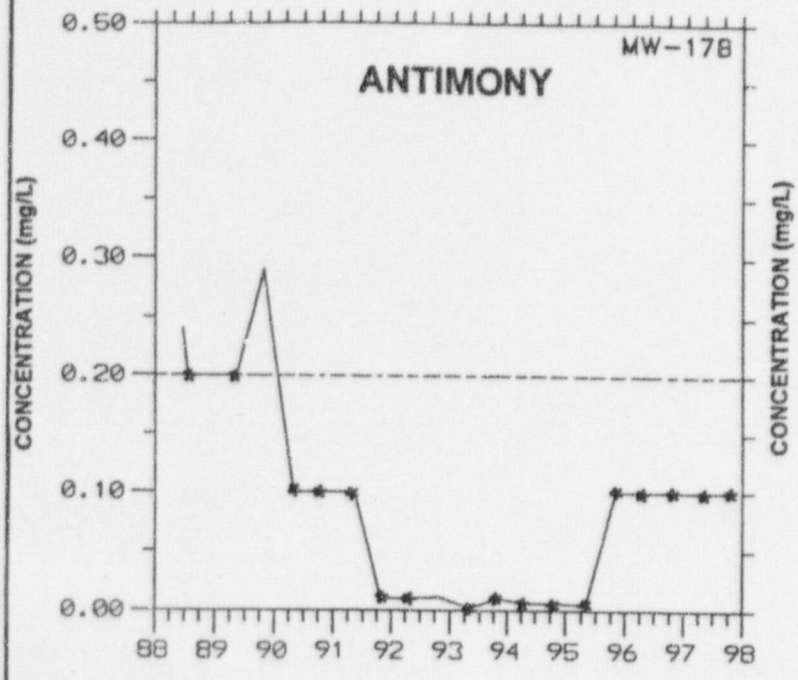

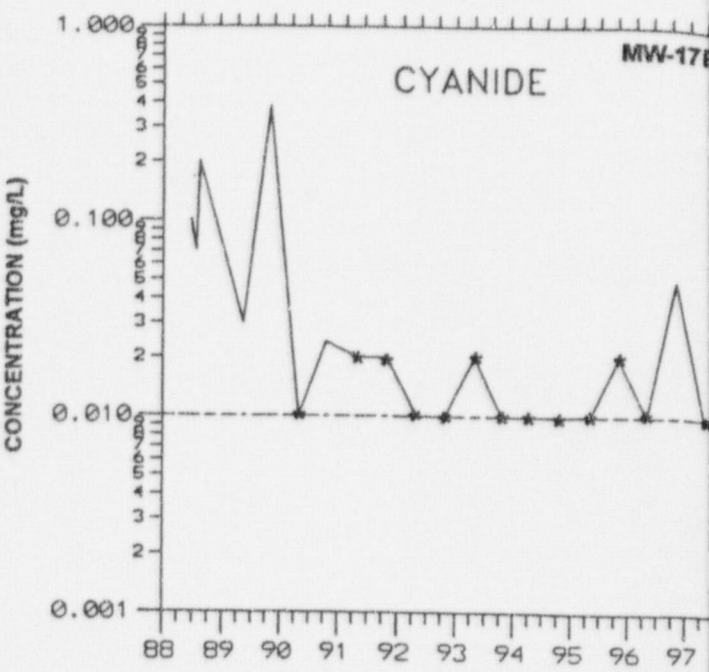

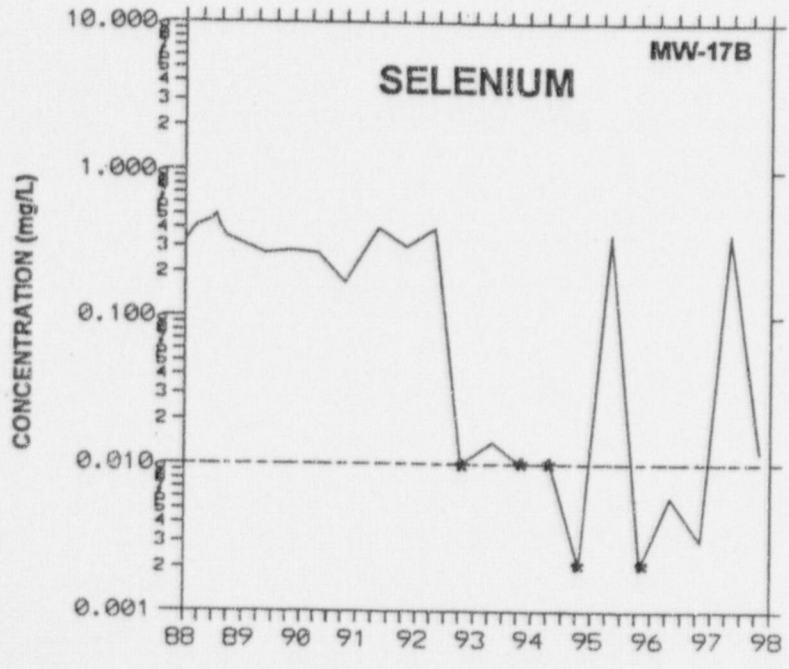

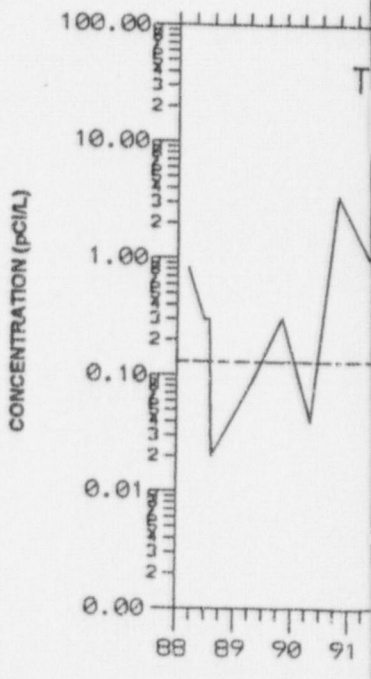

- - - Groundwater Protection Standard

★ Not Detected, Value Plotted is Method Detection Limit

■ Only Analyzed for Ra226

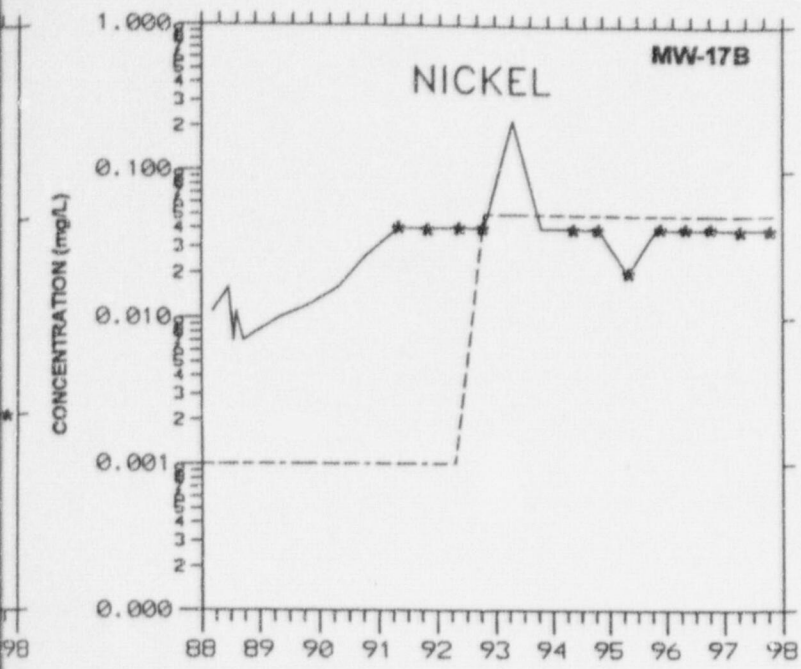

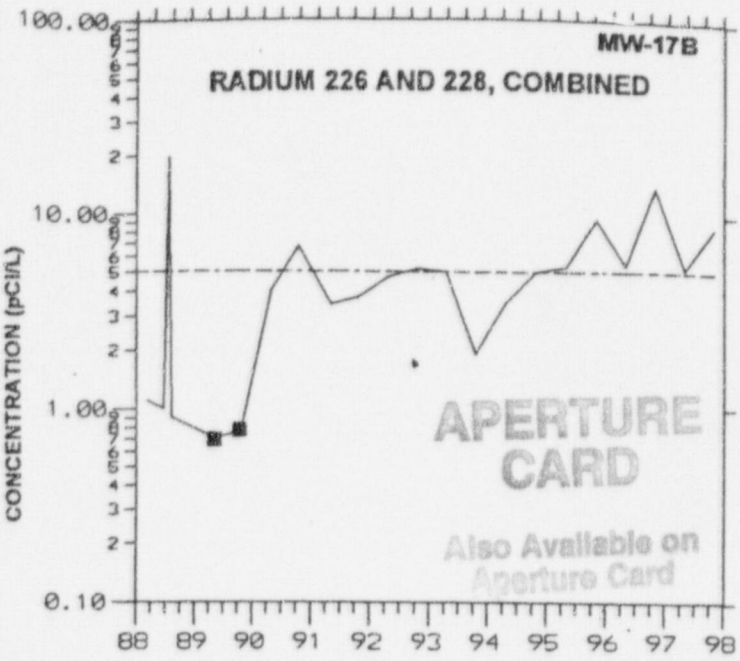

APERTURE CARD
Also Available on Aperture Card

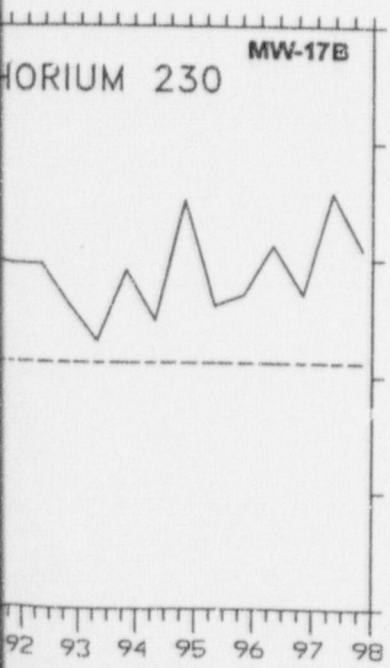

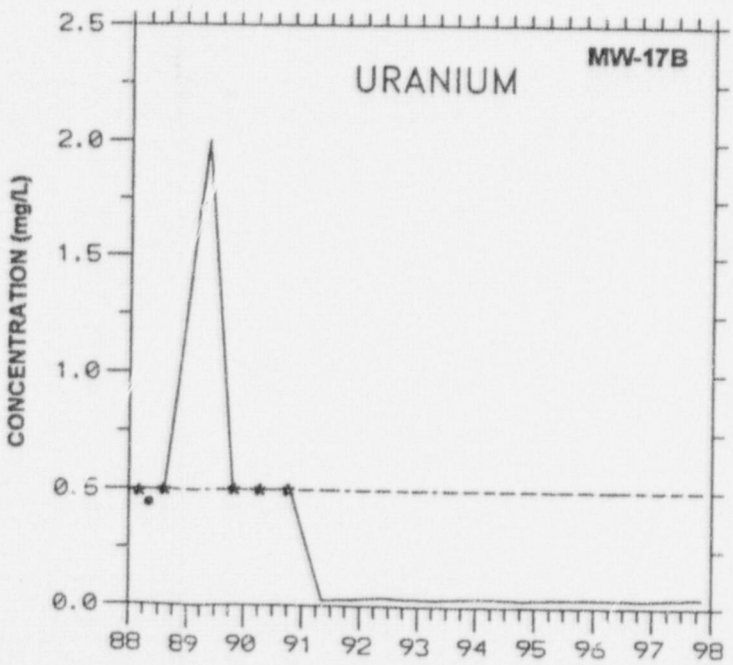

9903120203-02

DATE: 2/98	Concentrations at Point of Compliance Well MW-17B
REF: TKE 101	
DE&S Duke Engineering & Services	Figure C-2

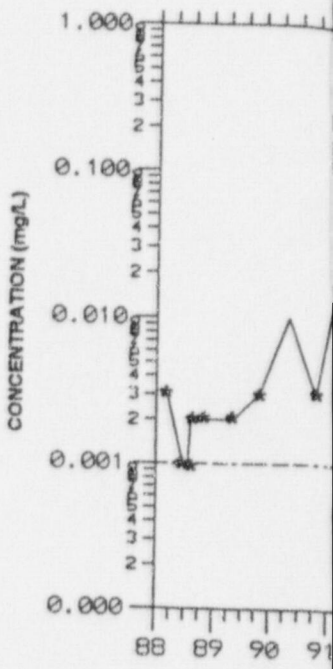

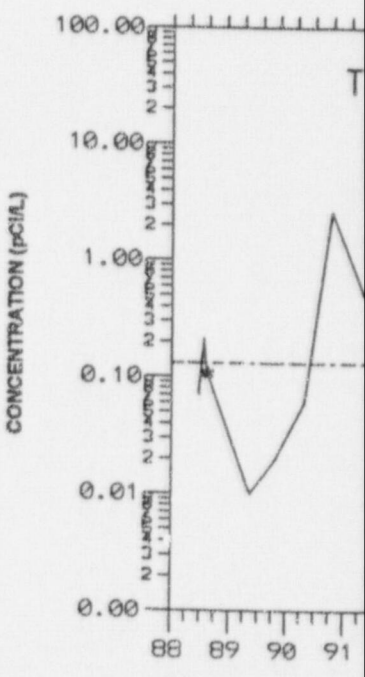

- - - Groundwater Protection Standard

★ Not Detected, Value Plotted is Method Detection Limit

■ Only Analyzed for Ra226

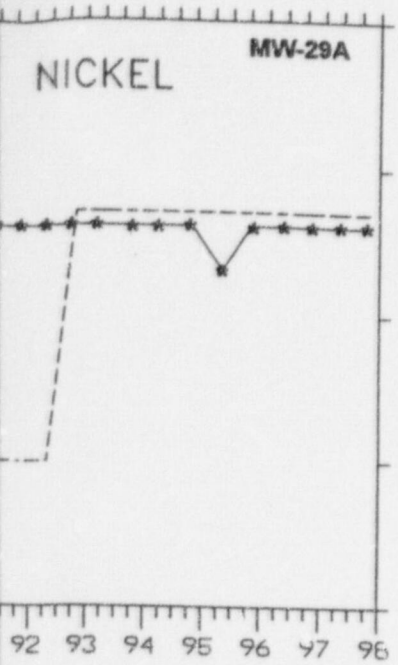

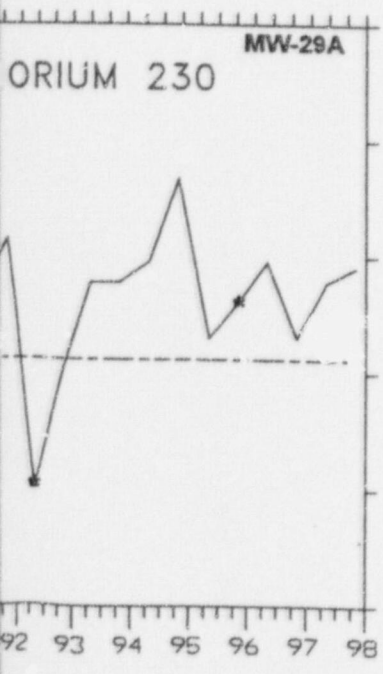

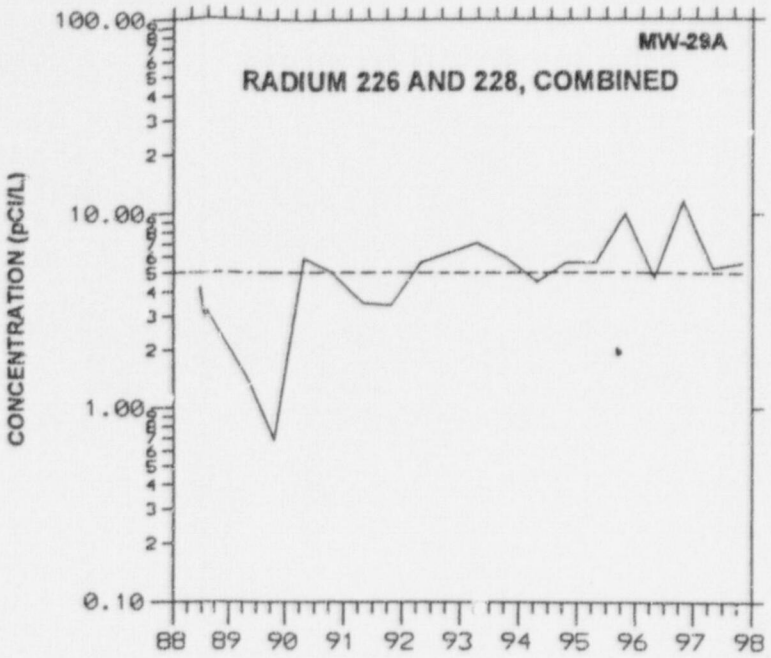

APERTURE CARD
Also Available on Aperture Card

9903120203-03

DATE: 2/98	Concentrations at Point of Compliance Well MW-29A
REF: TKE 101	
DE&S Duke Engineering & Services	Figure C-3

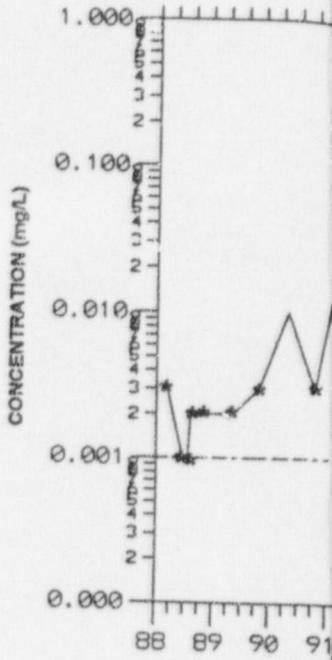

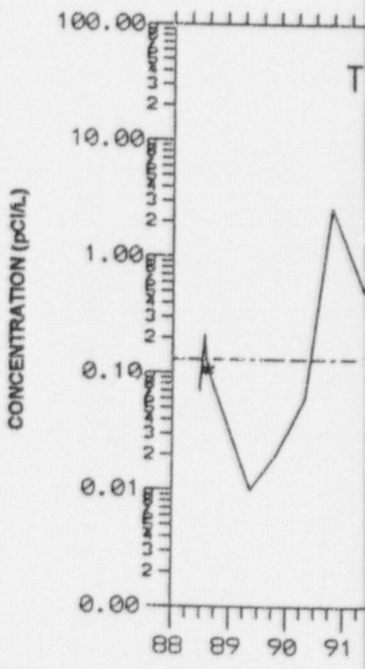

- - - Groundwater Protection Standard

★ Not Detected, Value Plotted is Method Detection Limit

■ Only Analyzed for Ra226

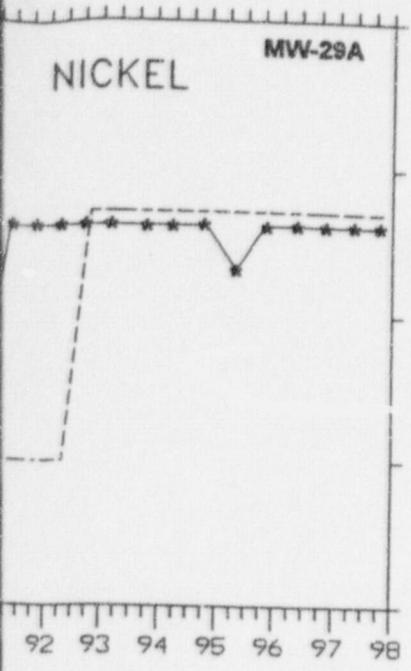

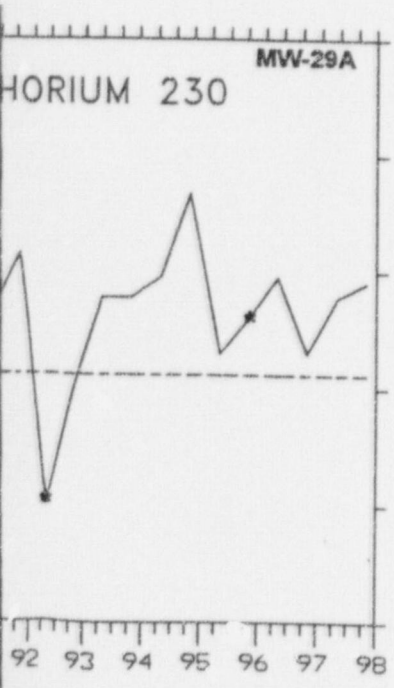

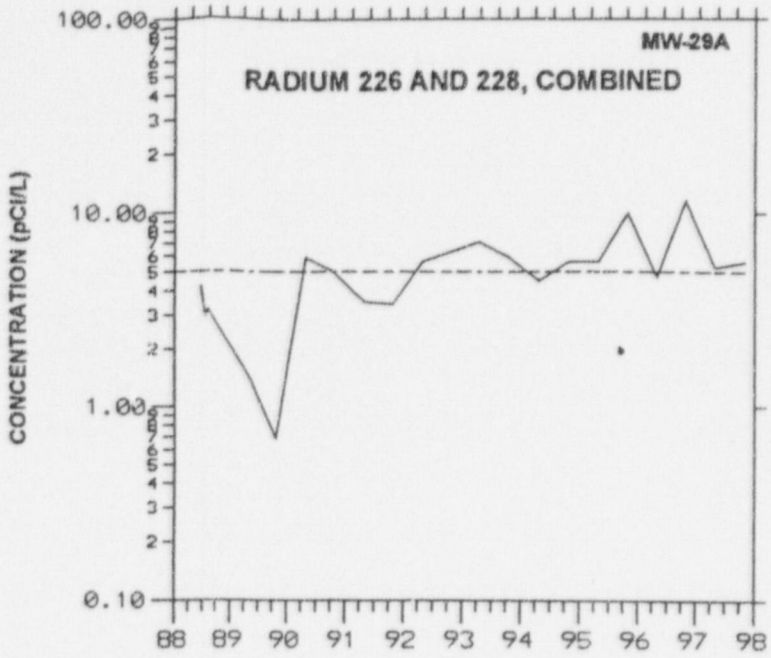

APERTURE CARD
Also Available on Aperture Card

9903120203-03

DATE: 2/98	Concentrations at Point of Compliance Well MW-29A
REF: TNE 101	
DE&S Duke Engineering & Services	Figure C-3

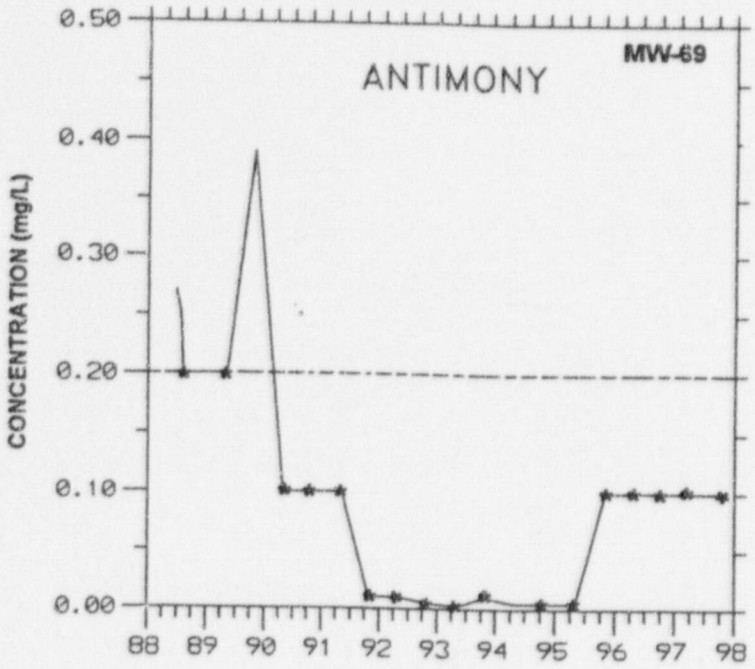

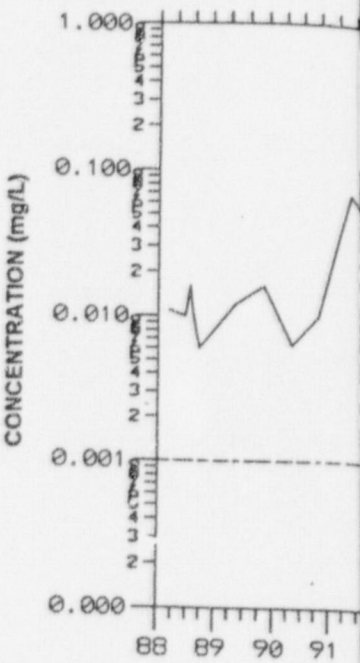

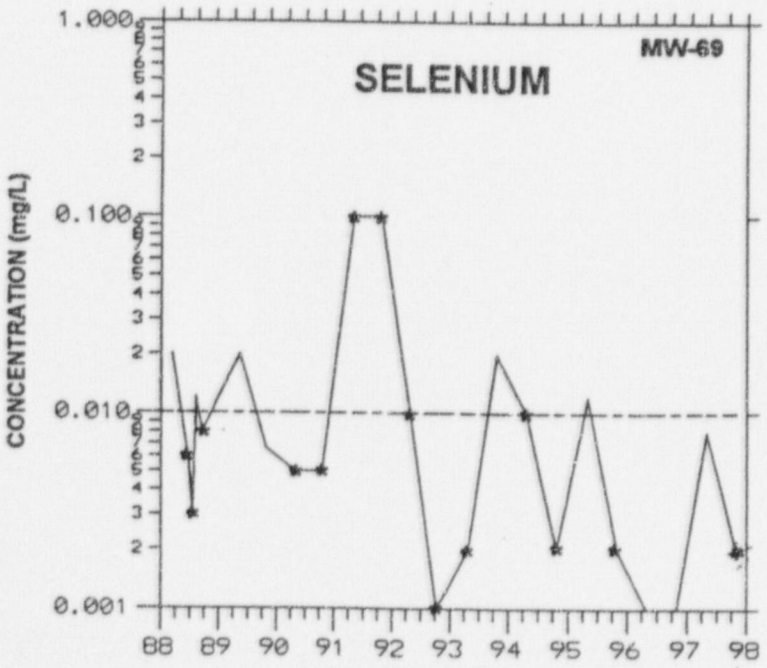

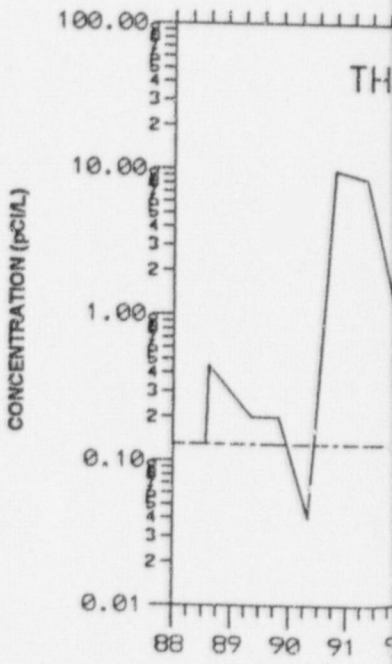

- - - Groundwater Protection Standard

★ Not Detected, Value Plotted is Method Detection Limit

■ Only Analyzed for Ra226

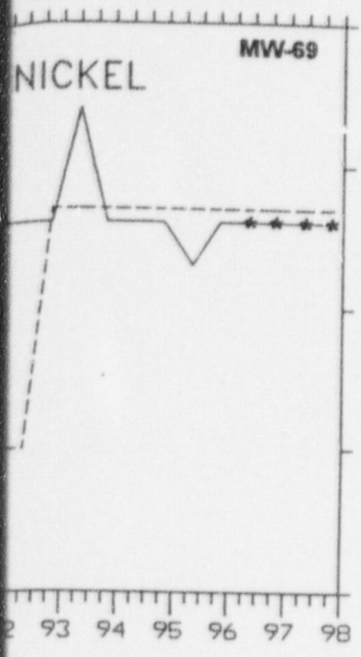

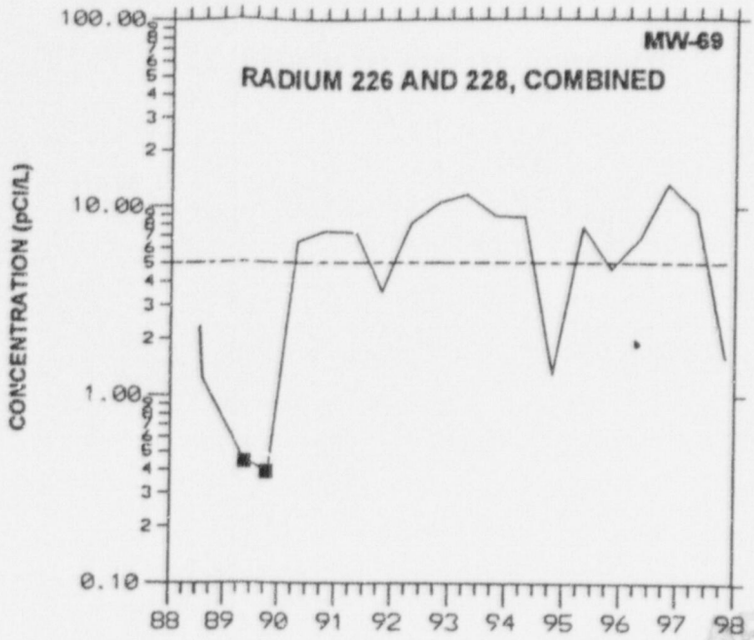

APERTURE CARD
Also Available on Aperture Card

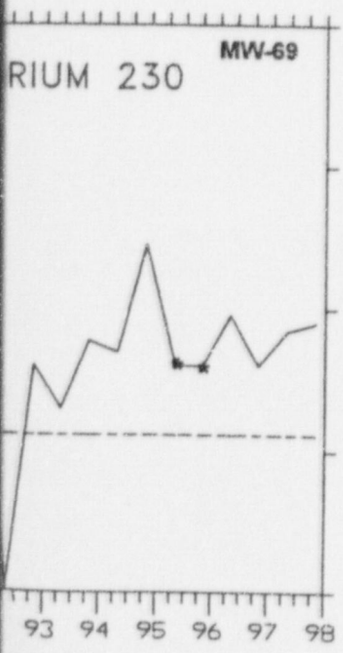

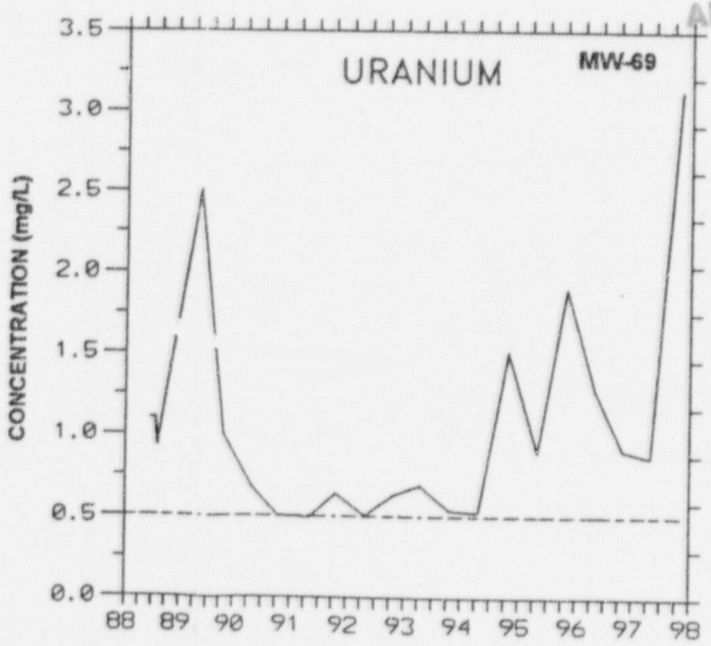

9903120203-04

DATE: 2/98	Concentrations at Point of Compliance Well MW-69
REF: TKE 101	
DE&S Duke Engineering & Services	Figure C-4

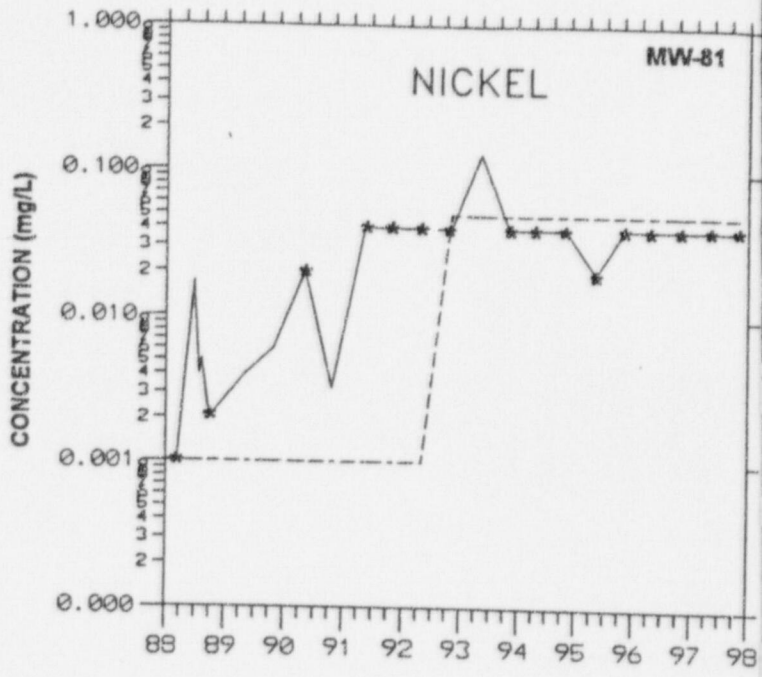

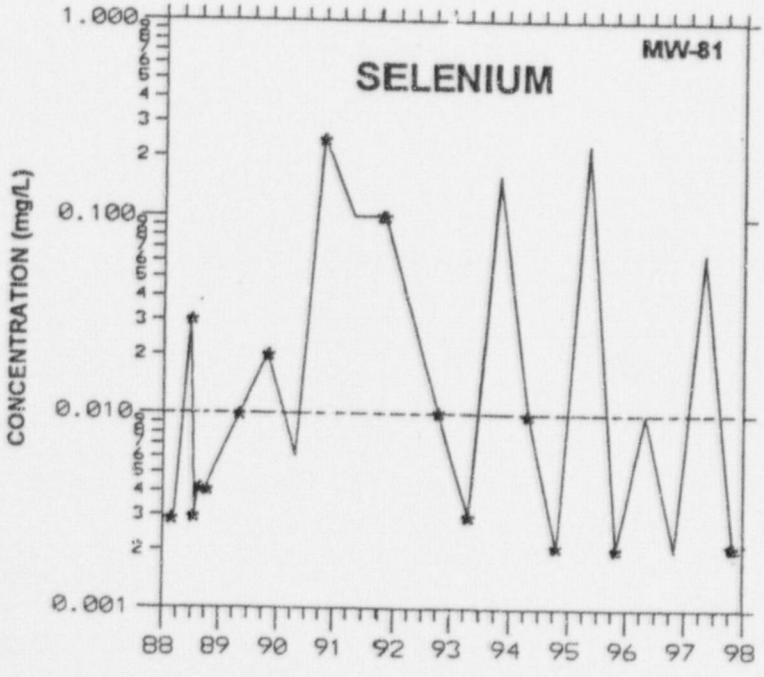

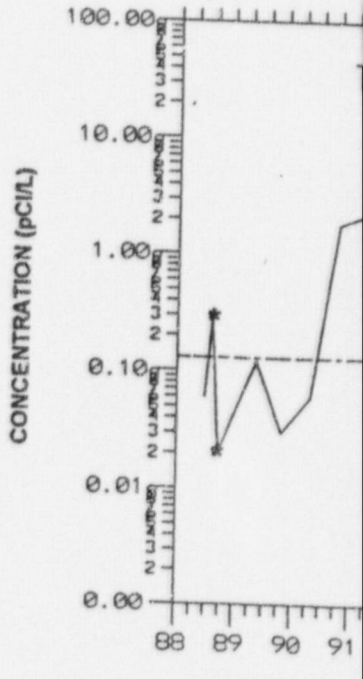

- - - Groundwater Protection Standard

★ Not Detected, Value Plotted is Method Detection Limit

■ Only Analyzed for Ra226

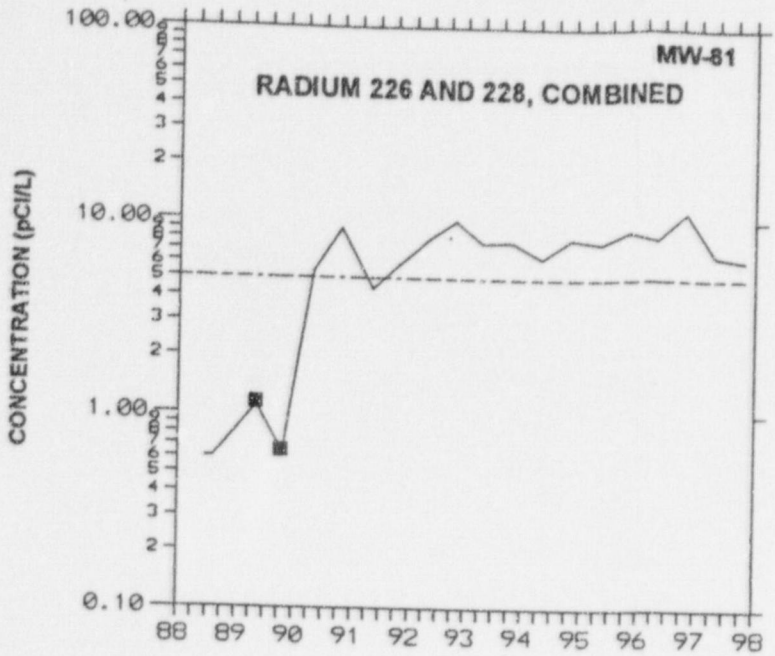

APERTURE CARD
Also Available on Aperture Card

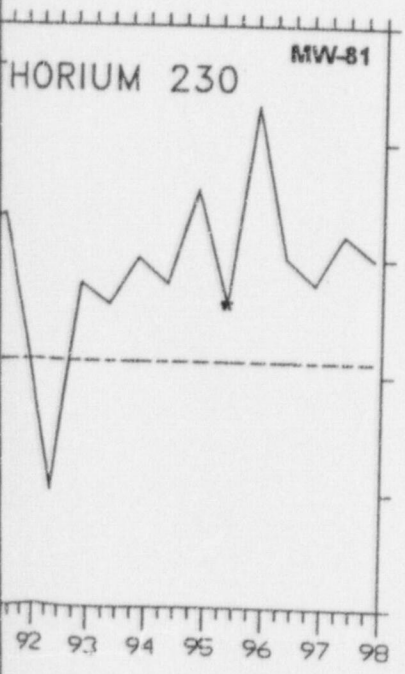

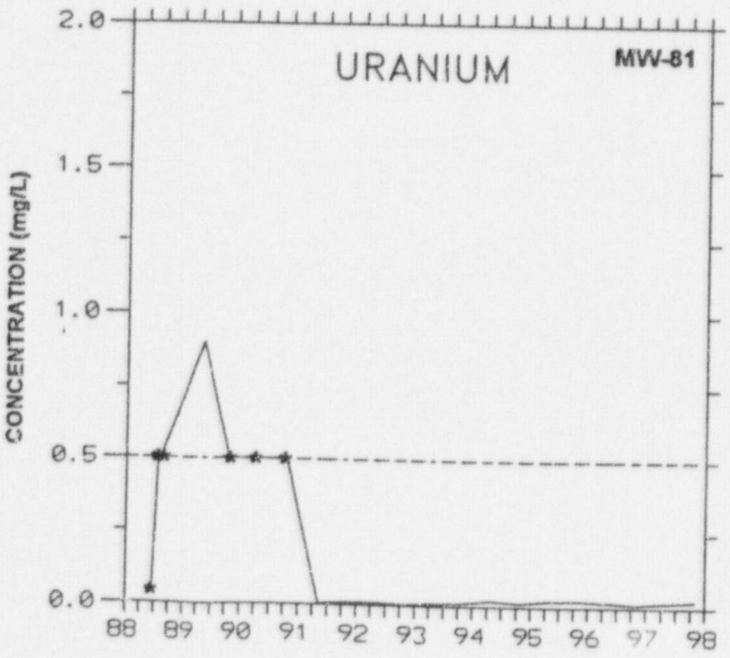

9903120203-05

DATE: 2/98	Concentrations at Point of Compliance Well MW-81
REF: TKE 101	
DE&S Duke Engineering & Services	Figure C-5